Exploring Outcome Measures of disease progression in Secondary Progressive Multiple Sclerosis

Floriana De Angelis

A thesis submitted to University College London
for the degree of Doctor of Philosophy

January 2020

Declaration

I, Floriana De Angelis, confirm that the work presented in this thesis is my own. Where information has been derived from other sources, I confirm that this has been indicated in the thesis.

The MS-SMART trial Team at UCL included several clinical research fellows, of whom I will provide a brief description in order to clarify the division of work in the data collection and analyses. When the trial was opened, in December 2014, the Team was composed by two clinical research fellows, including myself and Dr Domenico Plantone, who left the Team in April 2016. Dr Plantone screened 40% of the patients and performed a similar amount of baseline optical coherence tomography (OCT) scans; I performed the reminder of the screening visits (60%) and OCT scans at baseline (60%) and follow-up (100%). In September 2015, a third clinical research fellow, Dr Anisha Doshi, joined the trial team and contributed to data collection by performing clinical assessment of the enrolled patients (i.e. baseline, week 48 and week 96 visits) and analysing the number of persistent new T1 lesions at MRI. In April 2017, a further clinical research fellow, Dr Nevin John, joined the Team and contributed to clinical assessments and analysis of advanced MRI sub-study (spectroscopy).

The Research Nurses Tiggy Beyene, Vanessa Bassan, Nicola Stuart, Laura Brockway, Alvin Zapata were responsible for maintenance of the case record forms, taking blood and urine samples for patients' safety.

As far as my role was concerned, I performed the following: setting up the trial infrastructure at the UCL (London) site; advertising the trial in roadshows for

patients and conferences for neurologists; screening and recruitment of more than a half of the patients enrolled at the UCL site (n=176); organising patients visits for the screening, MRI and baseline visits at the UCL site; maintaining case report forms for the screening, baseline, and follow-up visits at 48 and 96 weeks; performing more than a half of the baseline retinal imaging using OCT, and all the imaging scans for the follow-up assessments; taking and processing blood, urine and cerebrospinal fluid (CSF) from most of the patients for the CSF sub-study; analysing spinal cord MRIs from the UCL site and new and enlarging T2 lesions for all trial scans at the 24 and 96 week timepoint scans; performing quality checks of all the baseline and follow-up (24 and/or 96 week) imaging for MRI brain segmentation, T2 lesion volume, and SIENA reports for all the trial scans (and sites); checking the quality of magnetic transfer ration (MTR) scans at baseline and 96 week follow-up for scans from the UCL and Edinburgh sites; checking quality, exporting data and entering data for OCT results for the UCL and Edinburgh sites; and the writing of this thesis.

The MS-SMART trial was designed by the UK Multiple Sclerosis Society Clinical Trials Network and led by Professor Jeremy Chataway as the Chief investigator of the study. The trial co-applicants were: Professor David H. Miller (later emeritus), Professor Sue H. Pavitt, Professor Gavin Giovannoni, Professor Claudia Gandini Wheeler-Kingshott, Professor Clive Hawkins, Professor Basil Sharrack, Mr Roger Bastow, Professor Christopher J Weir, Professor Nigel Stallard, Professor Siddharthan Chandran.

All the applications for ethics, MHRA, and R&D approval were carried out by Ms Moira Ross from the Edinburgh Clinical Trials Unit (ECTU).

Almudena Garcia Gomez and the admin staff from the Queen Square MS Centre performed the clinical data entry for the UCL site.

The sub-studies activated at UCL and Edinburgh (i.e. advanced MRI protocol sub-study, OCT sub-study, CSF sub-study) were designed by the Queen Square MS Team led by Professor David Miller, Professor Claudia Gandini Wheeler-Kingshott and Professor Jeremy Chataway.

The OCT scans at the Edinburgh site were performed by Dr James Cameron for the baseline visits and by Ms Dawn Lyle or local PhD students from the Anne Rawlings Neurodegenerative Clinic for the week 96 follow-up visit.

Professor Christopher Weir and Mr Richard Parker performed the statistical analyses for the primary outcome of the trial and for secondary and exploratory outcomes according to a pre-specified statistical analysis plan of the MS-SMART trial.

Professor Giovannoni and Dr Gnanapavan led the sample analyses for the CSF sub-study.

The MS-SMART sites and investigators were: Queen Square Multiple Sclerosis Centre, University College London Hospitals NHS Foundation Trust, London: Jeremy Chataway, Claudia Gandini Wheeler-Kingshott, Floriana De Angelis, Domenico Plantone, Anisha Doshi, Nevin John, Thomas Williams, Tiggy Beyene, Vanessa Bassan, Alvin Zapata, Marie Braisher; NHS Lothian, Anne Rowling Regenerative Neurology Clinic, Royal Infirmary of Edinburgh, Edinburgh: Siddharthan Chandran, Peter Connick, Dawn Lyle, James Cameron, Daisy Mollison, Shuna Colville, Baljean Dhillon; ECTU: Christopher J Weir, Richard

Parker, Moira Ross, Gina Cranswick; Barts and the London, London: Gavin Giovannoni, Sharmilee Gnanapavan; Imperial College, London: Richard Nicholas; Brighton and Sussex University Hospitals: Waqar Rashid, Julia Aram; Leeds General Infirmary, Leeds: Helen Ford; Southern General Hospital, Glasgow: James Overell; The Walton Centre, Liverpool: Carolyn Young, Heinke Arndt; The Royal Victoria Infirmary, Newcastle: Martin Duddy, Joe Guadagno; Queens Medical Centre, Nottingham: Nikolaos Evangelou; John Radcliffe Hospital, Oxford University Hospitals NHS Trust, Oxford: Matthew Craner, Jacqueline Palace; Derriford Hospital, Plymouth: Jeremy Hobart; Royal Hallamshire Hospital, Sheffield: Basil Sharrack, David Paling; University Hospital of North Staffordshire, Stoke-on-Trent: Clive Hawkins, Seema Kalra; Royal Cornwall Hospital, Truro: Brendan McLean. Statistics and Epidemiology, Division of Health Sciences, Warwick Medical School, University of Warwick, Coventry: Nigel Stallard. Patient Representative: Roger Bastow.

The MS-SMART trial was a project funded by Efficacy and Mechanism Evaluation (EME) Programme, an MRC and NIHR partnership. It was also supported by the UK Multiple Sclerosis Society, the National Institute for Health Research University College London Hospitals Biomedical Research Centre and University College London.

Abstract

Multiple sclerosis (MS) is a disabling and progressive neurological disease affecting more than 120,000 people in the UK and 2.5 million people worldwide. Most people diagnosed with relapsing-remitting MS (RRMS) experience a late phase of the disease characterised by gradual progression of impairment of neurological function, known as secondary progressive MS (SPMS). The underlying cause of disability accrual in SPMS is attributed to progressive neuro-axonal loss (neurodegeneration). Unlike RRMS, treatments for SPMS are lacking and research from clinical trials has provided only modest positive results.

This thesis concerns my work on a multi-centre, multi-arm, placebo-controlled phase 2B clinical trial (MS-SMART, ClinicalTrials.gov NCT01910259) investigating neuroprotection in SPMS. Through this trial, I investigated: (1) cross-sectional relationships between clinical and radiological outcomes that characterise a well-defined UK SPMS population not on disease-modifying therapy; (2) whether amiloride, fluoxetine and riluzole – the three pre-identified putative neuroprotective drugs used in the MS-SMART trial – reduced the rate of MRI-derived brain atrophy compared to placebo; (3) whether spinal cord MRI measures - reflecting cord damage and atrophy - were predictors of long-term disease course in people with SPMS and could be reliably used as outcome measures in future phase 2 trials; and (4) whether optical coherence tomography (OCT) measures were predictors of long-term disease course in people with SPMS and had a role in the measurement of neuroaxonal loss in future phase 2 trials.

I collected several measures of disability, which included the expanded disability status scale (EDSS), the symbol digit modalities test (SDMT), the multiple sclerosis functional composite (MSFC) and its sub-components (9-holep peg test, timed 25-

foot walk, paced auditory serial addition test), and multiple sclerosis impact scale (MSIS-29v2). To characterise the trial cohort at baseline and identify the variables that could better explain the sample variance, I used some sophisticated statistical analyses (principal component analysis, LASSO regression analysis) which helped to deal with the multiplicity of the variables. I also looked at some of the MS symptoms onset and comorbidities and their relationships with disease severity using multivariate analyses.

To investigate neuroprotection in the whole trial cohort, I measured MRI-derived percentage brain volume change, which is thought to reflect neuroaxonal integrity and disability. The percentage brain volume change was analysed with the SIENA method.

As MS-related disability is also referable to spinal cord damage, which is seen in up to 90% of patients with MS, I investigated spinal cord MRI abnormalities in the UCL cohort. I measured the cervical cord lesion number and volume, and calculated cord cross-sectional area using the active surface model. Additionally, I measured the cross-sectional area using two different pipelines to improve reduceing variability and get more reliable results.

Although MRI techniques are reliable and sensitive surrogate biomarkers of axonal pathology in MS, they are expensive, time consuming and not easily accessible. OCT is an emerging imaging technique that enables the measurement of the neural retina, whose layer thinning reflect axonal loss. In order to do so, I used a Heidelberg Spectralis OCT machine and measured the peripapillary retinal nerve fibre layer and the ganglion cell plus the inner plexiform layer thicknesses. Both participants from UCL and Edinburgh trial sites were included.

From December 2014 to June 2016, I actively recruited 176 subjects at UCL. In total, 445 subjects were enrolled in the MS-SMART trial across the UK.

The baseline analysis of the whole cohort showed that none of the clinical measures could explain the sample variance in isolation and that the SDMT – a measure of processing speed – emerged as the strongest explanatory component, although it could not explain more than 30% of the sample variance. The SDMT and the body mass index were the strongest predictor of whole brain volume. I also found that a history of optic neuritis at MS onset did not predict a better SPMS prognosis, while a history of hypertension was related to higher disease severity.

The primary trial analysis findings were negative, meaning that there was no difference in terms of percentage brain volume change between any of the three active arms and the placebo. This suggested that amiloride, fluoxetine and riluzole had no neuroprotective effects. The annualised percentage brain volume change was -0.87%. In the fluoxetine arm, there was a significant pseudoatrophy at 24 weeks suggesting perhaps possible neuromodulation with some anti-inflammatory effects.

Spinal cord atrophy occurred at a rate of -0.66% per year on average. Both spinal cord area and brain volume measures at baseline were significantly associated with EDSS at baseline and at 96 weeks. However, only spinal cord area at baseline, and not brain volume, seemed to predict confirmed disability progression at 96 weeks (OR= 0.94; 95% CI= 0.89 to 0.98, p= 0.01). The results from the two different spinal cord MRI analysis pipelines showed that head position into the scanner and lack of registration between baseline and follow-up would lead to substantial variability. However, when the sample size was larger, the two pipelines seemed to offer similar results.

OCT measures showed significant mean annual thinning independent of age. Additionally, baseline OCT measures could significantly predict clinical changes as measured by the two most common clinical metrics (EDSS and MSFC) and with the MRI-derived percentage brain volume change at 96 weeks. There was no correlation between annualised atrophy rates of OCT measures and MRI percentage brain volume change or EDSS change.

In summary, the cross-sectional analysis of the baseline characteristics of the trial cohort showed that the SDMT is an important clinical variable which correlates significantly with other clinical and MRI parameters. My study suggests that SDMT should be collected in all cross-sectional studies in SPMS.

I found that multi-arm trials are feasible in a UK population of people with SPMS. None of the three drugs – amiloride, fluoxetine, and riluzole - had neuroprotective effects, suggesting that future trials in SPMS should focus on different agents with different mechanisms of action. The role of fluoxetine as an anti-inflammatory was questionable and might deserve more investigations in the future.

I also found that the annual rates of brain volume and spinal cord atrophy were similar, although brain volume atrophy was slightly higher than spinal cord atrophy. However, both these measures were significantly associated with EDSS. Brain volume had the advantage of being associated with the timed 25-foot walk measure; whereas, spinal cord area had the advantage to predict confirmed disability progression at 96 weeks.

OCT measures significantly decreased over time independently of patients' age. Baseline OCT measures could predict EDSS changes and EDSS at 96 weeks, but

the percentage change of OCT measures had no relation with EDSS changes, suggesting that the observation time of 96 weeks was insufficient to detect clinically meaningful OCT changes.

In conclusion, analysing a large cohort of patients with SPMS enrolled in a phase 2B trial provided a large data set which served to explore outcome measures of disease progression. I found that none of the clinical, MRI or OCT variables was optimal, in isolation, to measure SPMS disability or progression. OCT and spinal cord MRI did not seem to provide better outcomes compared to MRI brain measures alone, implying that they could measure different aspects of the pathology underlying SPMS. My work suggests that investigation of composite outcome measures of multimodal variables might be the way forward to find more sensitive outcome measures for quantifying disability changes. Finally, my work also shows that multi-arm trials investigating different agents at the same time are feasible and advantageous in SPMS and should be replicated in MS and extended to other chronic neurological disorders.

Acknowledgements

I am grateful to all the patients who took part in the MS-SMART trial and, particularly, those who were enrolled at UCL. Their motivation and hope to help in research despite living with major disability caused by their MS have been extremely inspirational for me. Now, more than ever, I know that the cause of researching for patients with SPMS needs more effort.

I would like to thank my supervisors. Professor Jeremy Chataway provided support and encouragement when the situation became difficult. I am grateful to Professor Frederik Barkhof for his critical review of my work and for his suggestions and availability to help in the MRI analyses. I would also like to thank Emeritus Professor David Miller who supervised me during the first two years of my PhD before retirement. I will always remember him as a supportive and strong figure who kept encouraging me also in his retirement.

I would like to thank my co-fellows who shared with me good and bad moments during these years of work: Dr Anisha Doshi, Dr Domenico Plantone and Dr Nevin John.

I would like to thank all the team at the Queen Square MS Centre for their expertise, patience and support in this work. Marie Braisher, Tina Holmes, Charlotte Burt, and Jon Steel provided administrative and technical support. The physics team led by Prof Claudia Gandini Wheeler-Kingshott significantly contributed to development of the MRI protocols and image-analysis pipelines used in the study. I would like to acknowledge particularly the work of Dr Ferran Prados, Dr Rebecca Samson and Dr Bhavana Solanky. I am sincerely grateful to the kindness and

professional expertise of the Trial Office Team led by Mr David MacManus. Particularly, I thank Almudena Garcia and Jonathan Stutters.

I would like to thank Professor Christopher Weir and Mr Richard Parker from the Edinburgh Clinical Trials Unit who substantially helped me in the statistical analyses of my thesis. I bothered them many times, and they never denied help. I also thank Ms Moira Ross who worked as clinical trial coordinator at Edinburgh Clinical Trials Unit during the entire duration of the MS-SMART trial.

I am thankful for the support and friendship of Dr Rosanna Cortese, Dr Francesca Tona, Dr Carmen Tur, Dr Wallace Brownlee, Dr Alberto Calvi, Dr Thomas Williams. A special thank goes to Ms Tiggy Beyene, Ms Vanessa Bassan, Mr Alvin Zapata, Ms Sarah Alexander, Ms Iwona Pisarek. I also thank Dr Francesco Grussu and Dr Marco Battiston whom I remember as the first people I met when I started my adventure at Queen Square.

I would like to thank my partner, Dr Arman Eshaghi, for his patience, support, and critical review of this work.

I thank my sister Rosanna De Angelis and her husband Sabatino De Fusco, who were a continuous source of encouragement, human warmness and joy.

Finally, I would like to thank my father who does not know how much I am grateful for everything he has done for me.

Impact Statement

My PhD work has contributed to the research in a chronic neurological disorder for which there is no current cure. The MS-SMART trial did not show any evidence of neuroprotective effect of three agents - amiloride, fluoxetine and riluzole - in secondary progressive multiple sclerosis despite suggestive early animal and human work. These findings were surprising as the three agents were deliberately chosen to target different mechanistic pathways with strong preceding animal and positive phase IIA evidence. The trial findings suggest that academic studies should focus on other mechanisms of neuroaxonal damage other than the one addressed by the MS-SMART trial. Additionally, neuroprotection in secondary progressive multiple sclerosis might not be enough to slow down disability accrual and future research should consider combination therapy including anti-inflammatory and neuroprotective drugs.

Other implication for the academic environment is that investigator-led multi-arm, multi-centre trials are feasible and could be efficiently used also for other neurodegenerative diseases. These kinds of studies have the potential to examine promising experimental and early phase agents in a timely fashion. The results have implications for future experimental paradigms. This style of approach is necessary to accelerate treatment discovery in an area where there has been limited progress with implication for patients with progressive neurodegenerative disorders like multiple sclerosis.

My work has an impact locally, in the London area, and nationally, in the UK. However, the MS-SMART paradigm could be applied internationally in other academic environments.

The results of my work are being published in scholarly journals.

Table of contents

List of tables

List of figures

Abbreviations

3D: three-dimensional

9HPT: 9-hole peg test

AMD: adjusted mean difference

ARR: annualised relapse rate

ASIC: acid-sensing ion channel

ATP: adenosine tri-phosphate

BBSI: Brain Boundary Shift Integral

BDI-II: Beck Depression Index II

BDNF: brain-derived neurotrophic factor

BICAMS: Brief International Assessment of Cognition for multiple sclerosis

BPF: brain parenchymal fraction

BPI: brief pain inventory

BRNB: brief repeatable neuropsychological battery

CDP: confirmed disability progression

CI: confidence interval

CIS: clinically isolated syndrome

CNS: central nervous system

CSF cerebrospinal fluid

CRF: clinical research fellow

DMT: disease modifying treatment

DNA: deoxyribonucleic acid

DTI: diffusion tensor imaging

EAE: experimental autoimmune encephalomyelitis

EBV: Epstein Barr virus

EDSS: expanded disability status scale

EMA: European Medicines Agency

EQ-5D-5L: EuroQuol 5-level version

ETDRS: Early Treatment Diabetic Retinopathy Study

FDA: Food and Drug Administration

FAMS: functional assessment of multiple sclerosis

FLAIR: fluid attenuated inversion recovery

FS: functional System

FSE: fast spin echo

CI: confidence interval

GC: ganglion cell

GCL: ganglion cell layer

GIF: Geodesical Information Flows

GM: grey matter

gRNFL: global retinal nerve fibre layer

HCVA: high-contrast visual acuity

HLA: human leukocyte antigen

HR: hazard ratio

IFNb: interferon beta

IQR: interquartile range

IPL: inner plexiform layer

LASSO: least absolute shrinkage and selection operator

MACFIMS: minimal assessment of cognitive function in multiple sclerosis

MANOVA: multivariate analysis of variance

MNI: Montreal Neurological Institute

MRI: magnetic resonance imaging

MRS: magnetic resonance spectroscopy

MS: multiple sclerosis

MSFC: multiple sclerosis functional composite

MSIS-29v2: multiple sclerosis impact scale-29 (items) version 2

MSQoL-54: multiple sclerosis quality-of-life questionnaire

MSWSv2: multiple sclerosis walking scale v2

MTR: magnetization transfer ratio

MV: macular volume

NAWM: normal-appearing white matter

NFI: neurological fatigue index

NMDA: N-methyl-d-aspartate

NPRS: numerical pain rating score

NPS: neuropathic pain scale

OCT: optical coherence tomography

ON: optic neuritis

OR: odds ratio

PASAT: paced auditory serial addition test

PBVC: percentage brain volume change

PCA: principal component analysis

PC: principal component

PD: proton density

PI: principal investigator

PPMS: primary progressive multiple sclerosis

PRMS: progressive-relapsing multiple sclerosis

pRNFL: peripapillary retinal nerve fibre layer

PROM: patient-reported outcome measure

PSIR: phase-sensitive inversion recovery

QC: quality check

RN: research nurse

RNFL: retinal nerve fibre layer

RRMS: relapsing-remitting multiple sclerosis

SBC: Schwarz Bayesian Criterion

SDMT: symbol digit modalities test

SIENA: structural image evaluation using normalization of atrophy

SIENAX: Structural Image Evaluation using Normalization of Atrophy Cross-sectional

SLCVA: Sloan low contrast visual acuity

SPM: statistical parametric mapping

SPMS: secondary progressive multiple sclerosis

SSRI: serotonin-reuptake inhibitor

tRNFL: temporal retinal nerve fibre layer

T2LV: T2 lesion volume

T25FW: timed 25-foot walk

TNF: tumour necrosis factor

UCL: University college London

VBM: voxel-based morphometry

WM: white matter

Publications associated with this thesis

Floriana De Angelis, Peter Connick, Richard A Parker, et al. *Amiloride, fluoxetine or riluzole to reduce brain volume loss in secondary progressive multiple sclerosis: the MS-SMART four-arm RCT*, Efficacy and Mechanism Evaluation, No. 7.3, NIHR Journals Library; 2020 May.

Jeremy Chataway, Floriana De Angelis, Peter Connick, et al. *Multiple Sclerosis-Secondary Progressive Multi-Arm Randomisation Trial (MS-SMART): a multi-arm phase 2B randomised, double-blind, placebo-controlled clinical trial comparing the efficacy of three neuroprotective drugs in secondary progressive multiple sclerosis.* The Lancet Neurology, *in press*

Floriana De Angelis, Jeremy Chataway. *Novel Multiple Sclerosis Drugs in the Pipeline.* Clin Pharmacol Ther. 2019 May;105(5):1082-1090.

Floriana De Angelis, Nevin A John, Wallace J Brownlee, *Therapeutics for multiple sclerosis.* BMJ. 2018 Nov 27;363:k4674.

Floriana De Angelis, Domenico Plantone, Jeremy Chataway. *Pharmacotherapies in secondary progressive multiple sclerosis: slowing and preventing.* CNS Drugs, Jun 2018, 32 (6), 499-526.

Peter Connick, Floriana De Angelis, Richard Parker et al. *MS-SMART: Multiple Sclerosis-Secondary Progressive Multi-Arm Randomisation Trial. The first multi-arm phase 2b randomised, double blind, placebo-controlled clinical trial comparing the efficacy of three neuroprotective drugs in secondary progressive multiple sclerosis.* BMJ Open, *BMJ Open, 8 (8), 2018 Aug 30*

Domenico Plantone, Floriana De Angelis, Anisha Doshi, Jeremy Chataway. *Secondary Progressive Multiple Sclerosis: Definition and Measurement.* CNS Drugs. 2016 Jun;30(6):517-26. Review.

Chapter 1. **Background**

1.1 **Epidemiology of MS**

Multiple sclerosis (MS) is the most common acquired disabling neurological disease affecting young adults in temperate latitudes. It is estimated that there are over 120,000 people with MS in the UK and more than 2.5 millions worldwide (World Health Organization, 2008; Browne *et al.*, 2014; Mackenzie *et al.*, 2014). Although MS occurs throughout the world, there are geographical differences in prevalence and incidence rates. Classically, the prevalence rates of MS were divided into geographical latitudes (Figure 1.1), with higher prevalence moving away from the equator (Browne *et al.*, 2014). The latitudinal prevalence gradients have been confirmed by a large meta-analysis (Simpson *et al.*, 2011).

Figure 1.1 Worldwide prevalence of multiple sclerosis by country

This figure was removed due to copywrite.

The figure is available on

http://www.msif.org (Browne et al., 2014)

The prevalence of multiple sclerosis is higher in countries of higher latitude and in Western countries. Adapted from the Atlas of MS (2013), MSIF http://www.msif.org (Browne *et al.*, 2014).

Both prevalence and incidence of MS have been increasing over the past decades. The rise in prevalence is predominantly due to longer survival. The increase in

incidence is partially explained by better ascertainment of cases. Furthermore, studies from several countries, including Australia, the USA, Canada, and Japan suggest that the overall raised incidence is driven by a progressively increased incidence of the disease in women, leading to higher male to female sex ratios (Orton *et al.*, 2006). Indeed, MS is more common in females, with a current sex ratio close to 3:1 (F:M) in most developed countries.

Migration studies have showed that the risk for the disease in early life is linked with the birthplace. Adult migrants from low risk countries, such as the West Indies, to Europe are at low risk of developing MS; however, children born to migrants in Europe are at high risk. Moves from high to low prevalence countries showed retention of birthplace risk only for people aged >15 years; whereas opposite moves indicated susceptibility limited to some 11–45 year olds (Kurtzke, 2013).

The increase in the male to female sex ratio and the evidence from migration studies strongly support the existence of environmental influence on the risk of MS (Dean, 1967; Ascherio *et al.*, 2012; Kurtzke, 2013).

1.2 **Aetiology**

MS is an immune-mediated inflammatory disease of the central nervous system (CNS) characterised by demyelination and neuro-axonal loss. We have a limited understanding of the mechanisms underlying MS, and the ultimate cause of this disease is unknown. Many factors have been investigated in the pathophysiology of MS, although no specific trigger has been identified. Whether a CNS extrinsic or intrinsic factor drives MS is still not known. It is believed, though, that genetic, environmental and endogenous factors all concur to drive inflammation and ultimately neurodegeneration in MS (Kawachi and Lassmann, 2016).

The link between genetics and MS seems to be determined by the human leukocyte antigen (HLA) complex. Genome-wide association studies and other large-scale genotyping projects have revealed that only few common genetic variants exist that exert relatively large effects (odds ratio [OR] ranging from 1.3 to 3), all of which are located in the HLA locus. The remainder of the genetic risk spectrum is likely determined by a large number of susceptibility variants exerting much smaller effects. Changes in the HLA-DRB1 gene are the strongest genetic risk factors for developing MS. Variations in several HLA genes have been associated with increased MS risk; particularly, the HLA-DRB1*15:01 allele is the most strongly linked genetic risk factor (OR 3.10), whereas the HLA-A*02:01 allele is considered as a protective factor (OR 1.3) (Sawcer *et al.*, 2014). However, many genes seem associated with MS, but their individual pathologic influence is not fully understood. In two studies promoted by the International MS Genetics Consortium, the authors identified 110 variants outside the major histocompatibility complex that are confidently associated with susceptibility to MS. The associated loci identified so far account for only about a quarter of the heritability reported in MS, leaving an obvious question about what determines the remainder. About a half of the remainder is likely to be the result of as-yet-undefined interactions between risk factors; whereas the remaining half probably relates to risk alleles that are yet to be discovered (Compston *et al.*, 2008; Sawcer *et al.*, 2011; International Multiple Sclerosis Genetics Consortium, 2013).

Amongst the environmental risk factors, the role of infectious and non-infectious determinants has been considered. One hypothesis is of an external agent responsible for primary infection or neuronal disturbance within the brain, which could lead to activation of the immune system and result in inflammation of the CNS, as a secondary response. Amongst the infectious agents, Ascherio and

Munger reported that Epstein Barr virus (EBV) is a strong risk factor of MS. They showed that there is at least a 20-fold increase in risk of MS amongst individuals with a history of mononucleosis (OR of MS in EBV seronegative vs seropositive subjects was 0.06; 95% confidence interval [CI] 0.03-0.13), although an important or even critical role of other known or unknown microbes cannot be excluded (Ascherio and Munger, 2007). Being EBV negative, instead, protects from developing MS (Ascherio and Munger, 2007; Pakpoor *et al.*, 2013).

Amongst the non-infectious determinants, it was reported that the strongest risk factor was a low serum level of vitamin D. Moreover, a number of studies have showed an association between smoking habit and MS (O'Gorman *et al.*, 2014; Poorolajal *et al.*, 2016). The evidence for other risk factors, e.g. dietary fat, dietary oxidants, salt intake, and sex hormones remains unproven. Belbasis and colleagues, who undertook an umbrella review examining associations between environmental (non-genetic) factors and MS, confirmed that EBV IgG seropositivity (OR 4.46, 95% CI 3.26–6.09), infectious mononucleosis (OR 2.17, 95% CI 1.97–2.39), and smoking (OR 1.52, 95% CI 1.39–1.66) have the strongest consistent evidence of an association with MS. Despite the association of higher serum vitamin D with lower MS incidence previously reported, they showed that low serum vitamin D concentrations is a weak risk factor for MS (OR 0.44, 95% CI 0.24–0.78) (Belbasis *et al.*, 2015).

1.3 **Pathophysiology**

Historically, MS has been defined as a chronic inflammatory disease of the CNS leading to focal lesions in the white matter of the brain and spinal cord characterised by primary demyelination with a variable extent of axonal loss. Whether the inflammatory process is the primary driving force of tissue damage,

or whether the lesions are initiated by a neurodegenerative process amplified or modified by the inflammatory reaction in MS is still controversial. Two main hypotheses about the pathogenesis of MS, which do not necessarily exclude each other, have emerged. An “inside-out” hypothesis, which would better explain the progressive stages of the disease, suggests that a primary central process causing neuronal damage in the CNS triggers the peripheral immune system with subsequent attacks to the CNS and progressive neuronal damage. This view is supported by a study from Barnett and Prineas, whose findings suggest that initial MS lesions are formed in the absence of inflammation by T cells and B cells, although these cells accumulate in advanced lesion stages after the initial destruction of oligodendrocytes by apoptosis and demyelination (Barnett and Prineas, 2004). The alternative “outside-in” hypothesis, most commonly accepted, proposes that a primary aberrant peripheral activation of the immune system triggers a chain of events causing a not fully understood immune-mediated inflammatory process in the CNS. Indeed, quantitative studies following this primary observation from Barnett and Prineas showed that in the earliest stages of lesions there are already perivascular inflammatory infiltrates containing T cells and B cells. Macrophages and microglia from the innate immune system, and T and B lymphocytes from the adaptive immune system are the major contributors of this inflammatory process (Hemmer *et al.*, 2015). From the peripheral immune system, autoreactive T-helper cells are primed and stimulated to infiltrate the CNS where they activate microglia and macrophages, causing demyelination. Loss of myelin sheath and inflammation induce acidosis, virtual hypoxia and production of reactive oxygen and nitric oxide species, which in turn lead to mitochondrial dysfunction and energy failure (see also Paragraph 1.3.1). Because of the energy failure, the concentration of calcium and sodium inside the axon progressively increase. Additionally, there is an increased extracellular release of glutamate. These concomitant processes, i.e. acidosis, intracellular ion imbalance and

glutamate-mediated excitotoxicity and mitochondrial disfunction, conclude with oligodendrocytes apoptosis, axonal damage and ultimately neuronal death (Ciccarelli *et al.*, 2014).

The pathological hallmark of all MS phenotypes are focal plaques characterised by demyelination associated with various degrees of inflammation, mostly localised around postcapillary venules. MS plaques occur in both white matter and grey matter and can be found throughout the CNS, including brain, optic nerve and spinal cord. Kutzelnigg and colleagues reported that brains of people with MS are affected by three different pathologies dominating during different stages of the disease (Table 1.1). Focal demyelinated plaques are present in all stages of the disease; however, classical active plaques are predominantly formed in patients with relapsing-remitting disease, while focal white matter plaques in progressive MS are either inactive or show slow expansion on their edges. In contrast, cortical demyelination and diffuse white matter injury were most prominent in patients with primary-progressive MS (PPMS) or secondary progressive MS (SPMS) (Kutzelnigg *et al.*, 2005; Lassmann, 2018).

Table 1.1 Pathology of MS lesions

Lesion Type	Features	Degree of inflammation	MS Sub-type
Classical active lesions	Demyelination associated with phagocytic cells (activated microglia and macrophages) and signs of acute axonal injury (disturbed fast axonal transport or axonal end bulbs). Microglia activation is most pronounced at the lesion edge; macrophages are most pronounced in the lesion centre.	High. In the initial lesions, there is a low number of T cells; in the advanced lesions (when demyelination and tissue damage increase), T cells increase.	Abundant in relapsing-remitting MS
Slowly expanding active lesions	The lesion centre is inactive. The lesion rim is characterised by activated microglia with some macrophages containing myelin degradation products.	Low	Abundant in progressive MS

	There are signs of acute axonal injury.		
Inactive lesions	There are signs of demyelination, partial axonal preservation, and reactive gliosis. A variable degree of microglia activation is present in the periplaque white matter; microglia is reduced in the lesion centre.	Low	Abundant in all MS
Cortical lesions (type 1, 2 and 3)	Type 1: cortico-subcortical lesions located at the border involving both grey and white matter. Type 2: perivenous intracortical lesions. Type 3: located in the subpial layers of the cortex. Type 3 are the most abundant cortical lesions. They are associated with inflammation in the meninges.	Variable	Abundant in progressive MS

Magnetic resonance imaging (MRI) studies showed that, in the acute focal white matter plaques - more frequently seen in relapsing-remitting MS (RRMS) - there is breakdown of the blood-brain barrier resulting in trafficking of immune cells into the brain associated with leakage of the paramagnetic contrast agent on MRI (Cotton *et al.*, 2003). Additionally, a new MRI method has been developed to identify slowly expanding lesions *in vivo* (Elliott *et al.*, 2019). Indeed, in progressive MS, inflammation is compartmentalised behind an apparently normal blood-brain barrier, and acute plaques are rare, while chronic plaques are abundant and show a slowly expanding rim of activated microglia and macrophages containing myelin degradation products at borders (Kawachi and Lassmann, 2016; Lassmann, 2017). The concept that the blood-brain barrier is intact in progressive MS, though, has been recently challenged by a study showing that there is a marked deposition of fibrin(ogen) – a marker of blood-brain barrier disruption - in the cortex of progressive MS patients (Yates *et al.*, 2017).

Post-mortem analyses (Bjartmar *et al.*, 2001) support the hypothesis that axonal loss - including synaptic loss - and grey matter damage contribute to irreversible

neurological disability in MS patients, particularly in the progressive stages of the disease (Kutzelnigg *et al.*, 2005; Kapoor, 2006; Compston and Coles, 2008; Trapp and Nave, 2008; Lucchinetti *et al.*, 2011; Popescu and Lucchinetti, 2012; Hauser *et al.*, 2013; Mandolesi *et al.*, 2015). Degenerative changes in axons within white matter lesions and secondary degeneration of fibre tracts distal to these lesions have been documented (Kornek and Lassmann, 1999). Trapp and colleagues studied active and chronic white matter lesions. They showed that axonal transection was ubiquitous, specific and extensive feature of demyelinating lesions. The density of transected axons was over 10 per mm^3 in the centre of active inflammatory lesions. In chronic inactive lesions, instead, ongoing axonal damage was less abundant, but still considerably higher than the level of axonal damage observed in white matter from neurologically healthy controls (Trapp *et al.*, 1998).

A recent study from the Netherland brain bank cohort showed that demyelinating and innate inflammatory lesion activity is substantial at time of death in progressive MS patients with long-standing disease and that clinical disease course, disease severity and sex strongly correlate with MS lesion characteristics in autopsy tissue (Luchetti *et al.*, 2018). Luchetti et al. analysed post-mortem tissues of MS subjects including 100 SPMS and 56 PPMS patients. Notably, in this cohort, 57% of demyelinated white matter and mixed grey–white matter lesions were either active or mixed active/inactive (chronic active), showing that there is considerable inflammatory lesion activity even in autopsy patients with long-term progressive disease. Additionally, they found that, even in patients with the longest disease duration (42–64 years), active or mixed active/inactive lesions accounted for 34% of all lesions, supporting the notion that lesion activity is substantial in the progressive late phase of the disease. Other interesting findings from this study are that the lesion load positively correlated with the proportion of mixed

active/inactive lesions, reactive sites, microglia/macrophages activity and inversely with remyelinated lesions, and with disease severity. The findings from Luchetti et al. contrast with previous observations from Frischer et al. where inflammatory disease processes were found to decline in long-term disease (Frischer *et al.*, 2015). However, the Netherland brain bank cohort has the characteristic of including mainly MS patients with progressive course and long disease duration.

Post mortem and *in vivo* studies found that cortical demyelination, which can be found also in the early stages of the disease, is prominent in patients with progressive phenotypes and seems to be pathognomonic of MS (Prineas *et al.*, 2001; Kutzelnigg *et al.*, 2005; Fisher *et al.*, 2008; Fisniku *et al.*, 2008). Diffuse white matter injury and widespread changes in the normal-appearing white and grey matter are prominent in PPMS and SPMS, where there is evidence of perivenous inflammatory infiltrates surrounded by rims of demyelination, diffuse astrocytic gliosis, microglia activation and axonal degeneration (Bjartmar *et al.*, 2001; Rocca *et al.*, 2003; Rammohan, 2007; Popescu *et al.*, 2013). Mahad *et al*. confirmed these findings showing that degeneration of chronically demyelinated axons, diffuse pathology in the normal-appearing white/grey matter, cortical demyelination and concomitant remyelination failure were the main pathological features of progressive MS (Mahad *et al.*, 2015).

The exact pathogenesis of cortical lesions is debated, but they seem to extend along the subpial surface of the cortex and are believed to be linked to local accumulation of pro-inflammatory cells or soluble factors from the meninges. In areas of reduced cerebrospinal fluid (CSF) flow, meningeal ectopic B cell follicle-like structures have been identified and associated with SPMS, suggesting that meningeal inflammation may play a role in neurodegeneration (Magliozzi *et al.*, 2006; Howell *et al.*, 2011). Lisak and colleagues also demonstrated that B cells

from patients with RRMS, but not from healthy controls, secrete factors *in vitro* toxic to neurons and oligodendrocytes, which are independent of immunoglobulins, not complement-mediated, and involved in apoptosis. They hypothesised that B cells entering the meninges and CSF from the peripheral immune system could secrete soluble factors different from antibodies causing the characteristic damage of MS in the underlying cortical grey matter (Lisak *et al.*, 2012, 2017).

As discussed, grey matter pathology in cortical MS lesions, which includes axonal and dendritic transection, neuronal death by apoptosis, and demyelination, appears to be widespread and extensive, especially in SPMS patients, while the amount of inflammatory cell is reduced compared to white matter lesions. The discrepancy between low inflammation in the cortical MS lesions and neuroaxonal loss has also raised the question of whether neurodegeneration could be the primary neuropathological processes in MS (Peterson *et al.*, 2001; Vercellino *et al.*, 2005). This theory, however, is contradicted by a study carried out by Lucchinetti and colleagues (Lucchinetti *et al.*, 2011). They found that cortical demyelination is common in the early stages of the disease, and the characterisation of the cortical lesions underscored inflammatory character. Therefore, cortical demyelination that occurs close to the onset of MS substantially differs from that seen in chronic MS, and this does not support a primary (noninflammatory) neurodegenerative process of MS.

Another matter of debate in the pathogenesis of MS is whether or not neurodegeneration is a direct consequence of demyelination. Indeed, it seems possible that some axons may degenerate in MS in the absence of demyelination. DeLuca et al. found only a weak correlation between axonal loss and plaque load in post-mortem MS tissue (DeLuca *et al.*, 2006). In these cases, despite the intact axon and sodium channels distribution, an inadequacy of adenosine tri-phosphate

(ATP) might still induce Ca2+-mediated axonal injury (Dutta *et al.*, 2006). We know from pathology and MRI studies in MS that only 52-55% of cerebral T2-weighted white matter lesions are demyelinated (De Groot *et al.*, 2001; Fisher *et al.*, 2007) and that T2-weighted cerebral white matter lesions account for less than 30% of the variance in the rate of brain atrophy (Korteweg *et al.*, 2009).

Furthermore, clinical disability is not fully explained by the overall T2-weighted lesion burden observed (Barkhof, 1999). All these findings suggest that grey matter demyelination may be independent of white matter lesions in MS, a hypothesis that seemed to be confirmed by a recent neuropathology study by Trapp et al., who defined a new subtype of MS termed as “myelocortical MS”. In fact, they found that in 12% of the analysed post mortem tissues from patients with MS there were spinal cord and subpial lesions, but not white matter cerebral lesions (Trapp *et al.*, 2018).

New evidence from immunology and pathology are changing our understanding of MS, which is no longer felt as a two-stage disease but rather a *continuum*, where both inflammation and neurodegeneration are contemporarily present at any moment in the course of the disease (Steinman, 2001; Lassmann, 2017).

1.3.1 Mechanisms of neuronal injury in MS

A precise understanding of the mechanisms of neurodegeneration in MS is an essential prerequisite for achieving therapeutic progress. There are several mechanisms of neuronal injury that lead to the CNS damage in chronic MS (Figure 1.2) (Kapoor, 2006; Su *et al.*, 2009; Ciccarelli *et al.*, 2014):

Figure 1.2 Mechanisms of axonal damage in multiple sclerosis

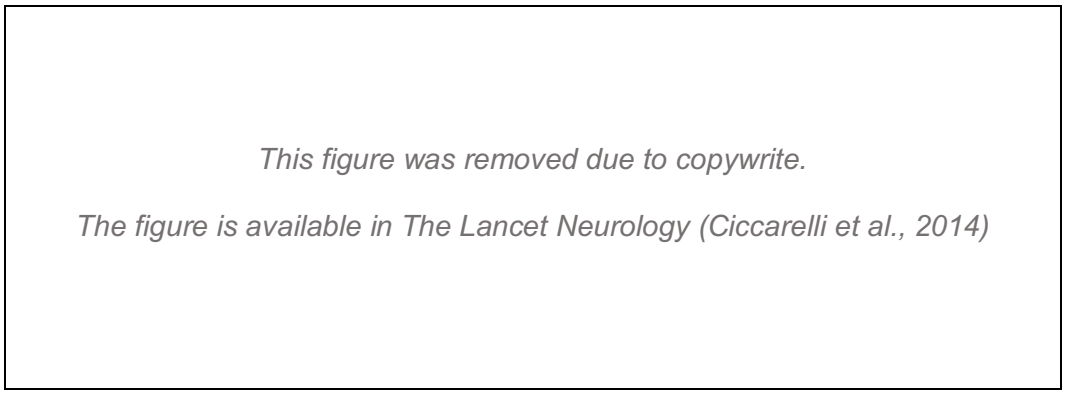

Adapted from Ciccarelli et a., Lancet Neurology 2014 (Ciccarelli *et al.*, 2014)

1. ***Direct neuronal damage.*** Neuronal cell bodies and axons may be damaged directly by the inflammatory process triggered by lymphocytes, particularly in axons that have lost their myelin sheath. Less is known about the mechanisms of injury to the grey matter, where microglial activation predominates over the lymphocytic response. This mechanism is present in the active and relapsing stage of the disease.

2. ***Loss of trophic support.*** Axons may degenerate once demyelination is established because a loss of myelin removes the trophic support provided by adjacent oligodendrocytes.

3. ***Mitochondrial dysfunction.*** In the denuded demyelinated axon, there is a redistribution of sodium (Na^+) channels, previously restricted to nodes of Ranvier. This electrophysiological adaptation induces an increased influx of Na^+ ions into the axon. In the attempt to restore a balanced intracytoplasmic Na^+ concentration, there are two main axonal mechanisms: 1) increasing the activity of the Na^+/calcium (Ca^{2+})

exchanger, which normally exchanges axoplasmic Ca^{2+} for extracellular Na^{+}; 2) increasing the activity of the Na^{+}/potassium (K^{+}) pump, which exchanges axoplasmic Na^{+} for extracellular K^{+}. According to the first mechanism, if the axonal Na^{+} rises above the concentration of approximately 20 mM, the Na^{+}/Ca^{2+} exchanger will start operating in the reverse mode (i.e. expelling sodium and introducing calcium) (Stys *et al.*, 1992). The second mechanism implies high consumption of energy in the form of ATP provided by mitochondria. In the context of inflammation, however, innate immune cells – especially macrophages and microglia – are stimulated to produce nitric oxide (NO) (Bogdan, 2001), which has inhibitory function on the mitochondrial respiration process (i.e. oxidative phosphorylation), reducing the overall production of ATP (Smith *et al.*, 2001; Waxman, 2006). This status of increased energy demand and a reduced ATP-producing capacity – called by some authors as "virtual hypoxia" - leads to deregulation of Ca^{2+} homeostasis. Chronic increases in axoplasmic Ca^{2+} concentrations depolymerise microtubules and activate proteases that fragment neurofilaments, alter the cell cytoskeletal structure and axonal transport, and eventually cause axonal degeneration and transection (Trapp *et al.*, 1998; Stys, 2004). Additional sources of intra-axonal Ca^{2+} are the endoplasmic reticulum and mitochondria, which normally stores this cation, Ca^{2+}-permeable cation channels, including the glutamate-gated receptors (Trapp and Stys, 2009), and activated acid-sensing ion channel (ASIC) 1A on the axon membrane (Friese *et al.*, 2007). The ASICs are activated in situations of prolonged acidity, which is obtained by persistent inflammation and neuronal energy deficit. Finally, some studies have raised the possibility that, in addition to extrinsic inhibitors of mitochondrial respiration, there may exist inherent genetic

defects in these organelles in MS that may further compromise energy-producing capacity (Dutta *et al.*, 2006).

4. ***Oxidative stress.*** This phenomenon occurs when the production of oxygen radical species exceeds the cellular antioxidant capacity leading to protein, lipid, and deoxyribonucleic acid (DNA) damage, with consequent cellular changes and cytotoxicity. In the CNS, reactive-oxygen species (ROS) are produced by activated microglia and macrophages, but also mitochondria (Su *et al.*, 2009). Macrophages and microglia produce large amounts of ROS and NO, which are used to disactivate phagocyted material, activate kinases, express transcription factors and genes (e.g. proinflammatory genes), or regulate proliferation and apoptosis (Bedard and Krause, 2007).

5. ***Excitotoxicity.*** Glutamate is an essential excitatory neurotransmitter that acts on specific receptors located on the post-synaptic membrane of neurons. Upon binding and activation of these receptors, ion channels open allowing cations like Na+, K+, and Ca^{2+} to enter the cell. Excess of glutamate in the synaptic space is regulated by astrocytes, oligodendrocytes, and microglia, which convert glutamate in glutamine that is taken by neurons and regenerated as glutamate. Glutamate excitotoxicity occurs when there is elevated release (or inadequate reuptake) of glutamate into the synaptic space. Activated immune cells such as macrophages and microglia produce large quantities of glutamate. The accumulation of glutamate overactivates signalling pathways, many of which causing the intracellular Ca^{2+} influx and concentration to increase. This increase in intracellular Ca^{2+} activates several enzymes including

phospholipases, endonucleases, and proteases, which damage DNA, disrupt the cytoskeleton, and alter membrane lipids (Trapp and Stys, 2009).

1.4 **Clinical phenotypes**

MS has a heterogeneous clinical course. In 80-85% of people developing MS, the initial course is characterised by the occurrence, recurrence, or worsening of neurologic symptoms (relapses) followed by a complete or partial recovery (i.e. RRMS) (Polman *et al.*, 2011). A clinically isolated syndrome (CIS) is often the first presentation of RRMS and it is characterised by a neurological clinical event suggestive of MS not fulfilling the current diagnostic criteria (Lublin *et al.*, 2014; Thompson *et al.*, 2017). In 10-15% of people with MS, the initial course is characterised by a steady progression of neurologic symptoms and a slow increase in disability over time (i.e. PPMS). Almost 60% of the patients with RRMS convert to a secondary progressive course (i.e. SPMS) after 15-20 years, and more than 80% after 25 years, from initial disease onset (Tremlett *et al.*, 2008; Scalfari *et al.*, 2010). SPMS is characterised by a gradual increase in disability over time, with or without superimposed relapses.

The accumulation of irreversible disability in patients with relapse-onset MS is driven by two separate processes: (i) relapses, where inflammatory demyelination results in permanent axonal injury with residual neurologic impairment; (ii) onset of SPMS. However, the change in disease course from relapsing to progressive MS is the major determinant of long-term disability in relapse-onset MS.

Definitions of the disease course of MS have been recently updated (Lublin *et al.*, 2014) and have included additional disease modifiers to better describe the different clinical phenotypes (Figure 1.3). Patients are classified as relapsing or

progressive with an additional descriptor of whether the disease is active or not. The terms ‘disease activity’ or ‘active disease’ are used to indicate the presence of ongoing inflammatory activity shown by clinical relapses or new, enlarging or contrast-enhancing MRI lesions (Lublin *et al.*, 2014; Scolding *et al.*, 2015). Patients with progressive MS are further classified based on whether the disease is clinically progressing or not progressing. Disease progression is defined as an objective increase in neurological disability, confirmed after 6-12 months (Lublin *et al.*, 2014).

Figure 1.3 MS phenotypes

This figure was removed due to copywrite.

The figure is available in Neurology, (Lublin et al., 2014)

Relapsing disease (left panel) and progressive disease (right panel) (adapted from Lublin et al., Neurology, 2014).(Lublin *et al.*, 2014)

An early and accurate diagnosis of MS and the degree of the disease activity are essential since many disease-modifying therapies that reduce relapses, accumulation of new MRI lesions and possibly delay disability progression are now available for RRMS. For progressive MS, ocrelizumab has recently been licenced for PPMS (Wingerchuk and Weinshenker, 2016; Montalban *et al.*, 2017; De Angelis *et al.*, 2018a). In March 2019, the U.S. Food and Drug Administration (FDA) approved siponimod for SPMS. In Europe, in November 2019, the European Medicines Agency (EMA) has recommended that a licence should be granted for siponimod for the treatment of active SPMS, defined as people experiencing relapses or showing signs of inflammation in MRI scans.

1.5 **The challenge of SPMS: definition and measurement**

There are no specific clinical or diagnostic criteria to determine the moment that RRMS converts to SPMS. Indeed, the disease course transition is usually gradual (Lublin *et al.*, 2014). As a consequence, the definition of progression, particularly in SPMS, is not straightforward and has been object of several debates.

In 1996, after an international survey, the definition of SPMS was standardised as an initial relapsing-remitting disease course followed by progression with or without occasional relapses, minor remissions and plateaus (Lublin and Reingold, 1996). In most clinical contexts, SPMS is diagnosed retrospectively by a history of many years of gradual worsening after an initial relapsing disease course, with or without acute exacerbations during the progressive course. The word “progression” denotes the continuous worsening of neurological impairment, independent of relapses, over a fixed period of time (Confavreux *et al.*, 1992). Many studies have used the term “sustained worsening” – rather than “progression” - as a clinical trial outcome, referring to a worsening of the Expanded Disability Status Scale (EDSS) score that persists for a specified period of time (usually 3 or 6 months) (Rudick and Kappos, 2010). Other studies, instead, have shown that improvement in EDSS scores after relapses continues beyond 3 months in a substantial proportion of patients, which suggests that confirmation of worsening by assessment at 6 months would indicate long-term accrual of disability more reliably than confirmation at 3 months (Lublin *et al.*, 2003). Clinical progression is not uniform, but may plateau and be characterised by periods of relative stability (Lublin *et al.*, 2014).

As far as disease progression is concerned, it is important to note that distinguishing between SPMS and PPMS is often difficult. Clinical, natural history

studies, imaging, and genetic data suggest that PPMS is a part of the spectrum of progressive MS phenotypes and that any differences between SPMS and PPMS are relative rather than absolute. Nevertheless, it is still recommended to consider PPMS as a separate course from SPMS, because of the absence of exacerbations prior to clinical progression (Lublin *et al.*, 2014).

More recently, Lorschreider and colleagues have attempted to provide a standardised objective definition of SPMS. Using MSBase, a large, prospectively acquired, global cohort study, these authors analysed the accuracy of 576 data-derived onset definitions for SPMS, from which they extracted the five best performing definitions that were further investigated in a total of 17,356 patients. The best definition included a 3-strata progression magnitude in the absence of a relapse, confirmed after 3 months within the leading Functional System and required an Expanded Disability Status Scale step ≥4 and pyramidal score ≥2. If applied broadly, this new definition of SPMS has the potential to strengthen the design and improve comparability of clinical trials and observational studies in SPMS (Lorscheider *et al.*, 2016).

Definition apart, investigating new drugs in progressive MS presents many other challenges (Khan, 2007; Ontaneda *et al.*, 2015; Plantone *et al.*, 2016). Firstly, trial participants should have homogeneous features in order to reduce confounders due to clinical variability (e.g. mixing patients with PPMS and SPMS). Secondly, participants should have a confirmed pre-enrolment disability progression rate (the minimum time required goes from 6 to 18 months in most of the trials) independent of relapses. Thirdly, trials should be appropriately designed with the choice of outcomes that are adequate to measure the planned endpoints within the trial timeframe. Ideal outcome measures should be easily reproducible and sensitive to change in a relatively short time. Additionally, they should be able to reflect the

pathology causing irreversible physical disability typical of disease progression (i.e. neuro-axonal damage and loss). Finally, drop outs in progressive MS trials is frequent, due to the natural clinical decline of patients; however, to reach statistical power, retention of participants should be monitored and constantly encouraged.

The design of modern clinical trials in progressive MS with 1–3-year follow-up infers long-term irreversible disability outcomes from short-term confirmed progression events. However, assessment of disability outcomes in MS therapeutic trials is a complex task due to high individual and time-dependent variability (Kalincik *et al.*, 2015). Several clinical, imaging and laboratory outcome measures alone or in combinations have been used in clinical trials for progressive MS. Outcome measures vary also according to the phase of the trial. Indeed, the focus of trials on progressive MS is evaluating disease progression directly, using clinical measures, or indirectly, using laboratory or imaging measures. The former approach is commonly used in phase III clinical trials, which are able to detect significant changes of neurologic disability in a short-period of time thank to the high number of participants enrolled. The latter approach is typical of phase II studies, where the evaluation time is short and the number of participants is low. Finding surrogate biomarkers of disability is relevant, as phase II investigations are proof of concept studies able to detect, in a very early stage, the potential efficacy of a drug providing the rationale for larger phase III trials.

In the following section, I will give an overview of the most commonly used outcome measures to assess disease progression (and indirectly neurodegeneration) in MS, which for simplicity can be divided into: clinician and patient-reported measures; imaging measures, such as MRI and optical coherence tomography (OCT); laboratory measures, such as CSF and serum biomarkers.

1.5.1 Clinician and patient-reported measures

Clinical measures of disability progression are generally used as primary outcome measures in phase III trials. Outcomes related to disability progression can be classified into five groups: metrics that quantify progression as a continuous phenomenon; metrics that consider progression as a binary phenomenon, such as the proportion of patients with or without confirmed disability progression (CDP); metrics that quantify confirmed improvement in disability as a binary phenomenon; metrics that quantify the time to CDP; and composite outcome measures (Tur *et al.*, 2018).

The Kurtzke Functional System (FS) and EDSS remain by far the most widely used clinical scoring system in MS for both clinical and research purposes. The EDSS is an ordinal, nonlinear scale that explores eight FS (visual, brainstem, pyramidal, cerebellar, sensory, bowel and bladder, cerebral and other functions), by scoring the level of impairment of each of them. The results of the ratings from each FS are combined with the measured walking distance and independence with activities of daily living and a final score from 0 to 10 is given with higher scores indicating more severe disability (Figure 1.4). However, the scale is heavily weighted towards motor and lower limb functions, which leads to a decreased sensitivity for detecting more subtle forms of disease progression, like progression of bladder, cognitive or upper limbs impairment (Kurtzke, 1983; Amato and Ponziani, 1999). Moreover, this scale has also shown a high intra and inter-observer variability, being based on the standard neurological examination which is inherently subjective and based on vague definitions of what qualifies disability as mild, moderate or severe. The known lack of sensitivity to change of the EDSS may account in part for the apparent lack of effect on the EDSS score despite

treatment benefits on other outcome measures in some phase II clinical trial (Cohen *et al.*, 2002). An independent platform for training and certification of the EDSS has been recently developed with the purpose of standardising the neurological examination and improving the scale's reliability ('Neurostatus.net', n.d.).

Figure 1.4 Expanded Disability Status Scale score and ambulation score

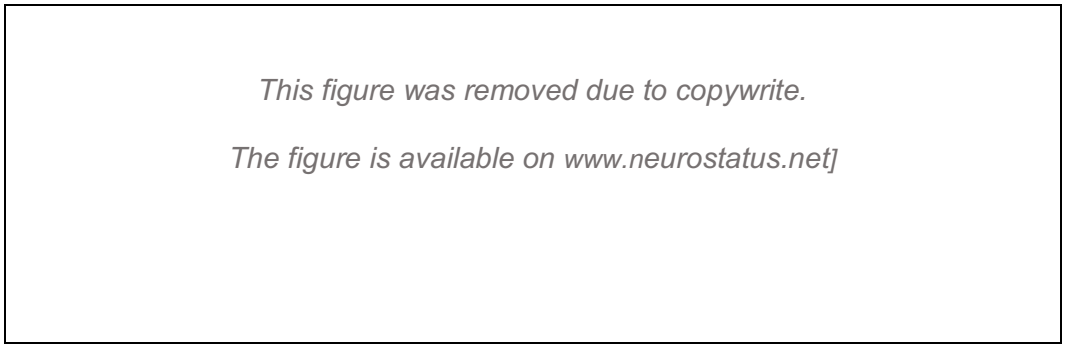

Adapted from Neurostatus.net.

To address the insensitivity and poor reliability of the EDSS, the National MS Society's Clinical Outcomes Assessment Task Force recommended an alternative outcome measure for clinical trials, the MS functional composite (MSFC) (Whitaker *et al.*, 1995; Rudick *et al.*, 1997). This is a composite score characterised by three components: walking speed (timed 25-foot walk [T25FW]), arm function (9-hole per test [9HPT]), and cognition (paced auditory serial addition test - 3 seconds [PASAT]) (Cutter *et al.*, 1999; Fischer *et al.*, 1999) (Figure 1.5). The PASAT assesses auditory information processing speed, which is one of the main cognitive domains affected in MS. The three components of the MSFC are partially independent of each other and correlate to a similar extent with the composite

score. Because the components differ in direction of change (deterioration indicated by higher scores on the 9HPT and T25FW vs lower scores on the PASAT) and units of measurement (time vs number correct), the MSFC composite score is reported as a Z-score that is computed from individual Z-scores for each component. Lower MSFC scores compared with baseline or prior measurements indicate neurologic deterioration. A Z-score is a standardized score that compares a patient's performance with that of a reference population. Z-scores are the number of standard deviations between scores for the individual and the reference population. The reference population used to create Z-scores can be derived from a standard MS population such as the pooled dataset used to develop the MSFC, the entry scores from patients enrolled in a particular study, or healthy controls. The choice of the reference population (e.g., patients with MS vs healthy controls) will influence weighting of the individual components (Polman and Rudick, 2010). The MSFC has a good inter-rater variability and the administration is very easy. However, a major concern with this method is the unknown clinical meaning of a change in the Z-score with respect to a patient's actual function in the three domains tested. Additionally, comparisons are difficult between Z-scores across studies because they are based on different reference populations. Moreover, the PASAT has been criticised by clinical trialists because of practise effects and patient frustration with the test. Moreover, the MSFC does not include measures of visual function, which is often impaired in MS. Therefore, it has been proposed to substitute the PASAT with other cognitive measure, e.g. the symbol digit modalities test (SDMT), and to include a measure of visual function, such as the Sloan low-contrast visual acuity (SLCVA) measures (Brochet *et al.*, 2008).

Figure 1.5 Multiple Sclerosis Functional Composite subcomponents

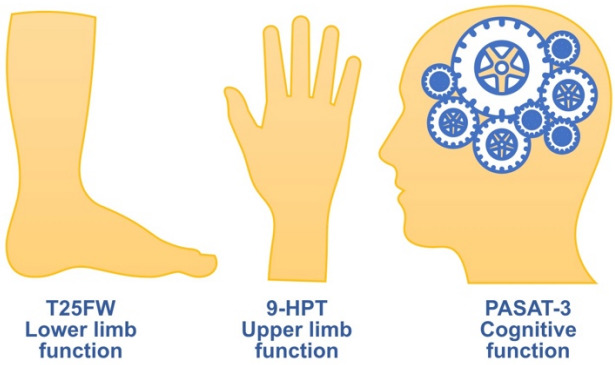

9-HPT: 9-hole peg test. PASAT-3: paced auditory serial addition test 3 seconds. T25FW: timed-25-foot walk test.

SLCVA letter charts have been investigated as possible additional outcome measures in MS, as these were shown to be sensitive to visual impairment even amongst patients with Snellen acuities of 20/20 or better. SLCVA letter charts have a standardised format based on the Early Treatment Diabetic Retinopathy Study (ETDRS) visual acuity charts, the standard used in ophthalmology clinical trials, and have several advantages over standard Snellen charts or near vision testing cards as traditionally used in MS trials: (i) SLCVA letter charts are designed to be equally detectable for normal observers; (ii) each line has an equal number of 5 letters; (iii) spacing between letters and lines is proportional to the letter size; (iv) change in visual acuity from one line to another occurs in equal logarithmic steps; (v) visual acuity for high-contrast may be specified by Snellen notation for descriptive purposes by the number of letters identified correctly (Balcer *et al.*, 2003, 2015). The SLCVA letter will be discussed further in Chapter 7.

In terms of cognitive function, the Rao brief repeatable neuropsychological battery (BRNB) and the minimal assessment of cognitive function in MS (MACFIMS) represent the most used and validated cognitive assessments in MS patients. The Brief International Assessment of Cognition for MS (BICAMS) (Langdon *et al.*,

2012) is a further battery of tests optimised for small centres that is getting more and more popular due to its simple administration. The SDMT (Smith A, 1982) is a test that can stand alone or be included in the neurocognitive batteries to assess visual processing speed and working memory. It has shown a sensitivity of 82% and a specificity of 60% for the assessment of information processing speed (Parmenter *et al.*, 2007). Furthermore, Van Schependom and co-workers have shown that the SDMT is an easy, low-cost and fast test useful to detect cognitive impairment in everyday clinical practice (Van Schependom *et al.*, 2014).

Patient-reported outcome measures (PROMs) are assuming an increasingly important role in clinical trials, and MS-specific measures have been developed, such as the MS quality-of-life questionnaire (MSQoL-54), the functional assessment of MS (FAMS), and the MS impact scale (MSIS-29v2) (Hobart *et al.*, 2001; Hobart and Cano, 2009). These multidimensional scales measure several domains, such as health distress, sexual function, overall quality of life, cognitive function, energy, pain, walking, sleep quality, fatigue, and social function. However, patient-reported outcomes can also focus on single domains, such as ambulation (MS walking scale-12), depression (Beck depression inventory and patient health questionnaire-9), or fatigue (modified fatigue impact scale) (Cohen *et al.*, 2012b).

The MSIS-29, currently version 2 (MSIS-29v2) consists of 29 items: 20 related to the physical impact of MS and 9 related to the psychological impact of MS. Each question is scored from 1 to 4 with higher scores denoting greater impact on life, giving score ranging 20–80 for the physical impact and 9–36 for the psychological impact (Hobart and Cano, 2009). The psychometric properties of the MSIS-29 have shown strong internal consistency, reproducibility and satisfaction of scaling assumptions for both components (Riazi *et al.*, 2002) and the scale has been

suggested as a valuable outcome measure in intervention studies of patients with MS (McGuigan and Hutchinson, 2004).

1.5.2 Imaging measures

Amongst the imaging measures widely used in MS trials, MRI and, more recently, OCT are becoming more and more popular. In this Chapter, I will focus on the description of MRI outcome measures for progressive MS trials. OCT imaging, instead, will be extensively discussed in Chapter 7.

MRI is divided into structural and functional techniques. Structural MRI, commonly used in research and clinical practice, can help to quantify two main phenomena in MS (Filippi *et al.*, 2014):

1) Active Inflammation, usually measured by the counting of new or enlarged T2 white matter lesions and gadolinium-enhancing lesions that reflect disease activity.
2) Neurodegeneration, usually measured by calculating whole or regional brain volume changes over time (atrophy) that is believed to reflect irreversible tissue damage.

Quantitative MRI measures have been extensively used as primary outcomes in RRMS phase III trials due to their sensitivity to disease activity (Barkhof *et al.*, 1997; Miller *et al.*, 2003; Kappos *et al.*, 2006; Polman *et al.*, 2006; Cohen *et al.*, 2010). Following the example of trials in RRMS, MRI has been considered as a reasonable primary outcome for phase II trials in progressive MS.

In progressive MS, the main MRI metric used to investigate neurodegeneration is the change (reduction) in brain volume, defined as “brain atrophy”. Studies of atrophy in clinically stable and untreated MS patients have shown that brain volume loss occurs at a rate of about 0.5–1% per year compared with 0.1–0.3% in healthy controls (Miller *et al.*, 2002a). Even though a decrease in brain volume is seen at all stages of MS, it is particularly pronounced in SPMS (Losseff *et al.*, 1996a; Kalkers *et al.*, 2001; Fisher *et al.*, 2008; De Stefano *et al.*, 2010). Neuroaxonal tissue constitutes a large proportion of brain volume (Miller *et al.*, 2002b) and the increased rate of brain atrophy has been interpreted as evidence for ongoing neuroaxonal loss (Figure 1.6). Moreover, brain atrophy significantly correlates with disability and cognitive impairment in MS (Bermel and Bakshi, 2006). Hence, the rationale in using MRI-derived atrophy metrics as surrogate of disability and prognostic predictors in MS trials (Filippi *et al.*, 2014).

Figure 1.6 MRI showing brain atrophy in secondary progressive multiple sclerosis

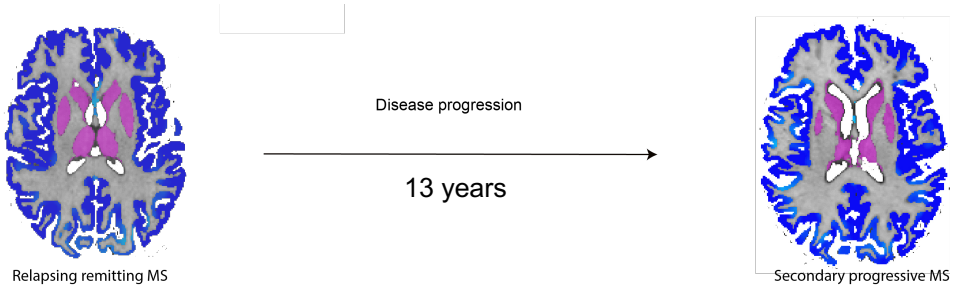

The figure shows MRI-derived brain atrophy occurring in a real patient with relapsing-remitting MS (left brain scan), who developed secondary progressive MS (right brain scan) after 13 years. The cortical grey matter is shown in blue, and the deep grey matter is shown in purple. *Courtesy of Arman Eshaghi.*

Different approaches have been developed to quantify brain volume and atrophy, which can be divided into “segmentation-based” and “registration-based” techniques, used to measure brain volume cross-sectionally or longitudinally respectively (De Stefano *et al.*, 2014; Plantone *et al.*, 2016). Cross-sectional methods (e.g. Structural Image Evaluation using Normalization of Atrophy Cross-

sectional [SIENAX], brain parenchymal fraction [BPF], Geodesical Information Flows [GIF]) estimate brain volume at a particular time point using a single MRI scan. Longitudinal methods (e.g. Structural Image Evaluation using Normalization of Atrophy [SIENA], Brain Boundary Shift Integral [BBSI]) calculate change in brain volume over time by comparing MRI scans acquired at two different time points. Some cross-sectional methods (e.g. BPF) can also be applied in longitudinal studies to measure brain volume changes over time. These methods work in a fully- or semi-automated way and can estimate whole or regional brain volumes or both. BPF and SIENA are the best-studied and most frequently used methods to measure brain volume in MS trials (Barkhof *et al.*, 2009).

In recent years, as previously reviewed, there has been increasing recognition of the importance of grey matter damage in MS. Clinically, the burden of grey matter damage is of extreme relevance. Indeed, grey matter atrophy – and particularly deep grey matter and thalamus atrophy - in the brains of patients with MS is associated with cognitive impairment (Nocentini et al., 2014; Riccitelli et al., 2011), cognitive and clinical decline (Bermel et al., 2003; Houtchens et al., 2007; Pagani et al., 2005). Grey matter can be assessed in vivo by using imaging acquired with quantitative MRI techniques. The volume of grey matter tissue is lower in MS patients compared with healthy subjects and quantification of grey matter atrophy represents a good potential outcome measure of clinical trials in progressive MS. Fisniku and colleagues demonstrated that, relative to the white matter, grey matter atrophy is more abundant and more clinically significant in progressive compared with relapsing disease (Fisniku *et al.*, 2008). Fisher et al showed that grey matter fraction change was 14-fold greater in SPMS than in healthy controls, and that the grey matter atrophy rates in SPMS patients was significantly greater than grey matter atrophy rate in healthy control subjects ($p = 0.005$) (Fisher *et al.*, 2008).

Most of the MRI analysis methods provide grey matter volume of regional areas from the brain, which have been used to predict disease worsening and stratify patients (Nourbakhsh *et al.*, 2016; Azevedo *et al.*, 2018; Eshaghi *et al.*, 2018b).

Amongst the disadvantage of MRI measures of disability, it is important to mention that longitudinal MRI-based brain volume measures are useful to detect changes at the group level and, therefore, can be used in clinical trials; however, their application at the individual level is not proven and currently they cannot be used in clinical practice (Barkhof, 2016). Indeed, many factors, such as physiological variability in brain volumes (Franke *et al.*, 2015; Nakamura *et al.*, 2015) motion artefacts (Reuter *et al.*, 2015) or technical features between different scanners or scanner upgrades (Takao *et al.*, 2011; Keshavan *et al.*, 2016) make the longitudinal brain volume measures not reliable at the individual level. Furthermore, some of the methods used to calculate brain volumes need manual lesion masking in order to correctly classify lesions as white matter. One more problem to consider when drug trials are designed is to account for a temporary loss of brain volume that can happen as a consequence of drug treatment, as shown by Zivadinov and colleagues in the early phase of treatment following administration of steroids (Zivadinov *et al.*, 2008) or disease-modifying drugs like interferon-beta-1a and natalizumab. Such an acute reduction of brain volume is likely to reflect the resolution of inflammation-associated oedema, a phenomenon described as “pseudoatrophy”. This suggests that, at least for some treatments, quantification of brain atrophy might not be the ideal outcome measure of treatment response in studies of short duration (1 year or less), and that the contribution of pseudoatrophy should be measured to reduced bias. An example of pseudoatrophy is shown in the phase II trial of lamotrigine versus placebo in patients with SPMS. Lamotrigine treatment was unexpectedly found to be

associated with greater annual cerebral volume loss in the first year compared with placebo (Kapoor *et al.*, 2010).

CNS damage in MS does not involve only the brain, but also the spinal cord. Focal spinal cord lesions are commonly seen in patients with MS – reported in in 80–90% of patients - and much of the locomotor disability that occurs in MS patients is attributable to spinal cord involvement (Kearney *et al.*, 2015b). However, the MRI of the spinal cord is challenging due to its own morphology and anatomical location, which lead to many artefacts due to breathing, cardiac rhythm, CSF flow, and aortic flow. New coil technology and scanners with magnetic high field strength have improved conventional and quantitative MRI techniques, which have gained better image resolution and signal-to-noise ratio, making spinal cord imaging more reliable (Gass *et al.*, 2015).

Studies on diverse cohorts of patients with MS have shown that, in MS, atrophy is more pronounced in the cervical segments of the spinal cord and that the atrophy is more pronounced in the progressive sub-types (Evangelou *et al.*, 2005; Klein *et al.*, 2011; Kearney *et al.*, 2015b). A popular method to estimate spinal cord atrophy is to measure the change in spinal cord area – commonly measured as cross-sectional areas in the cervical region in the area from C2 to C5 – between two time point MRI scans (Kearney *et al.*, 2015b). A more detailed description of spinal cord atrophy measures in SPMS is provided in Chapter 6.

Quantitative non-conventional MRI techniques are being investigated in clinical trials in MS as they can provide additional information to the traditional measures and are regarded as potential biomarkers of the disease evolution.

Magnetization transfer ratio (MTR) is an MRI measure that strongly reflects the amount of myelin in the brain, but can also be influenced by inflammation and axonal density. MTR is based on the interactions between protons in a free environment and motional restricted protons that are bound to macromolecules. With an off -resonance radiofrequency pulse, the magnetisation of bound protons is saturated and transferred to the mobile protons, thus reducing the signal intensity of the observable magnetisation. Since in the CNS the bound protons are mainly associated with myelin lipids and proteins, the amount of signal decrease is thought to suggest damage to myelin or to the axonal membranes. The measure provides an indication of the extent of axonal loss associated with new inflammatory-demyelinating white matter lesions. Decreased in MTR prior to the appearance of a white matter lesion on T2-weighted MRI or gadolinium-enhanced T1-wighted MRI suggests early myelin pathology not detectable by conventional MRI. The evolution of MTR within new lesions varies from lesion to lesion: mean lesional MTR may recover over 1–5 months, suggesting remyelination; or, it may remain low, or decrease further, suggesting on-going demyelination. MTR of non-lesional brain tissue, which predicts disability progression, has also been found to be abnormally low in MS patients, in both normal-appearing white and grey matter. MTR has provided many insights regarding the evolution of demyelination and remyelination and may be useful in measuring the potential benefit of remyelinating and neuroprotective therapies (Fox *et al.*, 2011).

Other quantitative MRI measures include magnetic resonance spectroscopy (MRS) and diffusion tensor imaging (DTI).

MRS is able to detect and quantify different metabolites in the CNS, and has been widely studied in MS. N-acetyl aspartate (synthesised in the neurons within the mitochondria), myoinositol (a glial metabolite), glutamate (a neurotransmitter

inducing excitotoxicity), creatine (a marker of gliosis) and choline (a marker of membrane phospholipids, highly suggestive of ongoing inflammation when elevated) can be quantified with MRS and can improve the specificity for the pathological processes. Although the longitudinal studies in SPMS patients and the application of MRS in SPMS clinical trials are still under review, guidelines for using MRS in multicentre clinical MS studies have been developed (Plantone *et al.*, 2016).

DTI can quantitatively detect brain microstructural changes by calculating parameters such as mean diffusivity, which is determined by the overall water motion and fractional anisotropy that reflects the uniformity of the direction of the diffusion of water molecules. DTI measures may be considered as markers of demyelination and axonal loss (Sbardella *et al.*, 2013).

Further emerging MRI techniques are based on physiopathological findings about mitochondrial function and the redistribution of sodium channels in demyelinated axons, which are now regarded as two key processes in neurodegeneration in MS. These processes induce a modification of sodium content in the CNS, which can be studied with a relatively recent MRI technique called sodium (^{23}Na) MRI. Demyelinating lesions, normal-appearing white matter and grey matter in MS all have higher concentrations of sodium and there is correlation with clinical disability, supporting its application as a future possible outcome measure in SPMS trials (Inglese *et al.*, 2010; Paling *et al.*, 2013).

1.5.3 Animal models of MS

Although experimental autoimmune encephalomyelitis (EAE) is commonly studied as an animal model of MS, there is no perfect animal model of the human disorder.

Using direct human tissues is challenging because brain tissue is rarely biopsied in patients with MS, and because the time lag between death and removal of tissue for post-mortem study - usually a few hours - limits the molecular analysis.

Actively induced EAE in rodents is achieved through a subcutaneous immunisation with a myelin-related antigen. Therefore, EAE can be considered as an autoimmune disease, whilst MS is an immune-mediated disease, since the antigens of the immune response have not been found (Bjelobaba *et al.*, 2018).

Although acute and relapsing-remitting forms of EAE, which are T cell dependent, are accepted to represent relapsing-remitting phases of MS, most of the treatments later on used in people with RRMS that showed efficacy in suppressing EAE in rodents were found to be ineffective or even dangerous (e.g. anti-TNF-alpha) in MS (Batoulis *et al.*, 2014; Kemanetzoglou and Andreadou, 2017). Whether animal models of MS are helpful to test drugs that work on humans, especially in progressive MS, is currently matter of debate (Fox *et al.*, 2012). This is because animal models of MS give only limited insight into the pathophysiology of the disease, especially of progressive MS (Kipp *et al.*, 2017). Although EAE models, such are the secondary progressive (chronic) EAE stage in Biozzi ABH mice, represent the progressive phase of MS better, they can only provide a partial explanation of SPMS from a pathological perspective (Hampton *et al.*, 2008). In the absence of better experimental models of progressive MS, EAE in rodents is still the most widely animal model in use.

1.6 **Treatment and clinical trials in progressive MS**

The therapeutic approach to MS aims at: (i) managing relapses; (ii) treating residual symptoms of disability; (iii) preventing the occurrence of relapses and new CNS inflammatory lesions; (iv) delaying or preventing disability accrual. The management of relapses is based on steroids and physiotherapy, as appropriate (Galea *et al.*, 2015). Many symptomatic non-MS specific therapies are in use for the management of MS-related residual symptoms such as overactive bladder, spasticity, and neuropathic pain. The prevention of exacerbations, new lesion accumulation, and disability is treated using disease-modifying therapies, which are MS-specific. During the past two decades, findings in the pathophysiology of MS have been translated into new therapeutics that mainly target the immune system centred on RRMS. Glatiramer acetate and betainterferons represent the first-generation of disease-modifying therapies in MS, followed by a second-generation of drugs initiated by natalizumab and fingolimod. Further agents such as teriflunomide, alemtuzumab, dimethyl fumarate, ocrelizumab and cladribine have been approved for RRMS by the principal regulatory agencies (Figure 1.7) in Europe and the USA (Wingerchuk and Weinshenker, 2016; De Angelis *et al.*, 2018a). Ocrelizumab is also approved for PPMS. Interferon beta-1b and mitoxantrone have indication for relapsing SPMS; however, the role of these two drugs in SPMS is unclear and clinical trials have shown contradictory results ('Managing multiple sclerosis - NICE Pathways', n.d.; European Study Group on interferon beta-1b in secondary progressive MS., 1998; Panitch *et al.*, 2004; Edan *et al.*, 2011). Indeed, the immunomodulatory and immunosuppressive strategies derived from RRMS have proven no or limited efficacy when extended into SPMS and it has been postulated that Disease-modifying therapies should be used early in the course of the disease to delay or prevent the disease progression (Coles *et al.*, 2006). Siponimod has been recently approved by the FDA for relapsing MS, including relapsing SPMS.

Figure 1.7 Timeline of approval of disease-modifying therapies for multiple sclerosis

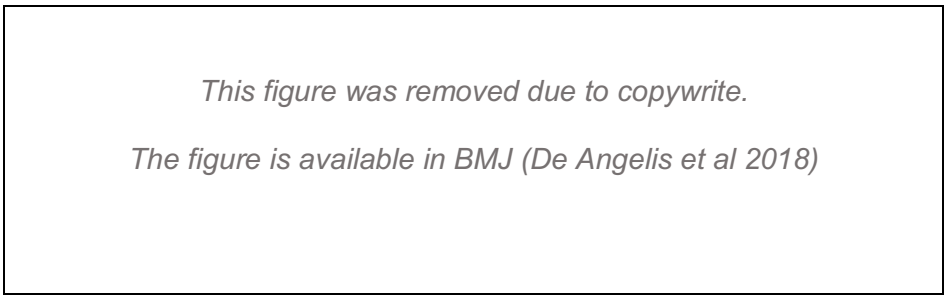

The figure shows drugs approved by the Food and Drug administration (FDA) (top) and the European Medicines Agencies (EMA) (bottom). *Adapted from De Angelis et al. BMJ 2018.* Additionally, in March 2019, the FDA has approved Siponimod for the treatment of relapsing-MS and SPMS. Siponimod is currently being reviewed by the EMA.

To date, there are no disease-modifying therapies that are efficacious in stopping the disease progression in SPMS and there is an urgent need to treat SPMS and, according to the current theories, stopping neuroaxonal loss may improve SPMS prognosis. There are three possible pharmacological approaches that are being pursued in clinical trials in SPMS (De Angelis *et al.*, 2018b): immune-modulation neuroprotection and remyelination (or reparative). Neuroprotective drugs would be able to decrease the neuroaxonal loss preventing oligodendrocyte and axonal degeneration (Figure 1.8). Several drugs with putative neuroprotective properties have been investigated in phase II trials (e.g. simvastatin, lipoid acid, ibudilast) and attempted in a phase III study (i.e. dronabinol). Natalizumab, fingolimod and siponimod, which notoriously are immune-modulatory agents, have been investigated in progressive MS as experimental evidence suggested they might have additional neuroprotective properties.

In the following sections, I will summarise the most relevant phase III and phase II trials reported so far in progressive MS. Thereafter, I will give an overview of agents currently under investigation. Finally, I will discuss future strategies for drug discovery in SPMS.

Figure 1.8 Phases of relapsing multiple sclerosis and pharmacological agents

This figure was removed due to copywrite.

The figure is available on www.clevelandclinicmeded.com

(Hersh CM and Fox RJ, 2018)

Adapted from Multiple Sclerosis, Disease Management website, Cleveland Clinic.

1.6.1 Phase III trial in progressive MS

All of the phase III trial in SPMS have shown negative results, with the exception of the SPECTRIMS and MIMS trials and the recently reported EXPAND study (Kappos *et al.*, 2018). Studies investigating betainterferon in SPMS, such as the European and North American trials, have found opposite results (European Study Group on interferon beta-1b in secondary progressive MS., 1998; Secondary Progressive Efficacy Clinical Trial of Recombinant Interferon-beta-1a in MS (SPECTRIMS) Study Group, 2001; Panitch *et al.*, 2004), with the European study being positive and the North American negative. It has been hypothesised that the discrepant findings were due to differences in study populations. In fact, subjects in the European study were younger with a shorter duration of disease and higher pre- and on-study relapse rates. Furthermore, the IMPACT (Cohen *et al.*, 2002) study of interferon-beta in SPMS showed beneficial effects on the MSFC, but this effect was driven mainly by the 9HPT and PASAT as no benefit was for the T25FW and EDSS. The MIMS trial investigating mitoxantrone in SPMS showed positive results; however, its effect was mostly attributed to anti-inflammatory properties. Moreover, mitoxantrone causes toxicity and increased risk of malignancy and is no longer recommended (Cocco and Marrosu, 2014), although it can still find

indication in specific cases (Edan *et al.*, 2011; Le Page *et al.*, 2011; Edan and Le Page, 2013).

Table 1.2 shows the phase III trials that have been reported so far in progressive MS over the past 30 years. Most of them have not met their primary endpoints (Ontaneda *et al.*, 2015; De Angelis *et al.*, 2018b).

Table 1.2 Reported phase III trials in progressive multiple sclerosis

Trial	Year	Drug	MS course	Size	Primary outcome	Results
British and Dutch MS Azathioprine Group (Group, 1988)	1988	Azathioprine	Any MS (19% SPMS; 14% PPMS)	354	EDSS Ambulation	Negative
Cyclosporine MS Study Group ('The Multiple Sclerosis Study Group.', 1990)	1990	Cyclosporine	PMS	547	EDSS	Positive but modest clinical benefit.
Canadian Cooperative MS Study Group (' The Canadian Cooperative Multiple Sclerosis Study Group.', 1991)	1991	Cyclophosphamide	PMS	168	EDSS	Negative
Mayo Clinic-Canadian Cooperative Trial (Noseworthy *et al.*, 1998)	1998	Sulfasalazine	Any MS (11% SPMS; 13% PPMS)	199	EDSS	Negative
European Study Group on interferon beta-1b in SPMS (European Study Group on interferon beta-1b in secondary progressive MS., 1998)	1998	Interferon beta-1b	SPMS	718	EDSS	Positive
North American Linomide Investigators; (Noseworthy *et al.*, 2000)	2000	Linomide (Roquinimex)	SPMS&RRMS (87% SPMS)	715	EDSS	Early termination (serious adverse events).
Cladribine and progressive MS (Rice *et al.*, 2000)	2000	Cladribine	PMS (70% SPMS)	159	EDSS	Negative
SPECTRIMS (Secondary Progressive Efficacy Clinical Trial of Recombinant Interferon-beta-1a in MS (SPECTRIMS) Study Group, 2001)	2001	Interferon beta-1a	SPMS	618	EDSS	Negative
IMPACT (Cohen *et al.*, 2002)	2002	Interferon beta-1a	SPMS	436	MSFC	Negative but MSFC showed no worsening.
***Mitoxantrone in progressive MS* (Hartung *et al.*, 2002)**	2002	Mitoxantrone	SPMS&RRMS (50% SPMS)	194	EDSS Ambulation Relapses	Positive
Subcutaneous Interferon beta (Andersen *et al.*, 2004)	2004	Interferon beta–1a	SPMS	371	EDSS	Negative

North American Study Group on Interferon beta-1b in SPMS (Panitch *et al.*, 2004)	2004	Interferon beta-1b	SPMS	939	EDSS	Negative
European Study on Immunoglobulin in MS trialists;	2004	Immunoglobulin	SPMS	318	EDSS	Negative
Intravenous immunoglobulin in progressive MS (Pöhlau *et al.*, 2007)	2007	Immunoglobulin	PMS (85% SPMS)	231	EDSS	Positive for PPMS. Negative for SPMS.
PROMiSE (Wolinsky *et al.*, 2007)	2007	Glatiramer acetate	PPMS	943	EDSS	Early termination (lack of efficacy)
OLYMPUS (Hawker *et al.*, 2009)	2009	Rituximab	PPMS	439	EDSS	Negative but subgroup analyses suggested positive effect for younger patients, with active disease.
MAESTRO (Freedman *et al.*, 2011)	2011	Myelin basic protein 8298 (Dirucotide)	SPMS (with HLA-DR2 or DR4 positive)	612	EDSS	Negative
CUPID (Zajicek *et al.*, 2013)	2013	Dronabinol	PMS (61% SPMS)	498	EDSS MSIS-29	Negative
PROMESS (Brochet et al., 2017)	2012	Methylprednisolone vs Cyclophosphamide	SPMS	138	EDSS	Cyclophosphamide more effective than methylprednisolone at reducing progression but both were poorly tolerated
INFORMS (Lublin et al., 2016)	2014	Fingolimod	PPMS	969	EDSS T25FW 9HPT	Negative
MS-SPI (Tourbah et al., 2016)	2015*	Biotin (MD 1003)	SPMS&PPMS (41% SPMS)	154	EDSS T25FW	Positive
ASCEND (Kapoor *et al.*, 2018)	2015	Natalizumab	SPMS	889	EDSS T25FW 9HPT	Negative
SUPREMES Phase II/III (NCT00799890)	2016	Sunphenon EGCG (Epigallocatechin-Gallat, EGCG)	PMS	60	BVC	Results not reported
ORATORIO (Montalban et al., 2017)	2017	Ocrelizumab	PPMS	732	EDSS	Positive
EXPAND (Kappos et al., 2018)	2017#	Siponimod	SPMS	1651	EDSS	Positive

Abbreviations: 9HPT: 9-hole peg test; BVC: brain volume change. EDSS: expanded disability status scale; HLA: Human Leukocyte Antigen; MSFC: multiple sclerosis functional composite; MS: multiple sclerosis; MSIS-29v2: multiple sclerosis impact scale 29 items version 2; PMS: progressive multiple sclerosis; PPMS: primary progressive multiple sclerosis; RRMS: relapsing-remitting multiple sclerosis; SPMS: secondary progressive multiple sclerosis; T25FW: timed 25-foot walk.
*This is the only trial that looked at improvement rather than worsening of EDSS.
Extension phase ongoing.
(clinical trials have been searched on https://clinicaltrials.gov).

The most relevant results from phase III trials of the past 15 years come from two trials, ORATORIO and EXPAND, which tested ocrelizumab in PPMS and siponimod in SPMS respectively. The story of the development of ocrelizumab – a humanised anti-CD20 monoclonal antibody - is interesting, as it shows why proof-of-concept studies can be useful and how we can learn from negative trials. In 2008, the phase II HERMES trial found that rituximab - a B-cell–depleting chimeric

anti-CD20 monoclonal antibody – significantly reduced the number of gadolinium-enhancing lesions and relapses in RRMS when compared to placebo (Hauser *et al.*, 2008). These findings changed the traditional view of the MS pathophysiology as an inflammatory disorder principally mediated by T cells. Rituximab was later on investigated in the phase III trial in PPMS, the OLYMPUS (Hawker *et al.*, 2009) study, which reported negative results. Nevertheless, in a subgroup analysis of younger patients with active inflammatory lesions, the OLYMPUS investigators found that the selective B-cell depletion obtained with rituximab could reduce disease progression. Based on this last finding, other researchers developed ocrelizumab, pharmacologically similar to rituximab, and tested it in the ORATORIO study (Montalban et al., 2017), recruiting a population with less than 55 years of age[1], evidence of CSF IgG oligoclonal bands, and disease duration no longer than 10 or 15 years according to EDSS. Ocrelizumab showed a relative risk reduction of 24% vs. placebo of 12-week confirmed disability progression as measured by EDSS.

Similarly, the results of the EXPAND trial (Kappos *et al.*, 2018) suggest that younger and less disabled patients with shorter disease duration and ongoing disease activity were the ones that had greater benefits from receiving siponimod. Siponimod reduced the risk of 3-month confirmed disability progression by 21% compared with placebo (hazard ratio [HR] 0.79, 95% CI 0.65–0.95; p=0.013) as measured by EDSS.

Although ocrelizumab and siponimod were significantly associated with a reduction of the rate of disability progression, their efficacy was modest (Filippini, 2017; Metz

[1] Usually, the maximum eligibility age for trials in progressive MS is 65 years.

and Liu, 2018) and likely to be mediated by anti-inflammatory activity rather than direct interference with the neurodegenerative process underling disease progression.

Other interesting results were the ones obtained by the MS-SPI trial, a phase III study investigating biotin in patients with progressive MS. Biotin can increase energy production in demyelinated axons and enhance myelin synthesis in oligodendrocytes, behaving as both neuroprotective and myelin repair drug (Peyro Saint Paul *et al.*, 2016). The MS-SPI is one of the few examples of trials in progressive MS where, instead of looking at stopping disease progression, the investigators were looking at disease improvement, due to the potential remyelinating induction of biotin. In the MS-SPI trial, Tourbah and colleagues found a reverse of MS-related disability in 12.6% of the patients, and a reduced proportion of patients with confirmed EDSS progression (Tourbah *et al.*, 2016). The confirmatory phase III SPI-2 trial investigated biotin in a larger number of patients with progressive MS is underway (Table 1.4).

1.6.2 Phase II trials in progressive MS

Phase III trials are expensive - up to £50 million ('A timeline of the research process | Multiple Sclerosis Society UK', n.d.) - and lengthy (more than 10 years). The failure of a phase III clinical trial, therefore, can have repercussions on the development of other studies, leading to reduce investments from pharmaceutical companies in the discovery of new drugs. An example is provided by the pharmaceutical company Biogen, who decided aborting the phase III trial INSPIRE on dimethyl fumarate in SPMS (NCT02430532) due the recent failure of the similarly designed ASCEND study (Kapoor *et al.*, 2018). There is a need to de-risk phase III trials. Appropriately targeted phase II trials have the potential to identify

the treatments most likely to succeed in phase III – as shown previously with the example of rituximab - and those with little chance of success.

Examples of phase II trials in progressive MS carried out in the past 10 years are reported in Table 1.3.

Table 1.3 Reported phase II trials in progressive multiple sclerosis

Trial	Year	Drug	Ms course	Size	Time frame	Primary outcome	Results
ASPIRE (Montanari et al., 2009)	2009	Azathioprine (add on to interferon beta-1b)	SPMS	85	2y	MSFC	Negative, but low completion rate (45/85)
Lamotrigine in SPMS (Kapoor et al., 2010)	2010	Lamotrigine	SPMS	120	2 y	Brain atrophy	Negative but high drop outs and evidence of pseudoatrophy
NAPMS (Romme Christensen *et al.*, 2014)	2012	Natalizumab	PMS (50% SPMS)	24	60w	Osteopontin	Positive
POEMS (Lovera *et al.*, 2015)	2013	Polyphenon E	SPMS & RRMS	11	1y	MRS-NAA	Terminated (liver toxicity)
Fluoxetine in progressive MS (Mostert et al., 2013)	2013	Fluoxetine	PMS (69% SPMS)	42	2y	EDSS, 9HPT, Ambulation	Negative but positive trends for EDSS and 9HPT
***EPO-ProgMS* (Schreiber *et al.*, 2017)**	2013	Erythropoietin (rhEPO)	PMS (34 SPMS 18 PPMS)	52	48w	MGD 9HPT TMT-B	Negative
COMTiMS (Ratzer *et al.*, 2016)	2013	Methylprednisolone	PMS (50% SPMS)	30	60w	Osteopontin	Negative
MS-STAT (Chataway et al., 2014)	2014	Simvastatin	SPMS	140		Brain atrophy	Positive
RIVITaLISe Phase I/II (Komori *et al.*, 2016)	2015	Rituximab (IT)	Ii-SPMS	44	3m	CSF CXCL13 CSF BAFF	Terminated (lack of efficacy)
Abili-T Press Release (Opexa Therapeutics, n.d.)	2016	Tcelna (imilecleucel-T)	SPMS	183	2y	Brain atrophy	Negative
Lithium in progressive MS (Rinker JR et al, n.d.)	2015	Lithium	PMS	20	2y	Brain atrophy	Negative
FLUOX-PMS (Cambron *et al.*, 2019)	2016	Fluoxetine	PMS (72 SPMS 55 PPMS)	127	2y	T25FW 9-HPT	Negative
ARPEGGIO Press Release (Active Biotech » Press Releases, n.d.)	2017	Laquinimod	PPMS	374	48w	Brain atrophy	Negative
*MIS416 in SPMS Press Release (Press Release Innate Immunotherapeutics , 2017) **	2017	MIS416	SPMS	93	1y	Neuromuscular function	Negative
Lipoic acid in SPMS (Spain *et al.*, 2017)	2017	Lipoid acid	SPMS	54	2y	Brain atrophy	Positive
IPPoMS Press Release ('Santhera Reports Outcome of Exploratory Trial	2018	Idebenone	PPMS	85	2y	CombiWISE (Kosa *et al.*, 2016)	Negative

with Idebenone in PPMS Conducted at the NIH', n.d.)							
IB-MS ECTRIMS 2018 [NCT02273635]	2018	Andrographolides	PMS	43	2y	Brain atrophy	Negative, but CDP was significantly lower in the active arm.
SPRINT-MS (Fox et al., 2018)	2018	Ibudilast	PMS (134 PPMS, 121 SPMS)	96	96w	Brain atrophy	Positive

In the past, alemtuzumab and cladribine were negative in phase-2 trials that included progressive MS patients. (Sipe *et al.*, 1994; Filippi *et al.*, 2000; Rice *et al.*, 2000; Giovannoni *et al.*, 2010; Cohen *et al.*, 2012a; Coles *et al.*, 2012; Brown and Coles, 2013; Leist *et al.*, 2014). Abbreviations: CDP= confirmed disability progression. CSF: cerebrospinal fluid. EDSS= expanded disability status scale. IT= intrathecal. li-SPMS= low inflammatory secondary progressive multiple sclerosis. m= months. MGD= maximum gait distance. MRS-NAA= magnetic resonance spectroscopy-n-acetyl aspartate. RCT= randomised controlled trial. MS= multiple sclerosis. PMS= progressive multiple sclerosis. PPMS = primary progressive multiple sclerosis. SPMS= secondary progressive multiple sclerosis. T25FWT= timed 25-foot walking test. TMT-B= Trail Making Test - part B. w= week. y= year. 9HPT= 9-hole peg test (clinical trials have been searched on https://clinicaltrials.gov).

Positive results have been obtained by neuroprotective trials assessing the efficacy of ibudilast (Fox *et al.*, 2018), simvastatin (Chataway *et al.*, 2014), and lipoid acid (Spain *et al.*, 2017) in reducing brain atrophy over about 2 years. Ibudilast has anti-inflammatory actions, and inhibits nitric oxide synthesis and tumour necrosis factor-alpha, which is released by activated astrocytes and microglia (Mizuno *et al.*, 2004; Rolan *et al.*, 2009). The phase II randomised placebo-controlled SPRINT-MS study (Fox *et al.*, 2018) recruited 255 patients with progressive MS (47% with SPMS) and tested the efficacy of ibudilast against placebo in reducing the rate of MRI-derived brain atrophy over 96 weeks. Ibudilast reduced the rate of brain atrophy by 48% compared to placebo as measured by BPF. Similarly, simvastatin - a lipid-lowering medication which exert also anti-inflammatory and protective properties in the CNS - was associated with significant reduction of the percentage of brain volume change in patients with SPMS in the placebo-controlled phase II trial MS-STAT (Chataway *et al.*, 2014) and is now being investigated in a phase III study (Table 1.4). Lipoic acid is an antioxidant promoting free-radical scavenging, metallic ion chelation, regeneration of intracellular glutathione, and oxidative damage repair of macromolecules. It also takes part in the mitochondrial oxidative respiration and nucleic acid synthesis, and

inhibits macrophage and microglial activation in EAE (Marracci *et al.*, 2002; Morini *et al.*, 2004). Spain and colleagues investigated the neuroprotective role of lipoid acid in 51 patients with SPMS (Spain *et al.*, 2017). They found a change in brain volume that corresponded to a 68% reduction in the rate of brain atrophy in the active arm versus placebo. However, this trial had a small sample size and showed a near significant increase in the T2 lesion volume (p=0.058) in the lipoic acid arm, a potential confounder.

Another example of phase II trial in SPMS is the lamotrigine trial (Kapoor *et al.*, 2010). Although this trial did not show positive results, it has been very useful for subsequent atrophy-based trials as it pointed out the occurrence of pseudoatrophy as a possible confounder.

1.6.3 Agents under investigation

As previously introduced, in order to modify the natural history of SPMS, preventing or delaying the accumulation of disability should be the goal of the treatment. Putative neuroprotective, remyelination agents and immune-modulation agents are currently under investigation in progressive MS (Table 1.4).

NeuroVax, differently from the other agents, has an innovative mechanism of action as it works in stopping the aberrant activation of the immune system in the CNS by inducing immune-tolerance.

Table 1.4 Agents under investigation in progressive multiple sclerosis

Drug	Study Name NCT identifier	Time	Participants	Status	Primary Endpoint	Agent Type
			PHASE II TRIALS			
ACTH	ACTH in Progressive Forms of MS [NCT01950234]	3y	100 PMS (target)	Active Not recruiting	T25FW	Immune-modulation

Dimethyl Fumarate	FUMAPMS [NCT02959658]	48w	90 PPMS (target)	NCT02959658	Neuro filament light chain	Immune-modulation
Domperidone (Open label)	Domperidone in SPMS [NCT02308137]	1y	62 SPMS	Recruiting	T25FW	Regenerative
Glatiramer Acetate Depot (Open label)	Safety and Efficacy of Monthly Long-acting IM Injection of 40 mg GA Depot in Subjects With PPMS [NCT03362294]	56w	24 PPMS	Recruiting	Safety	Immune-modulation
Hydroxychloroquine (Open label)	Hydroxychloroquine in PPMS NCT02913157	18m	35 PPMS	Recruiting	T25FW	Neuroprotective
Mesenchymal Cell Therapy	ACTiMuS [NCT01815632]	2y	80 PMS (target)	Recruiting	GEP	Regenerative
Autologous Mesenchymal Stem Cell-derived Neural Progenitors	MSC-NP [NCT03355365]	27m	50 PMS (target)	Recruiting	EDSS Plus	Regenerative
NeuroVax	A Study of NeuroVax™, a Novel Therapeutic TCR Peptide Vaccine for SPMS [NCT02149706]	48w	150 PMS (target)	Unknown	EDSS	Immune-modulation (immunisation)
Oxcarbazepine	PROXIMUS [NCT02104661]	48w	50 early SPMS (must be on DMT)	Completed	Neuro filament light chain	Neuroprotective (recently reported as negative)
Quetiapine (Open label)	NCT02087631			unknown		Regenerative
Rituximab (Open label)	Intrathecal Rituximab in PMS (EFFRITE) [NCT02545959]	180d	12 PMS	Completed	Osteopontin	Immune-modulation
		PHASE III TRIALS				
Biotin (MD1003)	SPI2 [NCT02936037]	15m	600 PMS	Active Not recruiting	EDSS or T25FW (improvement)	Regenerative
Masitinib	Masitinib in Patients with PPMS or Relapse-free SPMS** [NCT01433497] (combined phase II/III)	96w	450 PMS (target)	Active Not recruiting	EDSS	Immnune-modulation
Simvastatin	MS-STAT2 [NCT03387670]	3y	1180 SPMS (target)	Recruiting	EDSS	Neuroprotective
Ocrelizumab	O'HAND [NCT04035005]	5y	1000 PPMS (target)	Recruiting	9HPT	Antinflammatory

GEP= Global evoked potential. PMS= progressive multiple sclerosis. PPMS = primary progressive multiple sclerosis. SPMS= secondary progressive multiple sclerosis. T25FWT= timed 25-foot walking test. 9HPT= 9-hole peg test (clinical trials have been searched on https://clinicaltrials.gov).

1.7 **Future strategies for SPMS therapeutics**

Disability progression in MS is a continuous and slow process that can take years. Similarly, new drug discovery and testing could take up to 15 years with success not guaranteed. In order to expedite the finding of new treatments for SPMS, several ways have been proposed (Ontaneda *et al.*, 2015; Plantone *et al.*, 2016; Nandoskar *et al.*, 2017).

Within the wider context of issues relevant to drug development programmes, such as high costs and the prolonged time from target selection to regulatory approval, the failure of therapeutic development for SPMS using conventional pipelines has led to interest in novel approaches such as “drug rescue” (evaluating drugs at advanced stage of development but abandoned before approval) and “repurposing” (evaluating drugs already approved for other indications) (Mullard, 2012). These offer the potential to reduce both the cost and time-taken to achieve licenced approval status (Ashburn and Thor, 2004). Drug repurposing - also known as drug repositioning or drug re-profiling - is the application of already approved drugs to new diseases (Ashburn and Thor, 2004; Yang *et al.*, 2016). It is advantageous because the repurposed drugs have already passed the trial stages assessing safety in humans, reducing time and costs of drug development (Cuatrecasas, 2006; Campillos *et al.*, 2008; Keiser *et al.*, 2009; Oprea and Mestres, 2012). In the past, drug repositioning was merely a consequence of chance or unforeseen drug effects, whereas nowadays computational methods have been developed to predict new targets for established drug or different drugs that act on the same target (Ashburn and Thor, 2004; Keiser *et al.*, 2009; Wang *et al.*, 2012). Structurally similar molecules can predict similar biological effects (Schuffenhauer *et al.*, n.d.; Fliri *et al.*, 2005; Bajorath, 2008). Molecular activities of drugs can be also inferred based on their side-effects, or predicted from human genome (Hopkins and Groom, 2002; Campillos *et al.*, 2008). Faissner and colleagues looked for repurposed drugs with neuroprotective potential targeting iron deposition in the CNS, which is thought to mediate mitochondrial dysfunction neurotoxicity in progressive MS. They showed that tricyclic antidepressants, antipsychotics, and indapamide might work in progressive MS. They also showed that clomipramine was able to suppress or improve EAE (Faissner *et al.*, 2017). Vesterinen and colleagues developed an evidence based framework to select oral repurposed neuroprotective drugs to be tested in SPMS (Vesterinen *et al.*, 2015).

They found at least seven agents with putative neuroprotective properties (see also Chapter 2 and 4). Three of these agents have been investigated in the MS-SMART trial and two other agents (ibudilast and lipoic acid) have been successful investigated in the SPRINT-MS study (Fox *et al.*, 2016; Connick *et al.*, 2018) and the Lipoic acid study (Spain *et al.*, 2017).

Additionally, innovative trial design, such as adaptive trials or multi-arm proof-of-concept studies may help in increasing drug discovery efficiency and further cost cutting. Large-scale long-term placebo-controlled parallel group trials, using a 1:1 ratio, have been used so far to assess efficacy drug in progressive MS. The efficiency of clinical trials in SPMS can potentially be increased by allowing a number of treatments to be tried concurrently. Adaptive seamless designs are feasible in SPMS. Multistage or multiarm randomised trials have been successfully used in other medical research areas such as oncology for some time (James *et al.*, 2012) and an attempt has also been made to model in SPMS (Chataway *et al.*, 2011). In 1999, Bauer and Kieser proposed an adaptive two-stage design for the situation of multiple treatments to be compared with a control within a single confirmatory trial (Bauer and Kieser, 1999). Such a trial would allow for an interim analysis to determine early termination or continuation of the study towards a second stage. Adaptive design methods are also useful in the early phases of drug development because are dynamically informative (Likosky *et al.*, 1991; Vandemeulebroecke *et al.*, 2008).

Finally, drug efficacy can be increased by combining drugs with different mechanisms of action. Combination therapy (Figure 1.9) is widely used in medicine, including in the treatment of immune disorders, such as rheumatoid arthritis. The rationale for the use of combination therapy in MS, as highlighted by Conway and Cohen, is supported by the different mechanisms of action of the

various available Disease-modifying therapies that can also have additive or synergistic efficacy (Conway and Cohen, 2010).

Figure 1.9 Combination therapy options

This figure was removed due to copywrite.

The figure is available in The Lancet Neurology (Conway and Cohen, 2010)

Adapted from Conway and Cohen, Lancet Neurol. 2010.

Combination therapy has pros and cons, and drugs with different mechanisms of action can target different aspects of the disease pathogenesis, which is complex and heterogeneous, but can also have additive side effects. (Milo and Panitch, 2011) Some attempt at combination therapy has been done, but no convincing results have been found (Rudick *et al.*, 2006; Cohen *et al.*, 2009; Goodman *et al.*, 2009; Lublin *et al.*, 2013).

Consistent with the rationale of combining immunomodulators with distinct mechanism of action, other combinations have obtained additive or synergistic effects in preclinical studies, showing a positive effect of combining vitamin D and interferon-β. The combination of anti-inflammatory and neuroprotective agents has also been tried in small studies such as the phase II trial combining intramuscular interferon-β 1a with riluzole or the ones combining minocycline and interferon-β or glatiramer acetate in RRMS (Metz *et al.*, 2009; Conway and Cohen, 2010; Waubant *et al.*, 2014). The CombiRx trial, combining interferon-β 1a and glatiramer acetate, enrolled more than a thousand of patients with RRMS. Whereas the

combination therapy did not produce a significant clinical benefit, there was evidence of superiority of the combination therapy over single arm treatment in reducing new lesion activity and accumulation of total lesion volumes. (Lublin *et al.*, 2013)

1.8 **Conclusions and rationale for this thesis**

Relapsing MS is a common neurological disorder that starts early in life in young adults and last for decades. In the long-term, most of the patients with relapse-onset MS will develop significant neurological disability, which is currently irreversible. Neuroprotective drugs could prevent clinical worsening due to neuro-axonal loss in MS and, therefore, slow down the disease progression. However, as previously discussed, the mechanisms responsible for disease progression are still not fully understood and many drugs have been investigated in the attempt of stopping disability progression in SPMS. This phenotype is difficult to study within randomised-controlled trials due to several reasons: unclear conversion between RRMS and SPMS; lack of progression or inhomogeneity of the studies populations; slowness of disease progression; lack of sensitive biomarkers of progression.

Against this background, the major aims of this thesis are: (1) to test putative neuroprotective drugs in a pure cohort of patients with SPMS; (2) to test the feasibility and efficiency of a multi-arm randomised-controlled trial design, never used before in MS; and (3) to explore outcome measures of disease progression in SPMS using conventional and non-conventional MRI techniques and OCT.

To address these objectives, I conducted a clinical, MRI and OCT study in a cohort of people with SPMS who were enrolled in the phase II MS-SMART trial. I conducted screening, baseline and follow-up visits for 96 weeks for most of the

patients recruited at UCL and analysed most of the MRI data and all the OCT data from the whole UK cohort. The major results are presented in this thesis.

This introductory Chapter has provided appropriate background to MS and SPMS. In Chapter 2, I provide an overview of the MS-SMART trial. In Chapter 3, I report the results from the baseline data of the whole trial cohort baseline data studied, whereas in Chapter 4 I report the main longitudinal results. In Chapter 5, I mostly focus on the UCL cohort characteristics and recruitment data. In Chapter 6 and 7, I discuss the findings from exploratory sub-studies. Finally, in Chapter 8, I conclude my work commenting on the main points that have emerged during the running of the trial and that will be object of future analyses.

Chapter 2. **The MS-SMART trial**

In the previous Chapter, I provided an overview of MS, including physiopathology and clinical phenotypes, and focused on the challenges of clinical research in SPMS.

In this Chapter, I shall provide an overview of the MS-SMART trial, starting with the drug selection to conclude with the methodology applied to investigate the study outcomes. The section on the mechanisms of axonal damage in MS discussed in Chapter 1 is the reference background to understand the rationale behind the choice of the three study drugs.

In the next two Chapters (Chapter 3 and Chapter 4), I shall describe the results from the baseline and the longitudinal analyses.

2.1. Drug selection strategy and rationale

In 2007, the Clinical Trials Network - a group of researchers, people affected by MS and healthcare professionals supported by the UK MS Society - was initiated to support innovative and investigator-led clinical trials in progressive MS. Members of the Clinical Trials Network prospectively sought to identify existing putative neuroprotective drugs - based on the strategy of drug rescue or repurposing (Ashburn and Thor, 2004) - to target specific neurodegenerative-causing pathways and slowing disease progression in SPMS. A commissioned systematic review (Vesterinen *et al.*, 2015) was carried out to look for repurposed drugs showing neuroprotective properties in animal models of MS and in patients with MS or neurodegenerative disorders sharing common pathological pathways such as motor neurone disease, Huntington's, Alzheimer's and Parkinson's

diseases. Initially, 120 possible drugs were selected, from which 52 drugs where further shortlisted and subsequently reviewed at a specially convened international meeting of experts from the Cochrane MS group, neuroscientists, neurologists, brain imaging experts, people with MS, trial methodologists, and industry. Structured discussions on safety, efficacy, study quality, and study size of each of the short-listed drugs led to the identification of seven drugs - ibudilast, riluzole, amiloride, pirfenidone, fluoxetine, oxcarbazepine, and the polyunsaturated fatty-acid class - as lead candidates for therapeutic evaluation (Table 2.1). Amongst the seven candidates, ibudilast, riluzole and amiloride were initially chosen. However, ibudilast could not be supplied and was replaced by fluoxetine (Vesterinen *et al.*, 2015).

Table 2.1 Putative neuroprotective agents for progressive multiple sclerosis

Intervention	Current main clinical application and mechanism of action
Ibudilast	***Anti-inflammatory use in asthma*:** non-selective phosphodiesterase (PDE 3,4,10,11) inhibitor and macrophage Migration Inhibitor Factor (MIF) inhibitor.
Riluzole	***MND/ALS*:** glutamate release inhibitor/inactivation of voltage-dependent sodium channels.
Amiloride	***Diuretic*:** acid sensing ion channel blocker.
Pirfenidone	***Pulmonary fibrosis*:**antagonises synthesis of TGF-beta & TNF-alpha; antifibrotic/anti-inflammatory activity.
Fluoxetine	***Antidepressant*:** selective serotonin reuptake inhibitor.
Oxcarbazepine	***Anticonvulsant*:** voltage sensitive sodium channel blocker.
PUFA class (Linoleic Acid, Lipoic acid; Omega-3 fatty acid, Max EPA oil)	***None / dietary supplements*:** mechanism of action unclear.

PUFA = polyunsaturated fatty acids. MND/ALS = motor neurone disease / amyotrophic lateral sclerosis.

Adapted from Vesterinen et al., PloS One 2015.(Vesterinen *et al.*, 2015)

Subsequently, a phase IIb multi-arm randomised placebo-controlled trial (MS-SMART; NCT01910259) was set up to simultaneously evaluate the three oral repurposed and putative neuroprotective agents amiloride, fluoxetine, and riluzole.

MS-SMART tested the hypothesis that the treatment with amiloride or fluoxetine or riluzole versus placebo reduced the rate of brain atrophy in SPMS over 96 weeks.

2.1.1. Amiloride

Amiloride is a widely used diuretic that works as an ASICs blocker. As discussed in Chapter 1, inflammatory demyelination induces a modification of the distribution of Na^+ channels along the length of the affected axons, leading to excessive influx of Na^+ and accumulation of intracytoplasmic Ca^{2+}, which is toxic for the cell. But inflammation also raises the acidity of the axonal environment leading to the opening of ASICs. In an experimental model of stroke, ASIC1 was found to increase neuronal Na^+ and Ca^{2+} influx during tissue acidosis (Xiong *et al.*, 2004). Later on, two studies on MS animal models and cellular cultures showed that CNS inflammation induces acidosis and hypoxia, and that these two phenomena were associated with an increased expression of the gene Asic1, which indirectly reflects an increased expression of the ASIC1 (Friese *et al.*, 2007; Vergo *et al.*, 2011), and that blockade of ASIC1 was neuroprotective. In mice with EAE treated with amiloride, there was a blockade of ASIC1 and better clinical outcomes compared to non-treated mice. These experimental findings were translated into a clinical pilot study by Arun and colleagues, who undertook a phase II trial of 14 patients with PPMS. The study was divided in a pre-treatment phase followed by an open-label phase where patients were treated with amiloride 5 mg twice daily (Arun *et al.*, 2013). In the amiloride-treatment phase, there was a significant reduction in the whole brain atrophy rate compared to the pre-treatment phase ($p=0.009$).

2.1.2. Fluoxetine

Fluoxetine is a selective serotonin-reuptake inhibitor (SSRI) widely used for depression. Experimental studies, though, have shown that fluoxetine has other properties in the CNS. For instance, fluoxetine can stimulate glycogenolysis in astrocytes and release of lactate in the extracellular space, an intermediate metabolite that can be used by neurons as a substrate for their energy needs (Kong *et al.*, 2002; Allaman *et al.*, 2011). Allaman and colleagues also showed that fluoxetine induces astrocyte release of brain-derived neurotrophic factor (BDNF), a protein controlling neuron growth, maturation and survival. Additionally, fluoxetine might exert immune-modulatory activity by suppressing the antigen presenting ability of astrocytes (De Keyser *et al.*, 1999; Maes *et al.*, 2005). Mostert and colleagues carried out a double-blind, placebo-controlled exploratory study in 40 non-depressed patients with RRMS (90%) and relapsing-SPMS (10%), who received oral fluoxetine 20 mg or placebo daily for 24 weeks (Mostert *et al.*, 2008). They found a mean (standard deviation [SD]) cumulative number of new gadolinium-enhancing lesions 1.84 (2.9) in the fluoxetine group and 5.16 (8.6) in the placebo group ($p=0.15$) during the 24 weeks of treatment, with significantly less scans showing new enhancing lesions in the fluoxetine group ($p=0.04$). Although there was no effect of fluoxetine in the first 8 weeks of treatment, when the researchers focused on the last 16 weeks of treatment, they found a nearly significant reduction in the cumulative number ($p=0.05$) in the fluoxetine group compared with the placebo group, suggesting that it may take several weeks before fluoxetine becomes effective. In a second trial, 42 patients with progressive MS (SPMS 69%) were randomised in a 1:1 ratio to fluoxetine 40mg/placebo over 2 years. Whilst no statistical differences were seen in the overall progression, there were trends in favour of fluoxetine in the grey matter and white matter volume changes, but the study was underpowered and any definite conclusion could not be deduced. More recently, several years after the Clinical Trials Network had

convened and the MS-SMART designed, the FLUOX-PMS trial was initiated. This was a multi-centre, randomised-controlled, double-blind study that enrolled 127 patients with progressive MS (SPMS 57%) to test fluoxetine 40 mg daily or placebo for 108 weeks. They primary endpoint was the time to confirmed disease progression defined as either at least a 20% increase in the T25FW or at least a 20% increase in the 9HPT (Cambron *et al.*, 2014).

2.1.3. Riluzole

Riluzole is licenced for motor neurone disease. It has two modes of action of relevance to SPMS: (i) reduction of glutamate release; (ii) antagonism of voltage dependent Na^+ channels. I previously mentioned, in Chapter 1, that there is a redistribution of Na^+ channels in the whole axon following demyelination. However, there is also an upregulation of Na^+ channel expression within activated microglia and macrophages in MS (Craner *et al.*, 2005), which are commonly activated in progressive MS. These findings suggest that Na^+ channel blockers can exert their effect via direct neuroprotective action on axons, or by a parallel mechanism that reduces the inflammatory damage driven by microglia and macrophages (Stys, 2004; Waxman, 2006). Phenytoin, a nonspecific Na^+ channel blocker, has been shown to be protective in animal models of MS or in humans with optic neuritis (Lo *et al.*, 2003; Raftopoulos *et al.*, 2016). Lamotrigine, instead, did not significantly decrease the rate of brain atrophy in a phase II study in SPMS (Kapoor *et al.*, 2010), although the study was biased by high rate of drop-outs and pseudoatrophy, as discussed in Chapter 1. A number of studies have suggested that riluzole induce a persistent Na^+ channel block in central neurons. Lamanauskas and Nistri showed that riluzole could persistently block Na^+ and Ca^{2+} currents, as well as modulating glutamate release *in vitro* rat hypoglossal motoneurons (Lamanauskas and Nistri, 2008). Benoit and Escande showed that riluzole specifically blocked inactivated

Na^+ channels in isolated myelinated nerve fibre of frog (Benoit and Escande, 1991).

Sustained glutamate exposure, known as *excitotoxicity*, induces neuronal damage, mostly by activation of N-methyl-d-aspartate (NMDA) receptors, which are cation channels permeable to Ca^{2+} (Pitt *et al.*, 2000; Hardingham and Bading, 2010). Overstimulation of NMDA-receptor-activated channels is one mechanism for calcium overload in neurons. Activated inflammatory cells, such as microglia, release glutamate, activate NMDA receptors, which, when excessively stimulated, release higher quantity of nitric oxide and superoxide. All these phenomena triggered by glutamate toxicity and NMDA receptor activity can predispose to neuronal death, as shown in acute and chronic neurodegenerative diseases (Hardingham and Bading, 2010; Malarkey and Parpura, 2008). In preclinical studies, riluzole was found to modulate the glutamatergic transmission (Mizoule *et al.*, 1985; Martin *et al.*, 1993) and inhibit glutamate release in rat striatal slices (Jehle *et al.*, 2000). In rat motoneuron cultures, riluzole significantly reduced glutamate and NMDA neurotoxicity (Estevez *et al.*, 1995).

In a Phase II trial, 16 patients with progressive MS were studied for one year in a pre-treatment phase, followed by a second year of treatment with riluzole 50 mg twice daily (Killestein *et al.*, 2005). The primary outcome was the change in cervical spinal cord cross-sectional area. The researchers found a reduction from -2% (year 1) to -0.2% (year 2) of spinal cord atrophy. In addition, they looked at the number of new T1 hypointense lesions, which are believed to reflect neurodegeneration (van Waesberghe *et al.*, 1999), and found this was reduced from 15% in year 1 to 6% in year 2; moreover, there was a reduction in whole brain parenchymal/intracranial volume from -1.0% (year 1) to -0.7% (year 2).

2.2. Objectives

The primary objective of the MS-SMART study was to establish whether any of the three selected drugs - amiloride, fluoxetine, riluzole - slowed down the rate of brain volume loss in people with SPMS over 96 weeks as assessed by MRI-derived percentage of brain volume change (PBVC).

Secondary objectives were:

1. To establish that a multi-arm trial strategy was an efficient way of screening drugs in SPMS and can become the template for future work;
2. To explore any anti-inflammatory drug activity (measured by counting the new and enlarging T2-weighted white matter lesions);
3. To examine for evidence of pseudo-atrophy by MRI (to ensure reliability of the primary outcome measure);
4. To examine the clinical effect of neuroprotection as measured by clinician and patient reported outcome measures;
5. To collect basic health economic data to inform future phase III trials.

Exploratory objectives were:

1. To assess neuroprotection in new lesions by estimating persistent new T1-weighted hypointense lesion (black holes) count;
2. To assess cortical neuroprotection by evaluation of grey matter volume change;
3. To evaluate myelination using MTR;
4. To assess spinal cord neuroprotection using MRI;
5. To quantify neuronal mitochondrial dysfunction, prevention of glial cell inflammation, and prevention of excitotoxicity as measured by MRS metabolites;

6. To increase sensitivity and study interaction of treatment mechanisms by measuring composite MRI/disability scores;
7. To evaluate neuroprotection using OCT measures;
8. To quantify neuroprotection using CSF neurofilaments.

My thesis will not report on CSF, MRS and MTR analyses, as other investigators will take this work forward.

2.3. Methods

2.3.1. Study design and participants

MS-SMART was an investigator-led, multi-centre, multi-arm, double blind, placebo-controlled, parallel-group, randomised phase IIb trial that compared the three candidate neuroprotective therapies - amiloride, fluoxetine, and riluzole - against a shared placebo arm in people with SPMS. ClinicalTrials.gov number NCT01910259.

MS-SMART was carried out across thirteen UK research neuroscience centre in London, Edinburgh, Liverpool, Sheffield, Brighton, Truro, Oxford, Stoke-on-Trent, Plymouth, Newcastle, Leeds, Nottingham, and Glasgow. The UCL Queen Square Institute of Neurology in London (hereafter called UCL) and the University of Edinburgh, Anne Rowling Regenerative Neurology Clinic in Edinburgh (hereafter called Edinburgh) were the two principal trial sites.

To be eligible for the study, patients had to be aged 25–65 years, have a diagnosis of SPMS with evidence of disease progression independent of relapses in the two years proceeding recruitment, have an EDSS score of 4.0–6.5 at baseline, and be able to undergo an MRI. Exclusion criteria included use of immunosuppressants

or first-generation disease-modifying treatments within 6 months of baseline visit, or use of natalizumab, fingolimod, dimethyl fumarate, teriflunomide or experimental disease-modifying treatments within 12 months of baseline visit. Additional exclusion criteria were: systemic corticosteroid use in the previous 3 months, MS relapse in the previous 3 months, history of depression, glaucoma, or any other serious concomitant medical illness, pregnancy, serious cognitive impairment (such as inability to provide informed consent), commencement of fampridine within the previous 6 months, and use of SSRI within the previous 6 months. A full list of eligibility criteria is reported in Table 2.2.

The study was done in accordance with Good Clinical Practice and the Declaration of Helsinki. The protocol was approved by each study site's institutional review board, and all patients gave informed consent before entering the study.

Table 2.2 MS-SMART trial eligibility criteria

Inclusion criteria	Exclusion criteria
• Secondary progressive multiple sclerosis • Steady disability progression prior 2 years • EDSS 4.0-6.5 (inclusive) • Age 25-65 (inclusive) • Women and men with partners of childbearing using appropriate contraception • Willing and being able to comply with the trial protocol • Written informed consent provided	• Relapsing-remitting or primary progressive multiple sclerosis • Baseline MRI scan not of adequate quality for analysis • Significant organ co-morbidity or blood test abnormalities • Relapse within 3 months of baseline visit • Steroid treatment within 3 months of baseline visit • Use of an SSRI within 6 months of the baseline visit • Use of Simvastatin at 80mg dose within 3 months of baseline visit • Commencement of fampridine within 6 months of baseline visit • Use of immunosuppressants or β-interferons and glatiramer within 6 months of the baseline visit • Use of other disease modifying drugs (mitoxantrone, natalizumab, alemtuzumab, daclizumab, fingolimod, dimethyl fumarate, teriflunomide) or experimental drugs within 12 months of the baseline visit • Epilepsy/seizures • Glaucoma • Depression or BDI-II score of ≥19 • History of bleeding disorders or on anticoagulants • Pregnancy or breastfeeding • Current use of tamoxifen, St. John's Wort, potassium supplements • Use of lithium, chlorpropamide, triamterene, spironolactone, monoamine oxidase inhibitors, phenytoin, L-tryptophan and/or neuroleptic drugs within 6 months of the baseline visit • Receiving or previously received Electro-Convulsive Therapy • Known hypersensitivity to the active substances and their excipients to any of the active drugs for this trial • Abnormal screening blood values: o LFTs > 3 x upper normal limit; K^+ <2.8mmol/l or >5.5mmol/l; Na^+ <125mmol/l; Creatinine >130µmol/l; WBCs <3 x 10^9/l; Lymphocytes <0.8 x 10^9/l; Neutrophil count <1.0 x 10^9 /l; PLT count <90 x 10^9 /l; Hgb <80g/l

BDI-II: Beck depression index-II. EDSS: expanded disability status scale. LFT: liver function test. MRI: magnetic resonance imaging. PLT: platelet. SSRI: serotonin selective reuptake inhibitor. WBC: white B cells.

2.3.2. Randomisation and masking

Eligible patients were randomised by an independent statistician via a secure web-based randomisation service on a 1:1:1:1 basis using a minimisation algorithm balanced according to sex, age (< or ≥ 45 years), baseline EDSS score (4.0-5.5; 6.0-6.5), and centre with a random component to maintain unpredictability of treatment allocation. Participants and all other personnel directly involved in the study were masked to treatment allocation. Amiloride, fluoxetine, riluzole and placebo capsules were over-encapsulated to obtain an identical appearance to ensure that treatment allocation remained concealed to both staff and participants.

2.3.3. Procedures

Participants were identified through different routes: General Practitioners and Consultant Neurologist referrals, existing MS Research Databases at each site, and a dedicated website (www.ms-smart.org) where patients could register their interest. Potential participants were contacted by the trial investigators at each site for a telephone pre-screening questionnaire to check that they met the main eligibility criteria. At the UCL site, I administered most of the pre-screening telephone questionnaires, which had an average duration of 20 minutes, and helped to identify the majority of the recruited patients (see also Chapter 5). After the pre-screening telephone questionnaire, suitable patients were sent - via e-mail or post - the trial participant information leaflets and invited to take part into a formal face-to-face screening visit. At the screening visit, informed consent was obtained and medical history, concomitant medications, EDSS and Beck depression index score recorded. Disease duration was calculated from the estimated date of the subject's first neurological symptom. Patients also underwent a full physical clinical examination, and vital signs and blood tests were collected. The entire screening visit took an average of 3 hours.

Patients passing the screening phase underwent a baseline brain MRI. In most of the sites, it was possible to perform the baseline MRI scan on the day of the screening visit, reducing travel costs and time commitment for participants. All sites carried out a standard mandatory MRI protocol (defined as *core MRI*). In addition, UCL and Edinburgh sites performed optional MRI scan protocols (defined as *advanced MRI*), which included brain MTR, spectroscopy and DTI scans at the Edinburgh site, and brain MTR, spectroscopy and upper cervical cord at UCL. The imaging obtained at each site were transferred to the Queen Square MS Centre Trial Unit for central quality control and approval. Upon acceptance of the core MRI scans, the participants were then invited to take part to the baseline visit, which included detailed neurological evaluation, randomisation and collection of participant self-reported questionnaires. Rejection of the advanced MRI protocol only (i.e. *core* MRI was accepted but *advanced* MRI was rejected) did not preclude the enrolment of patients and, whenever possible, the rejected advanced MRI scans were repeated at baseline visit. After completion of the baseline visit and randomisation, participants were provided with the study drugs, emergency card, and patient diary.

After the baseline visit, participants were reviewed at weeks 4, 8, 12, 24, 36, 48, 72, and 96 (Figure 2.1 and 2.2). At week 48 and 96 visits, participants underwent full neurological assessment and completed self-reported questionnaires. The MRI scan, instead, was repeated at week 24 and week 96. At each visit, standard clinical laboratory blood tests (chemistry and haematology) were taken for safety monitoring. Finally, at week 100, a safety telephone call was performed.

Figure 2.1 MS-SMART individual visit schedule

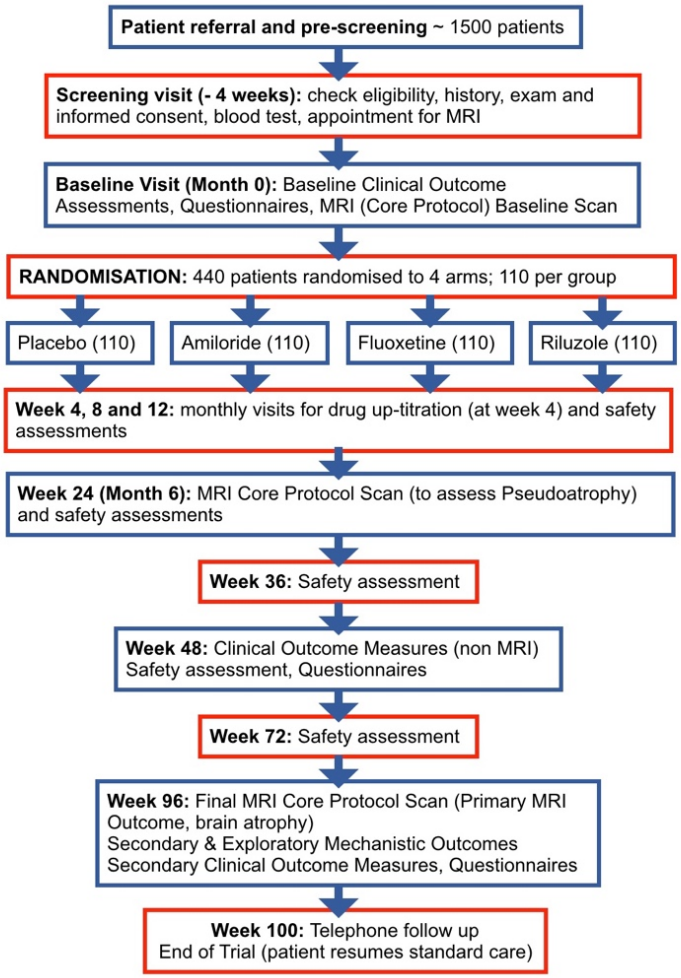

At each study site, there were treating physicians and research nurses (responsible for dose adjustment and adverse event monitoring) and trained NeuroStatus certified assessing physicians masked to patients' history, (responsible for baseline and yearly neurological assessments). Wherever possible, the follow-up assessments were undertaken by the same assessing physician to ensure consistency.

Figure 2.2 Patient flow

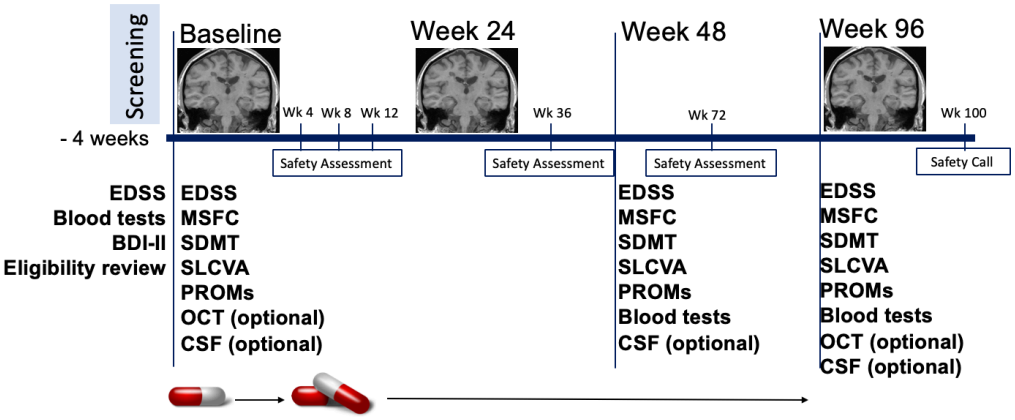

Abbreviations: EDSS= expanded disability status scale, MSFC= multiple sclerosis functional composite, SDMT= symbol digit modalities test, SLCVA= Sloan low contrast visual acuity, PROMs= patient-reported outcome measures, OCT= optical coherence tomography, CSF= cerebrospinal fluid, BDI-II= Deck depression index version II.

Finally, at UCL and Edinburgh, further sub-studies were carried out including OCT (at both Edinburgh and UCL) and CSF (at UCL) (Figure 2.3). OCT and CSF data were collected during the baseline and week-96 visits (Figure 2.2).

Figure 2.3 Main study and sub-studies across sites

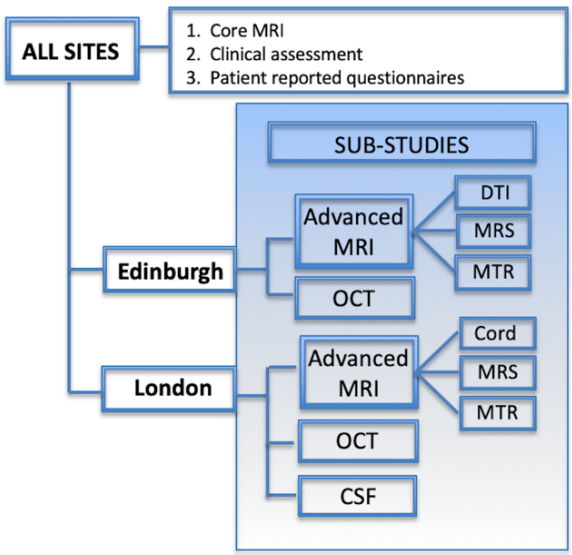

CSF= cerebrospinal fluid; DTI= diffusion tensor imaging; MRI= magnetic resonance imaging; MRS= magnetic resonance spectroscopy; MTR= magnetic transfer ratio; OCT= optical coherence tomography.

2.3.4. Outcomes

2.3.4.1 Primary and secondary endpoints

The predefined primary endpoint was the MRI-derived PBVC over 96 weeks measured with the SIENA method (see also Chapter 1 page 55). Brain atrophy was used as a marker of neurodegeneration and an interim endpoint for the progression of clinical disability (Bermel and Bakshi, 2006).

Secondary endpoints included MRI, clinical scores and patient-reported measures.

The secondary MRI endpoints were the count of new and enlarging T2-weighted lesions (to explore any anti-inflammatory drug activity), and evaluation for evidence of pseudoatrophy on active treatment arms calculating brain atrophy with the SIENA method after 24 weeks from recruitment (to ensure reliability of the primary outcome measure).

Clinical outcomes included EDSS, MSFC, SDMT, relapse frequency, high and low contrast visual acuity testing. For high contrast visual acuity assessment, the 100% logMAR letter charts were used. For low contrast visual acuity assessment, 5%, 2.5% and 1.25% SLCVA letter charts were used.

To investigate physical and psychological well-being, walking, pain, and fatigue, we asked the participants to fill the following questionnaires:

- MS Impact Scale-29 v2 (IMSIS29v2)
- MS Walking Scale v2 (MSWSv2);
- Numerical Pain Rating Score (NPRS);
- Brief Pain Inventory (BPI);
- Neuropathic Pain Scale (NPS);

- Neurological Fatigue Index (NF).

The EuroQuol (EQ-5D-5L) was also assessed to collect basic health economic data.

2.3.4.2 Exploratory endpoints

Exploratory outcomes to evaluated putative neuroprotection were:

(i) proportion of new and enlarging T2 lesions at 24 weeks being persistently T1 hypointense at week 96 (i.e. persisting blackholes);

(ii) grey matter brain volume change.

These endpoints were measured at all trial sites.

Additionally, at UCL and Edinburgh, further advanced metrics were measured:

(iii) MRS metabolites (N-acetyl aspartate, myo-inositol, glutamate);

(iv) whole brain volume, lesional, grey and white matter MTR;

(v) cervical cord cross sectional area (at UCL only);

(vi) fractional anisotropy, axial diffusivity, radial diffusivity, mean diffusivity, and peak width of skeletonised diffusivity for each of these DTI metrics (at Edinburgh only);

(vii) peripapillary retinal nerve fibre layer (RNFL) and ganglion cell + inner plexiform layer (GCIPL) with OCT;

(viii) CSF neurofilament levels (at UCL only).

The analyses of the proportion of persisting blackholes and grey matter brain volume change are not part of my PhD project and are being analysed by Dr Anisha Doshi - my co-fellow – as part of her PhD. Amongst the advanced metrics mentioned above, MRS will not be described further here being the topic the PhD research project of Dr Nevin John, another of my co-fellows. The CSF analysis,

instead, will be analysed by Dr Sharmilee Gnanapavan, sub-principal investigator of the CSF sub-study at Queen Mary University of London. The MTR analysis will be analysed in the future by other investigators.

Spinal cord MRI and OCT measures are discussed in Chapter 6 and 7.

2.3.5 MRI acquisition and analysis

At all sites, the following MRI core protocol was acquired:

1. Axial proton density (PD)-weighted fast spin echo (FSE), in plane resolution 1mm^2, slice thickness 3mm;
2. Axial T2-weighted FSE, in plane resolution 1mm^2, slice thickness 3mm;
3. Axial fluid-attenuated inversion recovery (FLAIR), in plane resolution 1mm^2, slice thickness 3mm;
4. Axial two-dimensional (2D)-T1-weighted sequence in plane resolution 1mm^2, slice thickness 3mm;
5. Axial three-dimensional (3D)-T1 spoiled gradient-recalled echo with 1mm^3 resolution (this scan was acquired twice at the baseline visit).

The core MRI protocol parameters were adjusted according to scanner vendor and strength of the magnet (Table 2.3) available at each trial site.

Upon receipt images to the central MRI facility (Queen Square MS Centre Trial Office) and after quality control performed by an experienced neuroimaging analyst blind to patient's details, approved MRI scans were analysed.

Table 2.3 Core MRI acquisition parameters according to scanner model

Scan	Dual echo PD/T2 weighted FSE/TSE	T2 weighted FLAIR	T1 weighted SE	3D-T1 weighted volumetric MPRAGE/IRF SPGR/TFE
Slice orientation	Axial-oblique	Axial-oblique	Axial-oblique	Sagittal-oblique
1st TE Siemens 1.5T/3T	11/26ms	122/100ms	12/6.8ms	3.45/4ms
1st TE GE 1.5T/3T	21/24ms	128/127ms	20/20ms	5/3ms
1st TE Philips 1.5T/3T	16/13ms	120/120ms	20/10ms	4/3.2ms
2nd TE Siemens 1.5T/3T	86/97ms	n/a	n/a	n/a
2nd TE GE 1.5T/3T	86/85ms			
2nd TE Philips 1.5T/3T	100/90ms			
TR Siemens 1.5T/3T	2680/2700ms	9500/9500ms	518/600ms	2400/2400ms
TR GE 1.5T/3T	2900/2600ms	10000/9500ms	650/700ms	13/8ms
TR Philips 1.5T/3T	3300/2900ms	10000/9500ms	600/600ms	12/6.9ms
TI Siemens 1.5T/3T	n/a	2400/2400ms	n/a	1000/1000ms
GE 1.5T/3T		2200/2400ms		650/450ms
Philips 1.5T/3T		2400/2400ms		950/830ms
Number of slices	≥46	≥46	≥46	≥176
Slice thickness	**3mm**	**3mm**	**3mm**	**1mm**
Slice gap	**0mm**	**0mm**	**0mm**	**0mm**
Echo train length Siemens 1.5T/3T	5/7	19/15	n/a	n/a
Echo train length GE 1.5/3T	8/10	19/19		
Echo train length Philips 1.5/3T	6/5	19/19		
Field of View	**25cmsx100%**	**25cmsx100%**	**25cmsx100%**	**25cmsx100%**
Image matrix acquisition (frequency x phase)	**256x256**	**256x192**	**256x256**	**256x256**
Image matrix reconstruction (frequency x phase)	**256x256**	**256x256**	**256x256**	**256x256**
Reconstructed pixel size	**0.976**	**0.976**	**0.976**	**0.976**
Frequency encoding	**a/p**	**a/p**	**a/p**	**s/i**
Phase encoding	**r/l**	**r/l**	**r/l**	**a/p**
No of averages (excitations) 1.5T/3T	**1/1**	**1/1**	**2/1**	**1/1**
Flip angle Siemens	**-**	**-**	**-**	8°
Flip angle GE				20°
Flip angle Philips				8°

Reference parameters guidance depending on scanner model (i.e. Siemens, Philips, GE) and operating field strength (i.e. 1.5T or 3T). The values listed in bold were mandatory for all of the sites. Abbreviations: FLAIR= Fluid-Attenuated Inversion Recovery. FSE/TSE= Fast/Turbo Spin Echo. IRFSPGR: inversion recovery fast spoiled gradient echo. MPRAGE= magnetization prepared rapid gradient echo. PD= proton density. SE= Spin Echo. TFE= turbo field echo. a/p= anterior/posterior. s/i= superior/inferior; r/l= right/left.

The advanced MRI protocol - carried out as an optional sub-study at UCL and Edinburgh included the following additional MRI sequences at baseline and week 96:

- Brain MTR (at UCL and Edinburgh);
- Brain Proton (1H) MR spectroscopy (at UCL and Edinburgh);
- Brain DTI (at Edinburgh only);
- Cervical cord 3D-phase sensitive inversion recovery (3D-PSIR) (at UCL only).

Table 2.4 reports the acquisition parameters at both trial sites. The parameters differ between the two sites due to different scanners in use: at UCL, a Philips Achieva 3T scanner; at Edinburgh, a Siemens Verio 3T scanner.

Table 2.4 Advanced MRI acquisition parameters at UCL

	MTR	**MRS**	**3D-PSIR**
slice orientation	sagittal	axial	Axial oblique
first TE	2.7ms	35ms	6.147
second TE	4.3ms	n/a	n/a
TR	6.45ms	2000ms	12.38
TI	n/a	n/a	n/a
Number of slices	180	50	12
slice thickness	**1mm**	**15mm**	**3mm**
slice gap	0mm	0mm	0mm
Echo train length	4	n/a	128
Field of View	**25cms**x100%	2**4cms**x75%	**25cms**x50%
Image matrix acquisition (frequency x phase)	**256x256**	**240x240**	**512x512**
Image matrix reconstruction (frequency x phase)	**256x256**	**256x256**	**512x512**
Reconstructed pixel size	**1x1mm**	**1x1mm**	**0.5x0.5mm**
Frequency encoding	**a/p**	**a/p**	**s/i**
Phase encoding	**r/l**	**r/l**	**a/p**
number of averages (excitations)	**1**	**1**	**3**
Flip angle	**9°**	**-**	8°

MTR: magnetization transfer ratio. MRS: magnetic resonance spectroscopy. 3D-PSIR: 3-Dimensional phase sensitive inversion recovery.

2.3.5.1 T2 lesion analysis

An experienced MRI analyst identified T2-hyperintense brain lesions PD scans with the support of T2-weighted and FLAIR scans. A semi-automated edge-finding tool (JIM7, Xinapse systems, UK) was used to outline lesions and calculate T2 lesion volume (T2LV). The lesion load at baseline was recorded and quality-checked by a second image reader. I quality-checked n=110 T2LV masks at baseline (Figure 2.4).

PD/T2 scans between the follow-up timepoints 24 and 96 weeks were registered with the baseline scans. Registered FLAIR scans were also used to facilitate the identification of new lesions. For the count of new and enlarging T2 lesions, a scan was obtained from the intensity difference of two timepoint registered PD scans (i.e. between baseline and 24 weeks and between baseline and 96 weeks). This intensity subtraction scan facilitated the identification of newly developed hyperintensities, which were reviewed to confirm whether the new hyperintensities corresponded to new PD/T2 lesions. I checked all the PD subtraction scans at 24 weeks and 96 weeks (Figure 2.4).

Figure 2.4 T2 lesion analysis

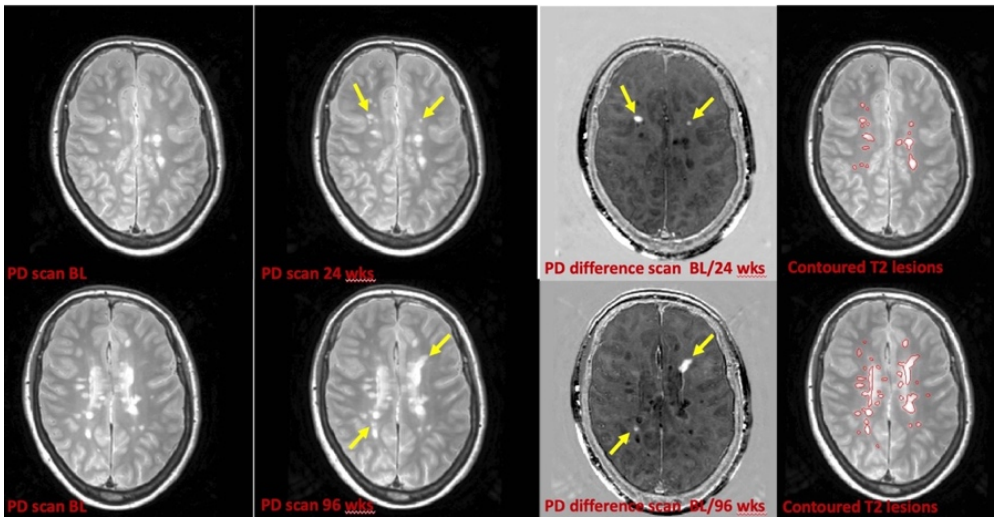

Yellow arrows: new lesions seen on PD scans and on subtraction scans.

2.3.5.2 Normalised brain volume analysis

We measured cross-sectional brain volume at baseline using the SIENAX method, part of the FMRIB Software Library (FSL, www.fmrib.ox.ac.uk/fsl). SIENAX is a registration-based method where each image voxel from each subject included in the study is geometrically aligned to a specific anatomical location of a template

image to ensure consistency across all subjects for group analysis. The standard template used in MS-SMART was the Montreal Neurological Institute (MNI)152 – the template most commonly used in registration-base cross-sectional analyses - which contains an average of 152 healthy adults (Smith *et al.*, 2002). The sequences used to measure brain volume are 3D-T1-weighted images.

The pipeline used for measuring normalised brain volume in MS-SMART is as follows (Figure 2.5):

1) ***Image reorientation.*** This is a rotation of the image necessary to rearrange its axes directions so that they match the MNI-152 standard template. In this template, the first image axis in the left-right axis, the second axis is the posterior-anterior axis, and the third axis is the inferior-superior axis.
2) ***Bias field correction.*** The bias field, caused by radiofrequencies inhomogeneities, results in parts of the image being brighter or darker than they should be. This can be avoided by bias-field correction. We bias field corrected the 3D-T1 scans using niftk (TIG, http://cmictig.cs.ucl.ac.uk).
3) ***T1-lesion filling.*** MS lesions influence the process of image analysis, causing tissue segmentation problems and biased morphometric estimates. We registered the T2-weighted scans on to 3D-T1 scans using reg_aladin (TIG, http://cmictig.cs.ucl.ac.uk) and registered the lesions to 3D-T1 scans using T2->T1 transform. Finally, we used the T2-weighted lesion masks (in T1 space) to fill the lesions on 3D-T1 using niftkT1PDT2lesions.ny (TIG, http://cmictig.cs.ucl.ac.uk). In other words, using the manually obtained T2-lesion mask, we applied a 3D-T1 lesion filling strategy based on in-painting techniques for image completion. This technique makes use of a patch-based Non-Local Means algorithm that fills the lesions with the most plausible texture, such as grey matter or white matter-like intensities (Prados *et al.*, 2014).

4) ***Brain extraction.*** In this step, non-brain structures are removed from the image to create a brain mask (i.e a binary image where voxels outside the brain contain a value of 0 and voxels inside contain a value of 1). This is useful to avoid non-brain parts from adversely affecting the results. In MS-SMART, the Geodesical Information Flows (GIF) algorithm, part of the NiftySeg software (TIG, http://cmictig.cs.ucl.ac.uk), was used to extract and segment the brain (Cardoso *et al.*, 2015).

5) ***Tissue segmentation.*** We performed a tissue-type segmentation to identify grey matter, white matter and CSF. This kind of segmentation is based on differences in the tissue intensities from T1-weighted imaging. However, noise and bias fields can affect voxel intensities and, ultimately, a correct segmentation. A common approach to overcome this, other than use a correction of the bias-field (as described above), is to use neighbourhood information in addition to the intensity information. For instance, if the intensity of a voxel matches that of white matter but all voxel surrounding this voxel have intensity matching grey matter, it is more likely that this voxel actually contains grey matter and that noise has caused the intensity to be abnormal. The GIF algorithm was also applied to segment the brain.

6) ***Registration to the MNI152 standard template and brain atrophy estimates.*** This step was done applying SIENAX, which uses brain extraction and tissue-type segmentation to find brain volume and then brain-and-skull-based registration to normalise (for head size) to standard space (using the skull image for the scaling), to reduce inter-subject variability. SIENAX uses the skull image to determine the registration scaling, in order to obtain the volumetric scaling factor to be used as a normalisation for head size. SIENAX has been shown to be accurate to

better than 1% error in normalised brain volume (FSL, www.fmrib.ox.ac.uk/fsl).

Figure 2.5 Normalised brain volume pipeline

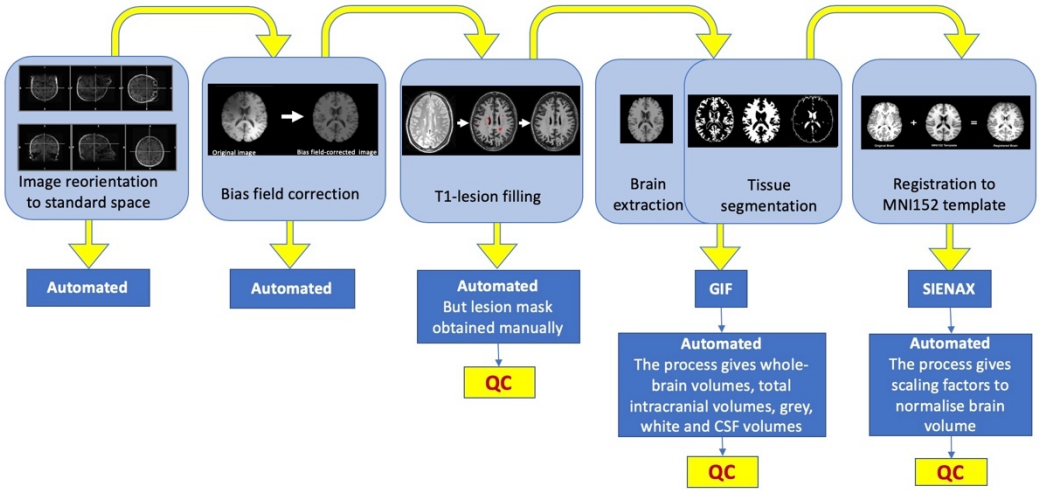

CSF= cerebrospinal fluid; GIF= Geodesical Information Flows; MNI= Montreal Neurological Institute; QC= quality check; SIENAX= Structural Image Evaluation, using Normalisation, of Atrophy cross-sectional.

2.3.5.3 Longitudinal brain atrophy analysis: PBVC

The PBVC was quantified using the SIENA method as previously described (Smith *et al.*, 2002, 2004). This method was used to calculate the PBVC at 96 weeks and to estimate occurrence of pseudoatrophy at 24 weeks.

As for the cross-sectional analysis of normalised brain volume, 3D-T1 baseline and follow-up scans (i.e. 24-week and 96-week scans) were reoriented, bias-field corrected and the 3D-T1 scans were lesion filled. The scans were then analysed with GIF, which extracted the brain and gave additional measures of total intracranial volume, grey matter (deep grey matter plus cortical grey matter), white matter, and CSF volumes for the two timepoint scans. The resulting brain volumes

between the two timepoints were co-registered and the SIENA algorithm was applied to calculate the PBVC. Differently from the normalised brain volume pipeline, here the registration is done between different timepoint scan in within subjects, and not across subjects by registering a single timepoint scan to a standard common template (Figure 2.6).

Figure 2.6 Longitudinal brain atrophy analysis pipeline

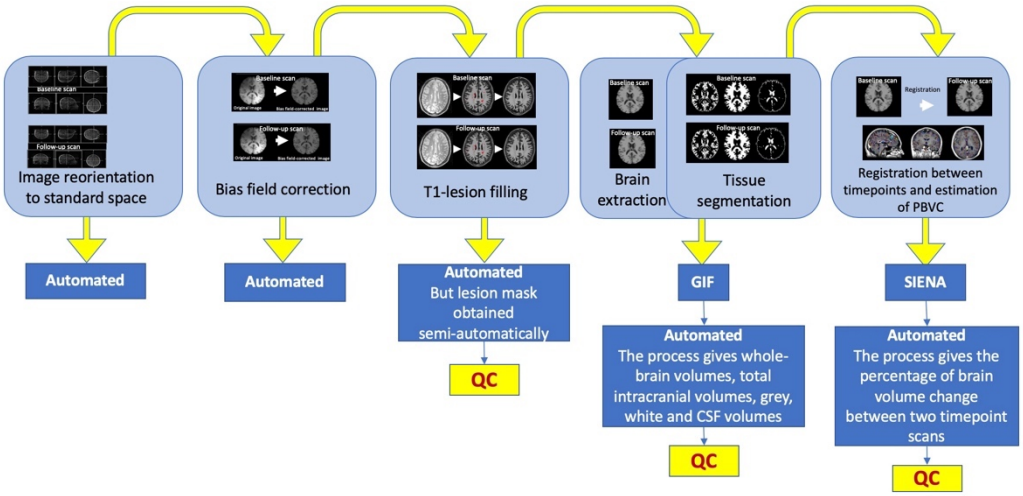

CSF= cerebrospinal fluid; GIF= Geodesical Information Flows; PBVC= percentage brain volume change; QC= quality check; SIENA= Structural Image Evaluation, using Normalisation, of Atrophy.

2.3.6 Statistical analysis for the longitudinal study

Exploratory summary methods were used to describe baseline characteristics: continuous variables are summarised using summary statistics (mean, standard deviation, median, interquartile range [IQR], minimum and maximum) by treatment group, and categorical variables are presented using frequencies and percentages by treatment group. Proportions of patients with missing 96-week MRI and follow-up visit data in each treatment group were summarised.

For the MSFC, Z scores were normalised with the study baseline scores. When a subject was unable to complete the 9HPT due to disability, a score of 777 seconds

was allocated (Cutter *et al.*, 1999). Where a subject was unable to complete the T25FW due to disability, a score of 180 seconds was allocated (Fischer *et al.*, 1999). In the event an individual patient was unable to complete the PASAT due to disability, a score of 0 was assigned.

2.3.6.1 Sample size

The sample size was calculated based on the study reported by Altmann and colleagues (Altmann *et al.*, 2009) for measurement of PBVC using the SIENA method in SPMS. Ninety patients per arm would give over 90% power to detect a 40% reduction in PBVC on any active arm compared to placebo and 80% power to detect a 35% reduction, using Bonferroni adjustment for multiple comparisons of three 1.67% two-sided tests, giving 5% overall two-sided significance level (Table 2.5). For a more exploratory analysis without adjusting for multiple comparisons, this sample size would give almost 90% power to detect a 35% reduction in atrophy (Table 2.5). Additionally, based on the experience from two UK phase II trials (Kapoor *et al.*, 2010; Chataway *et al.*, 2014), we expected 10% of the total cohort to drop out of the trial before week 48, and a further 10% of the total cohort to come for their week 96 visit, but be off medication. According to these figures, a total of 440 patients to be randomised equally (1:1:1:1) between the three active treatments and the placebo (i.e. 110 participants per treatment arm) would anticipate 90 participants per arm to complete the study.

Table 2.5 Required sample size per arm

MRI MEASUREMENT TIMES	**BASELINE - 96 WEEKS**			
2-sided significance level	0.0167		0.05	
Statistical power	**80%**	**90%**	**80%**	**90%**
Treatment effect:				
• **30%**	123	158	92	123
• **35%**	90	116	68	91
• **40%**	69	89	52	70

2.3.6.2 Primary MRI outcome measure

A normal linear model was used to compare each of the three active treatment group arms with placebo, adjusting for baseline normalised brain volume (BNBV) and minimisation variables: age, gender, treatment centre (as a fixed effect), and baseline EDSS. BNBV, age and baseline EDSS were entered into the model as continuous variables. Other minimisation variables were included in the models according to the categories used in the randomisation. The efficacy measure for each active treatment was the mean difference in PBVC change versus placebo. All patients for whom baseline and 96-week brain volume data were available were included in the analysis according to the treatment group to which they were randomised irrespective of which treatment(s) they might have received. Dunnett's method was used to adjust for the multiple pairwise comparisons versus a common placebo group. No formal comparisons of the active treatments were undertaken. The primary analysis was on complete cases. Three sensitivity analyses, based on pattern mixture modelling, standard multiple imputation and exclusion of extreme outliers on the primary outcome were used to explore the effect of missing data on the primary outcome analysis.

2.3.6.3 Counts of new and enlarging T2 lesions

Each active treatment group was compared with placebo for the number of new and enlarging T2 lesions between the baseline and 96-week MRI. Overdispersed Poisson regression models were used to estimate a rate ratio for each comparison after adjusting for baseline T2 lesion volume and the minimisation variables age, gender, treatment centre, and baseline EDSS.

2.3.6.4 Pseudoatrophy

Using the same methods as for the primary MRI outcome analysis, the mean difference in PBVC from baseline to 24 weeks between the placebo group and each of the active treatment groups was also assessed. If the reduction in PBVC was significantly greater in any treatment group, a secondary analysis was performed to compare PBVC from week 24 to week 96 between that treatment group and the placebo group using normal linear modelling as described for the primary outcome measure.

2.3.6.5 Clinical secondary outcome measures

If the change over time in continuous outcomes (EDSS, 9HPT, PASAT, MSFC, SDMT, SLCVA, MSIS29v2, MSWSv2, NFI, NPRS, NPS, BPI and EQ-5D-5L) was found to be normally distributed, following transformation where necessary, comparison was made between active treatments and the placebo group using normal linear models as for the primary outcome measure. If normality could not be assumed, an unadjusted non-parametric Mann-Whitney test was used to compare each active treatment to placebo. For NPS, the same method was used as for the other continuous outcome, but applied to the individual questionnaire items, with the exception of the components of item 8 which was analysed using logistic regression. Cox proportional hazard models (adjusting for the minimisation variables) were used for time to first relapse and T25FW, with the difference between each active treatment and placebo being expressed in terms of a hazard ratio.

Chapter 3. **MS-SMART: baseline results**

Mr Richard Parker from the Edinburgh Clinical Trials Unit performed the majority of the statistical analyses. Mr Jonathan Stutters assisted with the MRI analysis. Mrs Carolina Crespo helped with the manual segmentation of the T2 lesions. Dr Alberto Calvi helped with the T2 lesion segmentation quality check. Mr David MacManus, Dr Ferran Prados and Professor Frederik Barkhof reviewed uncertain image analysis results.

3.1. Introduction

The purpose of this study was to explore the baseline data from the MS-SMART trial cohort to identify clinical and MRI metrics that best characterised a large contemporary cohort of patients with SPMS in the UK. We also focused on the added value of patient-reported outcome measures in clinical trials.

In summary, in this Chapter, I:

1. Describe the trial recruitment phase;
2. Describe demographic, clinical and MRI characteristics of the trial cohort;
3. Investigate the strongest associations between clinical and MRI variables;
4. Identify clinical or MRI predictors of disease severity;
5. Look at the prognostic role of optic neuritis as a symptom at MS onset;
6. Explore the relationships between cardiovascular comorbidities and MS severity;
7. Investigate the relationships between patient and clinician-reported outcome measures.

3.2. Methods

3.2.1 Participants and outcomes

In this study, I included all the patients enrolled in the MS-SMART trial at the thirteen participating UK centres. The eligibility criteria are described in Chapter 2. The measures used in the statistical analyses are reported in Table 3.1.

Table 3.1 Variables used for the statistical analyses

DEMOGRAPHIC	CLINICAL	MRI
Age	EDSS	Whole Brain Volume
Sex	MSFC	Cortical Grey Matter Volume
Disease duration	T25FW	Deep grey matter Volume
Disease progression	9HPT	White matter Volume
Relapse number	PASAT	T2 lesion volume
BMI	SDMT	
Comorbidities	HCVA 100%	
- Hypertension	SLCVA 5%	
- Hyperlipidaemia	SLCVA 2.5%	
- Hypothyroidism	SLCVA 1.25%	
- Asthma	MSIS-29v2 total	
- Depression	MSIS-29v2 physical	
- Osteoporosis	MSIS-29v2 psychological	
- Hysterectomy	MSWSv2	
- Other	BDI-II	
	EQ-5D-5L	

9HPT: 9-hole peg test. BDI-II: Beck Depression Index version 2. BMI: body mass index. EQ-5D-5L: EuroQuol 5-level version. EDSS: expanded disability status scale. HCVA: high contrast visual acuity. SLCVA: Sloan low contrast visual acuity. MSFC: multiple sclerosis functional composite. MSIS-29v2: multiple sclerosis impact scale 29 items version 2. PASAT: paced auditory serial addition test. SDMT: symbol digit modalities test. T25FW: timed 25-foot walk test. MSIS-29v2: multiple sclerosis impact scale 29 items version2. MSWSv2: multiple sclerosis walking scale version 2.

As discussed in Chapter 2, the core MRI protocol was the same across the thirteen study sites, although sequence settings varied according to the available scanner vendor and magnet strength. The following baseline MRI measures were used for the purposes of this Chapter (Table 3.1): T2 Lesion volume, normalised (whole) brain volume, normalised deep grey matter volume, normalised cortical grey matter volume, and white matter volume.

I provide a detailed description of the MRI analyses in Chapter 2 and Figures 2.4-2.6.

3.2.2 Statistical analysis

For the descriptive statistics of the data, I used mean and standard deviation (SD) or median and minimum (Min) and maximum (Max) for continuous data, and proportions for categorical data. I present the data by mean of contingency tables.

The disease duration was defined as the number of years since the first clear neurologic symptom due to MS, as reported by patients and confirmed by medical records. The disease progression (or progression duration) was defined as the number of years since evidence of gradual clinical deterioration started independently of relapses. The relapse rate was the one calculated in the two years before trial recruitment.

All the statistical analyses presented in this Chapter were carried out at the patient level and not at the eye level. For that reason, visual measures (i.e. high and low contrast visual acuity) from only one of the two eyes were used per subject. We arbitrarily decided *a priori* to use the visual scores from left eyes only. This approach was adopted following recommended reporting guidelines (Cruz-Herranz *et al.*, 2016).

All the MRI brain volume measures used in this study were normalised using SIENAX.

The 9HPT values here are the result of the reciprocal of the average between right and left arm. This means that a higher 9HPT corresponds to less upper limb disability.

To analyse the relationship between clinical and MRI variables, we used several methods. Firstly, we performed correlation analyses between clinical and MRI variables. This analysis was useful to provide an overview on the data showing the strongest associations between the examined variables. We then performed more sophisticated analyses which included multivariate exploratory analyses using principal component analysis (PCA), least absolute shrinkage and selection operator (LASSO) regression analysis and multivariate analysis of variance (MANOVA).

Finally, I investigated in more details the cross-sectional relationship between clinical and patient-reported outcome measures using multivariable linear regression analyses.

3.2.2.1 Correlation analysis

Pearson's correlations were calculated for MRI and clinical variables.

3.2.2.2 Principal component analysis

The central idea of using PCA was to reduce the dimensionality of our data set consisting of a large number of interrelated variables, while retaining as much as possible of the variation present in the data set. PCA is a suitable method to achieve that, as the used variables are transformed to a new set of variables - the

principal components - which are uncorrelated and ordered so that the first few retain most of the variation present in all of the original variables (Jolliffe IT, 2002).

PCA was assessed separately in three models (Table 3.2): 1) a model including only MRI variables (MRI PCA); 2) a model including only clinical variables (Clinical PCA); 3) a combined model including MRI and clinical variables (Combined PCA). For the Clinical PCA model, we run two separate analyses: (i) Clinical PCA Model 1, which included both clinical and demographic data; (ii) Clinical PCA Model 2, which did not include demographic data and was restricted to clinician and patient-reported outcome measures (Table 3.2).

Table 3.2 Variables used in the principal component analysis models

PCA model	Variables
MRI PCA	- cortical grey matter volume - deep grey matter volume - T2 lesion volume - white matter volume - whole brain volume
CLINICAL PCA Model 1	- 9HPT - age - BMI - disease duration - disease progression - EDSS - MSIS-29v2 physical score - MSIS-29v2 psychological score - MSIS-29v2 total score - PASAT - SDMT - SLCVA 2.5% (left eye) - T25FW
CLINICAL PCA Model 2	- 9HPT - EDSS - MSIS-29v2 physical score - MSIS-29v2 psychological score - MSIS-29v2 total score - PASAT - SDMT - SLCVA 2.5% (left eye) - T25FW

COMBINED PCA	- Cortical grey matter volume - Deep grey matter volume - T2 lesion volume - White matter volume - Whole brain volume - 9-HPT - EDSS - MSIS-29v2 physical score - MSIS-29v2 psychological score - PASAT - SDMT - SLCVA 2.5% (left eye) - T25FW

9HPT: 9-hole peg test. BDI-II: Beck Depression Index version 2. BMI: body mass index. EDSS: expanded disability status scale. HCVA: high contrast visual acuity. SLCVA: Sloan low contrast visual acuity. MSFC: multiple sclerosis functional composite. MSIS-29v2: multiple sclerosis impact scale 29 items version 2. PASAT: paced auditory serial addition test. SDMT: symbol digit modalities test. T25FW: timed 25-foot walk test. MSIS-29v2: multiple sclerosis impact scale 29 items version2. MSWSv2: multiple sclerosis walking scale version 2.

3.2.2.3 LASSO regression analysis

LASSO regression is a regularisation and variable selection method for statistical models. It improves the prediction accuracy and interpretability of regression models by altering the model fitting process to select only a subset of the provided covariates for use in a final model. LASSO analysis identifies the most important variables (a sub-set of variables) associated with the response variable (or outcome). LASSO regression is a method that can help in interpretation of associations between variables when the number of variables is high and the number of observations is low. With LASSO, the regression coefficients for unimportant variables are reduced to zero, which effectively removes them from the statistical model, producing a simpler model that includes only the strongest predictors of outcome.

We used LASSO regression analyses to identify the clinical variables which could better predict a specific MRI outcome (i.e. whole brain volume or cortical grey

matter volume or deep grey matter volume or white matter volume, or T2 lesion volume).

In the first stage (Model A), a list of pre-specified clinical variables (EDSS, MSFC, 9HPT, T25FW, SDMT, PASAT, and SLCVA 2.5%) were included as explanatory variables in a LASSO regression model on each of the MRI variables separately (whole brain volume, deep grey matter volume, cortical grey matter volume, white matter volume, T2 lesion volume). The pre-selected variables were chosen based on the fact that they could give a comprehensive overview of disability severity from different perspectives: lower limb (walking) impairment, upper limb impairment, vision and cognitive performance, and overall disability.

In the second stage (Model B), we expanded the set of predictors by including BMI and number of years since diagnosis. We also included any additional baseline variables that did not add to the overall percentage of missing data. Variables not adding to the overall missing data percentage were: age, sex, race, relapse in past 2 years (yes/no), centre (as 3-category fixed effect), HCVA, SLCVA 5%, EQ-5D-5L, MSWSv2, Beck Depression Index II (BDI-II), MSIS-29v2 (i.e. total score and physical/psychological sub-scores), comorbidity (i.e. asthma, depression, hypertension, hypothyroidism, hyperlipidaemia, osteoporosis, hysterectomy, other).

The Schwarz Bayesian Criterion (SBC) was used to select the optimum shrinkage/penalty function and hence determine how many variables should be included in the models.

3.2.2.4 MANOVA analysis

To investigate the association between optic neuritis as MS symptom onset and disease severity outcomes (i.e. to understand the prognostic role of optic neuritis as symptom onset), and if a history of hypertension and hyperlipidaemia was able to drive a worse severity of MS, we performed multivariate two-group comparison test (comparison between patients with vision problems at onset and patients without vision problems at onset). In practice, we performed multivariate analysis of variance (MANOVA) based on all disease severity outcomes (EDSS, MSFC, SDMT, and SLCVA 2.5%). For the two-sample t-tests we used the Satterthwaite version of the t-test assuming unequal variances between groups for each outcome. The Cochran–Armitage test for trend was used to perform between-group comparisons for ordinal variables and confirm the results for EDSS score (which is an ordinal categorical variable rather than continuous). We used the same MANOVA method as above to compare patients: (i) with and without hypertension and (ii) those with and without hyperlipidaemia.

3.2.2.5 Association between clinician and patient-reported measures

To explore the relationship between patient and clinician-reported outcomes in the trial cohort, we used the two main clinical composite measures EDSS and MSFC, and the MSIS-29v2, which is one of the most common patient-reported questionnaires used in MS.

Firstly, we calculated Kendall's tau (τ) correlation coefficients to look at the direct relationship between the above variables.

To further investigate the association between MSFC/EDSS and total MSIS-29v2 score, considering that the association between clinical variables and patient

reported questionnaire might not be linear, we divided the MSFC and EDSS scores into quartiles and then included them in a multiple linear regression model with MSIS-29v2 score as the outcome variable and with the top three quartiles of MSFC or EDSS score as dummy variables (the lowest quartile of data was the reference category). We also adjusted for age, sex, disease duration, and site. Site was categorised into 4 categories for the regression model according to the largest sites (UCL, Edinburgh, Sheffield, Other site: with UCL as the reference category).

3.3. Results

3.3.1 Baseline characteristics

A total of 547 subjects were consented and screened between December 2014 and June 2016 at thirteen UK neuroscience centres. The first subject was screened on 18th December 2014, and the first subject was randomised on 29th January 2015. The last patient was randomised on 22nd June 2016, while the last patient last visit occurred on 4th July 2018.

Of the 547 subjects consented and screened, 445 (81% of total screened) met all eligibility criteria and were consecutively randomised onto one of the three active treatments or placebo. The rate of screening and randomisation are reported in Figure 3.1. There were 244 patients originally consented to the advanced MRI sub-study, 308 to the OCT sub-study and 84 to the CSF sub-study. There were 206 patients randomised to the advanced MRI sub-study, 260 to the OCT sub-study and 70 to the CSF sub-study.

The results of the spinal cord advanced MRI and OCT sub-studies are reported in Chapters 6 and 7.

Figure 3.1 Cumulative number of patients screened and randomised

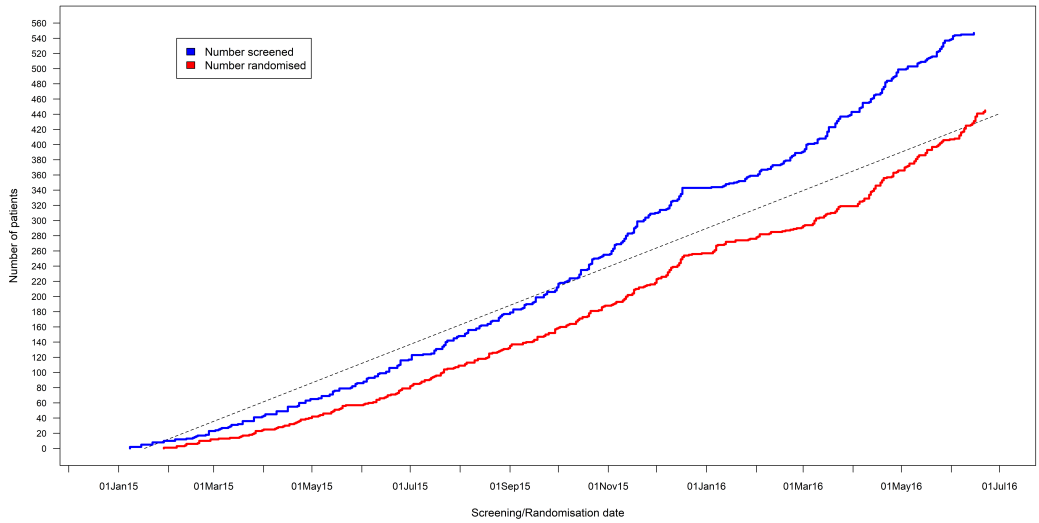

The proportion of patients randomised at each site and the distribution of treatment allocation across sites are reported in Figure 3.2.

Figure 3.2 Distribution of patients and treatment across the sites

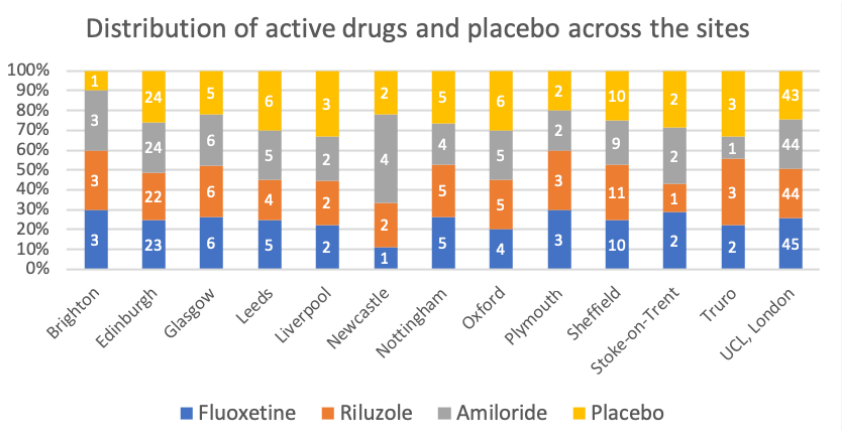

Demographic characteristics of the participants are shown in Table 3.3. The clinical characteristics, including EDSS, MSFC with three sub-components (9HPT, T25FWT, PASAT), SDMT, high and low contrast visual acuity and MSIS-29v2 total and the two sub-component scores (physical and psychological) are reported in Table 3.4.

Table 3.3 Baseline demographic characteristics

		Fluoxetine	Riluzole	Amiloride	Placebo	Overall
Age	*N*	111	111	111	112	445
	Mean	54.83	54.10	54.36	54.89	54.55
	SD	7.10	6.75	7.177	7.16	7.03
Gender						
Male	*N (%)*	37 (33.3)	37 (33.3)	36 (32.4)	37 (33)	147 (33)
Female	*N (%)*	74 (66.7)	74 (66.7)	75 (67.6)	75 (67)	298 (67)
Race						
White	*N (%)*	105 (94.6)	106 (95.5)	108 (97.3)	108 (96.4)	427 (96)
Black	*N (%)*	1 (0.9)	1 (0.9)	2 (1.8)	1 (0.9)	5 (1.1)
Asian	*N (%)*	4 (3.6)	3 (2.7)	1 (0.9)	2 (1.8)	10 (2.2)
Other	*N (%)*	1 (0.9)	1 (0.9)	0 (0)	1 (0.9)	3 (0.7)
Disease	*N*	110	109	107	109	435
duration,	*Mean*	22.47	21.94	21.40	20.73	21.64
years	*SD*	9.59	9.58	9.921	9.66	9.68
Disease	*N*	111	110	111	111	443
progression,	*Mean*	7.44	7.86	7.793	7.05	7.54
years	*SD*	5.74	5.7	5.520	5.66	5.65
Relapse	*N*	111	111	110	112	444
Count	*Mean*	0.1	0.09	0.19	0.15	0.13
(pre-	*SD*	0.36	0.42	0.57	0.51	0.47
enrolment),	*Media*					
number	*n*	0	0	0	0	0
	Min	0	0	0	0	0
	Max	2	3	4	3	4

Table 3.4 Baseline clinical characteristics

		Fluoxetine	Riluzole	Amiloride	Placebo	Overall
EDSS score	*N*	111	111	111	112	445
	Median	6.0	6.0	6	6.0	6.0
	Min	4.0	4.0	4	4.0	4.0
	Max	6.5	6.5	6.5	6.5	6.5
EDSS Band						
4.0-5.5	*N (%)*	28 (25.2)	28 (25.2)	29 (26.1)	29 (25.9)	114 (25.6)
6.0-6.5	*N (%)*	83 (74.8)	83 (74.8)	82 (73.9)	83 (74.1)	331 (74.4)
BDI-II	*N*	111	111	111	112	445
	Median	6	7	6	7	6.0
	Min	0	0	0	0	0
	Max	18	18	18	18	18

		Fluoxetine	Riluzole	Amiloride	Placebo	Overall
MSFC z-score	*N*	111	111	111	112	445
	Mean	-0.033	-0.10	-0.176	0.004	-0.077
	SD	0.61	0.96	1.195	0.912	0.942
PASAT no. correct answer	*N*	110	111	111	112	444
	Mean	36.6	36.91	39.018	41.464	38.509
	SD	15.17	16	13.667	13.864	14.784
T25FW sec	*N*	109	111	111	112	443
	Mean	15.7	19.84	25.136	18.633	19.842
	SD	12.38	28.46	38.843	28.530	28.819
9HPT - sec	*N*	111	111	111	112	445
	Mean	0.03	0.03	0.034	0.033	0.034
	SD	0.01	0.01	0.011	0.010	0.010
SDMT no. correct answer	*N*	111	109	109	112	441
	Median	46	45	46	46.500	46
	Min	17	18	17	13	13
	Max	67	74	72	75	75
HCVA 100% OD no. correct answer	*N*	111	110	106	110	437
	Mean	52.72	48.78	48.821	49.918	50.078
	SD	7.27	14.84	13.975	13.430	12.772
	Median	53	54	53.500	54	54
	Min	25	0	0	0	0
	Max	65	65	62	63	65
HCVA 100% OS no. correct answer	*N*	111	110	107	111	439
	Mean	51.12	48.56	50.093	50.423	50.052
	SD	11.09	14.92	11.211	12.708	12.574
	Median	54	54	53	55	54
	Min	4	0	0	0	0
	Max	65	65	62	64	65
SLCVA 5% OD no. correct answer	*N*	110	108	106	109	433
	Mean	35.15	30.71	31.660	34.147	32.938
	SD	10.46	15.38	14.521	14.624	13.935
	Median	35	32	35	38	35
	Min	0	0	0	0	0
	Max	57	56	60	60	60
SLCVA 5% OS no. correct answer	*N*	110	108	107	110	435
	Mean	32.93	29.96	32.579	33.927	32.359
	SD	12.82	16.13	13.401	14.575	14.311
	Median	34.5	34.5	35	36	35
	Min	0	0	0	0	0
	Max	56	55	59	60	60
SLCVA 2.5% OD no. correct answer	*N*	111	109	106	110	436
	Mean	19.86	19.12	19.896	20.736	19.906
	SD	12.28	14.50	13.155	13.692	13.395
	Median	19	18	20.500	22	19
	Min	0	0	0	0	0
	Max	50	55	48	58	58
SLCVA 2.5% OS no. correct answer	*N*	111	109	107	111	438
	Mean	17.65	18.81	19.103	20.847	19.103
	SD	12.36	14.16	12.709	13.978	13.331
	Median	18	20	19	22	20
	Min	0	0	0	0	0
	Max	39	50	45	58	58
SLCVA 1.25% OD no. correct answer	*N*	111	109	106	110	436
	Mean	8.94	7.69	9.066	9.845	8.885
	SD	10.190	10.68	10.247	11.326	10.616
	Median	5	1	5.500	5	4
	Min	0	0	0	0	0
	Max	40	43	42	42	43

		Fluoxetine	Riluzole	Amiloride	Placebo	Overall
SLCVA 1.25% OS no. correct answer	*N*	111	109	107	111	438
	Mean	6.94	7.08	8.17	9.86	8.02
	SD	9.59	10.66	10.67	11.88	10.76
	Median	2	0	3	5	2
	Min	0	0	0	0	0
	Max	34	43	35	44	44
MSIS-29v2 Total score	*N*	111	111	111	112	445
	Mean	65	69.15	63.91	66.07	66.04
	SD	13.83	15.01	13.37	14.39	14.25
	Median	64	68	65	66	65
	Min	32	31	33	35	31
	Max	98	106	98	97	106
MSIS-29v2 Psychological score	*N*	111	111	111	112	445
	Mean	16.66	18.16	15.95	17.1	16.97
	SD	4.76	5.43	4.511	4.98	4.98
	Median	16	16	15	17	16
	Min	9	9	9	9	9
	Max	28	33	32	30	33
MSIS-29v2 Physical score	*N*	111	111	111	112	445
	Mean	48.34	50.99	47.97	48.97	49.07
	SD	10.44	11.30	10.5	11.22	10.9
	Median	49	51	48	48.5	49
	Min	23	21	24	25	21
	Max	74	77	70	74	77
MSWSv2	*N*	111	110	111	112	444
	Mean	41.08	42.64	41.43	41.63	41.69
	SD	9.77	9.32	9.18	9.93	9.54
	Median	44	45	42	44	43
	Min	14	14	14	18	14
	Max	54	54	54	54	54
EQ-5D-5L index	*N*	111	110	111	111	443
	Mean	0.70	0.66	0.68	0.67	0.68
	SD	0.16	0.17	0.17	0.18	0.17
	Median	0.72	0.67	0.73	0.72	0.71
	Min	0.17	0.12	0.12	0.17	0.12
	Max	0.95	1	1	0.94	1

9HPT: 9-hole peg test. EDSS: expanded disability status scale. HCVA: high contrast visual acuity. MSFC: multiple sclerosis functional composite. OD: right eye. OS: left eye. PASAT: paced auditory serial addition test. SDMT: symbol digit modalities test. SLCVA: Sloan low contract visual acuity. T25FW: timed 25-foot walk. MSIS-29v2: multiple sclerosis impact scale 29 items version 2. MSWSv2: multiple sclerosis walking scale version 2. EQ-5D-5L

Comorbidities were also recorded and are shown in Table 3.5. Seven conditions of interest were captured: asthma, depression, hypertension, hypothyroidism, hyperlipidaemia, osteoporosis, and hysterectomy.

Table 3.5 Comorbidities at baseline

Comorbidity	**Fluoxetine** N (%)	**Riluzole** N (%)	**Amiloride** N (%)	**Placebo** N (%)	**Overall** N (%)
Asthma	9 (8.1)	5 (4.5)	9 (8.1)	8 (7.1)	31 (7)
Depression	6 (5.4)	11 (9.9)	4 (3.6)	8 (7.1)	29 (6.5)
Hypertension	12 (10.8)	17 (15.3)	15 (13.5)	16 (14.3)	60 (13.5)
Hypothyroidism	9 (8.1)	15 (13.5)	7 (6.3)	10 (8.9)	41 (9.2)
Hyperlipidaemia	10 (9)	11 (9.9)	11 (9.9)	9 (8.0)	41 (9.2)
Osteoporosis	7 (6.3)	2 (1.8)	6 (5.4)	7 (6.3)	22 (4.9)
Hysterectomy	5 (4.5)	6 (5.4)	6 (5.4)	12 (10.7)	29 (6.5)
Other Condition	25 (22.5)	27 (24.3)	27 (24.3)	27 (24.1)	106 (23.8)

Finally, MRI characteristics, including T2 lesion volume and brain volume measures, are reported in Table 3.6.

Table 3.6 Baseline MRI characteristics

		Fluoxetine *N= 111*	**Riluzole** *N= 111*	**Amiloride** *N= 111*	**Placebo** *N= 112*	**Overall** *N= 445*
Whole Brain Volume *(ml)*	*Mean*	1413.07	1414.19	1432.18	1431.02	1422.63
	SD	82.41	74.85	84.23	91.15	83.58
Deep Grey Matter Volume *(ml)*	*Mean*	44.04	44.21	45.06	45.28	44.65
	SD	4.14	3.87	4.04	4.22	4.09
Cortical Grey Matter Volume *(ml)*	*Mean*	787.47	786.21	794.58	791.01	789.82
	SD	48.32	37.85	40.93	49.11	44.30
White matter (ml)	*Mean*	581.55	583.76	592.53	594.73	588.16
	SD	38.81	42.89	47.91	46.89	44.48
T2 Lesion Volume (ml)	*Mean*	14.12	12.99	12.98	13.65	13.44
	SD	12.75	12.26	12.38	12.47	12.43

3.3.2 Correlation analyses

Cortical grey matter volume and white matter volume were both very strongly correlated with whole brain volume (Pearson correlation coefficient of ≥ 0.90). There was a weak negative correlation between T2 lesion volume and all the other brain volume measures (Table 3.7).

Table 3.7 Correlations between MRI variables

Pearson Correlations (N=445)					
	Whole Brain Volume	**Deep Grey Matter Volume**	**Cortical Grey Matter Volume**	**White Matter Volume**	**T2 Lesion Volume**
Whole Brain Volume	1	0.75	0.90	0.91	-0.32
Deep Grey Matter Volume	0.75	1	0.62	0.69	-0.34
Cortical Grey Matter Volume	0.90	0.62	1	0.65	-0.30
White Matter Volume	0.91	0.69	0.65	1	-0.26
T2 Lesion Volume	-0.32	-0.34	-0.30	-0.26	1

We included twenty clinical baseline variables and five MRI outcomes (Table 3.8). There were N=407 total observations used in this analysis. Pearson's correlation coefficients above 0.3 are highlighted in Tables 3.8.

BMI has a moderate negative correlation with cortical grey matter volume. The SDMT score appeared to be moderately correlated with all the MRI outcomes. The PASAT shows a moderate negative correlation with T2 lesion volume (Table 3.8).

Table 3.8 Correlations between clinical, demographic and MRI variables

	Whole Brain Volume	**Deep Grey Matter Volume**	**Cortical Grey Matter Volume**	**White Matter Volume**	**T2 Lesion Volume**
Age	-0.07	0.01	-0.16	0.03	0.13
Disease duration	-0.13	-0.12	-0.09	-0.14	0.17
Disease Progression	-0.04	-0.00	-0.02	-0.05	0.10
BMI	-0.24	-0.17	**-0.33**	-0.11	-0.12
EDSS	-0.09	-0.07	-0.06	-0.09	0.13
T25FW	-0.02	-0.02	0.01	-0.03	0.06
9HPT	0.28	0.29	0.21	0.29	-0.23
PASAT	0.12	0.20	0.09	0.12	**-0.35**
MSFC	0.14	0.17	0.09	0.16	-0.24
SDMT	**0.36**	**0.36**	**0.30**	**0.34**	**-0.46**
HCVA	0.19	0.15	0.14	0.20	-0.12
SLCVA 5% (left eye)	0.19	0.14	0.12	0.21	-0.17
SLCVA 2.5% (left eye)	0.19	0.13	0.13	0.21	-0.19
SLCVA 1.25% (left eye)	0.11	0.07	0.05	0.16	-0.12
MSIS-29v2 Total	-0.05	-0.05	0.00	-0.09	0.16

MSIS-29v2 Physical	-0.05	-0.04	0.00	-0.09	0.16
MSIS-29v2 Psychological	-0.05	-0.06	-0.01	-0.07	0.11
EQ-5D-5L	0.02	-0.06	-0.01	0.05	-0.05
MSWSv2	-0.09	-0.07	-0.05	-0.11	0.09
BDI-II	-0.04	-0.08	-0.06	-0.01	0.04

9HPT: 9-hole peg test. BDI-II: Beck depression index verion 2. BMI: body mass index. EDSS: expanded disability status scale. HCVA: high contrast visual acuity. MSFC: multiple sclerosis functional composite. PASAT: paced auditory serial addition test. SDMT: symbol digit modalities test. SLCVA: Sloan low contract visual acuity. T25FW: timed 25-foot walk. MSIS-29v2: multiple sclerosis impact scale 29 items version 2. MSWSv2: multiple sclerosis walking scale version 2.

3.3.3 Principal component analyses

3.3.3.1 MRI outcomes PCA

Whole brain volume, deep grey matter volume, cortical grey matter volume, white matter volume and T2 lesion volume were used in this PCA model.

The first principal component (PC1) explained 69% of the variance which increased to 86% with the addition of the second principal component, and then to 94% with the third principal component.

The first principal component had the following form:

*PC1=0.53** whole brain volume + *0.46** deep grey matter volume + *0.47** cortical grey matter volume *+0.48** white matter volume – *0.25*T2Vol*

Therefore, the first principal component mainly represents a combination of total brain, grey matter, and white matter volume since the highest loadings are on whole brain volume, deep grey matter volume, cortical grey matter volume, and white matter volume (Table 3.9).

The second principal component (PC2) has the following form:

*PC2=0.16 **</* whole brain volume + *0.0007** deep grey matter volume + *0.12** cortical grey matter volume *+0.19** white matter volume + *0.96*T2 lesion volume*

Therefore, the second principal component mainly represents T2 lesion volume.

The third principal component (PC3) has the following form:

*PC3= -0.19** whole brain volume + *0.68** deep grey matter volume *-0.66** cortical grey matter volume *+0.25** white matter volume + *0.06** *T2 lesion volume*

Therefore, the third principal component mainly represents the contrast between deep grey matter volume and cortical grey matter volume.

Table 3.9 Loading of MRI variables in principal components

Principal Component	PC1	PC2	PC3
Whole Brain Volume	**0.53**	0.16	-0.19
Deep Grey Matter Volume	**0.46**	0.00	**0.68**
Cortical Grey Matter Volume	**0.47**	0.12	**-0.66**
While Matter Volume	**0.48**	0.19	0.25
T2 Lesion Volume	-0.25	**0.96**	0.06

The table shows loadings of the variables included in the principal component analysis into the three principal components. The variables with the largest loadings into each of the principal components are shown in bold. PC: principal component.

The variances explained by principal components PC1, PC2, and PC3 are 3.43, 0.85 and 0.41 respectively (out of a total variance of 5). The amount of variance explained by the first two principal components is 4.3, which is 86% of the total variance.

This analysis suggests that all five MRI variables are important in explaining the total observed variance.

3.3.3.2 Clinical outcomes PCA

In the first analysis (Clinical PCA Model 1), we found that the first principal component explained only 25% of the variance, the second 15%, the third 12%, and the remainder less than 10% each. In order to explain a reasonable proportion of the variance, at least 7 principal components were required.

In the second analysis (Clinical PCA Model 2, Table 3.10), the first principal component explained only 31% of the variance, the second 17%, the third 15%, and the remainder less than 11% each. In order to explain a reasonable proportion of the variance, at least 5 principal components were required. The Clinical PCA Model 2 provided the following factor loadings on the first three principal components (Table 3.10):

Table 3.10 Loading of clinical variables in principal components in Model 2

Principal Component	PC1	PC2	PC3
9HPT	**0.64**	-0.03	0.40
EDSS	-0.53	**0.52**	-0.15
MSIS-29v2 Physical	**-0.68**	0.39	0.44
MSIS-29v2 Psychological	-0.48	0.06	**0.76**
PASAT	0.55	**0.51**	0.08
SDMT	**0.73**	0.45	0.21
SLCVA 2.5%	0.39	0.40	-0.031
T25FW	-0.32	**0.56**	-0.44

The table shows loadings of the variables included in the principal component analysis into the three principal components. The variables with the largest loadings into each of the principal components are shown in bold. All the variables have similar loadings into each of the principal components. The first principal component consisted of mainly SDMT, MSIS-29v2 Physical, and 9HPT. The second principal component consisted of mainly EDSS, PASAT and T25FW. The third principal component consisted of mainly of MSIS-29v2 Psychological.
9HPT: 9-hole peg test. EDSS: expanded disability status scale. MSIS-29v2: multiple sclerosis impact scale 29 items version 2. PASAT: paced auditory serial addition test. PC1: first principal component. PC2: second principal component. PC3: third principal component. SDMT: symbol digit modalities test. SLCVA: Sloan low contract visual acuity. T25FW: timed 25-foot walk.

As seen for Model 1, also in this Clinical PCA Model 2, the first principal component explained only 31% of the variance, the second 17%, the third 15%, and the remainder less than 11% each. In both models, in order to explain a reasonable proportion of the variance (>80%), at least 7 and 5 principal components were required respectively. The loadings on each principal component (including the first one) were not easy to interpret and no clear patterns emerged. Therefore, the principal component analysis of the clinical variables did not provide any useful conclusions.

3.3.3.3 Combined clinical and MRI outcomes PCA

The first principal component explained only 32% of the variance, the second 16%, the third 10%, and the remainder less than 10% each. In order to explain a reasonable proportion of the variance, at least 6 principal components were required. The first principal component consisted mainly of the MRI variables plus SDMT score and, to a less extent, also 9HPT. The second principal component consisted mainly of MSIS-29v2 Physical score (Table 3.11).

Table 3.11 Loading of clinical and MRI variables in principal components in the Combined Model

Principal Component	PC1	PC2	PC3
Cortical Grey Matter Volume	**0.76**	0.40	-0.13
Deep Grey Matter Volume	**0.77**	0.31	-0.07
T2 Lesion Volume	**-0.55**	0.19	-0.35
White Matter Volume	**0.81**	0.33	-0.17
Whole brain volume	**0.87**	0.40	-0.16
9HPT	**0.52**	-0.32	-0.21
EDSS	-0.25	**0.52**	0.47
MSIS-29v2 Physical	-0.28	**0.71**	0.20
MSIS-29v2 Psychological	-0.22	0.49	-0.16

Principal Component	PC1	PC2	PC3
PASAT	0.43	-0.33	**0.53**
SDMT	**0.69**	-0.31	0.34
SLCVA 2.5%	0.36	-0.15	0.30
T25FW	-0.11	0.36	**0.58**

The table shows loadings of the variables included in the principal component analysis into the four principal components. The variables with the largest loadings into each of the principal components are shown in bold.
9HPT: 9-hole peg test. EDSS: expanded disability status scale. MSIS-29v2: multiple sclerosis impact scale 29 items version 2. PASAT: paced auditory serial addition test. PC1: first principal component. PC2: second principal component. PC3: third principal component. SDMT: symbol digit modalities test. SLCVA: Sloan low contract visual acuity. T25FW: timed 25-foot walk.

3.3.4 LASSO regressions

As described in the methods section, we carried out two analyses on pre-selected variables (Model A) and on a wider range of variables (Model B).

3.3.4.1 MODEL A: Pre-selected variables only

Clinical variables that predict whole brain volume

Out of the chosen variables, the LASSO model selected three variables (Table 3.12): 9HPT, SDMT, and SLCVA 2.5%. SDMT had the highest standardised coefficient indicating the strongest relationship with outcome. EDSS, MSFC, and PASAT did not appear in the final model (i.e. their coefficients were constrained to be zero).

Table 3.12 LASSO analysis of clinical variables and brain volume

Parameter Estimates (N=435)		
Parameter	**Estimate**	**Standardised Estimate**
Intercept	1302376	0
9HPT	901004	0.113
SDMT	1861.15	**0.278**

Parameter estimates in the final model after LASSO regression. 9HPT: 9-hole peg test. SDMT: symbol digit modalities test.

The following diagram (Figure 3.3) shows how the magnitude of the standardised coefficients changes as the shrinkage parameter increases.

Figure 3.3 LASSO analysis of clinical variables predicting whole brain volume

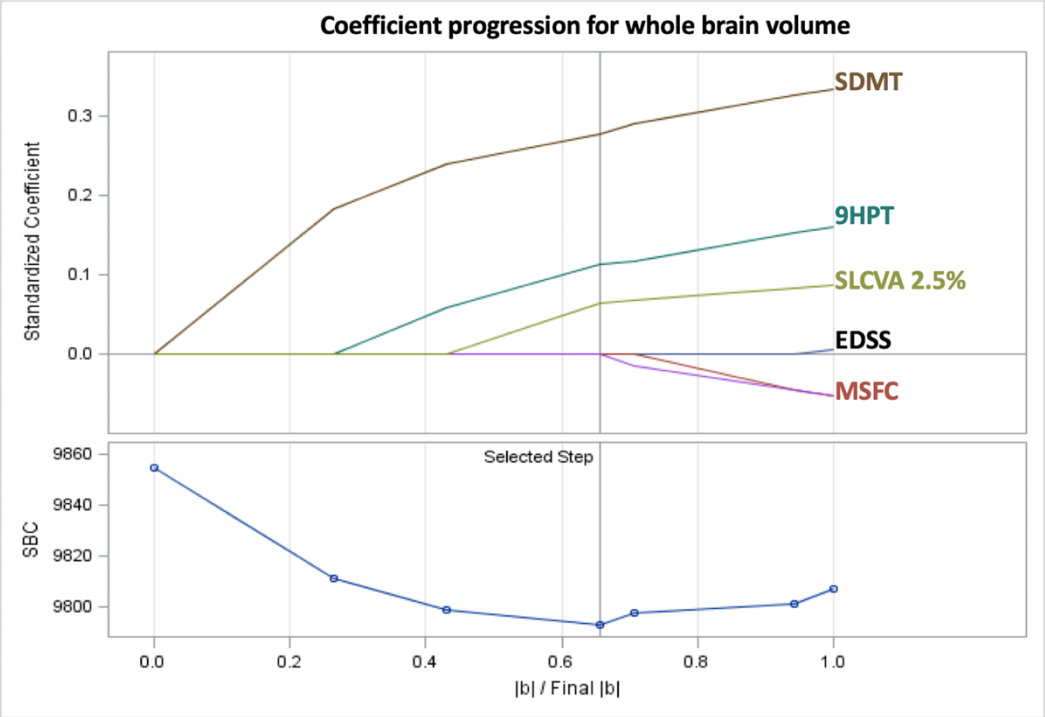

Whole brain volume is the response variable (dependent variable). Clinical metrics are explanatory variables (independent variables); these represent the input of the model. Each coloured line represents the value taken by a different coefficient in the model. The graphs show how the standardised coefficient of each variable (and statistical model) changes as the shrinkage parameter increases (top graph), and how the Schwarz Bayesian criterion (SBC) changes with the shrinkage parameter (bottom graph). Shrinkage parameter for the final model is chosen based on the lowest SBC. The variables that most influence the model are: SDMT, 9HPT and SLCVA 2.5%.
Abbreviations: EDSS: expanded disability status scale. MSFC: multiple sclerosis functional composite. SBC: Schwarz Bayesian Criterion. SDMT: symbol digit modalities test. 9HPT: 9-hole peg test. SLCVA: Sloan low-contrast visual acuity.

Clinical variables that predict deep grey matter volume

The LASSO analysis selected only 9HPT and SDMT, which appeared in the final model. SDMT gave the highest standardised coefficient (Table 3.13).

Table 3.13 LASSO analysis of clinical variables and deep grey matter volume

Parameter Estimates (N=435)		
Parameter	**Estimate**	**Standardised Estimate**
Intercept	39347	0
9HPT	41247	0.105
SDMT	88.91	**0.268**

Parameter estimates in the final model after LASSO regression. 9HPT: 9-hole peg test. SDMT: symbol digit modalities test.

Clinical variables that predict cortical grey matter volume

Once again, 9HPT and SDMT appear in the final model, with SDMT giving the highest standardised coefficient (Table 3.14).

Table 3.14 Lasso analysis of clinical variables and cortical grey matter volume

Parameter Estimates (N=435)		
Parameter	**Estimate**	**Standardised Estimate**
Intercept	742883	0
9HPT	161329	0.038
SDMT	940.45	**0.264**

Parameter estimates in the final model after LASSO regression. 9HPT: 9-hole peg test. SDMT: symbol digit modalities test.

Clinical variables that predict White matter volume

For this analysis, the final model included the variables: 9HPT, SDMT and SLCVA 2.5%. SDMT was the strongest predictor of white matter volume (table 3.15).

Table 3.15 LASSO analysis of clinical variables and white matter volume

Parameter Estimates (N=435)		
Parameter	**Estimate**	**Standardised Estimate**
Intercept	524764	0
9HPT	637636	0.150
SDMT	796.84	**0.223**
SLCVA 2.5%	340.40	0.103

Parameter estimates in the final model after LASSO regression. 9HPT: 9-hole peg test. SLCVA: Sloan low contrast visual acuity. SDMT: symbol digit modalities test.

Clinical variables that predict T2 lesion volume

SDMT and PASAT appear in the final model. SDMT has a very high standardised estimate of -0.37 (table 3.16). The higher the SDMT score, the lower the T2 lesion volume.

Table 3.16 Clinical variables that predict T2 lesion volume from LASSO analysis

Parameter Estimates (N=435)		
Parameter	**Estimate**	**Standardised Estimate**
Intercept	32491	0
SDMT	-371.77	**-0.371**
PASAT	-68.97	-0.082

Parameter estimates in the final model after LASSO regression. PASAT: paced auditory serial addition test. SDMT: symbol digit modalities test.

3.3.4.2 MODEL B: Pre-selected and additional variables

For this analysis, several variables were added to the model, in addition with the pre-specified ones.

Clinical variables that predict Whole brain volume

The variables in the final model are reported in the table below (table 3.17).

Table 3.17 LASSO analysis of additional clinical variables and whole brain volume

Parameter Estimates (N=422)		
Parameter	**Estimate**	**Standardised Estimate**
Intercept	1420642	0
9HPT	474972	0.061
SDMT	1526.28	**0.228**
BMI	-3184.33	**-0.210**
HCVA	234.31	0.035
Disease duration	-1126.11	-0.128
Male gender	-28925	-0.168
UCL centre	-15667	-0.095

Parameter Estimates (N=422)		
Parameter	**Estimate**	**Standardised Estimate**
White race/ethnicity	22538	0.053

Parameter estimates in the final model after LASSO regression. 9HPT: 9-hole peg test. BMI: body mass index. SDMT: symbol digit modalities test. HCVA: high contrast visual acuity.

Again, SDMT score has a relatively high standardised coefficient, closely followed by BMI.

The plot of coefficient progression is shown below (Figure 3.4).

Figure 3.4 Additional LASSO analysis coefficient progression

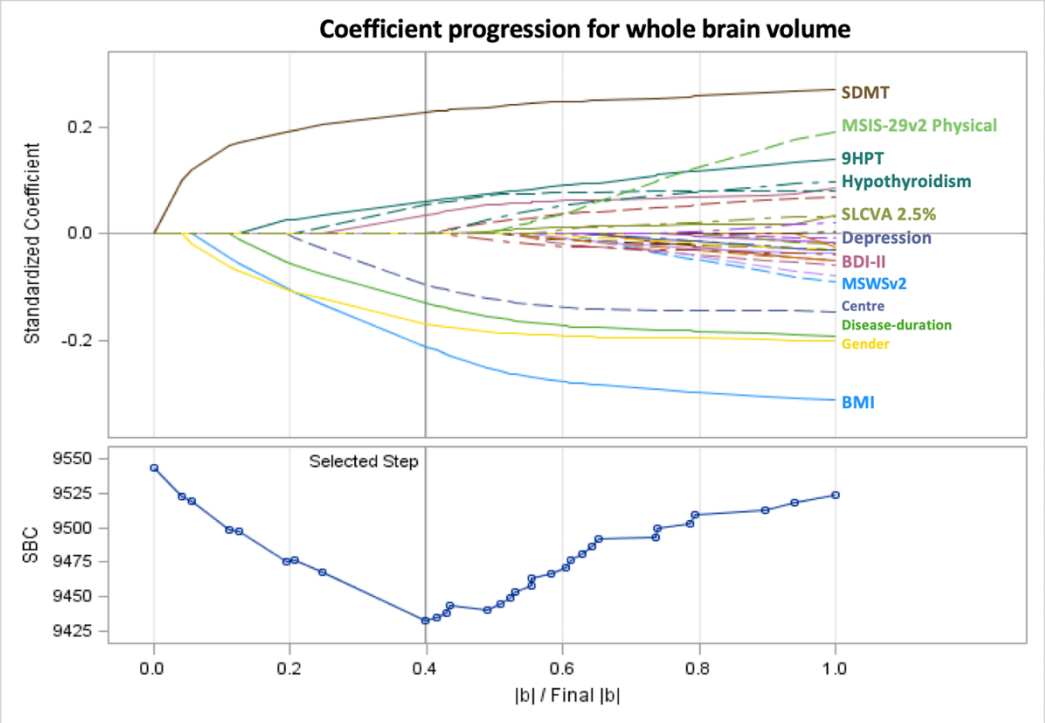

Whole brain volume is the response variable (dependent variable). Clinical and demographic metrics are explanatory variables (independent variables); these represent the input of the model. Each coloured line represents the value taken by a different coefficient in the model. The graphs show how the standardised coefficient of each variable (and statistical model) changes as the shrinkage parameter increases (top graph), and how the Schwarz Bayesian criterion (SBC) changes with the shrinkage parameter (bottom graph). Shrinkage parameter for the final model is chosen based on the lowest SBC.
The variables that most influence the model are: SDMT, 9HPT, BMI, gender and disease duration.
BDI-II: Beck depression index-II. BMI: body mass index. MSIS-29v2 Physical: multiple sclerosis impact scale 29 items version 2 physical sub-score. MSWSv2: multiple sclerosis walking scale version 2. 9HPT: 9-hole peg test. SDMT: symbol digit modalities test. SBC: Schwarz Bayesian criterion.

Clinical variables that predict deep grey matter volume

The variables in the final model are reported in the table below (Tab 3.18).

Table 3.18 LASSO analysis of additional clinical variables and deep grey matter volume

Parameter Estimates (N=422)		
Parameter	**Estimate**	**Standardised Estimate**
Intercept	43155	0
9HPT	26556	0.068
SDMT	76.26	**0.228**
BMI	-73.91	-0.098
Disease duration	-36.87	-0.084
Male gender	-1038.3	-0.121
UCL centre	178.67	0.022
Other centre	-76.43	-0.009

Parameter estimates in the final model after LASSO regression. 9HPT: 9-hole peg test. BMI: body mass index. SDMT: symbol digit modalities test.

Again, the strongest predictor was shown to be the SDMT score. The higher the SDMT score, the greater the deep grey matter volume.

Clinical variables that predict cortical grey matter volume

The variables in the final model were selected as per table 3.19.

Table 3.19 LASSO analysis of additional clinical variables and cortical grey matter volume

Parameter Estimates (n=422)		
Parameter	**Estimate**	**Standardised Estimate**
Intercept	836616	0
9HPT	132777	0.032
SDMT	633.576	**0.180**
BMI	-2150.4	**-0.270**
HCVA	104.839	0.030
Years since diagnosis	-440.5	-0.095
Age	-344.59	-0.057

Parameter Estimates (n=422)		
Parameter	**Estimate**	**Standardised Estimate**
Male Gender	-19895	**-0.220**
Edinburgh Centre	8019.97	0.076
White race/ethnicity	2664.06	0.012
Black race/ethnicity	-11000	-0.028
Hypertension	-3994.3	-0.031
Hyperlipidaemia	-1333	-0.009

Parameter estimates in the final model after LASSO regression. 9HPT: 9-hole peg test. BMI: body mass index. SDMT: symbol digit modalities test. HCVA: high contrast visual acuity.

BMI, male gender and SDMT score appear to be the strongest predictors of cortical grey matter volume.

Clinical variables that predict White matter volume

The variables in the final model were as follows (table 3.20):

Table 3.20 LASSO analysis of additional clinical variables and white matter volume

Parameter Estimates (n=422)		
Parameter	**Estimate**	**Standardised Estimate**
Intercept	557960	0
9HPT	371343	0.088
SDMT	795.098	**0.220**
SLCVA 2.5%	15.4352	0.005
BMI	-1106.3	-0.136
HCVA	163.278	0.045
SLCVA 5%	32.9542	0.011
Years since diagnosis	-629.95	-0.133
Male gender	-7405.1	-0.080
UCL centre	-16325	**-0.184**
Other centre	638.644	0.007
White race/ethnicity	19005	0.083
Hypothyroidism	8742.49	0.059

Parameter estimates in the final model after LASSO regression. 9HPT: 9-hole peg test. BMI: body mass index. SDMT: symbol digit modalities test. HCVA: high contract visual acuity. SLCVA: Sloan low high contrast visual acuity.

The strongest predictors of white matter volume from this model were SDMT score and UCL centre.

Clinical variables that predict T2 lesion volume

The variables in the final model are reported in table 3.21. Only SDMT score, PASAT and number of years since diagnosis appear in the final model.

Table 3.21 LASSO analysis of additional clinical variables and T2 lesion volume

Parameter Estimates (N=422)		
Parameter	**Estimate**	**Standardised Estimate**
Intercept	29296	0
SDMT	-323.34	**-0.322**
PASAT	-63.69	-0.076
Years since diagnosis	42.76	0.033

Parameter estimates in the final model after LASSO regression. PASAT: paced auditory serial addition test. SDMT: symbol digit modalities test.

Again, SDMT score appears to be a strong predictor of T2 lesion volume.

3.3.5 MANOVA

Briefly, two multivariate analyses were carried out to investigate if:

1) There was an association between vision problems (e.g. optic neuritis) at initial MS symptom onset and disease severity outcomes;
2) A history of hypertension or hyperlipidaemia drives a worse MS severity.

3.3.5.1 Association between optic neuritis at MS onset and disease severity outcomes

The disease severity outcomes used in this analysis, including EDSS, MSFC, SDMT, and SLCVA 2.5%, were compared between those patients with MS vision

problems (i.e. optic neuritis in one or both eyes) and those without vision problems at MS onset using a multivariate two group comparison test.

The MANOVA p-value was 0.613.

The results of the two-sample t-test (using a Satterthwaite version of the t-test assuming unequal variances for all outcomes) results are shown in the table below (Table 3.22).

Table 3.22 Two-sample t-test for optic neuritis at MS onset and disease severity

Outcome	Mean difference (Vision problems – no vision problems)	95% CI	P-value
EDSS	0.019	-0.133 to 0.170	0.808*
MSFC	0.099	-0.078 to 0.275	0.272
SDMT	-0.688	-3.246 to 1.870	0.597
SLCVA 2.5%	-0.920	-3.660 to 1.820	0.509

*Cochran-Armitage trend test for ordinal categorical variables gave a p-value of 0.806.
CI: confidence interval. EDSS: expanded disability status scale. MSFC: multiple sclerosis functional composite. SDMT: symbol digit modalities test. SLCVA: Sloan low contrast visual acuity.

There is insufficient evidence that vision problems at MS onset are related to disease severity outcomes.

3.3.5.2 Hypertension and hyperlipidaemia and MS severity

The analysis showed as follows:

- For a history of hypertension, the MANOVA p-value was 0.001;
- For a history of hyperlipidaemia, the MANOVA p-value was 0.199.

A history of hypertension appears to be related to disease severity, particularly disease severity as measured by EDSS (Table 3.23).

Table 3.23 Two-sample t-test for hypertension and disease severity

Outcome	Mean difference (Hypertension – no hypertension)	95% CI	P-value
EDSS	0.390	**0.276 to 0.502**	**<0.0001***
MSFC	-0.167	-0.472 to 0.138	0.279
SDMT	-3.332	**-6.414 to -0.251**	**0.034**
SLCVA 2.5%	-3.488	**-6.929 to -0.046**	**0.047**

*Cochran-Armitage trend test for ordinal categorical variables gave a p-value of 0.0002.
CI: confidence interval. EDSS: expanded disability status scale. MSFC: multiple sclerosis functional composite. SDMT: symbol digit modalities test. SLCVA: Sloan low high contract visual acuity.

There is insufficient evidence that a history of hyperlipidaemia is related to the disease severity outcomes overall (table 3.24).

Table 3.24 Two-sample t-test for hyperlipidaemia and disease severity

Outcome	Mean difference (Hyperlipidaemia – No hyperlipidaemia)	95% CI	P-value
EDSS	0.222	0.014 to 0.429	0.037*
MSFC	-0.109	-0.336 to 0.119	0.342
SDMT	-4.311	8.396 to -0.226	0.039
SLCVA 2.5%	-0.591	-4.655 to 3.472	0.771

*Cochran-Armitage trend test for ordinal categorical variables gave a p-value of 0.068.
CI: confidence interval. EDSS: expanded disability status scale. MSFC: multiple sclerosis functional composite. SDMT: symbol digit modalities test. SLCVA: Sloan low high contract visual acuity.

3.3.6 Association between clinician and patient-reported measures

This analysis included 445 participants. For 10 subjects, disease duration (i.e. number of years since first symptoms) information was missing. Therefore, the regression analyses, which included disease duration as a nuisance variable, only included 435 subjects.

The MSIS-29v2 total score and physical and psychological sub-scores were normally distributed (Figure 3.5).

Figure 3.5 Histograms showing the distribution of MSIS-29v2

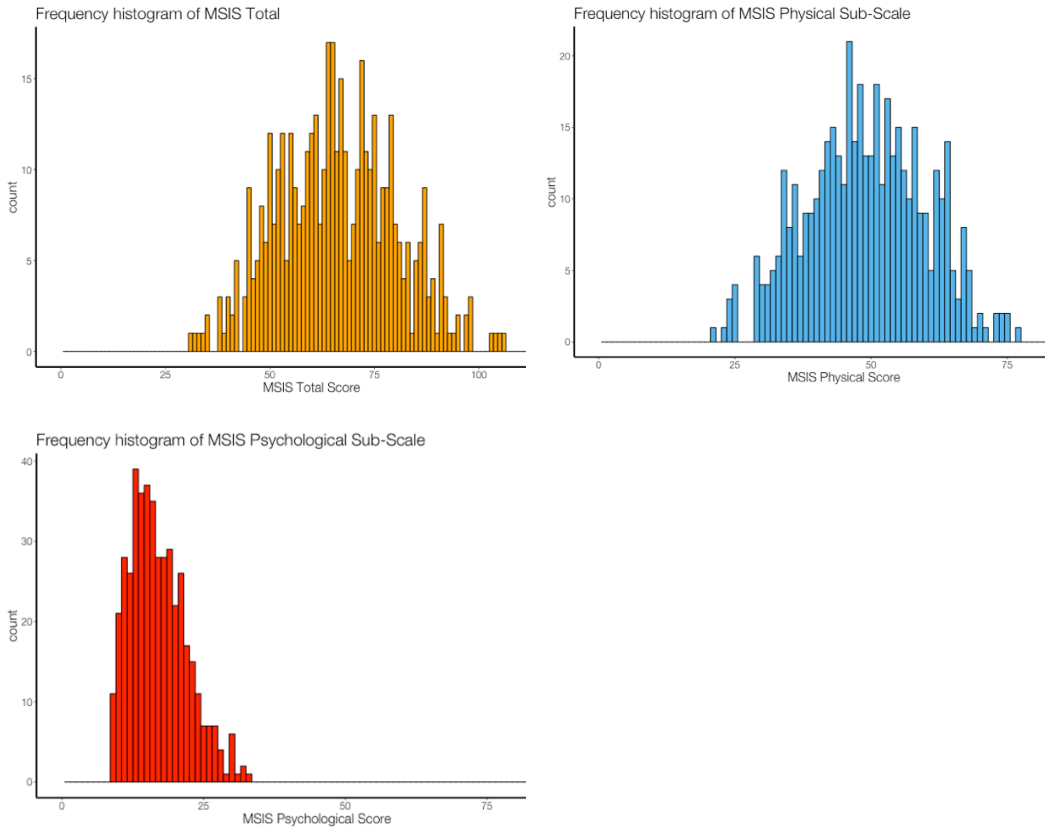

Weak correlations were found between MSFC and both the MSIS-29v2 Total score (τ= -0.21, p<0.001), Physical score (τ= -0.23, p<0.001) and Psychological score (τ= -0.08, p=0.010). A weak positive correlation was also found between EDSS and both the MSIS-29v2 Total score (τ= 0.26, p<0.001) and physical score (τ= 0.33, p<0.001), but not with the MSIS-29v2 psychological score (table 3.25 and Figure 3.6).

Table 3.25 Kendall's tau-b correlation coefficients

	MSIS-29v2 Total score	**MSIS-29v2 Physical subscale**	**MSIS-29v2 Psychological subscale**
MSFC	-0.21 (p<0.001)	-0.23 (p<0.001)	-0.08 (p=0.010)
EDSS	0.26 (p<0.001)	0.33 (p<0.001)	0.02 (p=0.608)

EDSS: expanded disability status scale. MSFC: multiple sclerosis functional composite. MSIS-29v2: multiple sclerosis impact scale 29 items version 2.

Figure 3.6 Correlation plots

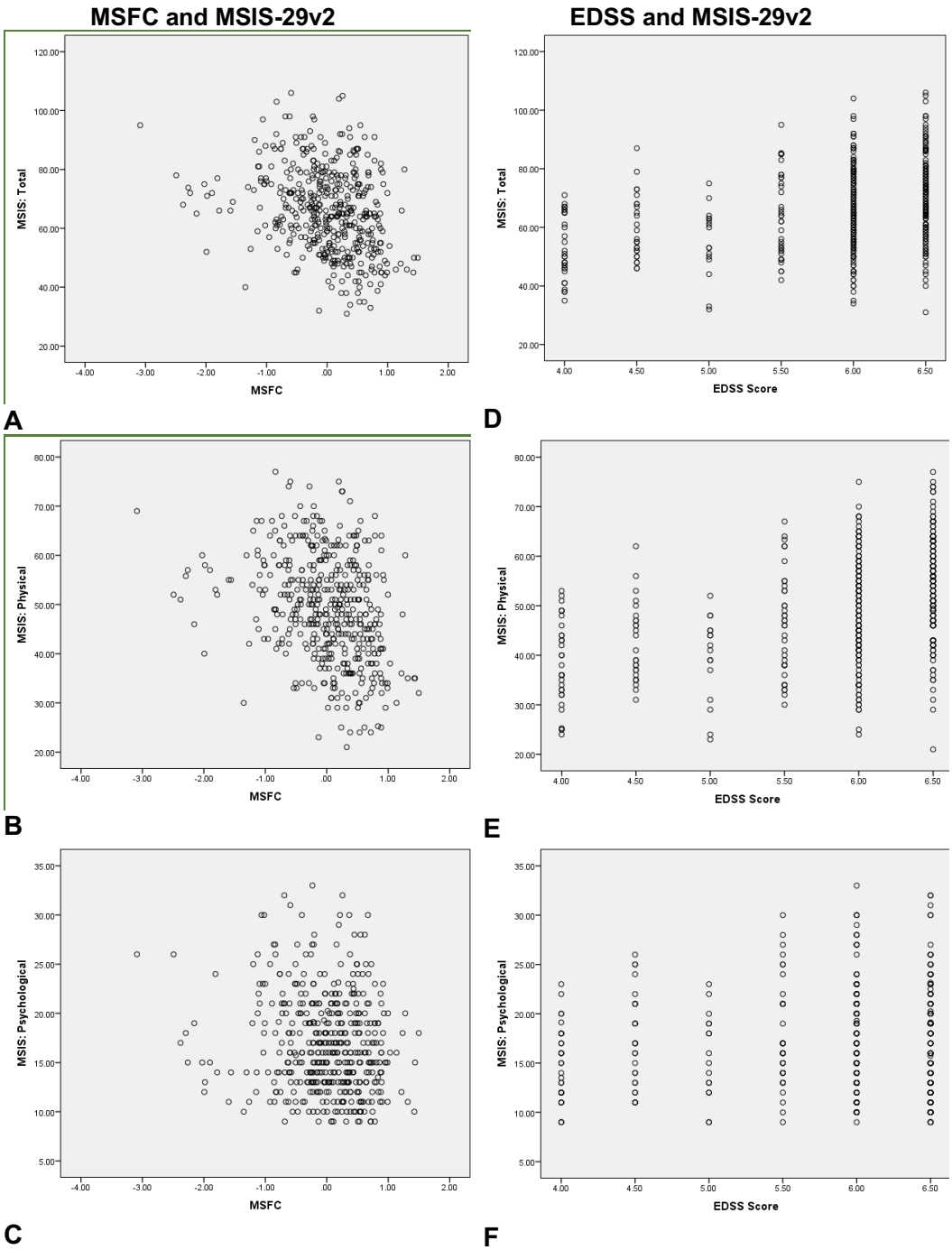

The figure represents bivariate scatterplots of the following associations: A) MSFC and MSIS-29 Total score; B) MSFC and MSIS-29 Physical sub-score; C) MSFC and MSIS-29v2 Psychological sub-score; D) EDSS and MSIS-29v2 Total score; E) EDSS and MSIS-29v2 Physical sub-score; F) EDSS and MSIS-29v2 Psychological sub-score.
EDSS: expanded disability status scale. MSFC: multiple sclerosis functional composite. MSIS-29v2: multiple sclerosis impact scale 29 items version 2.

The regression analyses confirmed these findings and showed that patients in the lowest quartile of MSFC had a significantly higher MSIS-29v2 total and physical scores than patients in each of the other quartiles (Table 3.26). Patients in the

lowest quartile of MSFC had also a significantly higher MSIS-29v2 psychological score than patients in the second and fourth quartiles (Table 3.26).

Table 3.26 Association between MSIS-29v2 and MSFC

	MSIS-29v2 Total			MSIS-29v2 Physical			MSIS-29v2 Psychological		
	AMD	**95% CI**	**P-value**	**AMD**	**95% CI**	**P-value**	**AMD**	**95% CI**	**P-value**
MSFC 1									
MSFC 2	-4.89	-8.57 to -1.12	**0.010**	-3.40	-6.19 to -0.60	**0.017**	-1.50	-2.83 to -0.16	**0.028**
MSFC 3	-8.14	-11.99 to -4.55	**<0.001**	-6.84	-9.64 to -4.03	**<0.001**	-1.31	-2.65 to 0.03	0.055
MSFC 4	-11.99	-15.08 to -7.64	**<0.001**	-9.90	-12.71 to -7.09	**<0.001**	-2.09	-3.43 to -0.75	**0.002**

The cohort is split in quartiles of MSFC. MSFC 1 is the reference category.
AMD: adjusted mean difference. MSFC: multiple sclerosis functional composite. MSIS-29v2: multiple sclerosis impact scale 29 items version 2.

Patients with EDSS score of 5.0 had a significantly lower MSIS-29v2 total and physical score than patients with EDSS score of 5.5 or 6.0 or 6.5 (Tab.3.27). However, no significant associations were found between EDSS and the MSIS-29v2 Psychological score.

Table 3.27 Association between MSIS-29v2 and EDSS

	MSIS-29v2 Total			MSIS-29v2 Physical			MSIS-29v2 Psychological		
	AMD	**95% CI**	**P-value**	**AMD**	**95% CI**	**P-value**	**AMD**	**95% CI**	**P-value**
EDSS 5.0									
EDSS 5.5	6.99	1.59 to 12.40	**0.011**	5.38	1.41 to 9.35	**0.008**	1.61	-0.40 to 3.62	0.116
EDSS 6.0	11.26	7.46 to 15.05	**<0.001**	9.65	6.86 to 12.44	**<0.001**	1.61	0.19 to 3.02	**0.026**
EDSS 6.5	16.00	12.16 to 19.85	**<0.001**	14.72	11.89 to 17.54	**<0.001**	1.29	-0.15 to 2.72	0.078

The cohort is split in quartiles of EDSS. EDSS 5.0 is the reference category (only the significant relationships are reported).
AMD: adjusted mean difference. EDSS: expanded disability status scale. MSIS-29v2: multiple sclerosis impact scale 29 items version 2.

3.4. Discussion

Research studies and clinical trials depend on valid and reliable outcome measures (Cohen *et al.*, 2012b; Ontaneda *et al.*, 2015). In this Chapter, I investigated a large UK SPMS cohort and I looked cross-sectionally at different outcome measures that characterised it.

Recruitment was effective and the target number of participants was reached. The enrolled cohort had a typical non-relapsing SPMS phenotype, with a median disease duration of 21 years, secondary progression for 6 years and an EDSS score 6.0. Over 90% of the patients were relapse free for at least 2 years before recruitment. When compared to natural history studies or other UK SPMS trial cohorts, the MS-SMART demographic and baseline characteristics were not dissimilar (Kapoor *et al.*, 2010; Koch *et al.*, 2010; Chataway *et al.*, 2014). In MS-SMART, similarly to other SPMS studies, like ASCEND or EXPAND, there was no limit to the disease duration at entry, provided that there was evidence that patients had been experiencing steady disability progression independently from relapses in the 2 years prior to enrolment. In ASCEND and EXPAND, however, patients had a shorted mean disease-duration (see Table 3.28 below for comparison).

Table 3.28 Key eligibility criteria and baseline characteristics of recent randomised-controlled trials in SPMS

	MS-SMART	MS-STAT1	LAMOTRIGINE	SPRINT-MS	LIPOIC ACID	EXPAND	ASCEND
Drug	Amiloride Fluoxetine Riluzole	Simvastatin	Lamotrigine	Ibudilast	Lipoic acid	Siponimod	Natalizumab
Trial phase	2	2	2	2	2	3	3
Primary outcome	Brain atrophy (SIENA)	Brain atrophy (BSI)	Brain atrophy (SIENA)	Brain atrophy (BPF)	Brain Atrophy (SIENA)	3-month CDP (EDSS)	6-month CDP (EDSS or T25FW or 9HPT)
Progression prior to enrolment	≥2y yrs	≥2 yrs	≥2 yrs	≥2 years	≥5 years	≥2 years	≥2 years
Trial duration	96 wks	2 yrs	96 wks	96 wks	2 years	Max 3 yrs	96wks$
Eligibility Age	25-65	18-65	18-55	21-65	40-70	18-60	18-58
Eligibility EDSS	4.0-6.5	4.0-6.5	4.0-6.5	3.0-6.5	≤6.0*	3.0-6.5	3.0-6.5
DMT	Not permitted	Not permitted	Not permitted	IFNb/GA permitted	IFNb/GA permitted	Not permitted	Not permitted
Trial Completion	2018	2014	2010	2017	2015	2016$	2015
Population	SPMS (n=445)	SPMS (n=140)	SPMS (n=120)	SPMS (n=122) PPMS (n=133)	SPMS (n=54)	SPMS (n= 1651)	SPMS (n=889)
Age (mean [SD])	54.9 (7.2)	51.1 (6.8)	50.1 (6.7)	55.6 (7.3)	59.7 (6.0)	48 (7.9)	47.2 (7.6)
Disease duration (mean [SD])*	20.7 (9.7)	20.3 (8.8)	18.9 (8.3)	11.9 (9.0)	29.1 (9.9)	16.2 (8.2)	16.5 (7.7)
EDSS (median (range)])	6.0 (4.0-6.5)	6.0 (4.0-7.0)	6.0 (4.0-7.5)	6.0 (2.5-6.5)	6.0 (3.0-9.0)	6.0 (2.5-7.0)	6.0 (5.0-6.5)
T2 lesion volume mL^3*	13.65 (12.47)	Not provided	26.6 (18.4)	10.3 (11.1)	14.9 (8.3)	14.7 (15. 6)	16.2 (16.4)
Brain volume, mL	1431 (91)	1098 (124)	255.0 (23.6) [Central cerebral volume]	0.80 (0.03) [BPF]	1395 (66)	1425 (88)	1426 (83)

*Due to slow recruitment during the first 8 months, the EDSS limit of 6.0 was eliminated. **The values refer to the placebo groups. $This time refers to the double-blind phase. BSI: brain boundary shift integral. CDP: confirmed disability progression. IFNb: interferon beta. GA: glatiramer acetate. DMT: disease-modifying therapy. BPF: brain parenchyma fraction. T25FW: timed 25-foot walk. 9HPT: 9-hole peg test. EDSS: expanded disability status scale. SIENA: Structural Image Evaluation, using Normalisation, of Atrophy. SD: standard deviation.

With the PCA of MRI variables, we found that the first two principal components – combinations of all the five MRI variables included in the model - explained 86% of the total patient sample variance. With the PCA of the clinical variables (including demographics), in order to explain a reasonable proportion of the variance (>80%), at least 5 or 7 principal components were required, not providing a clear pattern. However, when we focused on the pure clinical measures of disability, SDMT, MSIS-29v2 Physical score, and 9HPT emerged as stronger explanatory variables of variance, although the first principal component could explain only 31% of the variance. Additionally, when we combined clinical and MRI variables in the PCA model, the first principal component consisted mainly of the MRI variables plus SDMT score and, to a less extent, 9HPT. The second principal component consisted mainly of MSIS-29v2 Physical.

The SDMT is used to measure information processing speed. It has an excellent ability to differentiate between patients and healthy controls and has shown a high test–retest reliability and sensitivity to detect changes over time (Benedict *et al.*, 2017). Disadvantages of SDMT are its dependence on vision, which can be compromised in patients with MS (Cohen *et al.*, 2012b). Although SDMT is widely collected in MS studies, its use is mostly limited to assess presence or worsening of MS-related cognitive impairment. Studies using SDMT as a measure of overall disease severity are lacking. Additionally, there are no longitudinal studies investigating SDMT changes in a non-cognitively impaired population. Based on my analysis, I recommend collecting SDMT for any study in SPMS. Cross-sectionally, SDMT seems to reflect disability overall. However, prospective confirmation of its ability to detect treatment effects or meaningful clinical changes are warranted.

The 9HPT is regarded as the gold standard for manual dexterity in patients with MS. A 20% decrease in 9HPT score is associated with clinically meaningful worsening (Feys *et al.*, 2017). 9HPT has been used as an outcome measure of confirmed disability progression as part of a multicomponent measure of sustained disability progression (comprising EDSS and T25FW) in the phase III clinical trial ASCEND investigating the efficacy of natalizumab in SPMS (Kapoor *et al.*, 2018). In the ASCEND study, disease progression was defined as meeting one or more of the following three criteria: an increase of EDSS score (≥1.0 points from a baseline score of ≤5.5; or ≥0.5 points from a baseline score of ≥6.0); an increase of 20% or more from baseline on the T25FW; or an increase of 20% or more from baseline (on either hand) on the 9HPT. In a study investigating meaningful changes of clinical measures in 527 patients with MS by mean of a patient reported outcome, 9HPT seemed to reflect better than T25FW multiple system dysfunction (Kragt *et al.*, 2006). Indeed, while T25FW changes were mainly associated with impact on daily life with respect to lower limb function and fatigue; 9HPT changes indicated a more variable or diffuse impact of the disease. Of note, a phase III trial in primary progressive MS is on the way (NCT04035005) assessing the efficacy of ocrelizumab in reducing the time to confirmed upper limb disability progression as measured by 20% increase from baseline in 9HPT.

From a different angle, the wide LASSO analysis models seemed to confirmed the relevance of SDMT as a measure reflecting whole brain volume, which is one of the most widely used primary outcome measures in phase II trial in progressive MS (see also Chapter 1). SDMT clearly emerged as a strong predictor of neurodegeneration - under the pre-specified assumption that lower brain volume measured with MRI would be the result of neuroaxonal loss due to MS – in this cross-sectional fashion study. This finding could have potential implications in the approach to patients in clinical practice. Indeed, the SDMT is a quick and easy test

that can be measured during standard clinical consultations. As SDMT can predict MRI-derived brain atrophy measures, based on my results, one could potentially use it as a prognostic factor to infer the extent of brain atrophy. However, as I mentioned above, my analysis is cross-sectional and it is unclear whether longitudinal changes of SDMT are prognostic of disease severity or brain atrophy. An Italian study (Pitteri *et al.*, 2017) tested the hypothesis that cognitive impairment could represent a clinical marker of more aggressive grey matter pathology. They found that SDMT could predict cortical atrophy after 8 years, although they did not find significant associations between baseline SDMT and risk of disability progression. However, in other longitudinal studies, SDMT was found to predict not only disability progression, but also conversion to SPMS. For instance, in a French study, the SDMT measured very early during the course of RRMS was significantly correlated with EDSS worsening in the following 5 to 7 years (Deloire *et al.*, 2010). In a 10-year longitudinal study, patients with cognitive impairment – and particularly lower SDMT - at baseline had a two times greater rate of conversion to SPMS compared to patients without cognitive impairment (Moccia *et al.*, 2016).

The LASSO analysis also selected BMI as one of the main measures showing an inverse relation with whole brain volume and cortical grey matter volume. These findings are relevant as brain volume - and particularly grey matter volume - loss are associated with greater long-term disability in MS (Mowry *et al.*, 2018). Additionally, obesity is being regarded as a possible risk factor for MS (Langer-Gould *et al.*, 2013; Munger *et al.*, 2013). Mowry and colleagues (Mowry *et al.*, 2018) have recently reported that, amongst 469 people with clinically isolated syndrome and RRMS, higher BMI was independently associated with reduced grey matter volume (95% CI −1.8 to −0.5, p=0.001) and normalised brain parenchyma volume (95% CI −2.1 to −0.05, p=0.039) in multivariate models.

These results are of interest because obesity-related comorbid conditions have been associated with worse prognosis for people with MS (Marrie *et al.*, 2015). It must be noted that, in the study from Mowry et al., higher BMI values were statistically associated with lower brain volume measures; however, the BMI changes did not appear to be clinically meaningful. In another study, Bove et al found no longitudinal associations between BMI and EDSS (Bove *et al.*, 2016).

As far as other comorbidities and MS severity are concerned, the results from the multivariate analysis suggested that a history of hypertension was related to worse disease severity. Previous reports have found that vascular comorbidities are common in MS (Marrie *et al.*, 2011, 2012). Vascular comorbidities might directly influence MS pathophysiology by inducing increased peripheral inflammation and elevated inflammatory markers. Alternatively, vascular disease may have independent effects on disability, which are additive to the effects of MS (Marrie *et al.*, 2010). In a study from Conway et al. carried out in 2083 patients with RRMS, hypertension, diabetes, and obstructive lung disease, but not hyperlipidaemia, impacted clinical outcomes, including walking speed, self-reported disability, and depression. MRI outcomes were unaffected by comorbidities (Conway *et al.*, 2017). Of note, Enzinger and co-worker investigated MRI brain atrophy measures in neurologically asymptomatic elderly. They found that brain volume loss accelerated with age (Enzinger *et al.*, 2005).

Optic neuritis as MS onset symptom did not seem to predict a worse outcome in terms of disease severity in our cohort of patients.

When looking at the relationship between clinical and patient-reported outcome measures, we found that the total and physical scores of MSIS-29v2 correlated with MSFC and EDSS. This is an expected result because higher levels of disability

correspond to higher physical limitations. However, only MSFC and not EDSS correlated with the MSIS-29v2 psychological sub-scores, suggesting that MSFC might give a more balanced picture of the overall condition of people with SPMS.

Our study has several limitations, some of which are intrinsic to the nature of this study, that is, cross-sectional analysis of data from a randomised clinical trial. This means that I cannot conclude about causation or direction of effect. Selection bias should be considered when inferring generalisation in the SPMS population. For instance, in MS-SMART, we recruited patients who had already progressed in terms of disability with a median EDSS score of 6.0. This means that we have excluded a significant proportion of SPMS patients who still have good neurological function. Another limitation is the lack of MRI measures of brain regional volumes. I have not analysed, for instance, thalamic volumes, which have been regarded as a possible more sensitive outcome of neurodegeneration (Minagar *et al.*, 2013; Azevedo *et al.*, 2018). I do not know, therefore, whether the addition of thalamic volumes in the PCA model would have given a different explanation of the data variance. Finally, I do not have groups of healthy controls or other MS subtypes to compare my findings with and it is unclear whether the MRI measures or the SDMT have been affected by ageing or by comorbidities.

3.5. Conclusions

The overall findings from this chapter analysis suggest that SDMT, 9HPT, MSIS29v2, and MRI brain volume measures are relevant (based on the variance-explained) and should be collected in studies in SPMS. Additionally, comorbidities such as obesity and hypertension might have a direct effect on brain volume and should be considered as nuisance variables when analysing brain atrophy, particularly in an older population as the one represented by SPMS.

Despite the importance of the above outcome measures, the results of my analyses also showed that one single outcome measure, such as SDMT or 9HPT, was unable to explain most of the variance of the sample, supporting the notion that MS-related disability is the result of multiple neurological function damage (Hulst *et al.*, 2017). The use of composite endpoints might increase a study sensitivity by enabling a capture of data for multiple clinical domains of MS. However, interpretation of composite measures might not be straightforward (Cohen *et al.*, 2012b).

In conclusion, the analyses of the baseline data have highlighted several important points, which warrant further research. SDMT, 9HPT, BMI and hypertension are variables that should be considered in future trial of SPMS.

Further directions are looking at the prognostic role of BMI and hypertension in the longitudinal analysis. Additionally, the predictive role of SDMT and 9HPT should be investigated and the MRI analyses should also be extended to include regional volumes, such as thalamic volumes.

Chapter 4. **MS-SMART: longitudinal results**

I have discussed the objectives and main outcomes of the MS-SMART trial in Chapter 2. Briefly, the aim of the MS-SMART trial was to see whether amiloride, fluoxetine, or riluzole - three putative neuroprotective drugs – could slow down disease progression (neurodegeneration) in people with SPMS after 96 weeks, as measured by MRI-derived brain atrophy rates. This was the first multi-arm randomised controlled trial using different investigational agents against placebo ever done in multiple sclerosis.

In Chapter 2, I described the MRI and statistical analyses in use for the trial. These were prespecified in a statistical analysis plan.

In Chapter 3, I provided a detailed description of the baseline characteristics of the whole trial cohort and performed several trial non-prespecified statistical analyses as part of my PhD project, independently from the MS-SMART trial aims.

In the following pages of this Chapter, I shall provide a detailed description of the primary and secondary outcome results from the whole trial cohort from the thirteen UK centres. I will also report safety data.

The statistical analysis was carried out by Mr Richard Parker and Professor Christopher Weir on behalf of the Edinburgh Clinical Trials Unit (ECTU). Mr Jonathan Stutters assisted with the MRI analyses. Dr Anisha Doshi performed the count of new persisting T1 hypointense lesions. Mr David MacManus, Dr Ferran Prados, and Professor Frederik Barkhof reviewed uncertain MRI results. At UCL, I carried out 50% of the clinical assessments, reviewed comorbidities and safety for equally 50% of the patients, and ensured participant retention for the entire cohort

of 176 patients. Additionally, I quality checked one-by-one all the imaging outputs from GIF and SIENA for the 24-week and 96-week follow-up scans. I identified the new and enlarging T2 lesions for all of the 24-week and 96-week follow-up scans. Finally, I carried out the statistical analysis for the study of cross-sectional associations between patient-reported outcome measures and clinical outcomes.

4.1. Patients

From January 2015 to June 2016, 445 patients were randomly assigned in a 1:1:1:1 fashion to receive: amiloride (n=111), fluoxetine (n=111), riluzole (=111), and placebo (n=112) (Figure 4.1). Baseline characteristics and reasons for screening failure are described in the previous Chapter. Briefly, the four treatment arm baseline characteristics were well balanced with similar values across the arms. Mean age was 54 years (±7), disease duration 21.6 years (±9.8), median EDSS was 6.0. Patients had a low relapse count in the two years before screening (mean 0.13, SD 0.5). Hypertension was the major organ comorbidity (13%), with this condition being equally distributed across the four trial arms.

For the statistical analyses, the sites Brighton, Truro and Plymouth each had small numbers of patients (<11) and so these sites were combined in a “South Coast Other” category. Similarly, the sites Liverpool, Stoke and Newcastle also had small numbers of patients (<11) and so were combined into a “Northern Other” category.

Figure 4.1 Patient disposition

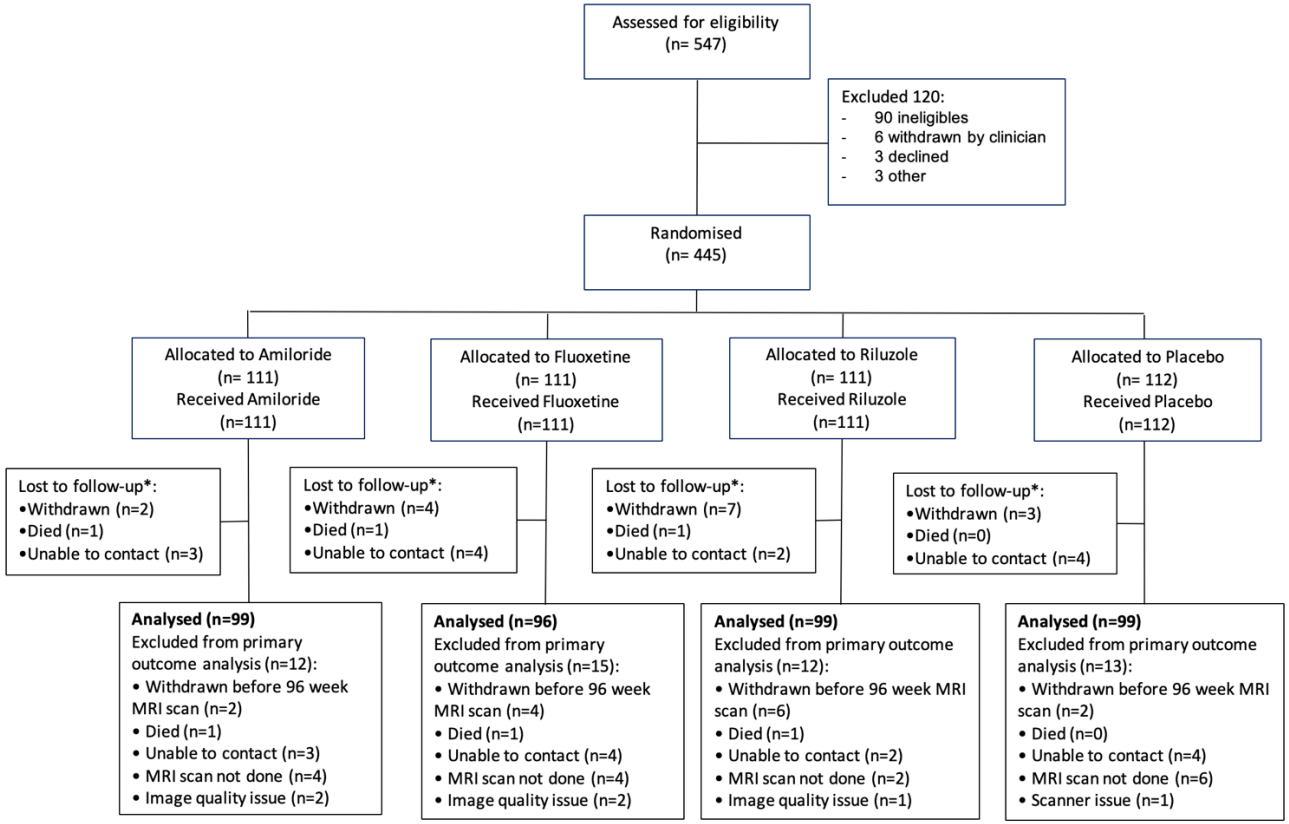

Two patients randomised to riluzole also received fluoxetine prescribed by their GP during follow-up towards the end of the study. Only 1 patient (randomised to riluzole) was a withdrawal by clinician: all other withdrawals were according to patient. Two withdrawals (one each from the riluzole and placebo groups) happened shortly after the 96-week MRI scan and so were still included in the primary outcome analysis. GP: general practitioner; MRI: magnetic resonance imaging; SSRI: serotonin selective reuptake inhibitor.
*Lost to follow-up refers to all patients lost to follow-up at any time during active follow-up (i.e. up to and including the 100-week telephone call). There were two patients who withdrew after the 96-week MRI scan, but before the end of the study (one in the Riluzole arm and one in the placebo arm).

4.2. Primary outcome measure

During the 96 weeks of MS-SMART, neither amiloride, nor fluoxetine, nor riluzole significantly reduced the rate of brain atrophy in the enrolled SPMS patients (Table 4.1 and Figure 4.2). These results were confirmed by sensitivity analyses.

Table 4.1 Primary outcome, PBVC at 96 weeks

	NBV (ml) at baseline	PBVC at 96 weeks	Adjusted mean difference in PBVC (Active– Placebo) and 95% confidence interval*	p-value*
Fluoxetine	1,414.88 (79.92)	-1.4 (1.5)	-0.1 (-0.5 to 0.3)	0.863
Riluzole	1,416.02 (75.04)	-1.4 (1.5)	-0.1 (-0.6 to 0.3)	0.771
Amiloride	1,426.92 (82.39)	-1.3 (1.0)	0.0 (-0.4 to 0.5)	0.995
Placebo	1,428.78 (91.53)	-1.3 (1.1)		

All tabulated results derived from the N=393 participants in whom 96-week outcome was recorded. A single model adjusted for minimisation variables (age, sex, treatment centre, baseline EDSS) and baseline normalised brain volume. CI: confidence intervals. NBV: normalised brain volume. PBVC: percentage brain volume change.
± Negative values indicate reductions in brain volume
*Accounted for multiple testing versus a common control group using Dunnett adjustment.

Figure 4.2 Primary outcome

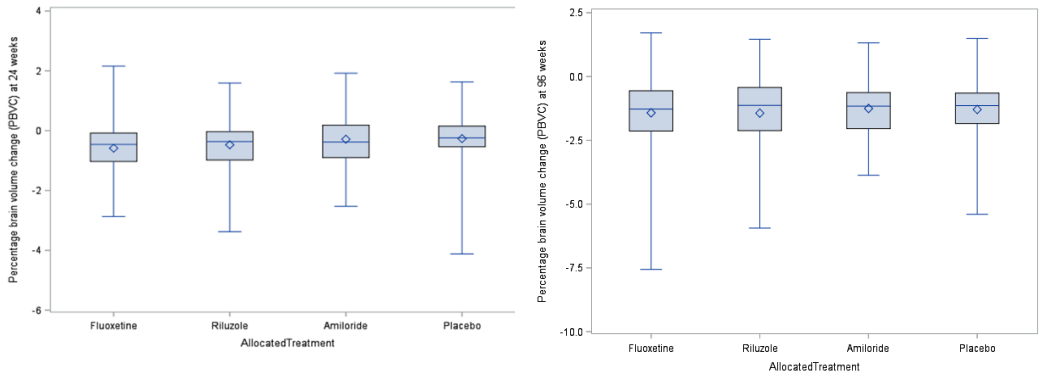

(a)

(b)

MRI-derived percentage brain volume change

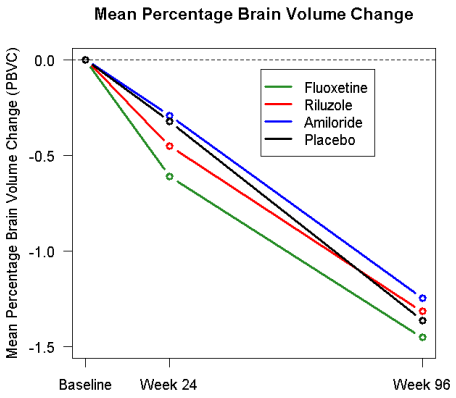

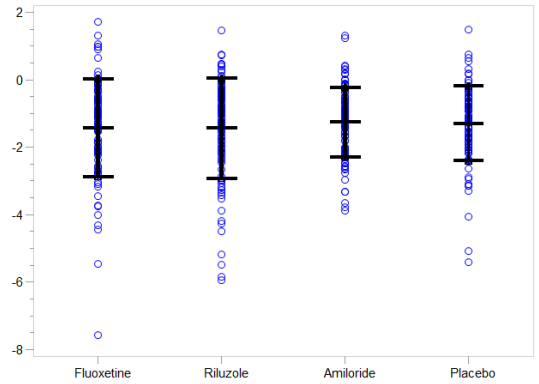

(c) (d)

Upper panel: boxplots of PBVC within randomised treatment group at (a) 24 weeks and (b) 96 weeks. Lower panel: (c) mean PBVC profile by treatment group (d) Dot Plot for MRI-derived percentage brain volume change at 96 weeks stratified by trial arm and vertical lines showing the mean +/- 1 standard deviation.

4.3. Secondary outcome measures

4.3.1 MRI endpoints

The number of new and enlarging T2 lesions after 24 and 96 weeks is reported in Table 4.2.

Table 4.2 New and enlarging T2 lesions

		fluoxetine	riluzole	amiloride	placebo	overall
Number of new and enlarging T2 lesions 0-24 weeks	**N**	106	98	103	105	412
	Mean	0.566	0.765	1.107	0.848	0.820
	SD	1.887	1.792	2.608	2.845	2.333
Number of new and enlarging T2 lesions 0-96 weeks	**N**	99	100	101	100	400
	Mean	1.768	2.830	3.743	2.950	2.828
	SD	5.278	5.708	8.054	6.897	6.594

SD: standard deviation.

The adjusted rate ratio for the number of new and enlarging T2 lesions detected at the 96-week MRI scan is reported in Table 4.3. An adjusted rate ratio of <1

indicates a lower rate of new and enlarging T2 lesions in the active treatment arm. The model was based on N=400 patients. The scale parameter was estimated to be 2.542.

Table 4.3 Adjusted rate ratio for the number of new and enlarging T2 lesions at 96 weeks

	Adjusted rate ratio for the number of new and enlarging T2 lesions at 96-week (Active– Placebo) and 95% confidence interval*	p-value*
Fluoxetine	0.54 (0.332 to 0.87)	**0.012**
Riluzole	0.95 (0.63 to 1.45)	0.814
Amiloride	1.24 (0.83 to 1.83)	0.291
Placebo		

*Adjusted for baseline T2 lesion volume and the minimisation variables (age, sex, treatment centre, EDSS).

4.3.2 Clinical endpoints

No treatment effect was detected in the four arms for the observed clinical variables (Table 4.4 and 4.5), with the exception of high contrast visual acuity in the amiloride group (adjusted mean difference amiloride-placebo 3.0, 95% confidence interval 0.5 to 5.6, p=0.020). Regarding the patient-reported outcome measures, the adjusted mean differences were significant for patients in the amiloride arm for MSIS-29v2 total score (p= 0.037), psychological score (0.025), with a trend towards significance for the physical score (p=0.089). The NFI physical and nocturnal sub-scores were also significant in the amiloride arm (p= 0.019 and p=0.013 respectively).

Table 4.4 Clinical outcomes at baseline, 48 and 96 weeks

			Allocated Treatment				Overall
			Fluoxetine	Riluzole	Amiloride	Placebo	
EDSS, score	Timepoint						
	Baseline	N	111	111	111	112	445
		Mean	5.901	5.838	5.878	5.871	5.872
		SD	0.710	0.748	0.745	0.773	0.742
	48 weeks	N	98	97	103	100	398
		Mean	5.985	6.036	6.005	5.905	5.982
		SD	0.889	0.814	0.769	0.909	0.845
	96 weeks	N	95	92	100	96	383

			Allocated Treatment				Overall
			Fluoxetine	Riluzole	Amiloride	Placebo	
		Mean	5.932	5.962	6.030	5.953	5.970
		SD	1.189	1.072	1.002	1.021	1.069
MSFC, z-score	Timepoint						
	Baseline	N	111	111	111	112	445
		Mean	-0.016	-0.092	-0.191	-0.003	-0.075
		SD	0.602	0.952	1.189	0.906	0.935
	48 weeks	N	97	96	103	99	395
		Mean	-0.249	-0.328	-0.211	-0.213	-0.249
		SD	1.089	1.477	1.255	1.357	1.297
	96 weeks	N	95	95	100	97	387
		Mean	-0.528	-0.473	-0.548	-0.409	-0.490
		SD	1.664	1.687	1.868	1.776	1.746
PASAT, no. of correct answers	Timepoint						
	Baseline	N	110	111	111	112	444
		Mean	36.600	36.910	39.018	41.464	38.509
		SD	15.171	16.003	13.667	13.864	14.784
	48 weeks	N	97	94	103	98	392
		Mean	36.361	39.936	38.049	41.459	38.936
		SD	15.710	14.250	15.428	14.092	14.965
	96 weeks	N	95	94	99	97	385
		Mean	36.779	38.394	41.061	41.907	39.566
		SD	16.322	15.554	14.340	16.728	15.826
T25FW, sec	Timepoint						
	Baseline	N	109	111	111	112	443
		Mean	15.699	19.836	25.136	18.633	19.842
		SD	12.381	28.459	38.843	28.530	28.819
	48 weeks	N	96	96	100	99	391
		Mean	23.639	31.248	25.510	26.498	26.710
		SD	31.874	49.335	38.401	43.941	41.323
	96 weeks	N	94	93	99	96	382
		Mean	33.899	33.953	38.988	32.882	34.976
		SD	50.680	52.529	56.050	52.372	52.831
9HPT, sec^{-1}	Timepoint						
	Baseline	N	111	111	111	112	445
		Mean	0.034	0.034	0.034	0.033	0.034
		SD	0.010	0.010	0.011	0.010	0.010
	48 weeks	N	97	96	103	99	395
		Mean	0.032	0.034	0.034	0.033	0.034
		SD	0.010	0.010	0.012	0.011	0.011
	96 weeks	N	95	95	100	97	387
		Mean	0.033	0.034	0.033	0.033	0.033
		SD	0.011	0.012	0.012	0.012	0.012
SDMT, no. of correct answers	Timepoint						
	Baseline	N	111	109	109	112	441
		Mean	44.153	44.514	43.908	44.107	44.170
		SD	11.410	13.065	12.400	12.778	12.386
	48 weeks	N	97	95	101	99	392
		Mean	44.454	45.105	43.584	44.960	44.515
		SD	12.177	13.075	14.505	13.093	13.215
	96 weeks	N	95	93	100	94	382
		Mean	44.779	44.892	42.960	46.096	44.654
		SD	13.743	14.219	14.906	14.480	14.339
HCVA RE, no. of correct answers	Timepoint						
	Baseline	N	111	110	106	110	437
		Mean	52.559	48.655	48.792	49.845	49.979
		SD	7.067	14.725	13.951	13.368	12.682
	48 weeks	N	97	95	99	99	390
		Mean	51.443	49.674	50.434	50.141	50.426
		SD	8.626	13.150	13.033	12.969	12.072
	96 weeks	N	96	93	98	95	382
		Mean	51.615	49.065	48.582	48.968	49.558
		SD	8.647	13.468	14.678	13.190	12.715

			Allocated Treatment				Overall
			Fluoxetine	Riluzole	Amiloride	Placebo	
HCVA LE, no. of correct answers	Timepoint						
	Baseline	N	111	110	107	111	439
		Mean	50.838	48.473	50.075	50.378	49.943
		SD	10.801	14.836	11.193	12.668	12.470
	48 weeks	N	96	95	99	98	388
		Mean	50.688	49.642	51.000	50.520	50.469
		SD	10.805	14.730	9.876	11.875	11.902
	96 weeks	N	96	93	98	95	382
		Mean	50.490	47.806	50.082	49.095	49.385
		SD	11.161	15.812	10.914	13.696	13.004
SLCVA 5% RE, no. of correct answers	Timepoint						
	Baseline	N	110	108	106	109	433
		Mean	35.155	30.713	31.660	34.147	32.938
		SD	10.462	15.382	14.521	14.624	13.935
	48 weeks	N	96	95	99	98	388
		Mean	32.573	32.768	32.556	34.000	32.977
		SD	11.663	15.226	14.146	14.485	13.904
	96 weeks	N	95	93	98	94	380
		Mean	32.621	30.677	31.888	31.915	31.782
		SD	13.014	16.682	14.957	15.368	15.008
SLCVA 5% LE, no. of correct answers	Timepoint						
	Baseline	N	110	108	107	110	435
		Mean	32.927	29.963	32.579	33.927	32.359
		SD	12.820	16.131	13.401	14.575	14.311
	48 weeks	N	96	95	98	97	386
		Mean	30.427	32.747	31.480	32.258	31.725
		SD	12.096	14.824	13.699	14.264	13.731
	96 weeks	N	95	93	98	94	380
		Mean	32.611	31.151	31.827	32.415	32.003
		SD	13.072	15.650	12.906	13.470	13.759
SLCVA 2.5% RE, no. of correct answers	Timepoint						
	Baseline	N	111	109	106	110	436
		Mean	19.865	19.119	19.896	20.736	19.906
		SD	12.277	14.504	13.155	13.692	13.395
	48 weeks	N	96	95	99	99	389
		Mean	17.177	19.137	19.162	20.505	19.008
		SD	13.018	14.164	14.178	13.128	13.631
	96 weeks	N	96	93	98	95	382
		Mean	17.021	18.065	17.857	19.632	18.139
		SD	13.666	14.433	13.115	12.318	13.379
SLCVA 2.5% LE, no. of correct answers	Timepoint						
	Baseline	N	111	109	107	111	438
		Mean	17.649	18.807	19.103	20.847	19.103
		SD	12.356	14.164	12.709	13.978	13.331
	48 weeks	N	96	95	98	98	387
		Mean	14.458	20.168	18.204	18.755	17.897
		SD	12.115	14.435	13.376	13.656	13.532
	96 weeks	N	96	93	98	95	382
		Mean	16.521	17.656	17.133	18.084	17.343
		SD	13.160	14.228	14.209	13.378	13.710
SLCVA 1.25% RE, no. of correct answers	Timepoint						
	Baseline	N	111	109	106	110	436
		Mean	8.937	7.688	9.066	9.845	8.885
		SD	10.190	10.685	10.247	11.326	10.616
	48 weeks	N	96	94	99	99	388
		Mean	5.792	7.564	7.697	9.535	7.662
		SD	8.870	11.121	10.570	11.310	10.559
	96 weeks	N	96	93	98	95	382
		Mean	5.000	6.430	6.286	7.600	6.325
		SD	8.554	10.774	8.949	10.533	9.741
SLCVA 1.25% LE, no. of	Timepoint						
	Baseline	N	111	109	107	111	438

			Allocated Treatment				Overall
			Fluoxetine	Riluzole	Amiloride	Placebo	
correct answers		Mean	6.937	7.083	8.168	9.865	8.016
		SD	9.592	10.657	10.670	11.878	10.759
	48 weeks	N	96	94	98	98	386
		Mean	4.833	7.660	7.000	8.398	6.977
		SD	8.347	11.074	10.045	10.845	10.181
	96 weeks	N	96	93	98	95	382
		Mean	4.042	6.065	5.184	6.779	5.508
		SD	8.173	10.351	8.836	9.725	9.316
MSIS29v2, score	Timepoint						
	Baseline	N	111	111	111	112	445
		Mean	65.000	69.154	63.915	66.072	66.036
		SD	13.828	15.011	13.374	14.389	14.251
	48 weeks	N	95	98	104	102	399
		Mean	66.232	71.677	68.630	69.357	68.993
		SD	14.817	14.873	15.935	15.749	15.430
	96 weeks	N	96	96	101	97	390
		Mean	69.749	72.902	72.332	69.533	71.140
		SD	15.117	15.799	16.335	17.173	16.137
MSIS29v2 Psychological Score	Timepoint						
	Baseline	N	111	111	111	112	445
		Mean	16.657	18.163	15.947	17.103	16.968
		SD	4.759	5.427	4.511	4.977	4.979
	48 weeks	N	95	98	104	102	399
		Mean	16.737	19.158	17.721	18.444	18.024
		SD	5.213	5.255	5.620	5.352	5.420
	96 weeks	N	96	96	101	97	390
		Mean	17.676	19.333	19.108	18.256	18.599
		SD	5.257	5.352	6.063	5.799	5.651
MSIS29v2 Physical Score	Timepoint						
	Baseline	N	111	111	111	112	445
		Mean	48.344	50.991	47.968	48.969	49.068
		SD	10.439	11.300	10.498	11.224	10.899
	48 weeks	N	96	98	104	102	400
		Mean	49.517	52.519	50.909	50.914	50.971
		SD	10.908	10.961	12.060	11.785	11.460
	96 weeks	N	97	96	101	98	392
		Mean	52.052	53.569	53.225	51.273	52.531
		SD	11.399	12.411	12.023	12.700	12.131
MSWSv2 Total Score	Timepoint						
	Baseline	N	111	110	111	112	444
		Mean	41.078	42.641	41.428	41.633	41.693
		SD	9.773	9.319	9.182	9.935	9.544
	48 weeks	N	95	98	104	102	399
		Mean	42.263	44.738	42.664	43.372	43.259
		SD	9.352	8.053	10.122	9.919	9.424
	96 weeks	N	96	96	102	96	390
		Mean	44.363	44.583	44.188	43.646	44.195
		SD	8.804	9.620	9.445	10.134	9.481
NFI Summary Interval Score	Timepoint						
	Baseline	N	110	109	111	108	438
		Mean	17.430	19.052	18.013	17.803	18.074
		SD	3.890	4.799	4.198	3.856	4.232
	48 weeks	N	93	98	104	101	396
		Mean	17.874	19.420	18.474	18.202	18.498
		SD	3.693	4.453	5.250	4.246	4.486
	96 weeks	N	97	96	100	98	391
		Mean	18.326	19.708	19.384	18.337	18.938
		SD	3.988	4.828	5.275	5.451	4.942
NFI Physical Interval Score	Timepoint						
	Baseline	N	111	109	111	110	441
		Mean	14.663	15.907	15.116	14.740	15.104
		SD	3.869	4.339	3.780	3.654	3.935

			Allocated Treatment				Overall
			Fluoxetine	Riluzole	Amiloride	Placebo	
	48 weeks	N	94	98	104	101	397
		Mean	14.939	16.238	15.340	15.307	15.458
		SD	3.365	3.799	4.582	3.984	3.986
	96 weeks	N	97	96	101	98	392
		Mean	15.424	16.381	16.323	14.991	15.782
		SD	3.801	4.213	4.535	4.842	4.392
NFI Cognitive Interval Score	Timepoint						
	Baseline	N	110	109	111	109	439
		Mean	6.215	7.065	6.517	6.306	6.525
		SD	2.243	2.331	2.207	2.380	2.307
	48 weeks	N	93	98	104	101	396
		Mean	6.583	7.076	6.905	6.609	6.796
		SD	2.070	2.163	2.523	2.334	2.286
	96 weeks	N	97	96	101	98	392
		Mean	6.768	7.410	7.094	6.757	7.007
		SD	2.059	2.092	2.544	2.889	2.429
NFI Diurnal Interval Score	Timepoint						
	Baseline	N	111	110	111	110	442
		Mean	9.611	10.244	10.068	9.679	9.900
		SD	2.932	3.104	2.780	2.504	2.841
	48 weeks	N	93	97	102	101	393
		Mean	10.299	10.214	10.012	10.342	10.214
		SD	2.447	2.479	2.764	2.457	2.537
	96 weeks	N	96	96	98	96	386
		Mean	10.272	10.686	10.664	10.609	10.558
		SD	2.851	2.475	3.240	2.582	2.799
NFI Nocturnal Interval Score	Timepoint						
	Baseline	N	111	111	111	111	444
		Mean	7.599	8.243	7.748	7.961	7.888
		SD	2.463	2.782	2.037	2.294	2.413
	48 weeks	N	94	98	104	102	398
		Mean	8.077	8.374	8.109	8.166	8.181
		SD	2.213	2.633	2.180	2.296	2.330
	96 weeks	N	97	96	100	97	390
		Mean	8.347	8.413	8.690	8.171	8.407
		SD	2.252	2.471	2.133	2.202	2.265
EQ-5D-5L index score	Timepoint						
	Baseline	N	111	110	111	111	443
		Mean	0.702	0.658	0.683	0.671	0.678
		SD	0.156	0.175	0.170	0.185	0.172
	48 weeks	N	94	98	103	102	397
		Mean	0.658	0.617	0.648	0.645	0.642
		SD	0.174	0.207	0.192	0.186	0.190
	96 weeks	N	96	96	102	98	392
		Mean	0.615	0.596	0.603	0.613	0.607
		SD	0.206	0.190	0.227	0.221	0.211
EQ-5D-5L VAS: Health State Score	Timepoint						
	Baseline	N	111	111	111	112	445
		Mean	67.523	61.730	66.126	65.241	65.155
		SD	19.478	21.009	16.901	20.335	19.547
	48 weeks	N	93	97	103	102	395
		Mean	66.140	58.608	63.563	62.961	62.797
		SD	18.584	20.666	21.224	22.427	20.913
	96 weeks	N	97	96	102	96	391
		Mean	61.938	59.625	61.765	64.281	61.900
		SD	20.698	21.547	20.557	21.745	21.115

9HPT: Nine Hole Peg Test. EDSS: Expanded Disability Status Scale. EuroQol-5 dimensions-5 level. HCVA: high contrast visual acuity. LE: left eye. MSFC: Multiple Sclerosis Functional Composite. MSIS29v2: multiple sclerosis impact scale 29 items version 2. MSWSv2: multiple sclerosis walking scale version 2. NFI: Neurological Fatigue

Index. PASAT: Paced Auditory Serial Addition Test. RE: right eye. SD: standard deviation. SDMT: Symbol Digit Modalities Test. SLCVA: Sloan Low Contrast Visual Acuity. T25FW: timed-25-foot walk. VAS: visual analogue scale.

Table 4.5 Secondary outcomes at 96 weeks. Adjusted mean differences

	Adjusted mean difference (Amiloride – Placebo) with 95% CI*	P-value	Adjusted mean difference (Fluoxetine – Placebo) with 95% CI*	P-value	Adjusted mean difference (Riluzole – Placebo) with 95% CI*	P-value
EDSS	0.1 (-0.1 to 0.2)	0.61	-0.1 (-0.3 to 0.2)	0.53	0.1 (-0.2 to 0.2)	0.63
MSFC**	0.1 (-0.1 to 0.3)	0.59	-0.1 (-0.3 to 0.1)	0.42	0.0 (-0.19 to 0.23)	0.84
PASAT	0.9 (-1.9 to 3.7)	0.51	-1.1 (-3.9 to 1.8)	0.47	0.4 (-2.4 to 3.3)	0.76
9HPT, s^{-1}	0.0 (-0.0 to 0.0)	0.36	0.0 (-0.0 to 0.0)	0.85	0.0 (-0.0 to 0.0)	0.27
SDMT	-1.0 (-3.1 to 1.0)	0.32	-1.1 (-3.2 to 0.9)	0.29	-0.8 (-2.9 to 1.3)	0.44
HCVA 100%	3.0 (0.5 to 5.6)	**0.02**	1.8 (-0.7 to 4.4)	0.16	1.6 (-1.0 to 4.2)	0.22
SLCVA 5%	1.0 (-1.8 to 3.8)	0.49	1.3 (-1.6 to 4.1)	0.38	1.5 (-1.4 to 4.3)	0.32
SLCVA 2.5%	0.9 (-2.0 to 3.7)	0.55	1.3 (-1.5 to 4.1)	0.37	1.7 (-1.2 to 4.6)	0.25
SLCVA 1.25%	-0.6 (-2.7 to 1.5)	0.58	-0.8 (-2.9 to 1.3)	0.45	0.7 (-1.4 to 2.9)	0.49
MSIS-29v2						
Total	3.7 (0.2 to 7.2)	**0.04**	0.5 (-3.0 to 4.0)	0.79	0.9 (-2.6 to 4.5)	0.60
Physical	2.2 (-0.3 to 4.7)	0.09	0.7 (-1.8 to 3.3)	0.56	0.6 (-2.0 to 3.1)	0.66
Psychological	1.5 (0.2 to 2.8)	**0.02**	-0.3 (-1.6 to 1.0)	0.68	0.5 (-0.9 to 1.8)	0.49
MSWSv2	0.5 (-1.6 to 2.5)	0.66	1.0 (-1.1 to 3.1)	0.35	0.6 (-1.5 to 2.8)	0.55
NFI						
Summary	0.9 (-0.2 to 2.0)	0.11	0.5 (-0.6 to 1.7)	0.36	0.7 (-0.4 to 1.9)	0.20
Physical	1.2 (0.2 to 2.3)	**0.02**	0.7 (-0.3 to 1.8)	0.17	1.0 (-0.0 to 2.1)	0.06
Cognitive	0.1 (-0.4 to 0.6)	0.70	0.2 (-0.4 to 0.7)	0.55	0.2 (-0.4 to 0.7)	0.55
Diurnal	-0.3 (-0.9 to 0.3)	0.36	-0.3 (-1.0 to 0.3)	0.29	-0.3 (-0.9 to 0.4)	0.40
Nocturnal	0.6 (0.1 to 1.1)	**0.01**	0.4 (-0.1 to 0.9)	0.12	0.1 (-0.4 to 0.6)	0.65
EQ-5D						
I*ndex*	-0.0 (-0.1 to 0.0)	0.69	-0.0 (-0.06 to 0.03)	0.52	-0.0 (-0.0 to 0.0)	0.82
VAS	-2.1 (-7.6 to 3.5)	0.47	-3.0 (-8.6 to 2.6)	0.29	-3.0 (-8.6 to 2.7)	0.30

The results for each outcome were derived from a single model analysing the N=393 participants in whom at least some 96-week outcome data was recorded. N's shown are maximums per group. The minimum sample size was N=380 for each secondary outcome (minimum per group: amiloride 98, fluoxetine 94, riluzole 92, placebo 94). The multiple regression model for each outcome included trial arm as an explanatory factor variable (with placebo as the reference category), the baseline measurement, and the minimisation variables: age, gender, treatment centre and EDSS at baseline. T25FW was analysed with Cox proportional hazards regression and results are given in the text. 9HPT: 9 Hole Peg Test; CI: confidence interval; EDSS: Expanded Disability Status Scale; EQ-5D-5L: EuroQol-5 dimension; HCVA: high contrast visual acuity; MSFC: Multiple Sclerosis Functional Composite score; MSIS29v2: Multiple Sclerosis Impact Scale 29 version 2; MSWSv2: Multiple Sclerosis Walking Scale v2; NFI: Neurological Fatigue Index; SDMT: Symbol Digit Modalities Test; SLCVA: Sloan Low Contrast Visual Acuity; VAS: Visual Analogue Scale.
*Confidence intervals (CI) calculated using 1000 bootstrap resamples.
**MSFC was signed-square root transformed prior to analysis.
***Effect sizes are adjusted mean difference and 95% CI.

4.4. Safety

No emergent safety issues were seen during the trial and no significant difference could be seen across the three active arm and placebo (Table 4.6) for the serious

adverse events. There were three deaths, one in each of the active arms; however, they were unrelated to the study drugs. Gastrointestinal, renal and urinary adverse events were higher in the three active arms (Table 4.6). In the fluoxetine arm, there were more cases of psychiatric and respiratory adverse events as compared to placebo (30% and 23% vs 22% and 16% respectively). Patients on fluoxetine also experienced injuries and underwent investigations more frequently than those of placebo. Two patients randomised to the Riluzole treatment arm were prescribed Fluoxetine by their GP during follow-up (these were protocol deviations). These two patients experienced a total of 5 adverse events and no serious adverse events. A few of the AEs for these patients occurred after Fluoxetine was prescribed and therefore, if adverse reactions, may be attributable to Fluoxetine rather than Riluzole (or a combination of the two).

Table 4.6 Adverse events

		Amiloride (N=111)	Fluoxetine (N=111)	Riluzole (N=109)	Placebo (N=112)
Total AEs		*609*	*738*	*634*	*582*
AE		*100 (90%)*	*105 (95%)*	*101 (93%)*	*103 (92%)*
	Blood and lymphatic system	5 (5%)	3 (3%)	2 (2%)	3 (3%)
	Cardiac	1 (1%)	3 (3%)	8 (7%)	2 (2%)
	Ear and labyrinth	5 (5%)	3 (3%)	1 (1%)	5 (4%)
	Endocrine	0 (0%)	0 (0%)	1 (1%)	0 (0%)
	Eye	13 (12%)	8 (7%)	9 (8%)	8 (7%)
	Gastrointestinal	46 (41%)	62 (56%)	49 (45%)	36 (32%)
	General disorders and administration	26 (23%)	28 (25%)	27 (25%)	32 (29%)
	Hepatobiliary	2 (2%)	3 (3%)	0 (0%)	1 (1%)
	Immune system	1 (1%)	1 (1%)	3 (3%)	0 (0%)
	Infections and infestations	68 (61%)	58 (52%)	62 (57%)	69 (62%)
	Injury, poisoning and procedural complications	26 (23%)	43 (39%)	29 (27%)	28 (25%)
	Investigations	10 (9%)	20 (18%)	17 (16%)	8 (7%)
	Metabolism and nutrition	2 (2%)	9 (8%)	7 (6%)	4 (4%)
	Musculoskeletal and connective tissue	37 (33%)	26 (23%)	37 (34%)	29 (26%)
	Neoplasms benign, malignant and unspecified	2 (2%)	1 (1%)	4 (4%)	2 (2%)
	Nervous system	48 (43%)	46 (41%)	47 (43%)	44 (39%)
	Psychiatric	21 (19%)	30 (27%)	22 (20%)	22 (20%)
	Renal and urinary	9 (8%)	13 (12%)	10 (9%)	5 (4%)
	Reproductive system and breast	4 (4%)	3 (3%)	2 (2%)	2 (2%)
	Respiratory	15 (14%)	23 (21%)	13 (12%)	16 (14%)
	Skin and subcutaneous tissue	16 (14%)	11 (10%)	13 (12%)	17 (15%)
	Surgical and medical procedures	6 (5%)	3 (3%)	8 (7%)	7 (6%)
	Vascular disorders	4 (4%)	2 (2%)	3 (3%)	6 (5%)
SAE		*10 (9%)*	*7 (6%)*	*12 (11%)*	*13 (12%)*
	Cardiac	0	1	2	0
	Gastrointestinal	1	0	0	1
	General disorders and administration	0	2	1	1

Hepatobiliary	1	1	0	1
Infections and infestations	4	1	4	4
Injury, poisoning and procedural complications	3	0	3	2
Investigations	0	0	0	1
Musculoskeletal and connective tissue	0	1	0	0
Neoplasms benign, malignant and unspecified	1	0	0	0
Nervous system	1	0	1	0
Psychiatric	0	1	1	1
Renal and urinary	1	1	0	0
Respiratory	1	0	1	0
Skin and subcutaneous tissue	0	0	0	1
Surgical and medical procedures	1	0	1	1
Vascular	0	0	0	1
SUSAR	*0 (0%)*	*0 (0%)*	*1 (1%)*	*0 (0%)*

Data are number of patients experiencing each type of event.
AE= adverse event. SAE= serious adverse event. SUSAR= suspected unexpected serious adverse reaction.

4.5. Discussion

For the first time, a multi-arm, multi-drug trial of neuroprotection was successfully carried out in SPMS. MS-SMART condensed three standard placebo-controlled phase 2 trials into a 4-year time frame, a process that would have taken longer if carried out in series. Such an approach is not new to medicine and adaptive multi-arm trial designs have been successfully used in oncology (James *et al.*, 2012) and is proposed as possible approach in other neurodegenerative diseases (Foltynie, 2019).

As discussed in Chapter 3, the trial population had a typical non-relapsing SPMS phenotype and the planned recruitment target number was reached with participant retention of over 90% and high adherence. Over 90% of the patients were relapse free for at least 2 years before recruitment. The PBVC observed in this SPMS population (0.65-0.7%/year) was in accordance with expectations. About 10% of patients experienced an on-study relapse over the study duration, with the number of new/enlarging lesions being very low with median 0 (interquartile range 0-2). Significant total cohort deterioration was seen in the EDSS, MS impact scale, measures of ambulation, low visual function, and health-

related quality of life. In contrast little change was seen for upper limb function, simple cognitive measures and binocular vision. The result is robust with effective blinding, narrow treatment effect confidence intervals and a generalisable disease phenotype. MS-SMART met the assumptions underlying the power calculations, suggesting that a drug effect would have been observed, if it had existed.

None of the three chosen drugs had any effect on the primary or secondary outcomes of this trial. Drug selection was based on two separate systematic reviews (Vesterinen *et al.*, 2015): firstly, clinical 2a trials in people with MS and four other neurodegenerative disorders sharing common key pathways of neurodegeneration; secondly, pre-clinical studies on demyelination, inflammation, axonal loss, and neurobehavioural changes in experimental EAE models of MS. Agents were excluded on: significant safety profile issues, being likely to produce only symptomatic benefit, an immunosuppressive mechanism of action, limited efficacy data or limited biological plausibility, and prior evaluation in relapsing-remitting MS. After the initial identification of 120 potential candidates, two further critical review steps led to seven agents of interest being identified: ibudilast, oxcarbazepine, pirfenidone, polyunsaturated fatty acids (including lipoic acid) as well as the drugs used is in the MS-SMART study. Recently, ibudilast and lipoic acid have demonstrated phase 2 success, confirming the candidate selection methodology (Spain *et al.*, 2017; Fox *et al.*, 2018).

The pathophysiology process of neurodegeneration in MS is incompletely understood: chronic inflammatory demyelination induces a modification in the distribution of sodium channels along the length of the affected axons, leading to excessive influx of sodium and ultimate accumulation of intracytoplasmic calcium, which is toxic for the cell (Bano and Ankarcrona, 2018). Activated microglia and macrophage, mostly responsible for inflammation in progressive MS, produce nitric

oxide and reactive oxygen species, which compromise the oxidative phosphorylation of mitochondria and decrease the adenosine-triphosphate production. Additionally, an inflammatory environment, which is persistent and compartmentalised in progressive MS, decreases the local pH inducing the opening of ASIC1 and the influx of additional calcium (Friese *et al.*, 2007). Axonal damage is also induced by increased release of extracellular glutamate from activated inflammatory cells (i.e. microglia, macrophages and dendritic cells) or the axons themselves in response to raised intracellular sodium (Lassmann, 2003; Trapp and Stys, 2009). In such a scenario, the ultimate process leading to axonal degeneration is axonal calcium overload and energy failure. Targeting one or more of these mechanisms using the three MS-SMART drugs, we aimed at decreasing axonal loss and preserving neuronal survival. However, the dynamics of calcium regulation in neurons is complex. For example, a recent study has identified axonal membrane disruptions <10 nm in size, defined as “nanoruptures”, caused by toxic mediators released during neuroinflammation in an animal model of MS (Choi *et al.*, 2010; Witte *et al.*, 2019). Extracellular calcium would then accumulate in the axoplasm through axoplasmic membrane nanoscale ruptures rather than from calcium channels. In such a context, it is likely that counteracting glutamate excitotoxicity or blocking ASICs with riluzole and amiloride might not be a key mechanism to prevent axonal degeneration in SPMS. We also note the recent failure of amiloride in an acute optic neuropathy trial (McKee *et al.*, 2017). With regard to fluoxetine, this seems to act on axons essentially through astrocytes, which are stimulated to release lactate through glycogenolysis providing essential energy substrates to neurons (Kong *et al.*, 2002; Allaman *et al.*, 2011). It is possible, however, that the astrocyte function in MS is compromised (Prineas and Lee, 2019). Furthermore, it should be noted that, if the mechanisms leading to excessive axoplasmic calcium influx discussed before are in place, mitochondria

may be damaged by the excess of calcium and, therefore, non-reactive to the energy substrate provided by astrocytes under the effect of fluoxetine.

The lack of efficacy may also reflect pharmacokinetic considerations such as limited bioavailability in the CNS. Fluoxetine and its active metabolites are highly lipophilic with high CNS penetrance, albeit with a slow (≥5 week) time to reach steady state (Henry *et al.*, 2005). In contrast, riluzole has 60% absolute bioavailability and is also known to have limited ability to cross the blood-brain barrier.(Parikh and Patel, 2016) No reliable data are currently available on the CNS bioavailability of amiloride. Differences from pre-clinical work in both dose and the route of administration may also have been relevant. Pre-clinical studies with amiloride were performed using much higher doses (10mg/kg body weight) than would be possible in humans (equivalent to 700mg/day); and intra-peritoneal rather than oral administration was used (Friese *et al.*, 2007; Vergo *et al.*, 2011; McKee *et al.*, 2017). Similarly, *in vitro* studies show that fluoxetine exerts CNS immune-modulatory activity at plasma concentrations of 10–50 μM(Diamond *et al.*, 2006), levels that are not achievable using the usual therapeutic daily doses of fluoxetine 20-40 mg (corresponding to concentrations ranging between 0.26 and 0.65 μM (Lundmark *et al.*, 2001).

Fundamental questions have also been repeatedly raised about the translational relevance of EAE models with respect to human disease pathobiology (Gilgun-Sherki *et al.*, 2003; Friese *et al.*, 2007; Bhat *et al.*, 2017) EAE is a widely used model of MS, but it is known to have several limitations, particularly when studying the chronic neurodegenerative component of the disease (Denic *et al.*, 2011; Fox *et al.*, 2012). Newer animal model of chronic progressive MS – such as the Theiler's Murine Encephalomyelitis Virus infection or the EAE in Biozzi ABH mice

– may be of more help in future preclinical studies in progressive MS (Hampton *et al.*, 2008; Denic *et al.*, 2011).

Separately, the mechanism of action for the three tested drugs targeted axonal pathobiology implicated in the neurodegenerative substrate of progressive MS. Amiloride blocks acid sensing ion channels and therefore targets axonal calcium overload, riluzole targets glutamate mediated excitotoxic injury, and fluoxetine stimulates astrocytic lactate release - aiming to provide an essential energy substrates to neurons (Kong *et al.*, 2002; Allaman *et al.*, 2011). While all of these processes represent biologically plausible targets for neuroprotection, they may represent a relatively “downstream” point of intervention within the causal chain of relevant pathobiology. The failure to date of all trials exclusively targeting axonal biology, stands in contrast to the emergent successes with agents that target more “upstream” inflammatory processes. Given our findings combined with the substantial body of prior evidence, it is possible that isolated targeting of axonal pathobiology represents an insufficient strategy to mitigate neurodegeneration in progressive MS. Future trials of such agents may therefore wish to reflect carefully on the potential need for combinatorial interventions. Such an approach might combine putative neuroprotective interventions with the use of anti-inflammatory DMTs to counter any overt or covert inflammatory activity. Although evidence for on-going focal inflammatory disease activity in this cohort (clinical/MRI) was low, evidence was not available on B-cell or microglial activity. In terms of successful phase 2 neuroprotection trials with reductions in brain atrophy rates of 43-68%, the rates of DMT usage have been between 0-45% (Sedel *et al.*, 2015; Spain *et al.*, 2017; Fox *et al.*, 2018). Moreover, in the context of recent positive results from the ocrelizumab (Montalban *et al.*, 2017) and siponimod (Kappos *et al.*, 2018) phase 3 trials, future work will likely stratify for the use of anti-inflammatory compounds in conjunction with possible neuroprotective agents.

Our finding that fluoxetine was associated with both a significant decrease in the PBVC at 24 weeks and the number of new/enlarging T2 lesions at 96 weeks should be interpreted with caution. These were secondary outcomes and the number of participants developing new and enlarging T2 lesion was overall low (median 0, IQR 0-2). Additionally, the MRI protocol did not include post-gadolinium scan at baseline and we were therefore unable to establish whether some of the fluoxetine patients had by chance a greater ongoing sub-clinical disease inflammatory activity at study entry. A paradoxical reduction in parenchymal brain volume compared to placebo ("pseudoatrophy") has been well described (Frank *et al.*, 2004; Hardmeier *et al.*, 2005; Miller *et al.*, 2007; Zivadinov *et al.*, 2008; Kapoor *et al.*, 2010; Tourbah *et al.*, 2016) in both immune-modulatory (e.g. natalizumab (Miller *et al.*, 2007)) and sodium channel blockade (e.g. lamotrigine(Kapoor *et al.*, 2010)) studies. Fluoxetine might therefore theoretically exert immune-modulatory activity such as decreased lymphocyte proliferation and suppressed interferon-γ production by acting on astrocytes (Diamond *et al.*, 2006). However the primary outcome of our study was negative, and is consistent with the lack of therapeutic effect in the recently reported negative results of the FLUOX-PMS trial involving 137 progressive MS patients (Cambron *et al.*, 2019).

One of the challenges in finding treatments for progressive MS is the lack of optimal outcome measures (Ontaneda *et al.*, 2015). It is possible that the primary outcome measure used in this trial – i.e. MRI-derived whole-brain volume change - was not sensitive enough to detect significant differences between active and placebo arms. Alternatively, it is possible that the observational period of 96 weeks was too short to detect significant changes. However, MRI-derived brain atrophy measures have been successfully used in phase 2 and 3 trials during about two years in patients with progressive MS. In the SPRINT-MS study, using a the brain

parenchymal fraction method, the investigators showed a statistically significant reductions of the loss of parenchymal fraction in patients taking ibudilast for 96 weeks (Fox *et al.*, 2018). In the MS-STAT trial, investigators used the boundary shift integral method to show efficacy of simvastatin in reducing brain atrophy after two years (Chataway *et al.*, 2014). The SIENA method used in MS-SMART has shown high reproducibility in measuring brain volume change in longitudinal studies and is one of the most popular techniques in use for measuring brain atrophy (Barkhof *et al.*, 2009). Indeed, the EXPAND trial used the same SIENA method to quantify brain atrophy, finding that brain volume decreased at a lower rate with siponimod than with placebo after 12 and 24 months. Recent studies have shown that regional volumes, such as thalamic volume, cortical or deep grey matter volumes, may reflect the progress of neurodegeneration better than whole-brain measures. Moreover, the progressive loss of grey matter is not homogeneous across different brain regions and MS subtypes (Azevedo *et al.*, 2018; Eshaghi *et al.*, 2018a, b). To further investigate this point in our trial, we carried out a non-pre-planned analysis looking at the treatment effect by using brain segmentation measures such as cortical grey matter, deep grey matter, and white matter volumes instead of whole brain volume measures changes over 96 weeks. This analysis did not show any statistical difference between the active arms and the placebo. We did not look at the single thalamic regional volume changes as this data was not collected for the pre-specified analysis. However, a post-hoc analysis of the MS-STAT trial did not show any significant change of thalamic volume over 2 years, possibly due to significant baseline thalamic volume loss in a cohort of patients with an average disease duration of about 20 years (Eshaghi *et al.*, 2019). It is very likely that the MS-SMART cohort shows thalamic baseline values similar to the MS-STAT ones given the similarities in the baseline characteristics of the two cohorts.

4.6. Conclusions

In conclusion, this study has shown that a multi-arm approach can be successfully used in proof of concept studies to expedite drug discovery in patients with progressive MS. The results from MS-SMART do not support the efficacy of amiloride, fluoxetine and riluzole in slowing down the disease progression in this stage of the disease, and suggest that further mechanisms of action and/or combinatorial strategies should be critically examined to help identify drugs with neuroprotective potential.

Chapter 5. **The UCL cohort: an in-depth overview**

The aim of this Chapter is to provide an overview of the baseline characteristics of the UCL cohort as I will mostly focus on this in the following Chapters dedicated to the MS-SMART sub-studies. Moreover, being based at UCL, I know this group of patients in considerable detail, as I have been directly involved in recruitment, assessment, data collection, and analyses.

I consented 50% of the patients and collected clinical history and important demographic data: age, disease onset, disease diagnosis, years since progression, number of relapses in the previous two years. I excluded significant organ comorbidities and carefully reviewed concomitant medications. I arranged for the baseline MRIs to be done on the same day of the screening visit and ensured good quality of the imaging by reviewing the scans with the radiographers at the time of imaging acquisition. I performed clinical assessments for about 50% of the enrolled patients at baseline.

In the following pages, I will talk about patient recruitment at UCL and explore the baseline characteristics of this cohort. I will also look at the relationships between clinical and MRI variables.

5.1. Participants and methods

For the purpose of this Chapter, the 176 patients recruited at UCL were included in the analysis. Metrics of interest for the statistical analysis were as follows: clinical disability scores EDSS, MSFC (including the sub-scales T25FW, 9HPT and PASAT), SDMT, and binocular SLCVA 2.5%; MRI metrics, including baseline (normalised) brain volumes, baseline T2-lesion volume, and new/enlarging T2

lesion counting. Additional measures were the patient-reported MSIS-29v2 questionnaire (including the total, physical and psychological scores).

Data were graphically inspected to asses normality. Statistical calculations were performed using R version 3.4.2 (The R Project for Statistical Computing, www.r-project.org). To investigate the cross-sectional relationships between clinical and MRI variables, I calculated Kendall's tau correlation coefficients. For the variables that showed significant correlations, I fitted linear regression models adjusting for age, sex, disease duration, T2 lesion volume, and visual function (as measured by SLCVA 2.5%) as appropriate. The linear regression model looking at the associations between normalised whole brain volume and SDMT was adjusted also for SLCVA 2.5% to account for low SDMT scores due to poor vision. Statistical significance was set at p <.05. Due to the exploratory nature of this study, there was no adjustment for multiple comparisons.

5.2. Results

5.2.1 Recruitment

UCL (London) was the principal trial site. At UCL, we recruited 40% of the overall national patient cohort (Figure 5.1).

Figure 5.1 Proportion of participants per site

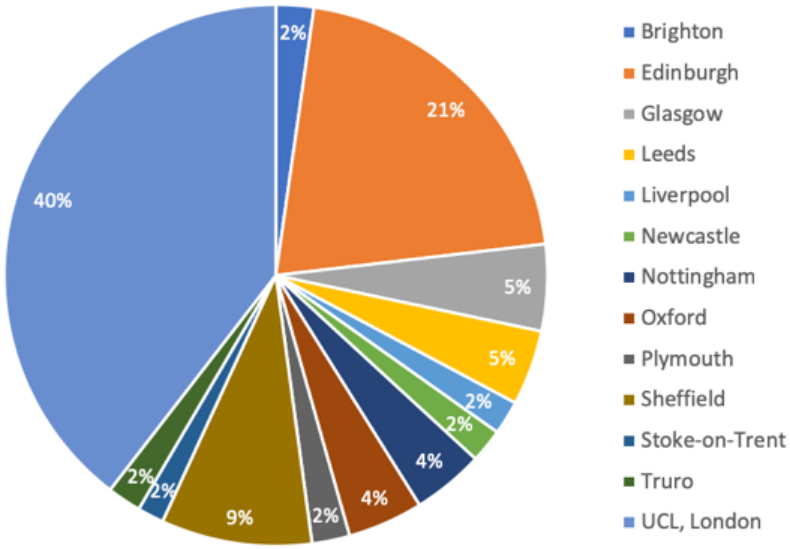

The UCL site was activated on 19th December 2014 after the first screening visit. The last screening visit was undertaken in June 2016. The recruitment rate is reported in Figure 5.2.

Figure 5.2 Recruitment at UCL

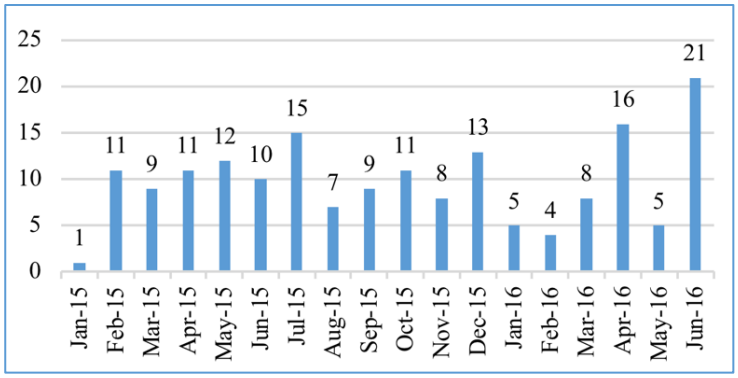

As mentioned in the previous Chapter, we received patient referrals from different roots: consultant referrals (22%); dedicated website (76%); local MS centre outreach meetings (0.4%), and MS nurse referrals (2%).

We used different ways to contact patients (emails, letters, telephone calls. Ultimately, before seeing patients for screening, we performed a telephone pre-screening questionnaire (Figure 5.3).

Figure 5.3 Pre-screening Telephone Questionnaire

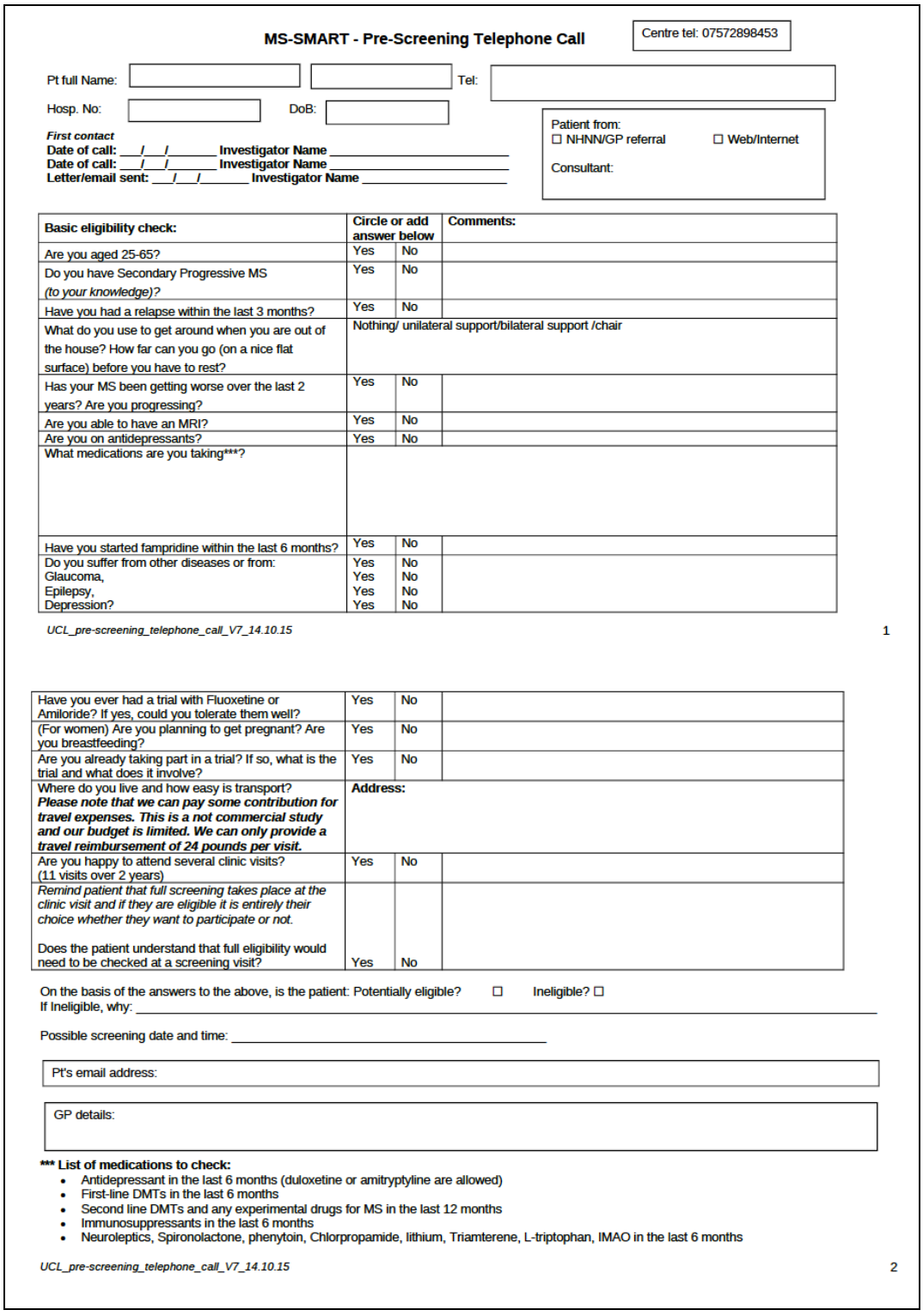

MS-SMART - Pre-Screening Telephone Call

Centre tel: 07572898453

Pt full Name: _____ _____ Tel: _____

Hosp. No: _____ DoB: _____

First contact
Date of call: ___/___/_____ Investigator Name _____
Date of call: ___/___/_____ Investigator Name _____
Letter/email sent: ___/___/_____ Investigator Name _____

Patient from:
☐ NHNN/GP referral ☐ Web/Internet

Consultant:

Basic eligibility check:	**Circle or add answer below**		**Comments:**
Are you aged 25-65?	Yes	No	
Do you have Secondary Progressive MS *(to your knowledge)?*	Yes	No	
Have you had a relapse within the last 3 months?	Yes	No	
What do you use to get around when you are out of the house? How far can you go (on a nice flat surface) before you have to rest?	Nothing/ unilateral support/bilateral support /chair		
Has your MS been getting worse over the last 2 years? Are you progressing?	Yes	No	
Are you able to have an MRI?	Yes	No	
Are you on antidepressants?	Yes	No	
What medications are you taking***?			
Have you started fampridine within the last 6 months?	Yes	No	
Do you suffer from other diseases or from: Glaucoma, Epilepsy, Depression?	Yes Yes Yes Yes	No No No No	

UCL_pre-screening_telephone_call_V7_14.10.15 1

Have you ever had a trial with Fluoxetine or Amiloride? If yes, could you tolerate them well?	Yes	No	
(For women) Are you planning to get pregnant? Are you breastfeeding?	Yes	No	
Are you already taking part in a trial? If so, what is the trial and what does it involve?	Yes	No	
Where do you live and how easy is transport? ***Please note that we can pay some contribution for travel expenses. This is a not commercial study and our budget is limited. We can only provide a travel reimbursement of 24 pounds per visit.***	**Address:**		
Are you happy to attend several clinic visits? (11 visits over 2 years)	Yes	No	
Remind patient that full screening takes place at the clinic visit and if they are eligible it is entirely their choice whether they want to participate or not. Does the patient understand that full eligibility would need to be checked at a screening visit?	Yes	No	

On the basis of the answers to the above, is the patient: Potentially eligible? ☐ Ineligible? ☐
If Ineligible, why: _____

Possible screening date and time: _____

Pt's email address:

GP details:

***** List of medications to check:**
- Antidepressant in the last 6 months (duloxetine or amitryptyline are allowed)
- First-line DMTs in the last 6 months
- Second line DMTs and any experimental drugs for MS in the last 12 months
- Immunosuppressants in the last 6 months
- Neuroleptics, Spironolactone, phenytoin, Chlorpropamide, lithium, Triamterene, L-triptophan, IMAO in the last 6 months

UCL_pre-screening_telephone_call_V7_14.10.15 2

The questionnaire was administered by myself and clinical fellows. The time needed to complete the questionnaire was variable (around 30 minutes).

About 800 potential candidates were contacted by phone, email and letter. We managed to perform a pre-screening questionnaire by telephone or email for approximately 500 patients. Of the total pre-screened patients, 264 patients seemed to fulfil the eligibility criteria, but not all of them accepted to be formally seen for screening. We screened 218 patients and randomised 176 of them (Figure 5.4). The reasons for screening failure are reported in Table 5.1.

Figure 5.4 Recruitment profile

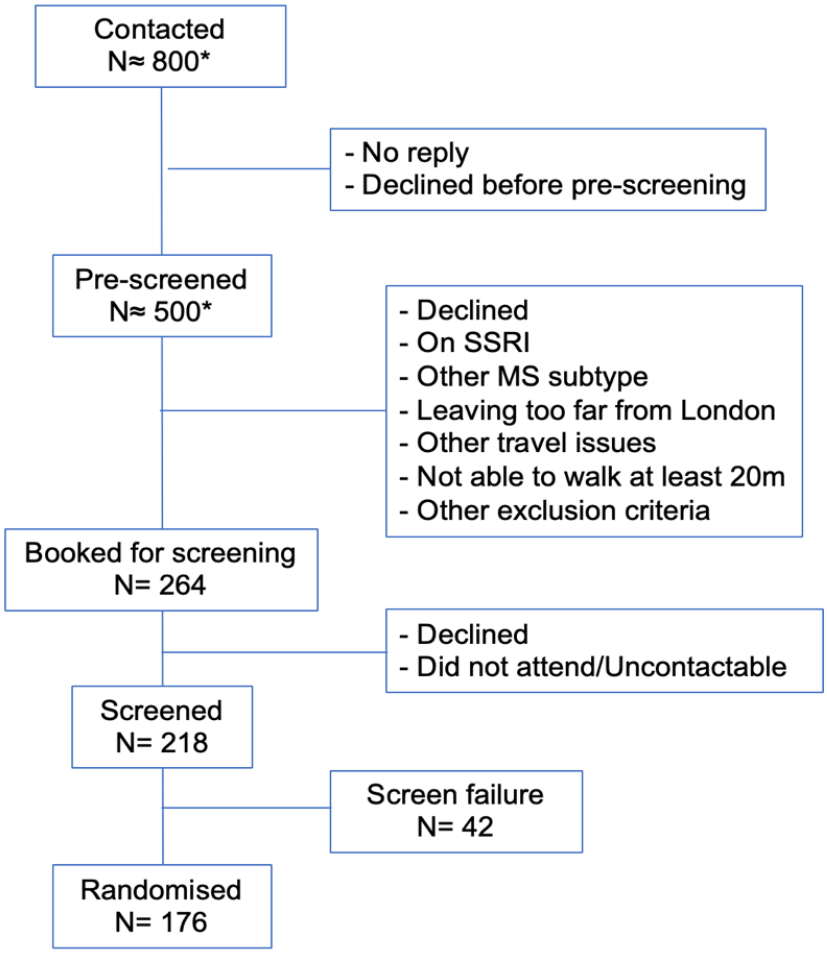

*Approximate number. SSRI: Selective Serotonin Reuptake Inhibitor.

Table 5.1 Screening failure at the UCL centre

REASON OF SCREENING FAILURE	N (%)
Travel issues	18 (43%)
On forbidden drugs (DMTs, warfarin, prednisolone)	4 (9.5%)
Depression	3 (7%)
Significant organ comorbidity	4 (9.5%)
Worried about side effects	4 (9.5%)
MRI not suitable for analysis	4 (9.5%)
Another MS phenotype (PPMS)	2 (4.8%)
Unhappy with the study team	1 (2.4%)
Disability score too high (EDSS>6.5)	1 (2.4%)
Claustrophobia (MRI not doable)	1 (2.4%)
	Total 42

5.2.2 Baseline characteristics

UCL patients baseline characteristics are reported in Table 5.2. The cohort was overall well balanced in terms of age, sex, physical disability and MRI metrics across the four treatment arms. The placebo arm, with a mean of 19.9 years, had a slightly shorted disease duration compared to the other trial arms (21.6 years for fluoxetine, and about 23 years for riluzole and amiloride). The population enrolled at UCL, similarly to the overall trial cohort, was mostly relapse free in the two years before recruitment.

As expected, data were skewed for T25FW, and EDSS.

Table 5.2 Baseline characteristics form the UCL cohort

Number randomised	Fluoxetine (n=45)	Riluzole (n=44)	Amiloride (n=44)	Placebo (n=43)	Overall (N= 176)
Sex					
Female N (%)	31 (69)	29 (66)	31 (70)	31 (72)	122 (69)
Male N (%)	14 (31)	15 (34)	13 (30)	12 (28)	54 (31)
Age					
Mean (SD)	54.5 (7.5)	54.1 (6.4)	54.1 (7.5)	53.3 (7.6)	54 (7.2)
Median (Min-Max)	56 (34; 65)	55 (39; 65)	55 (37; 65)	54 (36; 64)	55 (34; 65)
EDSS					
Mean (SD)	5.8 (0.7)	5.7 (0.8)	5.9 (0.7)	5.7 (0.8)	5.8 (0.8)
Median (Min-Max)	6 (4.0; 6.5)	6 (4.0; 6.5)	6 (4.0; 6.5)	6 (4.0; 6.5)	6 (4.0; 6.5)

Disease-duration					
Mean (SD)	21.6 (8)	23.8 (9.5)	23.2 (9.9)	19.9 (9.3)	22.1 (9.2)
Median (Min-Max)	19 (9; 40)	23 (8; 53)	22.5 (5; 47)	19 (5; 40)	21 (5; 53)
Progression duration					
Mean (SD)	7.7 (4.8)	9.7 (5.9)	8.5 (6)	8.4 (6.6)	8.6 (5.9)
Median (Min-Max)	6 (2; 20)	8.5 (2; 28)	7.5 (2; 28)	6 (2; 26)	7 (2; 28)
Patients with relapses previous 2 years					
N (%)	4 (9%)	3 (7%)	6 (14%)	3 (7%)	16 (9%)
MSFC					
Mean (SD)	-0.00 (0.7)	-0.23 (1.2)	- 0.02 (1.1)	-0.07 (1.3)	-0.08 (1.08)
Median (Min-Max)	0.14 (-1.2; 1)	-0.05 (-5.7; 0.9)	0.35 (-4.9; 1.2)	0.24 (-5.2; 1)	0.15 (-5.75; 1.24)
T25FW (average)					
Mean (SD)	16.6 (14.1)	22.4 (36.4)	22.5 (32.4)	24.4 (41.8)	21.5 (32.6)
Median (Min-Max)	12.2 (5.1; 82)	10.6 (5.3; 180	10.3 (4.2; 180	9.3 (4.4; 180)	10.6 (4.25; 180)
9HPT (average)					
Mean (SD)	33.2 (14.6)	35.5 (17.6)	36.9 (26.1)	34.6 (20.9)	35 (20.1)
Median (Min-Max)	29.3 (20.1; 104.6)	32.1 (20; 105.8)	28 (19.7; 138.7)	27.9 (18; 146.4)	28.8 (18; 146.4)
PASAT (N=175)					
Mean (SD)	38.2 (13)	38 (14.7)	42.5 (11.9)	44.2 (11.8)	40.7 (13.1)
Median (Min-Max)	40.5 (9; 57)	39.5 (0; 59)	43 (3; 60)	46 (13; 60)	43 (0; 60)
SDMT (N=175)					
Mean (SD)	44.9 (11)	45.5 (12.7)	47.4 (12.7)	45.5 (14.6)	45.9 (12.7)
Median (Min-Max)	48 (17; 67)	48 (20; 74)	49 (22; 72)	49 (13; 75)	48 (13; 75)
HCLVA 100% binocular (N=175)					
Mean (SD)	54.5 (7.8)	50.4 (13.7)	52.5 (7.2)	54.5 (7.6)	53 (9.6)
Median (Min-Max	58 (18; 60)	55 (0; 60)	54 (29; 60)	57 (28; 60)	55 (0-60)
SLCVA 5% binocular (N=175)					
Mean (SD)	39.4 (10.1)	35 (13.4)	37 (10.4)	40 (10.8)	37.84 (11.34)
Median (Min-Max)	40 (4; 54)	38 (0; 54)	39 (4; 52)	43 (0; 55)	40 (0-55)
SLCVA 2.5% binocular (N=175)					
Mean (SD)	24.9 (12.7)	22.9 (13.6)	23.7 (11.4)	25.7 (12)	24.3 (12.4)
Median (Min-Max)	29 (0; 41)	23 (0; 49)	24 (0; 40)	28 (0; 45)	27 (0-49)
SLCVA 2.5% binocular (N=175)					
Mean (SD)	10.7 (11)	8.3 (9.6)	11.5 (11.1)	11.4 (11.8)	10.5 (10.4)
Median (Min-Max)	7 (0; 34)	4 (0; 37)	9 (0; 31)	7 (0; 37)	7 (0-37)
MSIS-29v2 total					
Mean (SD)	66 (13.7)	72.3 (15.3)	63.2 (13.8)	68.3 (13.6)	67.5 (14.4)
Median (Min-Max)	64 (32; 91)	70 (45; 106)	64 (33; 87)	73 (38; 93)	67 (32; 106)
MSIS-29v2 Physical					
Mean (SD)	49 (9.5)	53.8 (11.5)	46.6 (10.6)	50.5 (11)	50 (10.9)
Median (Min-Max)	49 (23; 67)	51.5 (31; 77)	46 (24; 64)	53 (25.3; 74)	50 (23; 77)
MSIS-29v2 Psychol					
Mean (SD)	17 (5.1)	18.4 (5.8)	16.5 (4.7)	17.8 (4.8)	17.5 (5.1)
Median (Min-Max)	16 (9; 28)	16 (9; 33)	16 (9; 27)	18 (9; 30)	16.5 (9; 33)
Normalised brain volume (ml)					
Mean (SD)	1407.4 (88.3)	1402 (85.6)	1412.2 (86.9)	1427.4 (96.7)	1412.1 (89.2)
Median (Min-Max)	1389.8 (1145.3; 1615.8)	1393.2 (1145.4; 1579)	1421.2 (1133.6; 1545.1)	1438.4 (1215.4; 1591.2)	1410.6 (1133.6; 1615.8)

T2 Lesion Volume (ml)					
Mean (SD)	13.7 (10)	13.5 (10.3)	11.7 (9.1)	11.7 (11.6)	12.6 (10.2)
Median (Min-Max)	13 (1.1; 47.4)	11 (0.3; 38.5)	10 (0.6; 34)	8.8 (0.2; 52)	10.4 (0.2; 52)
Normalised deep grey matter Volume (ml)					
Mean (SD)	45.1 (4.3)	45 (4.4)	45.3 (4.3)	46.2 (4.7)	45.4 (4.4)
Median (Min-Max)	44.7 (31.9; 53.9)	44.6 (36.5; 53.2)	45.6 (32.5; 53.7)	45.7 (36.6; 56.9)	45.5 (31.9; 56.9)
Normalised Cortical grey matter volume (ml)					
Mean (SD)	788.4 (51)	784.1 (41.3)	792.4 (44.6)	795.7 (50.1)	790.1 (46.7)
Median (Min-Max)	789.8 (651.9; 901.3)	789.6 (655.6; 849.1)	793.8 (652.9; 859.6)	801.4 (674.3; 884.1)	794.8 (651.9; 901.3)

9HPT: 9-hole peg test. BDI-II: Beck Depression Index version 2. BMI: body mass index. EQ-5D-5L: EuroQuol 5-level version. EDSS: expanded disability status scale. HCVA: high contrast visual acuity. SLCVA: Sloan low contrast visual acuity. MSFC: multiple sclerosis functional composite. MSIS-29v2: multiple sclerosis impact scale 29 items version 2. PASAT: paced auditory serial addition test. SDMT: symbol digit modalities test. T25FW: timed 25-foot walk test. MSIS-29v2: multiple sclerosis impact scale 29 items version2. MSWSv2: multiple sclerosis walking scale version 2.

5.2.3 Relationship between clinical and MRI measures

I calculated Kendall's tau (τ) correlation coefficients between the clinical and radiologic variables (Table 5.3). I found stronger correlation coefficient between normalised brain volume and SDMT (τ= 0.25, p<0.001), 9HPT (τ= 0.2, p<0.001), SLCVA 2.5% (τ= 0.23, p<0.001) (Figure 5.5).

Table 5.3 Correlations between clinical and MRI variables

	EDSS	**MSFC**	**T25FW**	**SDMT**	**SLCVA 2.5%**	**9HPT**	**PASAT**
Whole brain volume	τ= -0.13 p= 0.017	τ= 0.19 p <0.001	τ= -0.1 p= 0.05	**τ= 0.25 p<0.001**	**τ= 0.23 p<0.001**	**τ= -0.2 p<0.001**	τ= 0.07 p= 0.15
T2 lesion volume	τ= 0.16 p= 0.01	**τ= -0.3 p <0.001**	τ= 0.11 p= 0.03	**τ= -0.39 p<0.001**	**τ= -0.28 p<0.001**	τ= 0.19 p<0.001	**τ= -0.29 p<0.001**

EDSS: expanded disability status scale. MSFC: multiple sclerosis functional composite. T25FW: timed 25-foot walk. SDMT: symbol digit modalities test. SLCVA: Sloan low contrast visual acuity. 9HPT: 9-hole peg test. PASAT: paced auditory serial addiction test.

In separate linear regression models, I assessed associations between normalised brain volume and the clinical variables showing stronger correlations, i.e. SDMT,

SLCVA 2.5% and 9HPT (Table 5.3). Normalised brain volume was an independent predictor of SDMT (standardised-beta= 0.2; p= 0.006; 95% CI= 0.06; 0.33; adjusted-R^2= 0.4). There were significant associations also between normalised brain volume, and SLCVA 2.5% (standardised-beta = 0.2; p= 0.01; 95% CI= 0.04; 0.32; adjusted-R^2= 0.2). The linear regression model looking at the associations between normalised brain volume and SDMT was also adjusted for SLCVA 2.5%. Finally, there was a trend towards significance for the 9HPT (p= 0.07).

Figure 5.5 Association between normalised brain volume and SLCVA or SDMT

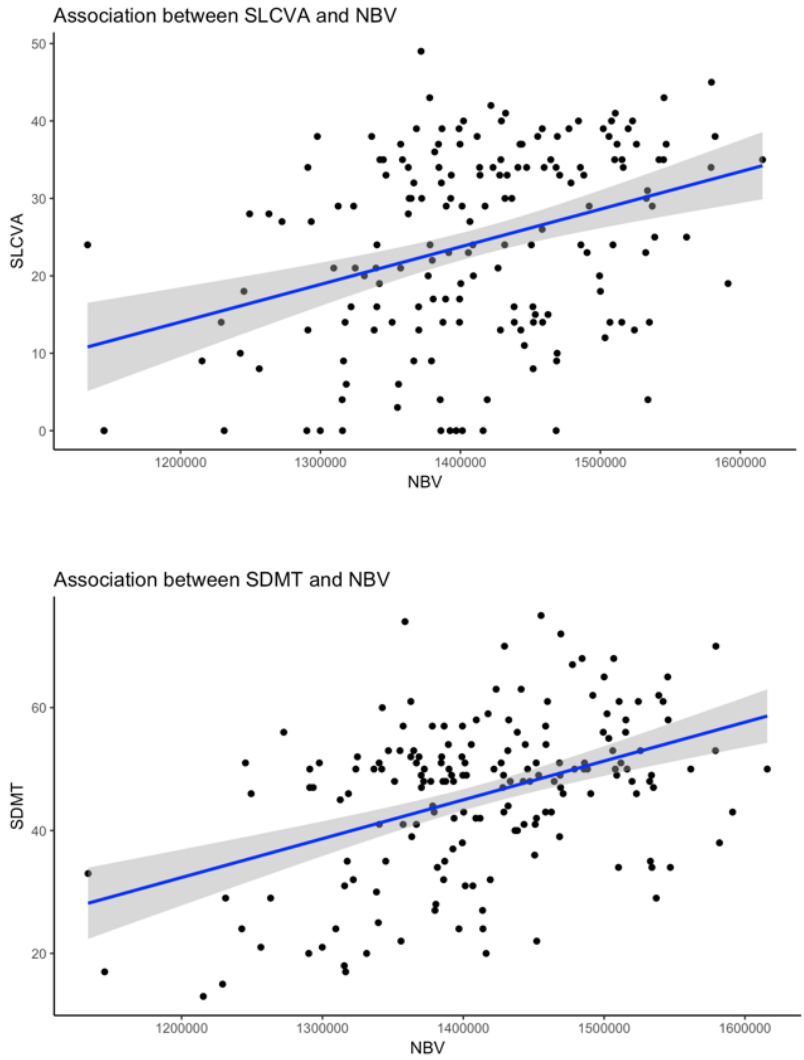

NBV: normalised brain volume. SDMT: symbol digit modalities test. SLCVA: Sloan low contrast visual acuity.

5.3 Conclusions

The demographic profile of the UCL patients was typical of people with SPMS with a mean age of 52 years and approximately two-thirds female. The disease duration was 22 years. There was homogeneity in patient demographics, clinical severity and MRI findings across the four arms, with just a slightly shorter duration of the disease in the placebo arm (19.9 vs 21.6-23.8). However, there was no difference in terms of pre-treatment relapse number or years since progression. When compared to the overall MS-SMART trial cohort, the demographic profile, the clinical severity and the MRI findings were also similar.

Correlation analyses showed no association (τ<0.3) between nomalised brain volume, T2 lesion volume and EDSS, T25FW, MSFC and PASAT. There were weak correlations between MRI metrics and SDMT, SLCVA 2.5% and 9HPT. When investigated in more details in regression models, adjusting for confounders, the associations between brain volume and SDMT or SLCVA was confirmed, whereas a trend towards significance was found between brain volume and 9HPT.

In the following Chapters, I will focus on the trial sub-studies including post-hoc analyses of interest. For each Chapter, I will firstly provide appropriate background before entering into the details of the analyses that I have carried out.

Chapter 6. **MRI sub-study: spinal cord**

6.1. Background: spinal cord in MS

The spinal cord is a compact structure organised into functional columns. Spinal cord focal lesions and diffuse abnormalities are seen on MRI in up to 90% of patients with MS and contribute to disability. Spinal cord lesions can occur at any level, but typically are seen in the upper cervical cord and can involve both white and grey matter. Because grey matter demyelination is associated with neuronal loss and secondary Wallerian degeneration, it is difficult to quantify whether axonal pathology in the cervical cord of MS patients is due to local damage or to retrograde and anterograde degeneration of neurons secondary to the injury of fibres traversing white matter lesions of the brain (Evangelou *et al.*, 2000). Indeed, previous MRI and pathology studies have demonstrated that individual lesions play a minor role in local atrophy (Bergers *et al.*, 2002; Evangelou *et al.*, 2005; Rashid *et al.*, 2006; Mann *et al.*, 2007). A recent study (Petrova *et al.*, 2018) suggested that axonal loss may not entirely account for atrophy seen on imaging, and that both gliosis and demyelination are significant contributors to the volume loss seen radiologically, questioning the utility of spinal cord atrophy measurements to assess disease progression. However, all the neuropathology changes occurring in the spinal cord contribute to development of cord atrophy in MS, an aspect that can be substantial in the progressive phases of the disease (Kearney *et al.*, 2015b).

Although spinal cord is affected in the majority of MS patients and cord atrophy is believed to reflect neurodegeneration, the role of spinal cord MRI measures – lesions and atrophy – as clinical outcome measures in clinical trials is still controversial.

With regard to the contribution of cord lesions to disease progression, there have been some inconsistent findings (Bot *et al.*, 2004; Evangelou *et al.*, 2005; Lukas *et al.*, 2013; Kearney *et al.*, 2015a). However, from a prognostic perspective, studies carried out in clinically isolated syndrome have shown that the presence of spinal cord asymptomatic lesions and cord atrophy at the time of presentation were associated with an increased risk of developing physical disability later on (Brownlee *et al.*, 2017; Arrambide *et al.*, 2018).

There have been several studies reporting strong associations between cord atrophy measures and clinical variables (Rocca *et al.*, 2011; Lukas *et al.*, 2013; Kearney *et al.*, 2015b; Schlaeger *et al.*, 2015). In a longitudinal study of a large cohort of patients with MS, spinal cord volume loss was independently associated with disease progression, and all MS patients showed a median decrease of spinal cord area of 1.5% per year, with higher values of -1.8%/year in SPMS (Lukas *et al.*, 2015).

In a recent systematic review and meta-analysis, which included 22 longitudinal studies of cord cross-sectional area from a pooled cohort of more than 1000 patients, Casserly and colleagues (Casserly *et al.*, 2018) supported the notion that spinal cord is atrophied in MS and that the magnitude of spinal cord atrophy is greater in progressive versus relapsing forms of the disease, and correlates with clinical disability. According to this study, the pooled annual rate of spinal cord atrophy was 1.78%/year (95% CI 1.28 to 2.27). This rate was greater than the one reported (0.4-0.6% per year) for brain atrophy in MS (De Stefano *et al.*, 2010), suggesting that the measurement of spinal cord area is highly relevant as an imaging outcome in MS clinical trials. In their review, Casserly and co-workers also estimated average values of cross-sectional area in all MS patients as 73.07 mm^2,

with lower values for patients with SPMS (68.55 mm^2). They estimated an average cross-sectional area of 80.87 mm^2 in healthy controls.

In a recent longitudinal study that included 51 SPMS patients (mean age 55, mean disease duration 19 years, median EDSS 4.5), spinal cord atrophy, quantified with cervical cord volume measurement, showed significant correlations with concurrent disability and could predict long-term outcome (Tsagkas *et al.*, 2018). In particular, the spinal cord atrophy rate was an independent predictor of physical disability as measured by EDSS, and was the strongest predictor of changes in the T25FW test, especially in patients with SPMS, although they found no statistical difference in the estimated annualised spinal cord atrophy between RRMS (-0.38%/year) and SPMS (-0.62%/year) (Prados and Barkhof, 2018).

A strong clinico-radiological association between spinal cord atrophy and disability measures in MS has been mostly found in progressive patients (Losseff *et al.*, 1996b; Stevenson *et al.*, 1998; Rocca *et al.*, 2011; Kearney *et al.*, 2015b). In cross-sectional studies, spinal cord measures differed between relapsing and progressive disease types, being more pronounced and strongly associated with clinical measures independently from brain measures particularly in progressive MS (Kearney *et al.*, 2015b). In a longitudinal study, Agosta and colleagues found that the cross-sectional area of the cervical cord at baseline, but not the MRI brain measures, was associated with accrual of disability at follow-up (Agosta *et al.*, 2007). However, in a 15-year follow-up study of 49 patients with PPMS (Rocca *et al.*, 2017), cord atrophy did not show statistical significance, in contrast to previous studies of PPMS with a shorter follow-up of 5 years (Sastre-Garriga *et al.*, 2005); whereas brain atrophy measures were good predictors of long-term clinical outcome. Rocca et al. argued that cervical cord atrophy may reach a floor effect after long disease-duration; therefore, no significant change could be detected.

6.1.1 Neuroimaging of the spinal cord

Performing quantitative spinal cord MRI measurements *in vivo* is technically challenging. This is mostly due to the small size of the cord, and the potential for cord motion during the scan, caused by both involuntary patient movement and physiological motion caused by cardiac and respiratory cycles (Wheeler-Kingshott *et al.*, 2014), particularly at the level of the thoracic spine. The cord is surrounded by a higher amount of bone, fat and CSF than the brain. Additionally, T2 or PD weighting imaging lack sensitivity and specificity to the MS-associated pathological changes in the spinal cord and the inherent contrast of spinal cord lesions against healthy cord signal is usually lower than in the brain parenchyma (Wheeler-Kingshott *et al.*, 2014).

Developments in spinal cord imaging in the past 5 years have improved both the qualitative characterisation and quantitative measures of spinal cord abnormalities. Reduced cross-sectional area of the upper cervical cord in patients with MS, in comparison with healthy controls, is thought to indicate atrophy of the cord. The most common method of assessing spinal cord atrophy is to measure the cross-sectional area at specific anatomical levels, typically in the cervical region in the area from C2 to C5. Indeed, the upper cervical cord can be considered as a surrogate of overall cord degeneration for two main reasons: a) lesions are more common in the cervical (Stankiewicz *et al.*, 2009) than thoracic cord; b) destructive processes in the thoracic cord should be reflected by Wallerian degeneration in the cervical cord.

Measures of cord cross-sectional area were initially manually performed, but over the past 20 years several semi-automated segmentation methods have been

developed. Losseff et al. reported a semiautomated edge-detection method involving the manual drawing of two regions of interest (one around the spinal cord and the other around the outer boundary of the surrounding CSF) and then calculating the mean signal intensity of the cord and surrounding CSF and using a signal intensity threshold halfway between the two to define the edge of the spinal cord, from which cross-sectional area could be calculated (Losseff *et al.*, 1996b). An evolution of this method, known as Active Surface Model (ASM) has been developed for automated cord edge detection and rapid measurement of the spinal cord size (Horsfield *et al.*, 2010). The ASM technique involves the normal placement of cord markers on some representative axial slices and subsequently an outline of the spinal cord is created automatically. Kearney et al. demonstrated that the active surface model can be combined with three-dimensional phase-sensitive inversion recovery (3D PSIR) images centred on C2-C3, which improves cord area measurement reproducibility (Kearney *et al.*, 2014, 2015b). More recently, fully automated spinal cord atrophy measurements have been implemented and validated (De Leener *et al.*, 2014, 2015).

An important issue in the spinal cord atrophy estimation is that spinal cord atrophy is conventionally measured using segmentation-based methods that quantify the spinal cord cross sectional area at each time point to obtain an indirect longitudinal cord atrophy measurement by numerical subtraction of the cord area between the two time points (Kearney *et al.*, 2014). Using this approach, longitudinal estimates of spinal volume or area loss can be affected by measurement noise at each time point, causing low reproducibility. To overcome this issue, registration-based techniques similar to the ones used for quantification of brain atrophy are being implemented (Moccia *et al.*, 2019).

Another important issue in the spinal cord MRI studies is finding the optimal normalisation factor for spinal cord atrophy measures in cross-sectional studies. Normalisation improves power for group comparisons by removing differences between patients that are related to biological variations not due to disease effects. A common cause of natural variation in cord cross-sectional area is subject's "size". Several metrics can be used to normalise spinal cord, such as spinal cord length, subjects' height, and intracranial volume measures (Healy *et al.*, 2012; Oh *et al.*, 2014).

6.1.2 Spinal cord measures in clinical trials

Table 6.1 shows phase 2 and 3 randomised controlled trials that used MRI-derived cervical cord cross-sectional area as an outcome measure (Tur *et al.*, 2018; Ciccarelli *et al.*, 2019).

Table 6.1 Randomised-controlled trials that used MRI-derived cervical spinal cord cross sectional area as an outcome measure

Trials	Patients	Duration	Change in MUCCA
Riluzole in PPMS (Kalkers *et al.*, 2002)*	PPMS (n=16)	24 months	Mean change in 1st year, without treatment: -2% Mean change in 2nd year, on treatment: -0.2%.
Interferon beta-1a in PPMS (Leary *et al.*, 2003)	PPMS (n=50)	24 months	-0.5% vs -1.0% vs 0.3% after 12 months (**ns**) and -3.7% vs 1.5% vs -1.3% after 24 months (**ns**)
Interferon beta-1a in RRMS and SPMS (PRISMS and SPECTRIMS trials) (Lin *et al.*, 2003)	RRMS (n=20) SPMS (n=18)	48 months	-1.5% vs -2.8% after 12 months (**ns**) -4.5% vs -5.7% after 48 months (**ns**)
interferon beta-1b in PPMS and transitional MS (Montalban *et al.*, 2009)	PPMS (n=49) SPMS (n=24)	24 months	-1.6% vs -1.3% after 12 months (**ns**) -0.9% vs -1.6% after 24 months (**ns**)

Lamotrigine for neuroprotection in SPMS (Kapoor *et al.*, 2010)	SPMS (n=120)	24 months	-1.60% vs -1.26% after 24 months (**ns**)
Fingolimod in PPMS (INFORMS trial) (O, n.d.) ECTRIMS 2018	PPMS (n=823)	24 months	-2.04% from baseline vs -2.44% after 24 months (**ns**)

PPMS = primary progressive multiple sclerosis, RRMS = relapsing-remitting multiple sclerosis, SPMS = secondary progressive multiple sclerosis.
None of the trials in this table showed treatment effects of the investigated experimental drug. * Run-in versus treatment trial (no specific treatment during the first year and all patients on riluzole during the second year).
Adapted from Tur et al.(Tur *et al.*, 2018) and Ciccarelli et al. (Ciccarelli *et al.*, 2019).

The trials reported in Table 6.1 have not shown a significant treatment benefit on spinal cord atrophy, which could be because of lack of absolute treatment effect, enrolment of non-informative study populations, or variability in the measurement techniques (Ciccarelli *et al.*, 2019) applied in the trials with a multicentre design. Interestingly, these clinical trials looking at spinal cord atrophy measures have mostly recruited PPMS rather than SPMS patients.

6.2 Objectives

The main objective of the spinal cord MRI study in MS-SMART was to investigate whether measurement of spinal cord atrophy could detect neuroprotection in the active arms versus placebo and could be used as an appropriate outcome measure for phase 2 trials in SPMS. In addition to the trial objective, I carried out a more detailed analysis of the spinal cord measures, investigating the clinical and radiological correlates of cervical cord cross-sectional area, cord lesions, and brain volume measures. Finally, I applied a new MRI analysis pipeline to improve the one already existing to quantify the mean upper cord cross-sectional area (MUCCA) and cord atrophy measurement.

In summary, the objectives of the study presented in this Chapter were as follows:

1) To explore the relationships of quantitative spinal cord MRI (MUCCA, cord lesion count, cord lesion volume) and clinical measurements of disease severity;
2) To compare the changes of upper cord cross-sectional area (cord atrophy) in the active treatment arms versus placebo to quantify possible MS-SMART study drug neuroprotection;
3) To assess whether there was a significant change in MUCCA between baseline and 96 weeks;
4) To investigate the relationship of spinal cord area/atrophy versus brain volume/atrophy as predictors of physical disability;
5) To assess whether cervical cord lesion volume was associated with disability independently from cord atrophy;
6) To test a new MRI analysis pipeline to reduce variability.

6.3 Methods

6.3.1 Participants

As previously discussed, advanced MRI imaging was an optional sub-study in place at the UCL and Edinburgh sites. MS-SMART patients who opted to take part in the advanced MRI sub-study at the UCL site underwent also cervical cord imaging as part of the scanning protocol. The inclusion/exclusion criteria for this sub-study were the same as the ones for the MS-SMART trial (see Chapter 2). Additionally, patients were excluded if the spinal cord imaging had poor quality.

6.3.2 Outcomes

For the purpose of this study, I used the following clinical measures of disability at baseline and week-96: EDSS, MSFC, 9HPT, T25FW, SLCVA 2.5% contrast, SDMT.

From an MRI perspective, I used the following metrics: MUCCA (at baseline and week-96), cervical cord lesion volume and count at baseline and week-96, brain volume at baseline, total intracranial volume at baseline, brain T2 lesion volume at baseline, and percentage brain volume change between baseline and week-96.

6.3.3 MRI: scans and analysis pipeline

All the participants were scanned at baseline and 96-week using a 3T Philips Achieva MRI system with RF multi-transmit technology (Philips Healthcare, Best, the Netherlands). Brain scans were performed with a 32-channel coil. A 16-channel neurovascular coil was used to acquire spinal cord scans. To minimise motion during scans, we placed a polystyrene-filled bag surrounding the neck. No major software upgrades were performed between baseline and follow-up.

The scanning protocol included:

- **Brain** (previously described):
    - 3D T1-weighted magnetization-prepared turbo field echo with slice thickness = 1 mm, TR = 6.8 ms, TE = 3.1 ms, TI= 824 ms; flip angle α = 8°; FOV = 256 × 256 mm2; voxel size = 1 × 1 × 1 mm3, NEX= 1; 180 sagittal contiguous slices.
    - Axial PD/T2-weighted images using a dual-echo turbo spin echo sequence with 3-mm slice thickness, TR = 3500 ms, TE1/TE2 =

19/85 ms, flip angle α = 90°; FOV = 240 × 180 mm2; voxel size = 1 × 1 × 3 mm3; NEX = 1; 50 axial contiguous slices.

- **Cervical cord:** T1-weighted 3D-phase sensitive inversion recovery (PSIR) sequence acquired in the axial plane without parallel imaging containing 16 contiguous slices, FOV=256×256 mm2, matrix=512×256, TR=8 ms, TE=3.7 ms, dual RF transmit, TI=843.6 ms and number of averaged signals=3. The voxel dimensions were 0.5×0.5×3 mm^3 and the acquisition time was 14:00 min. The cervical cord was imaged in the axial-oblique plane (i.e. slices perpendicular to the cord) from C2-C4 with the centre of the imaging volume positioned at the level of C2-3 intervertebral disc plane.

6.3.3.1 Brain imaging analysis

I provided a detailed description of the brain imaging analysis in Chapter 2. Briefly, the T2 lesion volume was manually measured at baseline on PD/T2-weighted scans and the lesion mask was used for lesion filling of the 3D-T1 scans. The 3D-T1 brain scans were then analysed using the GIF algorithm to extract and segment brain (Cardoso *et al.*, 2015). From the GIF analysis, which is fully automated, the following brain volumes were obtained: whole brain volume, white matter volume, grey matter volume (divided in deep grey matter and cortical grey matter volumes), and total intracranial volume. Differently from the analysis reported in Chapter 2, for the purpose of this Chapter, I did not use normalised brain volume measures. When I looked at the changes at the group level, I used total intracranial volume as normalisation factor to adjust for subject size (Healy *et al.*, 2012).

6.3.3.2 Spinal cord imaging analysis

To calculate the upper cervical cord lesion volume, I manually contoured lesions using a semiautomated edge-finding tool from JIM software (version 7.0, Xinapse systems, http://www.xinapse.com) (figure 6.1). Lesions were identified and outlined on the acquired 3D-PSIR scans (containing 16 contiguous 3-mm-thick axial slices) as focal abnormal areas with a visible hypointense abnormality with clearly defined margins (Kearney et al., 2015a). On 14 of the 16 axial slices from the 3D-PSIR scan, I manually contoured and counted the cord lesions; I excluded the top and the bottom 3D-PSIR axial slices (slice no. 1 and slice no. 16) as these were often affected by technical artefacts. Poorly demarcated areas of equivocal decrease in signal intensity were not outlined. Total lesion volume was obtained by the sum of the individual lesion volumes.

Figure 6.1 Contoured cord lesion

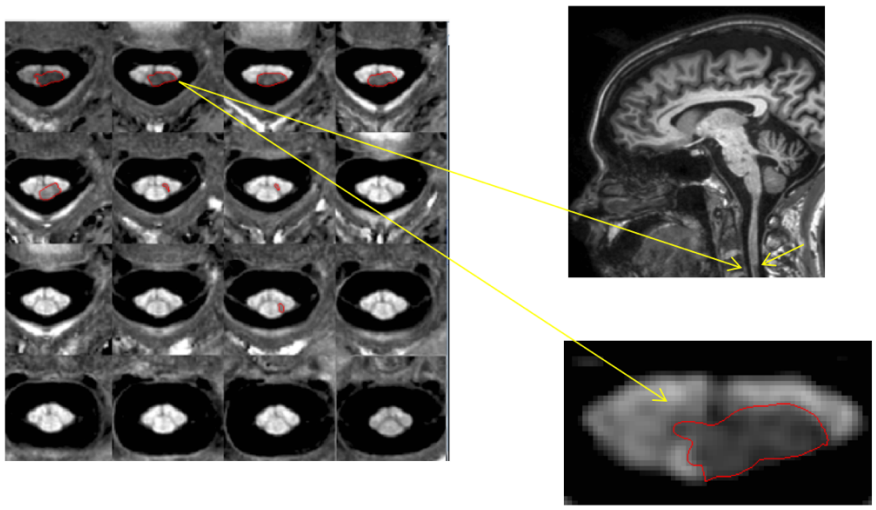

I calculated MUCCA using two methods, to which, for clarity, I will refer as the "established method" and the "implemented method". The established method refers to the MUCCA analysis pipeline already in use at the Queen Square MS Centre Trial Unit before I started my PhD. This pipeline was the one officially used

for the analysis of the spinal cord MRIs of the MS-SMART trial (Kearney *et al.*, 2014). The implemented method, as previously mentioned, emerged in due course of the trial MRI analyses during my PhD, and was developed with the aim of improving reproducibility and reduce variability of the MUCCA measurements.

MUCCA: established method

I calculated MUCCA using the active surface model on Jim software (version 7.0, Xinapse Systems, UK) from the 3D-PSIR image. To achieve this, I followed these steps (Figure 6.2):

1. I manually marked the centre of the five intermediate 3-mm thick slices of the 3D-PSIR scan (centred at C2–C3);
2. I ran the Jim software to automatically detect the cord edge and provide a marked cord area contour for each of the five selected slices;
3. I visually inspected the results for cord segmentation error and manually edited cord segmentation errors or re-positioned the central marker to re-ran software analysis if necessary;
4. I then recorded the five resulting cord area measures obtained with the Jim software and averaged these to have a final MUCCA.

I carried out this process for each patient scan and separately for each time point within the same patient (i.e. baseline and week-96). This semi-automated method of cord area detection showed good inter-rater and intra-rater reproducibility (Kearney *et al.*, 2014); however, the first step in this pipeline, corresponding to the manual positioning of a marker in the centre of each slices (step 1), was based on visual inspection. This implied that, for the same patient, the manual positioning of the central cord markers on the baseline scans did not correspond exactly to the same positioning of these markers on the week-

96 scans, potentially introducing a bias on the measurement of the longitudinal MUCCA change.

Figure 6.2 Cross-sectional area measurement

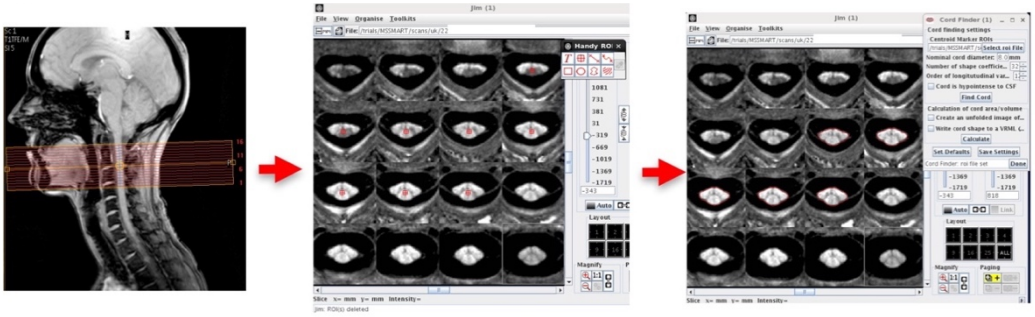

The left panel shows the positioning of the acquired volume scan (made of 16 slices) at the C2-C3 level. The middle panel shows the red cord markers that I manually positioned in the centre of the five cross-sectional slices acquired between C2-C3 (i.e. slices 7-11). Subsequently, I prompted the JIM7 software to run an automated cord edge detection tool, which found the cord area of the cross-sectional from the 5 slices I marked. MUCCA resulted from the average of the 5 cross-sectional areas.

MUCCA: implemented method

This implemented method aimed at making the MUCCA analysis almost fully automated reducing intra-subject variability. Despite controlling for head position and despite centring the scan acquisition volume parallel to the cord curvature on the C2-C3 intervertebral space for all subjects, I noted that different patient's neck positioning in the MRI scanner across two timepoints could also cause biased MUCCA quantifications. This could be due to physiological reasons, that is, when the neck is flexed, the cord is stretched, resulting in a relatively smaller MUCCA compared to when the neck is extended and the cord is relaxed. In order to confirm my observation based on a few patients, I scanned a healthy volunteer. Within the same scanning session, the cervical cord was scanned in three neck positions (extended, straight and flexed) (Figure 6.3) and MUCCA was obtained for each of the three contemporary scans and compared.

Figure 6.3 Different neck positions for acquisition of spinal cord scan

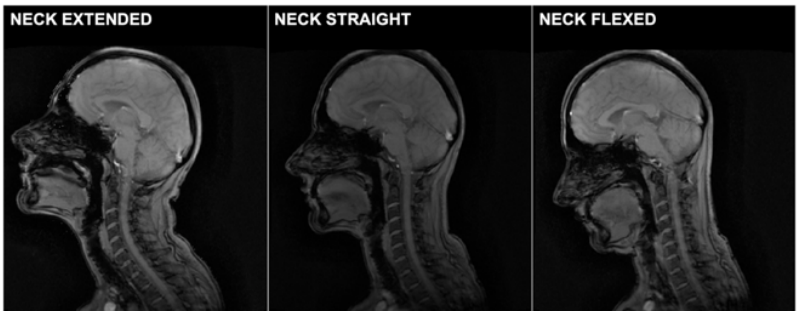

To decrease the MUCCA measurement bias due to the neck curvature and positioning, I re-analysed some of the already acquired scans using the following pipeline:

1) Each scan was computationally straightened using cord masks in the native space with geometric adjustment to account for cord curvature;
2) The axial imaging obtained with the cord straitening analysis were all centred in the same centre of gravity;
3) The 96-week follow-up scans were registered to the baseline scans;
4) The centre of the cord was marked using Jim7 in the 5 central cross-sectional scans for the first subject enrolled in the sub-study;
5) The same cord markers used from the first subject were then applied to all the other subjects at any timepoint, reducing manual input.

6.3.4 Statistical analysis

I explored baseline data looking at baseline associations between clinical and radiological variables using Pearson's or Spearman' correlation coefficients as appropriate. I corrected for multiple comparisons using false discovery rate (FDR) and Bonferroni corrections.

I looked at the comparison between change in MUCCA between trial arms using multiple regression models. These models included the trial arm as an explanatory factor variable (with placebo as the reference category), the baseline variable (corresponding to the outcome variable), and the minimisation variables age, sex, and EDSS at baseline.

I calculated the percentage MUCCA annual change between baseline and week 96 using the following formula: 100 × ([MUCCA at week 96− MUCCA at baseline]/[MUCCA at baseline]/[years between baseline and follow-up scans]). To confirm that this calculation was accurate and the change in MUCCA was statistically significant, I used paired t test and linear mixed effects models. I also looked at other variables changes using Wilcoxon test and/or mixed effects models for EDSS and for other clinical variables.

To investigate the associations between baseline brain volume, MUCCA and EDSS at week 96 or EDSS change between baseline and week-96, I used linear regression models where the EDSS at week-96 or EDSS change were the outcome variables, MUCCA and brain volume the predictors of interest, and age, sex, disease duration, and total intracranial volume were the variables of nuisance.

I reported the 9HPT score as the average time (seconds) between the two arms. I reported the T25FW score as the average (seconds) between the two walking attempts. I reported the SLCVA and SDMT as the number of correct answers (letters or numbers respectively).

Based on clinical scores, I divided participants into two groups: “progressed” and “non-progressed”. I defined disability progression if at week-96 there was at least one of these three criteria: i) an increase of 1.0 points or more when the baseline

EDSS score was <5.5 or an increase of 0.5 points or more when the baseline EDSS score was ≥5.5; ii) an increase of 20% or more from baseline on the T25FW; iii) or an increase of 20% or more from baseline on the 9HPT.

For T25FW and 9HPT, I calculated the percentage change with the following formula: 100 × ([Value at baseline – Value at week 96]/([value at baseline + value at week 96]/2)).

I used logistic regressions and reported odds ratio to investigate whether MUCCA, cord lesion volume, brain volume at baseline could predict disability progression at week 96. I used similar logistic models where the predictor was, in turn, T25FW or 9HPT and the outcome was disability progression.

6.4 Results

At UCL, 176 patients were randomised for the MS-SMART trial. Of these, 152 agreed in having the MRI advance protocol inclusive of the cervical cord 3D-PSIR scan (Figure 6.4). For two patients, we could not perform spinal cord imaging due to lack of time on the day of the trial visit. Eight scans were rejected due to poor quality, leaving 142 scans suitable for analyses. At 96 weeks, 131 scans were performed, but 9 were rejected due to poor quality, resulting in 122 scans available for the longitudinal analyses (Figure 6.4). Twenty scans at baseline and 6 at week-96 were unsuitable for the cord lesion analysis due to technical or motion artefacts, which did not affect the MUCCA measurement though (Figure 6.4). For all the patients, brain MRI and clinical metrics were available at baseline. At follow-up, for 1 out of 122 patients completing the spinal cord sub-study, the SIENA algorithm failed and percentage brain volume change was unavailable.

Figure 6.4 Patient disposition spinal-cord sub-study

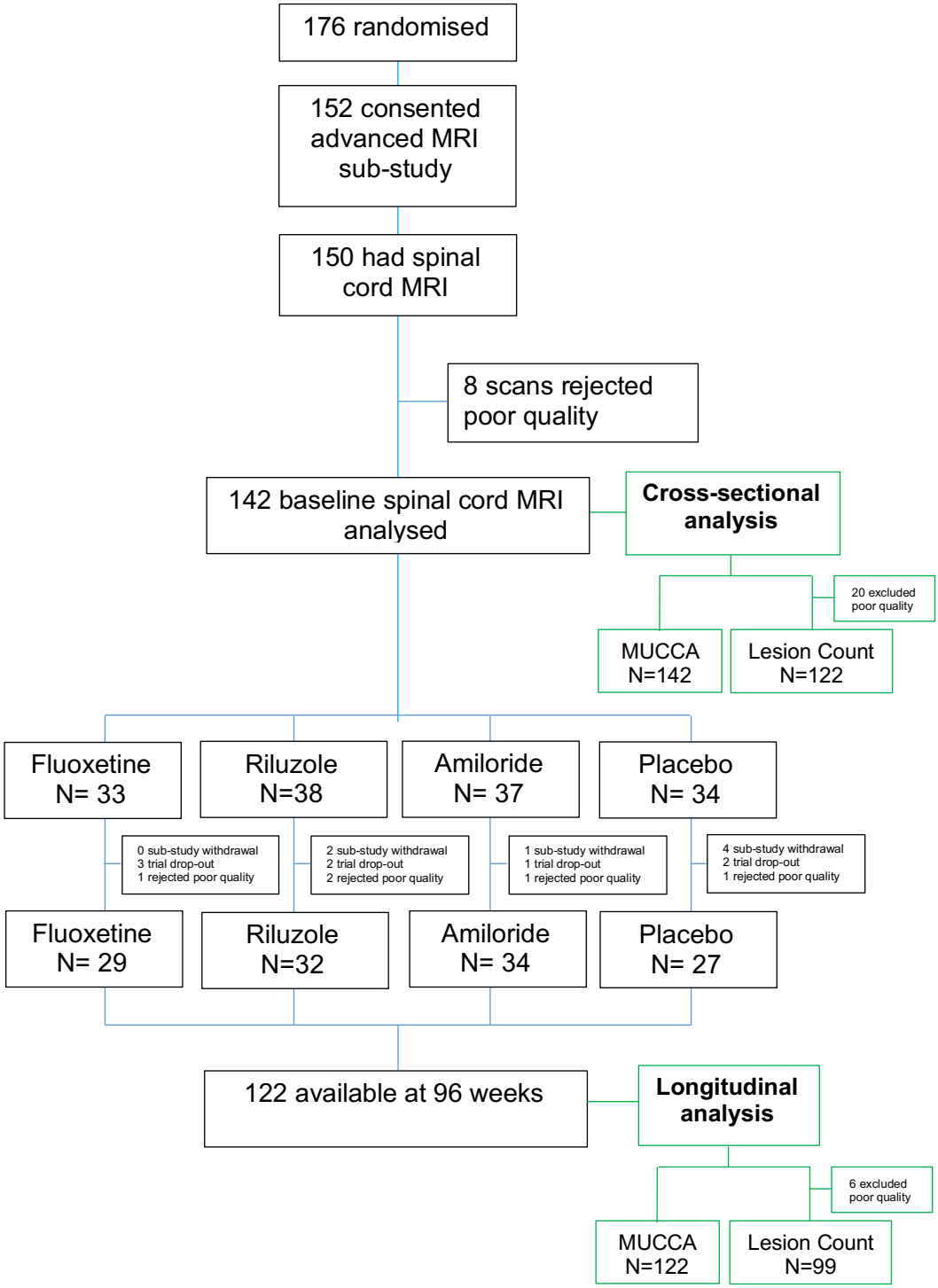

Sixty-two patients (51%) completing the spinal cord study showed disability progression. I was unable to measure disability progression in one of the 122 patients completing the spinal cord sub-study due to missing MSFC (and its sub-scores T25FW or 9HPT) at follow-up.

The baseline characteristics of the analysed patients who underwent the spinal cord MRI sub-study are reported in Table 6.2.

Table 6.2 Baseline characteristics spinal cord sub-study

Number randomised	**Fluoxetine (n=33)**	**Riluzole (n=38)**	**Amiloride (n=37)**	**Placebo (n=34)**	Overall **N= 142**
Gender					
Female N (%)	22	23	25	24	94 (66.2%)
Male N (%)	11	15	12	10	48 (33.8%)
Age					
Mean (SD)	55.7 (6.4)	54.4 (6.7)	55.5 (7)	54.1 (7.5)	54.9 (6.9)
Disease duration (yrs)	22.1 (8)	24 (10)	23.8 (10.2)	20.6 (9.5)	22.7 (9.5)
Mean (SD)					
Progression duration (yrs)					
Mean (SD)	7.2 (4.7)	9.9 (6.1)	9 (6.3)	8.9 (7.1)	8.8 (6.1)
Relapses prior 2 yrs	3	2	5	3	13 (9%)
N (%)*					
EDSS					
Median (Min-Max)	6 (4.0; 6.5)	6 (4.0; 6.5)	6 (4.0; 6.5)	6 (4.0; 6.5)	6 (4.0; 6.5)
MSFC					
Mean (SD)	0.08 (0.6)	-0.23 (1.3)	0.17 (0.6)	0 (1.2)	0.0 (1)
T25FW (average)					
Mean (SD)	16.4 (15.7)	23.5 (38.9)	17 (17)	23 (38)	20.1 (29.6)
9HPT (average)					
Mean (SD)	42.3 (67.7)	54.9 (86.4)	62.5 (106.4)	34.5 (22.2)	49.1 (78.3)
PASAT					
Median (Min-Max)	43 (9; 57)	40 (0; 59)	41 (15; 60)	46.5 (13; 60)	43.5 (0; 60)
SDMT					
Median (Min-Max)	48 (17; 67)	48 (20; 61)	49 (22; 70)	48 (15; 70)	48 (15; 70)
SLCVA 2.5% binocular					
Median (Min-Max)	30 (0; 39)	22.5 (0; 49)	24 (0; 40)	24 (0; 45)	26 (0; 49)
T2LV (ml)					
Mean (SD)	13.5 (9)	14.6 (11.7)	11.7 (9.4)	11.4 (10.3)	12.7 (9.8)
MUCCA (mm^2)	70.4 (9.6)	69.2 (9.2)	67.8 (7.6)	67.5 (10)	68.53 (9.27)
BV (ml)	1058.9	1069.6	1040.8	1059.5	1057.20 (93.7)
Mean (SD)	(87.9)	(92.9)	(86.5)	(108.4)	
DGMV (ml)	33.8 (3.3)	34.1 (3.4)	33.9 (4)	33.9 (4)	33.8 (3.6)
Mean (SD)					
CGMV (ml)	592.2 (48.8)	597.7 (50)	583.5 (42.4)	589.8 (54.1)	590.8 (48.7)
Mean (SD)					
TIV (ml)	1156.8	1179.9	1111.5	1128.8	1144.5 (204.5)
Mean (SD)	(220.1)	(203.6)	(186.2)	(210.5)	
SCLV (ml)	0.4 (0.4)	0.3 (0.2)	0.3 (0.3)	0.3 (0.2)	0.3 (0.3)
SCLN	2.4 (1.6)	2.6 (1.5)	2.4 (1.4)	2.2 (1.1)	2.4 (1.4)

MUCCA= mean upper cord cross-sectional area; EDSS= expanded disability status scale; MSFC= multiple sclerosis functional composite; 9HPT= 9-hole peg test; T25FW= timed 25-foot walk; PASAT= paced auditory serial addition test; SDMT= symbol digit modalities test;

SLCVA= Sloan low contrast visual acuity. FDR= false discovery rate; BV= brain volume; CGMV= cortical grey matter volume; DGMV= deep grey matter volume; T2LV= T2 lesion volume; SCLV= spinal cord lesion volume; SCLN= spinal cord lesion number; TIV= total intracranial volume.

6.4.1 Cross-sectional relationships between cervical cord MRI, brain MRI, and disease severity measures at baseline

When looking at the associations between MUCCA and clinical measures, there were significant correlations between MUCCA, EDSS and MSFC, also after adjusting for multiple comparisons (Table 6.3). There was a very weak correlation between MUCCA and T25FW or SDMT (Table 6.3); however, the *p* values of these correlations did not survive the multiple comparisons correction. There was no significant correlation between MUCCA and 9HPT, PASAT or SLCVA 2.5%.

Table 6.3 Correlations between MUCCA and clinical variables at baseline

		EDSS	MSFC	9HPT	T25FW	PASAT	SDMT	SLCVA 2.5%*
MUCCA	Correlation Coefficient	-0.29	0.26	-0.09	0.18	0.08	0.17	0.14
	p value	**<0.001**	**0.001**	0.27	0.03	0.3	0.04	0.09
	Adjusted p value (FDR)	**0.003**	**0.003**	0.3	0.07	0.3	0.07	0.12
	Adjusted p value (Bonferroni)	**0.007**	**0.007**	1	0.21	1	0.28	0.63
	Sample size N	142	142	142	142	142	141**	141**

*Binocular measure. **One subject had very poor vision and was unable to undertake the SDMT and SLCVA 2.5% testing. MUCCA= mean upper cord cross-sectional area; EDSS= expanded disability status scale; MSFC= multiple sclerosis functional composite; 9HPT= 9-hole peg test; T25FW= timed 25-foot walk; PASAT= paced auditory serial addition test; SDMT= symbol digit modalities test; SLCVA= Sloan low contrast visual acuity. FDR= false discovery rate.

When looking at the associations between MUCCA and MRI measures, there were significant correlations between MUCCA and all the considered MRI measures, also after adjusting for multiple comparisons (Table 6.4 and Figure 6.5). The strongest correlation was seen between MUCCA and cord lesion volume (rho= -0.43; 95% CI= -0.57 to -0.28; p<0.001).

Table 6.4 Correlations between MUCCA and MRI variables at baseline

		BV	CGMV	DGMV	WMV	T2LV	SCLV
MUCCA	Correlation coefficient	0.23	0.20	0.26	0.24	- 0.21	-0.43
	P-value	0.005	0.01	0.002	0.003	0.01	<0.001
	Corrected p value (FDR)	0.008	0.01	0.007	0.007	0.01	0.003
	Corrected p value (Bonferroni)	0.025	0.05	0.01	0.015	0.05	0.007
	Sample size N	142	142	142	142	142	122

Raw brain volume measures were used. MUCCA= mean upper cord cross-sectional area; BV= brain volume, CGMV= cortical grey matter volume; DGMV= deep grey matter volume; WMV= white matter volume; T2LV= T2 lesion volume; SCLV= spinal cord lesion volume.

Figure 6.5 Baseline correlation plots

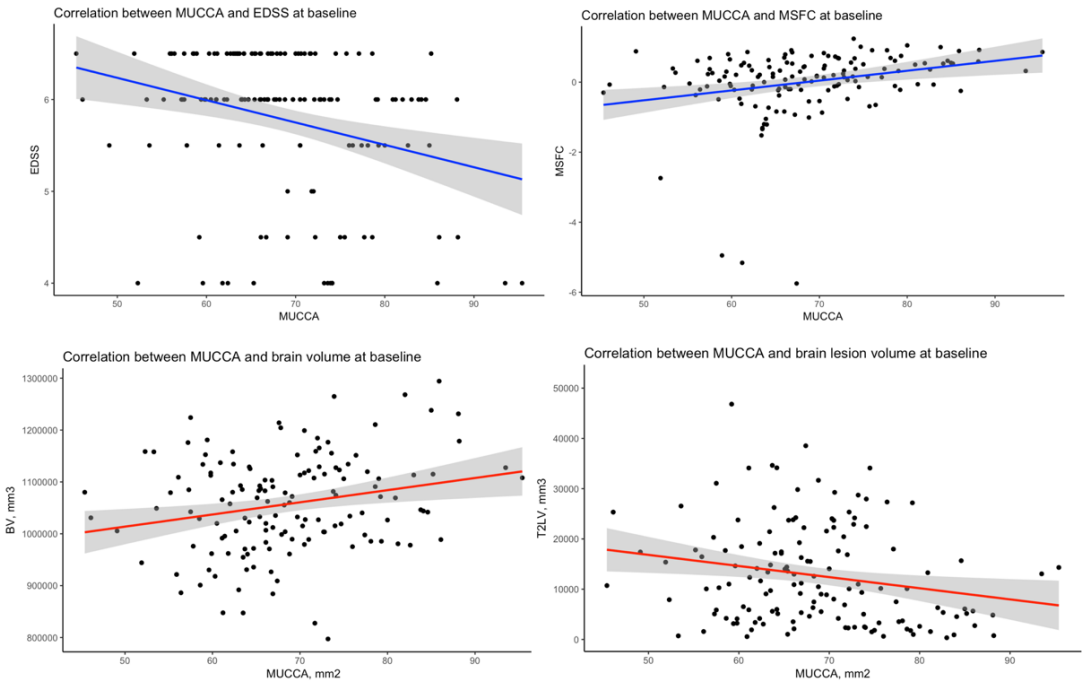

EDSS= expanded disability status scale; MSFC= multiple sclerosis functional composite; MUCCA= mean upper cord cross-sectional area; BV= brain volume, T2LV= T2 lesion volume.

6.4.2 Comparisons between treatment arms

There was no statistically significant difference in MUCCA changes between each active treatment arm and the placebo arm (Table 6.5)

Table 6.5 Comparison between arms versus placebo

	Adjusted mean difference of MUCCA change at 96-week (Active– Placebo) and 95% confidence interval*	p-value
Fluoxetine	-0.372 (-1.262 to 0.518)	0.410
Riluzole	-0.587 (-1.458 to 0.284)	0.185
Amiloride	-0.445 (-1.303 to 0.414)	0.307
Placebo		

6.4.3 Changes in MUCCA and key clinical variables between baseline and 96 weeks.

T-test showed a statistically significant change in MUCCA between baseline and week 96 (t= 5.6; 95% CI= 0.54 to 1.13; p<0.001). The change of EDSS between the two time points measured with Wilcoxon test was also significant (p= 0.05).

Mean cord percentage change for patients completing the week 96 study (n=122) was -0.66% (SD 1.31) per year.

These findings were confirmed by unadjusted linear mixed effects models. The annualised mean MUCCA atrophy rate was -0.0066 mm^2/year (standard error [SE]= 0.001; p<0.001), which corresponds to a percentage cord atrophy change of -0.66% per year. By using the same statistical model, EDSS significantly changed by a value of 0.068 per year (SE=0.029; p= 0.018). In comparison, for the same patients (except one for whom the SIENA algorithm failed), the percentage brain volume change during the 96 weeks of the trial was -1.6% (SD 1.54), corresponding to an annualised rate of - 0.87%.

When applied to MSFC and its sub-scores, adjusted linear mixed effect models showed as follows:

- MSFC: annualised change -0.14 z-score (SE=0.039; p<0.001);

- 9HPT: annualised change 4.4 sec (SE=3.4; p=0.079; trend to significance);
- T25FW: annualised change 4.65 sec (SE=1.25; p<0.001);
- PASAT: annualised change 0.39 number of correct answers (non-significant);
- SDMT: annualised change 0.26 number of correct answers (non-significant);
- SLCVA 2.5%: -1.04 number of correct answers (SE=0.35; p=0.003).

6.4.4 MUCCA is a predictor of physical disability

The results from the adjusted multivariable regression model showed that baseline MUCCA could predict EDSS at week 96 (Standardised beta: -0.35, SE= 0.085; adjusted R^2= 0.11; p<0.001) and EDSS changes (Standardised beta: -0.23, SE= 0.088; adjusted R^2= 0.054; p=0.01). In separate regression models, brain volume could predict EDSS at 96 weeks (Standardised beta: -0.52, SE= 0.17 adjusted R^2= 0.06; p=0.003) but not EDSS changes. When the two measures - baseline MUCCA and brain volume - were pooled in the same regression model (adjusted R^2= 0.06), MUCCA remained statistically significant (p=0.01); whereas, no statistically significant association was found with brain volume and EDSS change (p=0.93) (figure 6.6). When the outcome was EDSS at 96 weeks, both MUCCA (Standardises beta= -0.32, p<0.001) and brain volume (Standardises beta= -0.44, p=0.008) were significant (adjusted R^2= 0.16).

Figure 6.6 Association between MUCCA at baseline and EDSS change

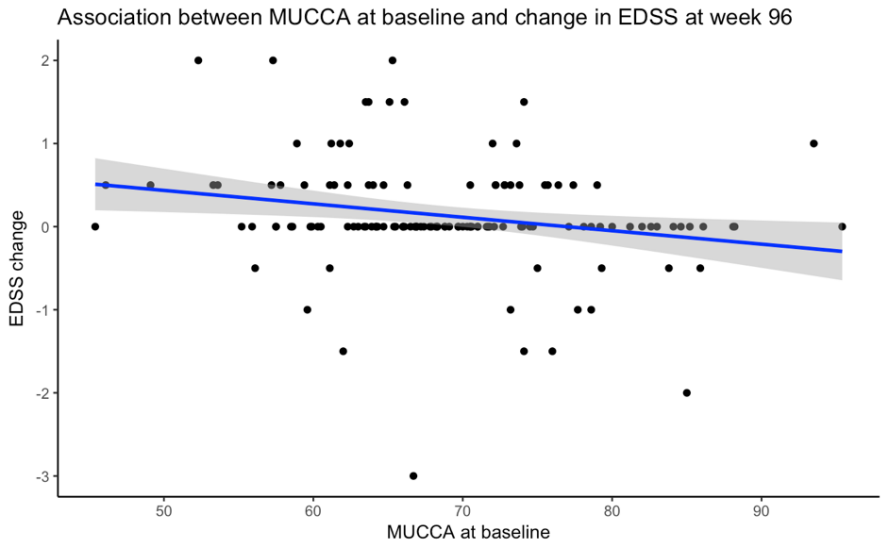

In an adjusted logistic regression model (adjusted for age, sex, disease duration and total intracranial volume) where the predictors were MUCCA and brain volume at baseline and the outcome was the occurrence of disability progression (as described in methods), MUCCA, but not brain volume, was significantly associated with the occurrence of disability progression (OR= 0.94; 95% CI= 0.89 to 0.98, p= 0.01). This means that, for every one unit (i.e every 1 mm^2) decrease in MUCCA, there was a 6% percent increase in the odds of disability progression.

When I looked at the percentage MUCCA change and percentage brain volume change and how these related to disability progression and EDSS change using logistic regression models, neither percentage MUCCA change nor percentage brain volume change could predict disability progression; however, percentage brain volume change showed trends towards significance though (p=0.064).

Finally, in separate linear regression models looking at the associations between EDSS, T25FW and 9HPT at 96 weeks with MUCCA and brain volume, I found that both MUCCA (Standardised B= -0.32, adjusted R^2= 0.16, p<0.001) and brain volume (Standardised B= -0.45, adjusted R^2= 0.16, p=0.008) at baseline could

significantly predict EDSS at 96 weeks. Only brain volume, but not MUCCA, could predict T25FW at 96 weeks (Standardised B= -0.47, adjusted R^2= 0.03, p=0.01). Neither MUCCA nor brain volume could significantly predict 9HPT at 96 weeks. Neither percentage MUCCA change nor brain volume change were statistically significantly associated with the three clinical measures at 96 weeks.

Table 6.6 summarises the results from this section.

Table 6.6 MUCCA as a predictor of physical disability

Predictor	Outcome	Statistical model	Variables of nuisance	P value
MUCCA at baseline	EDSS change	Linear regression	- Age - Sex - Disease-duration - Total intracranial volume - Baseline brain volume (**ns**)	0.01
MUCCA at baseline	Disability progression	Logistic regression	- Age - Sex - Disease-duration - Total intracranial volume - Baseline brain volume (**ns**)	0.01
MUCCA at baseline	EDSS at week-96	Linear regression	- Age - Sex - Disease-duration - Total intracranial volume - Baseline brain volume **(p=0.008)**	<0.001
MUCCA at baseline	T25FW at week-96	Linear regression	- Age - Sex - Disease-duration - Total intracranial volume - Baseline brain volume **(p=0.01)**	**ns**
MUCCA at baseline	9HPT at week-96	Linear regression	- Age - Sex - Disease-duration - Total intracranial volume - Baseline brain volume **(ns)**	**ns**
MUCCA % change	Disability progression	Logistic regression	- Age - Sex - Disease-duration - Total intracranial volume - Brain volume % change (**ns**)	**ns**
MUCCA % change	EDSS at week-96	Linear regression	- Age - Sex - Disease-duration - Total intracranial volume - Brain volume % change (**ns**)	**ns**

MUCCA % change	T25FW at week-96	Linear regression	- Age - Sex - Disease-duration - Total intracranial volume - Brain volume % change (**ns**)	**ns**
MUCCA % change	9HPT at week-96	Linear regression	- Age - Sex - Disease-duration - Total intracranial volume - Brain volume % change (**ns**)	**ns**

9HPT: 9-hole peg test. EDSS: expanded disability status scale. MUCCA: mean upper cord cross-sectional area. Ns: non-significant. T25FW: timed 25-foot walk.

6.4.5 Relationship between cervical cord lesions, cord area, brain volume and disability

There was no significant statistical change of cord lesion volume or count between baseline and follow-up. I looked at the associations between lesion volume in both cord and brain at baseline and EDSS at 96 weeks. In the same multivariable linear regression model, where EDSS at 96 weeks was the outcome variable and cord and brain lesion volumes at baseline were the predictors, both cord lesion volume (Standardised beta=0.2; SE= 0.93; p= 0.04; adjusted-R^2= 0.09) and brain T2 lesion volume (Standardised beta=0.25; SE= 0.99; p=0.01; adjusted-R^2= 0.09) could predict EDSS at 96 weeks after adjusting for age, sex, disease-duration and total intracranial volume. However, when I looked at the EDSS change as an outcome, none of the two measures (i.e. baseline cord lesion volume or brain T2 lesion volume) was significant. When I used disability progression as a binary outcome of a logistic regression model, none of the two measures reached statistical significance as a predictor, although brain T2 lesion volume showed a trend towards significance (p= 0.07).

Subsequently, in the adjusted multivariable regression model that included cord lesion volume, brain lesion volume, MUCCA and brain volume at baseline, cord and brain lesion volume were no longer significant, whereas both MUCCA and brain volume at baseline were independent predictors of EDSS at week 96. In this

model, brain volume seemed to be a slightly stronger predictor of EDSS (standardised beta= -0.43; SE= 0.21; p= 0.04) as compared to MUCCA (standardised beta= -0.20; SE= 0.10; p= 0.005). Using the same statistical model, but looking at EDSS change as outcome variable, I found that only MUCCA, and not brain volume, was able to predict this (Standardised beta= -0.26; SE= 0.11; p=0.03).

Using cord and brain lesion volumes, and MUCCA and brain volume at baseline, I fit a further logistic regression model, adjusting for age, sex, disease duration and total intracranial volume, to predict disability progression. The results of this analysis showed that, at baseline, only MUCCA could significantly predict disability progression (OR= 0.94; 95% CI= 0.88 to 0.99; p= 0.04) (Table 6.7). For every unit decrease in MUCCA, there is a 6% increase in the odds of disability progression.

Table 6.7 Logistic regression model results for cord and brain variables

Disability progression	OR	95% CI		P value
		Lower	*Upper*	
MUCCA, mm²	0.94	0.88	0.99	0.04
Brain volume, ml	1	0.99	1.0	0.26
Cord lesion volume, mm³	1	0.99	1.0	0.85
Brain T2 lesion volume, ml	1	0.99	1.0	0.48

Model adjusted for age, sex, disease-duration and total intracranial volume. OR= odds ratio; CI= confidence interval; MUCCA= mean upper cord cross-sectional area.

6.4.6 Improved spinal cord imaging pipeline

As mentioned in the method section, a healthy volunteer was consecutively scanned in the same MRI session to acquire 3D-PSIR in three different neck position (extended, straight and flexed). After the scan acquisition and using the established method for calculation of cord-area, I obtained the following MUCCA results: in the “flexed position”, MUCCA was 78.82 mm2, in the “straight position”

it was 78.94 mm2, and in the “extended position” it was 81.3 mm2. The corresponding differences between the three positions were as follows: difference “straight-extended” position 2.36 mm2; difference “straight-flexed” position 0.12 mm2; difference “extended-flexed” position 2.48 mm2 (Figure 6.7).

Figure 6.7 Different MUCCA values according to neck position during scan acquisition

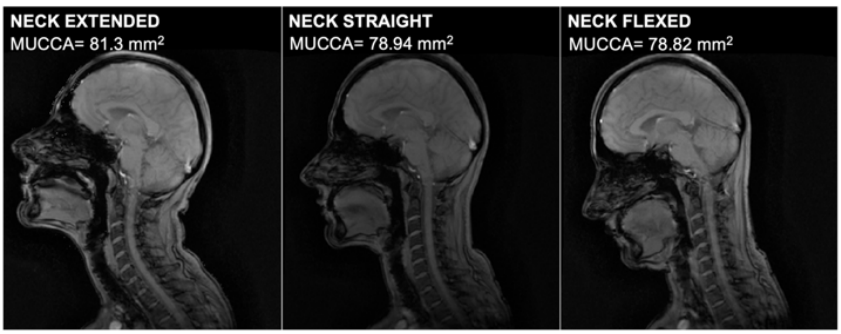

Based on these results, I applied six different methods to measure MUCCA with the aim of reducing the variability between the three neck positions (Figure 6.8).

Figure 6.8 Different chin positioning MUCCA analysis

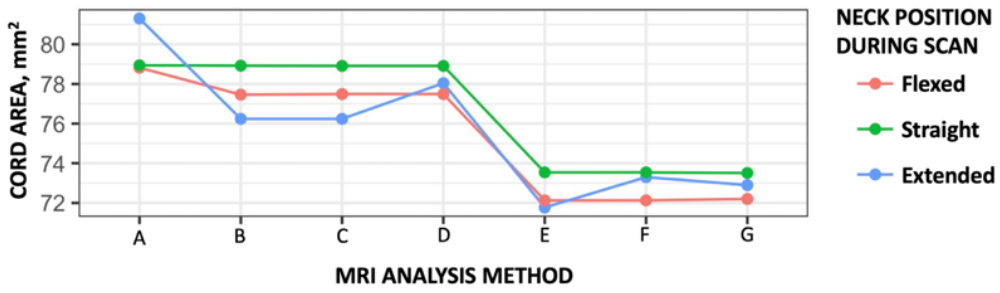

A= standard method (cord not straightened and central marker positioned manually on each scan); **B**= cord straightened and central marker positioned manually on each scan; **C**= cord straightened and same central marker for each scan; **D**= cord straightened, same central marker for each scan and correction of the orthogonal level; **E**= cord straightened, same central marker for each scan, and denoised; **F**= cord straightened, same central marker for each scan, correction of the orthogonal level and denoised; **G**= cord straightened, same central marker for each scan, correction of the orthogonal level, denoised, and intensity corrected.

As showed in Figure 6.8, all the alternative methods produced less variability in the three measurements of MUCCA. However, I noted that applying denoise and intensity correction significantly decreased the initial MUCCA value. Ultimately, method D showed consistent MUCCA results across the three measurements, with MUCCA values not too dissimilar to the ones obtained with the established method.

I then used the method D to compare the variance of MUCCA change between baseline and week- 96 versus the one from the standard method. I carried out an exploratory analysis in the first 19 consecutive enrolled subjects. As shown in Figure 6.9, the mean values between the MUCCA changes across the two methods showed similar median, but a wider variability.

Figure 6.9 Comparison of two methods to calculate longitudinal changes in MUCCA in the first 19 consecutive enrolled patients

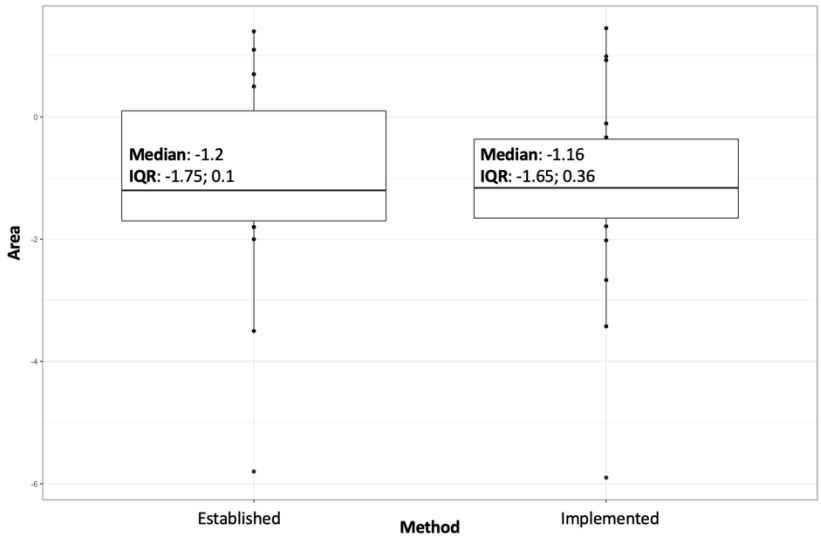

This suggested that the implemented method provided less variability in the measurement of the MUCCA changes. However, when I extended the analysis to the whole cohort (n=111), I found similar values of medians and IQRs (Figure 6.10). The implemented method failed for 11 follow-up scans.

Figure 6.10 Comparison of two methods to calculate longitudinal changes in MUCCA extended to the whole cohort

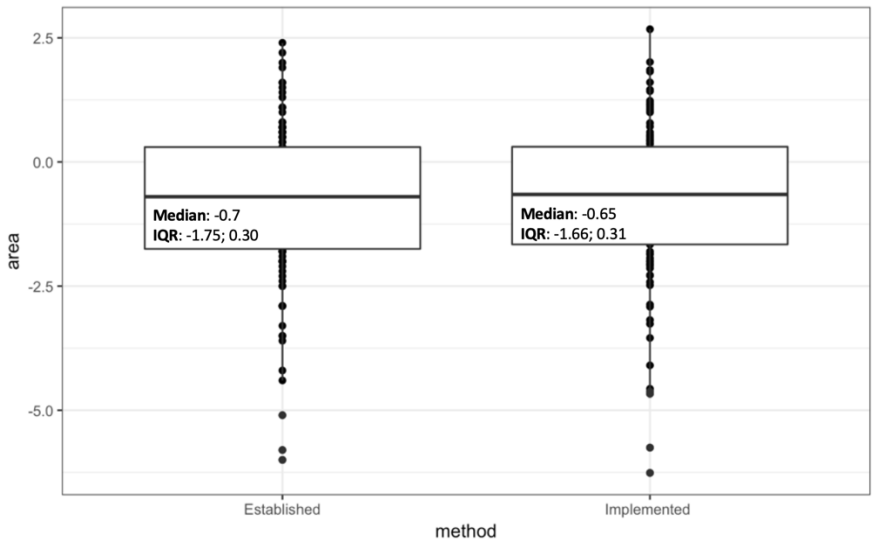

6.5. Discussion

To the best of my knowledge, this study represents the largest prospective spinal cord MRI investigation carried out in SPMS, including 142 subjects at baseline and 122 at follow-up. Clinical data were collected as part of a rigorous randomised-controlled trial; MRI scans were acquired at a single centre and imaging analyses were carried out by a single investigator, reducing biases related to heterogeneity of the sample, or inter-scanner and inter-rater variability.

The clinical and radiological characteristics of the MS-SMART trial participants included in this spinal cord sub-study reflected a real world SPMS population, with mean age of 55 years, mean disease-duration of about 22 years and median EDSS of 6.0.

The MS-SMART trial, as showed in the previous chapters, did not show any treatment effects. Not surprisingly, there was no statistically significant difference between MUCCA changes in the three trial arms versus the placebo arm. Nevertheless, a more detailed analysis of the spinal cord data showed that, cross-sectionally, MUCCA was significantly correlated with EDSS, MSFC, brain volume, brain T2 lesion volume and cord lesion volume. The relationship between MUCCA and EDSS at baseline was robust; it survived correction for multiple comparisons and was confirmed in adjusted multiple regression analyses, where MUCCA could also predict EDSS at 96 weeks and EDSS changes.

In line with previous reports (Kearney *et al.*, 2015b), I found that MUCCA and brain volume were independently associated with EDSS. As this clinical scale is a measure strongly weighted towards locomotion and spinal cord damage is known to cause mobility impairment, it seems plausible thinking that clinical progression is more related to spinal cord atrophy rather than brain pathology. However, when looking at other clinical variables T25FW, which reflects integrity of sensorimotor tracts through the spinal cord, this was only associated with brain volume and not with MUCCA. This finding is physiologically plausible, as sensory motor function not only rely on an intact spinal cord but also on neocortical and cerebellar neuronal integrity. Similar findings were seen by Furby et al (Furby *et al.*, 2008) who cross-sectionally analysed a cohort of 117 patients enrolled in the neuroprotective trial of lamotrigine in SPMS. They reported that cord area was significantly correlated with EDSS and 9HPT, but not with walking test; whereas, normalised brain volume measured significantly correlated with walking test and 9HPT, but not with EDSS. They explained this discrepancy arguing that the use of walking aids and orthoses by the majority of patients with SPMS would improve ambulation masking inter-individual variations in walking speed. Therefore, the timed-walk might not be an ideal measure of mobility at this late stage of the

disease. Another possible explanation of this clinic-radiological discrepancy can be drawn from the study by Petrova and co-workers, who showed that, in long-lasting MS, the magnitude of spinal cord atrophy (about 20%) does not reflect well the degree of axonal loss (about 60%) suggesting that MRI indices of spinal cord volume or area obtained in vivo are likely to underestimate the extent of axonal damage in the cord (Petrova *et al.*, 2018). Therefore, poor motor performance due to axonal loss might not be detectable with the standard quantitative MRI measures.

I found that the strongest correlation between baseline MRI variables and MUCCA was represented by the cord lesion volume. This finding was expected and supported by previous evidence suggesting that cord lesion in the cervical tract contribute to cord atrophy (Evangelou *et al.*, 2005; Lukas *et al.*, 2013; Kearney *et al.*, 2015a). Indeed, atrophy in MS has been attributed to a combination of local tissue loss within demyelinated lesions and Wallerian degeneration of fibre pathways (Miller *et al.*, 2002b). However, tissue loss within lesions does not seem to play a significant role in the size of the cord at the level of the lesion (Evangelou *et al.*, 2005) and a recent report from the MSBase Study Group found that the presence of spinal cord lesions in patients with RRMS did not increase the risk of conversion to SPMS (Fambiatos *et al.*, 2019), although other studies have shown that cord lesions can predict future disability (Dekker *et al.*, 2019) and patients with spinal cord lesions have are at higher risk of disability progression (Sombekke *et al.*, 2013; Brownlee *et al.*, 2017; Arrambide *et al.*, 2018). My analysis showed that cord lesion volume could predict EDSS at 96 weeks ($p= 0.04$), but this association was lost when I included measures of MUCCA and brain volume in the statistical models, suggesting that MUCCA was the only independent cord measure predictor of EDSS at week 96.

Regarding changes over time, the percentage brain volume change during the 96 weeks of the trial was -0.87% per year. In comparison, MUCCA significantly changed after 96 weeks with a percentage rate change of -0.66% per year. This annual rate of cord atrophy is lower than the ones reported in other studies. In a recent meta-analysis of spinal cord atrophy in MS (Casserly *et al.*, 2018), the authors described cord atrophy rates up to -1.78%-2%/year. In previous publications, Lukas and colleagues found rates of cord area loss of -1.8% per year in SPMS (Lukas *et al.*, 2015). In the SPMS cohort of the lamotrigine trial (Kapoor *et al.*, 2010), Furby and colleagues found percentage rates of cord area change of -1.8% per year (Furby *et al.*, 2010). The explanation of these differences may rely on the characteristics of the study populations and the MRI analysis method used to obtain cord area. Despite recruiting SPMS patients with mean age and disease-duration similar to the ones from MS-SMART, the participants enrolled in the lamotrigine trial were on average about 5 years younger and had about 4 years shorter disease duration. In the study from Lukas et al, there were 73 patients with SPMS pooled from two centres (Amsterdam and Basel) with median age of 54 years, median disease-duration of 18 years and median EDSS at baseline of 5.5, which is lower than the one from MS-SMART (i.e. 6.0). Furthermore, in the study from Lukas and colleagues, patients had a baseline MUCCA of 79.7 mm^3, which is higher than the one in MS-SMART (i.e. 68.53mm^2). These considerations may support the hypothesis formulated by Rocca et al, who did not find significant change in cord area in a long-term observational longitudinal study in PPMS possibly due to the fact that cervical cord atrophy may reach a floor effect after long disease-duration, not showing detectable significant changes (Rocca *et al.*, 2017). Additionally, Lukas and colleagues found that higher MUCCA at baseline were associated with faster spinal cord atrophy rates and it can be speculated that the rate of spinal cord tissue loss slows down over time, with already highly atrophied structures exhibiting slower atrophy rates (Lukas *et al.*, 2015).

Interestingly, Tsagkas and colleagues (Tsagkas *et al.*, 2018) recently found annualised spinal cord atrophy rates of -0.62%/year in their SPMS group of 51 patients, although they measured cord atrophy by mean of spinal cord volume. Their SPMS cohort was similar to the MS-SMART one in terms of demographics and disease duration, but participants were less disabled with a median EDSS 4.5.

MRI analysis of spinal cord atrophy varies across studies and mostly relies on semi-automated non-registration-based methods. As discussed in the introduction, the methods in use across studies are not directly comparable. Additionally, being semi-automated, they imply manual inputs that could potentially bias the results. Furby et al, in the lamotrigine trial, applied the same method as Lukas to calculate cord atrophy obtaining similar annualised cord atrophy rates. The active surface model that I used to calculate MUCCA required minimal manual input, similarly to the method used by Tsagkas et al, who analysed cord volumes using the *Cordial* toolbox (Amann *et al.*, 2016). In a study comparing the different semi-automated and fully-automated methods to quantify cord area, repeated measurements of cross-sectional area seem to differ according to the method used to obtain it, with lower values provided by fully automated methods than semi-automated methods, with differences in reproducibility according to the cervical level and the type of scan analysed (ECTRIMS Online Library. Lukas C. Oct 11, 2018; 231981; 232). I can only speculate that the Lukas method might overestimate cord atrophy changes overtime and the active surface model might underestimate cord atrophy changes. However, there is no study that has compared these two methods longitudinally in SPMS.

As far as the relationships between brain volume, MUCCA and clinical measures are concerned, both MUCCA (Standardised Beta= -0.32, $p<0.001$) and brain volume (Standardised Beta= -0.44, $p=0.008$) could independently predict EDSS at

week 96. However, only brain volume, and not MUCCA, could predict T25FW at 96 weeks (Standardised B= -0.47, adjusted R^2= 0.03, p=0.01) and neither MUCCA nor brain volume could significantly predict 9HPT at 96 weeks, although the 9HPT values did not significantly change over time. Finally, MUCCA, but not brain volume, was significantly associated with the occurrence of disability progression in the logistic regression model (OR= 0.94; 95% CI= 0.89 to 0.98, p= 0.01).

Limitations of this study include the use of a semi-automated method to obtain MUCCA that, as discussed, could have introduced bias due to the manual input and the lack of a pure registration-based method between baseline and follow-up scans. Additionally, the way the percentage cord atrophy change was computed differed from the one used for the percentage brain volume change, which was based on the SIENA method. Other limitation includes the lack of a control group of matched healthy subjects to compare MS-related spinal cord atrophy versus age-related cord atrophy. Additionally, I analysed together the three active arms and the placebo arm. I cannot exclude that the study drugs – amiloride, fluoxetine and riluzole – had an effect on cord atrophy; however, this seems extremely unlikely, given that all the primary and secondary trial outcomes were negative.

In conclusion, this study supports previous findings showing that there is a significant correlation between spinal cord atrophy and disability in SPMS patients with more than 20 years of disease-duration. The relationship between cord area and clinical disability as measured by EDSS is independent of brain atrophy, suggesting that irreversible tissue loss occurs in the spinal cord of patients with greater disability. Whereas baseline brain volume predicted T25FW at 96 weeks, spinal cord measures could not explain other clinical measures, including T25FW, suggesting that these MRI measures do not capture all clinically relevant pathology in MS. This could be due to MRI analysis limitations either for lack of registration-

based method for the spinal cord atrophy or due to the intrinsic factors which make quantitative MRI measures unable to estimate axonal loss accurately. Cord lesions certainly contribute to cord atrophy, but are not sufficient to explain neurodegeneration or disability, at least in the short period of 96 weeks. Cord and brain atrophy rates were very similar (0.66% and 0.87% respectively) suggesting that, in longstanding SPMS, cord area loss is still detectable, but it likely slows down compared to earlier stages of the disease where higher levels of atrophy rates were seen by other investigations.

Based on my findings, spinal cord atrophy measures are strongly associated with EDSS both cross-sectionally and longitudinally. Nevertheless, when compared with brain atrophy measures, cord measures do not seem to offer a clear advantage in the detection of neurodegeneration in this SPMS phase 2 clinical trial cohort. Future studies should implement registration-based cord atrophy measures and possibly integrate more advanced MRI techniques, such as diffusion imaging or magnetisation transfer, capable to detect more accurately axonal loss in the cord, which might be underestimated otherwise.

Chapter 7. **OCT sub-study**

In this Chapter, I shall describe briefly the anterior visual pathway anatomy and function, and the advantage of using OCT to visualise the optic disc and retina. Subsequently, I will provide a detailed description of the cohort undergoing OCT at the London site. Finally, I will report the cross-sectional study that I carried out on the overall OCT cohort including the participants from the London and Edinburgh site.

7.1. Background

7.1.1. The anterior visual pathway: a window on the brain

The anterior visual pathway is part of the CNS. It includes the neurosensory retina, traditionally divided into ten layers, including five major cell types arranged in three cellular layers (ganglion cell layer [GCL], inner nuclear layer and outer nuclear layer) and separated by two synaptic layers (inner plexiform layer [IPL] and outer plexiform layer) (Figure 7.1). The outer nuclear layer contains cell bodies of photoreceptors; the inner nuclear layer includes horizontal, bipolar, and amacrine cells; and the GCL contains ganglion cells and some displaced amacrine cells.

Figure 7.1 Retinal layers

This figure was removed due to copywrite.

The figure is available in Neurology (Ratchford et at, 2013)

Adapted from Ratchford et al, Neurology 2013 (Ratchford *et al.*, 2013).

The macula is located temporal to the optic nerve and measures approximately 5.5 mm in diameter. The macula is further divided into the fovea (1.5 mm in diameter) and foveola (0.35 mm). The fovea corresponds to the retinal area where vision is sharpest and coincide with the centre of gaze that we direct toward the objects of our attention. In the foveola - the very centre of gaze - the inner layers of the retina including the RNFL, GCL, inner plexiform layer, outer and inner nuclear layers are shifted aside (Figure 7.2) and nearly disappear in a way that light has direct access to the underlying photoreceptors without distortion. Ganglion cells are not present at the centre of the fovea, but their number is greatest around the fovea (forming up to nine layers of ganglion cells).

Figure 7.2 Refraction of light onto the retina

This figure was removed due to copywrite.

The figure is available in Principles of Neural Science by Eric Kandel, James Schwartz, Thomas Jessell, 2000

Light from an object in the visual field is refracted by the cornea and lens and focused onto the retina at centred at the level of the fovea. Adapted from Kandel, 2000.

The photoreceptor cells, in the outermost layer, absorb light and, through a series of cellular connections, convert it into a neural signal - a process known as phototransduction - which is relayed to retinal ganglion cells in the innermost layer, whose axons compose the RNFL and serve as the final common output pathway of the retina, the optic nerve (Kandel, 2000; Frohman *et al.*, 2006).

The optic nerve can be divided in into 4 portions according its course: intraocular (optic nerve head), intraorbital, intracanalicular, and intracranial. The intraocular portion, or optic nerve head, is located approximately 4.5mm nasal to the fovea and is visible on fundoscopy. Retinal axons enter the optic disc at a 90 degrees angle. Each optic nerve is composed of approximately 1.2 million retinal ganglion cell axons. In the intraorbital part of the optic nerve, the nerve fibres are arranged in bundles separated by secta and are unmyelinated at this point. The optic nerve travels posteriorly through the lamina cribrosa to exit the back of the globe, where it becomes myelinated and increases in diameter from 3 mm to 4 mm. It is also at this point that the optic nerve becomes ensheathed in the meninges and CSF fills the tube-shaped subarachnoid space between nerve and sheath.

The axons of ganglion cells travel in the RNFL, enter the optic nerve, travel through the chiasm and tract, and then finally synapse primarily in the lateral geniculate nucleus of the thalamus. Studies in human eyes indicated that the axons within the RNFL have a rough topographic organisation within the optic nerve head. Foveal ganglion cells send axons directly to the temporal aspect of the optic disc in the papillomacular bundle, whereas fibres from areas temporal to the fovea are displaced to more superior and inferior regions to form arcuate bundles coursing above and below the fovea and finally enter the superior and inferior portions of the optic nerve. Finally, axons originating nasal to the disc enter the nasal portion of the optic nerve (Fitzgibbon and Taylor, 1996; Frohman *et al.*, 2006). The axons of the papillomacular bundle are smaller in diameter compared to axons elsewhere in the retina. The small size of axons possibly makes the papillomacular bundle particularly vulnerable, explaining the frequently seen temporal thinning of the RNFL in MS. Axons of the RNLF are unmyelinated as the refractile characteristic of myelin may interfere with vision. However, these axons are ensheathed by the

surrounding processes of glial cells such as astrocytes and Müller cells, which are present in the RNFL.

7.1.2. Visual impairment and low contrast letters in MS

Visual disturbances are common in MS and both afferent and efferent visual pathways may be damaged by the disease. Optic neuritis is the most common afferent visual pathway manifestation in MS, being the presenting symptom of the disease in 25% of cases and occuring during the disease in about 70%. Disorders of the efferent visual pathway such as diplopia, nystagmus, oscillopsia are also common and affect approximately 40 to 76% of patients (Toosy *et al.*, 2014; Costello, 2016).

Axonal loss is recognised as a major cause of irreversible disability in MS and impaired visual function after optic neuritis. In acute optic neuritis, RNFL thickness increases due to optic nerve swelling. Subsequently, the optic nerve lesion leads to retrograde degeneration of the RNFL which will result in reduced thickness as a consequence of significant axonal loss (Toosy *et al.*, 2014). In the setting of acute inflammatory demyelination of the optic nerve, axonal loss is a consequence of the direct damage and axonal transection (Trapp *et al.*, 1998). Hickman and colleagues demonstrated the presence of optic nerve atrophy following monoloateral optic neuritis in a cross-sectional study (Hickman *et al.*, 2001). Another study has shown that, although most patients make a good clinical recovery after optic neuritis, the RNFL thickness in the affected eye decreases of about 20% (Henderson *et al.*, 2010a).

However, axonal loss also occurs as a result of chronic demyelination and this is likely to affet eyes of people with progressive MS (Henderson *et al.*, 2010b).

Indeed, the anterior visual system is a frequent target of the MS disease process and, on post-mortem analysis, almost all patients with MS are found to have characteristic changes in the retina and optic nerve, regardless of whether they have previously experienced acute optic neuritis (Ikuta and Zimmerman, 1976; Toussaint *et al.*, 1983). These data suggest that the visual system has a very high predilection for developing disease-related disability both from acute episodes of optic neuritis and from the more-constitutive elements of the disease process that contribute to an MS-related chronic optic neuropathy. These could, therefore, be used effectively to illustrate the histopathology of the disease process in MS.

The spatial resolution of the visual system can be assessed clinically using visual acuity measures. Traditionally measured with the Snellen charts, visual acuity is nowadays better estimated in research studies by mean of logMAR scores, requiring Early Treatment Diabetic Retinopathy Study (ETDRS) charts (Early Treatment Diabetic Retinopathy Study research group, 1985). A standard ETDRS chart measures the logarithmic (base 10) minimum angle of resolution at 4 m or less and provides a linearly continuous variable (Figure 7.3).

Figure 7.3 ETDRS chart representing high contrast (100%) contrast chart

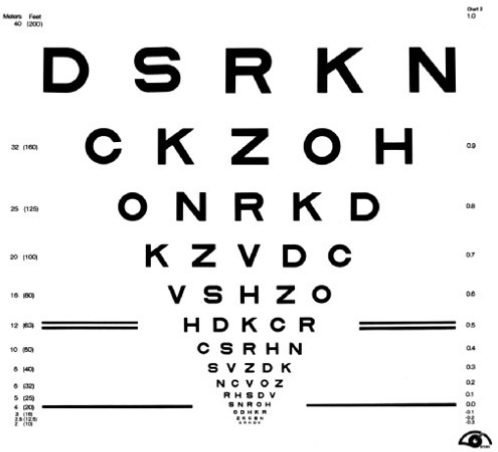

Low-contrast letter acuity charts are more sensitive than standard-contrast acuity charts at detection of visual dysfunction in MS. Contrast is defined as the quantity of lightness or darkness contaned by an objcect with respect to its background. Low-contrast letter acuity measure corresponds to the identification of grey letters of different intensity on a white background. As for the high contrast letters, the format of the low-contrast letter acuity may be the standardised ETDRS visual acuity charts in the form of the Sloan low constrast visual acuity (SLCVA) charts. In this Logmar-type charts, each line of letters gets progressively smaller whilst the contrast remains the same. Charts have varies contrast levels, e.g. 1.25%, 2.5% and 5% (Figure 7.4). The charts are scored by counting the number of correct letters (Balcer *et al.*, 2017).

Measures of low contrast vision in optic neuritis and MS have been shown to be reliable and sensitive to visul impairment, despite normal scores of the high contrast vision (Beck *et al.*, 2004; Balcer *et al.*, 2017). In the IMPACT trial (assessing the efficacy of interferon-beta 1b vs placebo in SPMS), for instance. they found that low-contrast letter acuity scores were significantly lower in patients than in controls (Balcer *et al.*, 2003).

Figure 7.4 Sloan low contrast visual acuity charts

This figure was removed due to copywrite.

The figure is available in Multiple Sclerosis Journal (Balcer et al., 2017)

Different contrast charts (5%, 2.5% and 1.25%) are shown.

Additionally, SLCVA are associated with T2 lesion load, MRI-derived brain volume and OCT measures of RNFL thickness (Talman et al 2010).

7.1.3. Optical coherence tomography

OCT is an ocular imaging technique first described by Huang et al. in 1991. It was used to scan the retina for the first time in vivo in 1993 and provided evidence of retinal pathology in early studies in 1995. Since these pivotal studies, OCT machines and techniques have evolved making the anatomy of the anterior visual pathways easily visualiseble *in vivo* and several studies have shown a good correlation between OCT retinal layers and retinal histopathology (Frohman *et al.*, 2006).

OCT is a non-invasive tool analogue of B-mode ultrasound, but based on light reflections instead of acoustic waves. OCT relies on interferometry of near-infrared light to construct very high-resolution images of the retinal layers. In retinal OCT imaging, a light source, represented by a superluminescent diode, emits a low-coherence, laser light wave, which is directed onto the retina through the pupil of the person being scanned. Differently from ultrasonography, direct detection of light echoes from tissues is not possible because light waves have a high speed compared with acoustic waves. Therefore, the laser light wave emitted by the diode reaches a beam splitter or a partial mirror, which splits the light wave in half. One part of the light wave – the reference wave - travels to a reference mobile mirror that reflects it directly back towards the beam splitter. The other part of the light wave - the sample wave - enters the eye and travels to the sample tissue (in our case, the retina). Depending on the optical properties of the tissue, some amount of light may be absorbed, refracted or reflected. More specifically, the light directed onto the retina crosses the transparent structures of the eye and is partially

absorbed, whereas a larger fraction is backscattered by the different retinal layers. In physics, when two light waves of the same length and constant phase difference meet, they are combined through superposition, a phenomenon called interference. If the light waves are in phase, they add together in constructive interference; if they are out of phase, they cancel each other out in destructive interference. Applying this principle to the specific case of retinal OCT scanning, the reflected portion of the sample light wave from retinal tissue travels back towards the beam splitter, where it meets with the reference light wave. When the sample and reference light waves meet, they either intensify or diminish depending on how the sample light interacts with the tissue. As a results of the co-occurrence of the two wave fronts, an interference signal is induced and registered by a photodetector or spectrometer to create a pixel for the specific tissue. The retinal OCT image is the result of the registration of repeatedly incoming interference signals from the retina and cross-sectional imaging is achieved by performing successive axial measurements of back-reflected light at different transverse positions (Frohman *et al.*, 2008; Hamdan *et al.*, 2012) (Figure 7.5).

Figure 7.5 Basic physics of OCT functioning

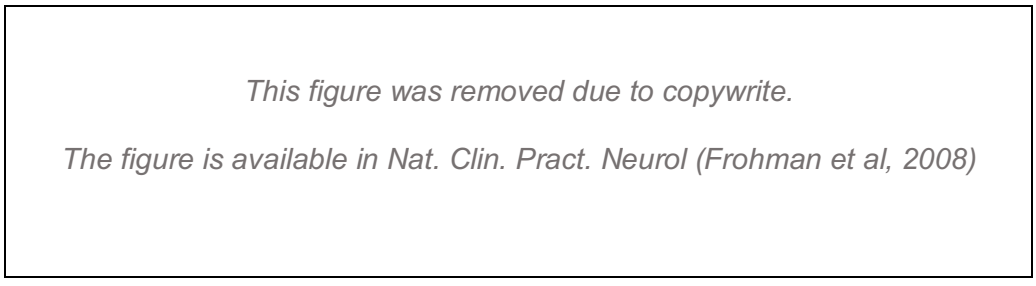

Adapted from Frohman et al, 2008

OCT performs cross-sectional and volumetric imaging by measuring the magnitude and echo time delay of backscattered light. Cross-sectional images are

generated by transversely scanning the incident optical beam and performing sequential axial measurements of echo time delay (axial scans or A-scans). This produces a two-dimensional data set which represents the optical backscattering in a cross-sectional plane through the tissue. Images, or B-scans, can be displayed in false colour or grey scale in order to visualize internal tissue structure of pathology (Drexler and Fujimoto, 2015).

OCT allows measurement of retinal layers and RNFL thickness. As the RNFL is principally composed of unmyelinated axons originating from the ganglion cells located in the ganglion cell layer within the macula, by measuring RNFL thickness, OCT provides an estimation of axonal integrity. OCT also allows measurement of the GCL in the form of ganglion cell and inner plexiform layer (GCIPL) complex.

There are several OCT machine vendors, but the two most widely used OCT scanners are provided by Carl Zeiss, Dublin, CA, USA (Cirrus OCT device) and Heidelberg Engineering, Heidelberg, Germany (Spectralis OCT device). Indeed, the vast majority of the published OCT studies in MS show data collected by mean of either of the above OCT machines.

In MS, retinal neuronal layer pathology can be primary (Saidha *et al.*, 2011b), due to a neurodegenerative process independent of demyelination, or secondary to optic nerve demyelination, resulting in retrograde axonal degeneration. Cross-sectional studies of OCT have shown that peripapillary global RNFL (gRNFL) and inner retinal layer thicknesses are reduced in MS and correlate with clinical disability and MRI-derived brain volume measures. These findings have been confirmed by longitudinal studies showing that gRNFL exhibits accelerated thinning in MS compared to healthy controls and that the GCL thickness was decreased in MS and mostly in SPMS (Saidha *et al.*, 2011a).

Many studies have reported an inverse correlation between RNFL thickness and EDSS in MS, and the strongest correlation was found for patients not affected by optic neuritis (Petzold *et al.*, 2010). Abnormalities of the retinal layers other than the gRNFL have been observed in post-mortem specimens from patients with MS, where 79% of eyes exhibited ganglion cell loss and 40% showed amacrine and bipolar cell loss in the inner nuclear layer. These findings have been corroborated *in vivo* by OCT, demonstrating thinning of the GCL and IPL (inner plexiform layer), and associated with reductions in visual function and vision-specific quality of life. These retinal findings demonstrated by OCT also correlate with more general clinical and imaging measures of MS disease activity and severity (Balcer *et al.*, 2015).

Frohman and colleagues, in an extensive review of the literature, confirmed that using OCT in MS can provide valid, reliable, and reproducible data to track the process of neurodegeneration within the retina of patients with MS with optic neuropathy. gRNFL thickness and macular volume analyses can serve as a surrogate biomarker and primary outcome measure to confirm the neuroprotective effects of new drugs (Frohman *et al.*, 2006).

In addition to the gRNFL, measures of GCIPL atrophy appears to mirror MRI-derived whole-brain atrophy measures, particularly grey matter atrophy, especially in progressive MS (Saidha *et al.*, 2015).

Martinez-Lapiscina and colleagues (Martinez-Lapiscina *et al.*, 2016), seeking for a putative biomarker to predict the course of MS, undertook a study to assess whether a single measurement gRNFL thickness or macular volume with OCT in eyes without optic neuritis could reflect the risk of disability worsening in patients

with MS. They showed that patients with MS and gRNFL thickness of up to 87 μm (with Cirrus OCT machine) or 88 μm (with Heidelberg OCT machine) in eyes without optic neuritis had roughly twice the risk of disability worsening during follow-up compared with patients with thicker gRNFL. This risk was independent of other factors known to be associated with disability worsening, including age, disease duration, baseline level of disability (EDSS), and the use of disease-modifying therapies. It has been suggested that the process of neurodegeneration within the retina is an indication of similar processes occurring more diffusely within the brain and spinal cord of patients with MS.

In conclusion, during the past decade, OCT has evolved into a sensitive method for imaging of neurodegeneration in MS. Since the retina is the only location where a tissue layer made up of axons can be imaged directly, quantification of the RNFL has the potential to open a window for the monitoring of neurodegeneration (Petzold *et al.*, 2010). OCT has a good analytical reproducibility, is cost-effective, correlates with clinical measures (loss of visual function or EDSS), and is predictive of a clinical outcome (poor visual recovery) (Petzold *et al.*, 2010).

Finally, reports from recent research studies measuring neurodegeneration in MS on one side (Saidha *et al.*, 2015) and clinical trials of neuroprotection in optic neuritis on the other side (Raftopoulos *et al.*, 2016), have shown that gRNFL and GCIPL thicknesses can be measured using OCT to provide a plausible biomarkers of axonal loss, supporting their use as outcome measures in clinical trials or neuroprotection in MS.

7.2. Objective

For clarification, I will divide the objectives (and analyses) of this Chapter in two sections:

a) **Section1- PhD Analysis:** this was designed for my PhD project and aimed at looking at the cross-sectional and longitudinal relationships of peripapillary RNFL (global [gRNFL] and temporal [tRNFL] sector) and GCIPL thicknesses with clinical and MRI measures.
b) **Section 2 - Trial Analysis:** this included the statistical analysis carried out in accordance with the pre-specified statistical analysis plan of the MS-SMART trial. According to the trial protocol, the OCT measures were collected as part of the exploratory objectives where peripapillary gRNFL and GCIPL thicknesses were obtained to quantify neuroprotection between active and placebo trial arms.

7.3. Methods

7.3.1. Participants

Participants recruited for the MS-SMART trial at the UCL and Edinburgh sites were invited to take part in this optional OCT sub-study. In addition to the eligibility criteria of the MS-SMART trial (see Chapter 2), participants were excluded if they had ocular pathology not due to MS or had refractive errors greater than ±6 dioptres. Medical history with respect to visual symptoms was obtained. History of optic neuritis (ON) was collected based on patient reports and medical records. Sub-study specific consent forms were obtained for all participants before performing OCT scans.

7.3.2. Clinical outcomes

For the purpose of this sub-study, the following variables (collected at baseline and week 96) were used: EDSS, MSFC (and the three sub-scores 9HPT, T25FW, PASAT), SDMT, SLCVA 2.5%.

7.3.3. OCT imaging and outcomes

OCT imaging was performed on a spectral domain OCT (software version 6.9.4.0 Spectralis, Heidelberg Engineering, Heidelberg, Germany) at both the UCL and Edinburgh sites. Table 7.1 shows imaging acquisition parameters at the two sites participating in the OCT sub-study.

Table 7.1 OCT scan acquisition parameters

RNFL	**Edinburgh and UCL parameters**	
Peripapillary circular scan	Nsite protocol: pre-set RNFL-N Circular scan diameter: 3.4 mm (12º) A-scans: 1536 ART 100 Eye-Tracking enabled Follow-up function enabled	
MACULA	**Edinburgh parameters**	**UCL parameters**
Macular volume scan	Retina protocol: pre-set PPole Volume: 30x 25º A-scans: 768 B-scans: 61 Alignment: posterior pole 7.0º ART: 12 Follow-up function enabled	Nsite protocol: pre-set RNFL-N Volume: 20x 20º A-scans: 1024 B-scans: 25 Alignment: vertical 90º ART: 9 Follow-up function enabled

RNFL: retinal nerve fibre layer; ART: automatic real time.

Scans were taken in condition of room-lighting dimmed, with no pharmacological pupil dilation. Peripapillary gRNFL and tRNFL, and GCIPL mean thickneses – measured in microns (μm) - were collected at baseline and 96 weeks.

To obtain peripapillary RNFL, a circular scan (table 7.1) was manually centred around the optic nerve head. The OCT machine automatically calculated average

thicknesses of the gRNFL and its sub-quadrants including the temporal one for tRNFL (Figure 7.6 and 7.7).

Figure 7.6 Peripapillary RNFL scan with sectors

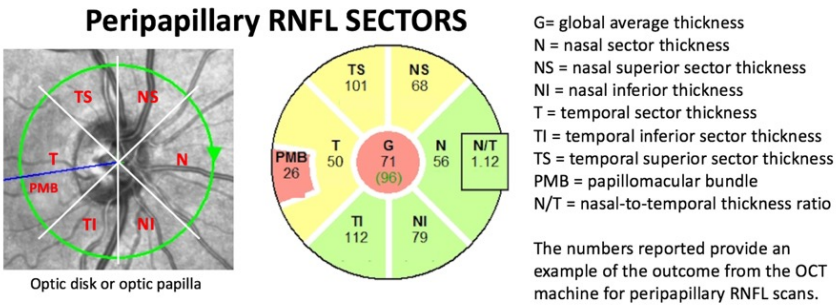

Figure 7.7 Peripapillary RNFL scan

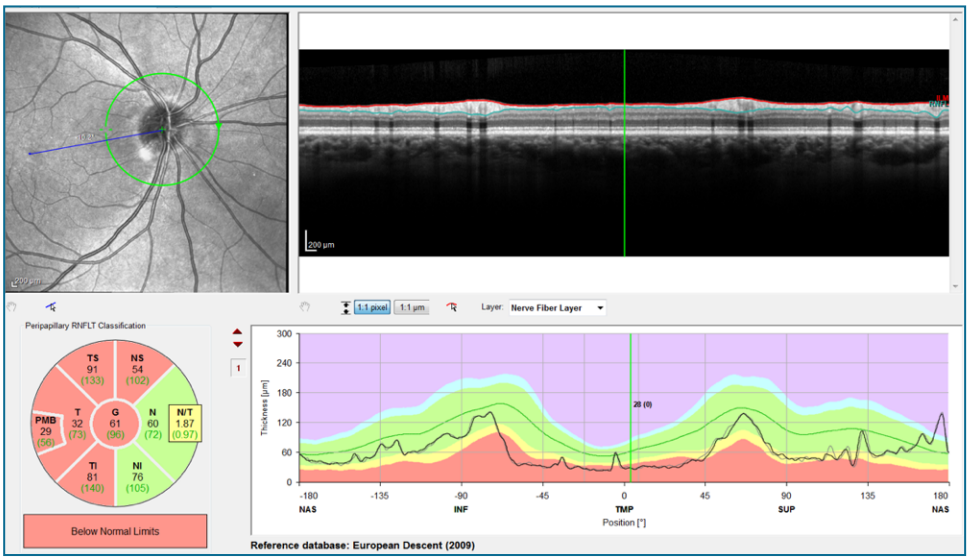

To obtain GCIPL thickness, we acquired volume scans of the macula (table 7.1), centred around the fovea (Figure 7.8). For the macular scan, we recorded the values using a thickness map on a 1-, 3-, and 6-mm ETDRS grid (Early Treatment Diabetic Retinopathy Study research group, 1985) (Figure 7.9).

Figure 7.8 Macular volume scan

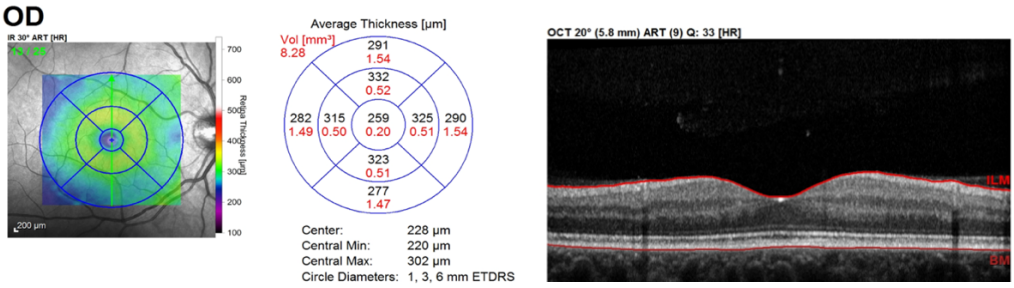

OD: right eye.

Macular layer segmentation (Figure 7.9) for quantification of the GCIPL thickness was obtained by an automated segmentation software provided by the manufacturer (Spectralis, Heidelberg Engineering, Heidelberg, Germany).

Figure 7.9 Macular layer segmentation

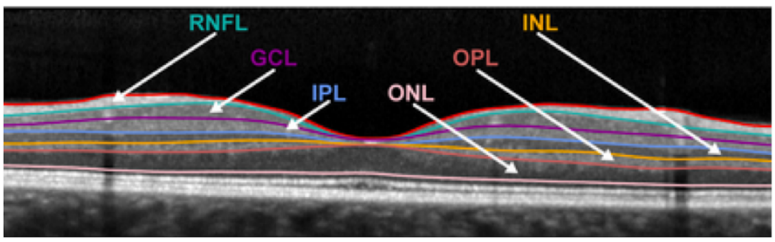

The picture shows some of the macular layers that can be segmented and measured with OCT and these are listed below:

RNFL= macular retinal nerve fibre layer
GCL= ganglion cell layer
IPL= inner plexiform layer
INL= inner nuclear layer
OPL= outer plexiform layer
ONL= outer nuclear layer

To calculate the GCIPL thickness average, we measured the mean thickness values of the inner quadrants of the ETDRS grid (i.e. mean of thickness of T1, S1, N1 and I1 quadrants, as shown in figure 7.10), as previously described (Balk *et al.*, 2014).

Figure 7.10 ETDRS sectors

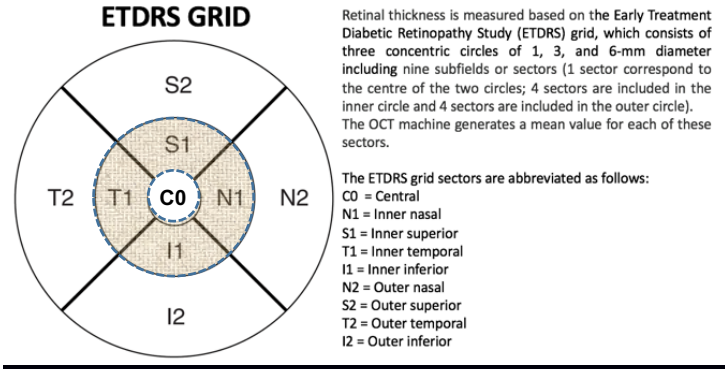

The OCT scans were performed by trained staff blinded to treatment allocation. At the UCL site, I performed about 50% of the baseline scans and 100% of the week-96 scans. In Edinburgh, a qualified ophthalmologist performed all of the baseline scans; the week-96 scans were performed by PhD students and an MS Research Nurse appropriately trained.

A rough initial quality check was performed by each operator at the moment of the OCT scan acquisition. Subsequently, I performed a final, and more accurate, quality check for all the scans obtained at UCL and Edinburgh in accordance to validated international consensus criteria OSCAR-IB (Schippling *et al.*, 2014). I also inspected OCT imaging checking for software algorithm segmentation failure. In case of automated segmentation failure, wherever possible, I performed minimal manual correction of the segmented scans. If segmentation failure was substantive, I rejected the scans due to reproducibility issues.

7.3.4. MRI acquisition and analysis

I have described the details of the MRI acquisition in the previous Chapters. Briefly, MRI scans were obtained on a 3T Philips Achieva scanner (Philips Healthcare, Best, Netherlands) at the UCL site and on a 3T Siemens Verio scanner (Siemens

Healthcare, Erlangen, Germany) at the Edinburgh site. As previously described, we calculated PBVC (percentage brain volume change) as a measure of whole-brain atrophy using the SIENA method. Normalised whole-brain volume measures were also obtained at baseline as well using a combination of GIF and SIENAX. We also obtained measures of grey matter (inclusive of deep grey matter and cortical grey matter) and white matter volumes using the GIF algorithm at baseline and 96 weeks. Finally, we manually measured the T2 lesion volume at baseline, and counted the new/enlarging T2 lesions at 24 and 96 weeks.

7.3.5. Statistical analysis

7.3.5.1. PhD analysis

I presented the baseline results using contingency tables. I provided a CONSORT diagram to illustrate participant disposition. I compared baseline characteristics between patients with and without optic neuritis using independent 2-group t-test or Wilcoxon rank sum test according to the parametric or non-parametric nature of the analysed variables.

To account for patients or eyes with optic neuritis, the following assumptions were used: for patients with sub-clinical optic neuritis (i.e. when the gRNFL inter-eye difference was >20%, as previously described (Martinez-Lapiscina *et al.*, 2016)), I assumed they had optic neuritis and included them in the optic neuritis patient subgroup; for patients where history of optic neuritis was undefinable (i.e. data not available, patient unsure about visual symptom), I assumed they had optic neuritis.

For the cross-sectional analysis, I looked at simple correlations between OCT and clinical/MRI variables. I used Pearson's or Spearman's correlation methods as appropriate for continuous or categorical variables respectively. As the correlation

analysis was carried out at the patient level and not at the eye level, I considered only one OCT measure per patient obtained as follows:

- For patients with no previous history of optic neuritis, I calculated the OCT measures average thickness between the two eyes, in order to have only one value for each patient;
- For patients who had had optic neuritis in one eye, I included in the analyses only the OCT measures belonging to fellow eyes (i.e. the eyes with no previous optic neuritis);
- I excluded from this analysis patients with bilateral or unknown history of optic neuritis.

Similarly, for the same reason as above (i.e. analyses done at the patient level), I calculated the average of SLCVA 2.5% following the same rules described above for the OCT measures in non-optic neuritis eyes in order to have only one visual acuity measure for each patient.

For the longitudinal analysis, I used linear mixed-effects models to calculate annualised rates of atrophy of gRNFL, tRNFL and GCIPL and to determine the relation between follow-up period and change in g/tRNFL thickness from baseline. I measured annualised rates of atrophy in patients with optic neuritis and without optic neuritis history, and in the pooled cohort including all subjects. I also looked at the single rate of changes in the four treatment arms and compared the rate of changes from the active arms versus placebo. I adjusted for age, sex, disease duration, site, and optic neuritis history. Additionally, because both eyes (if available) for each patient were included in the analyses in these longitudinal analyses, I adjusted for within patient inter-eye correlations. When comparing rates of OCT measure changes in the active arms versus placebo, I included also optic neuritis eye as fixed effect.

To calculate relationships between OCT measure percentage changes and PBVC between baseline and week 96, I calculated the OCT measure percentage changes per eye per subject, excluding patients with bilateral optic neuritis. When patients had history of optic neuritis in one eye, I only included OCT measure percentage changes from the unaffected eye (i.e. eye with history optic neuritis were excluded). I then performed linear regression analyses adjusting for age, sex, disease-duration and trial site.

Finally, I used logistic regression models - accounting for age, sex, disease-duration, site and EDSS score at baseline - to investigate the association of gRNFL, tRNFL and GCIPL thinning with confirmed clinical progression. As the MS-SMART trial included neurological evaluations only at three timepoints – i.e. baseline, week 48, week 96 - I included in this analysis only patients who had undergone all the clinical reviews and contributed to clinical variable collection. Furthermore, I included patients who had been assessed only at two timepoints if the clinical variables collected at these timepoints were unchanged (i.e. I considered as if these patients had not progressed). The diagram below (Figure 7.11) shows the criteria I used to select patients to exclude from this analysis. I defined confirmed clinical progression (i.e. disability worsening) as a documented increase in neurological disability detected by at least one of the following measures:

- 1-point increase in EDSS if the baseline score was 4.0–5.0, or a 0.5-point increase if the baseline score was 5.5–6.5 at week 48, confirmed at week 96;
- worsening of at least 20% from baseline in the timed 25-foot walk test (T25FW) at week 48, confirmed at week 96;

- worsening of at least 20% from baseline in the 9-hole peg test (9HPT) at week 48, confirmed at week 96.

Figure 7.11 Patient selection criteria for logistic regression analyses

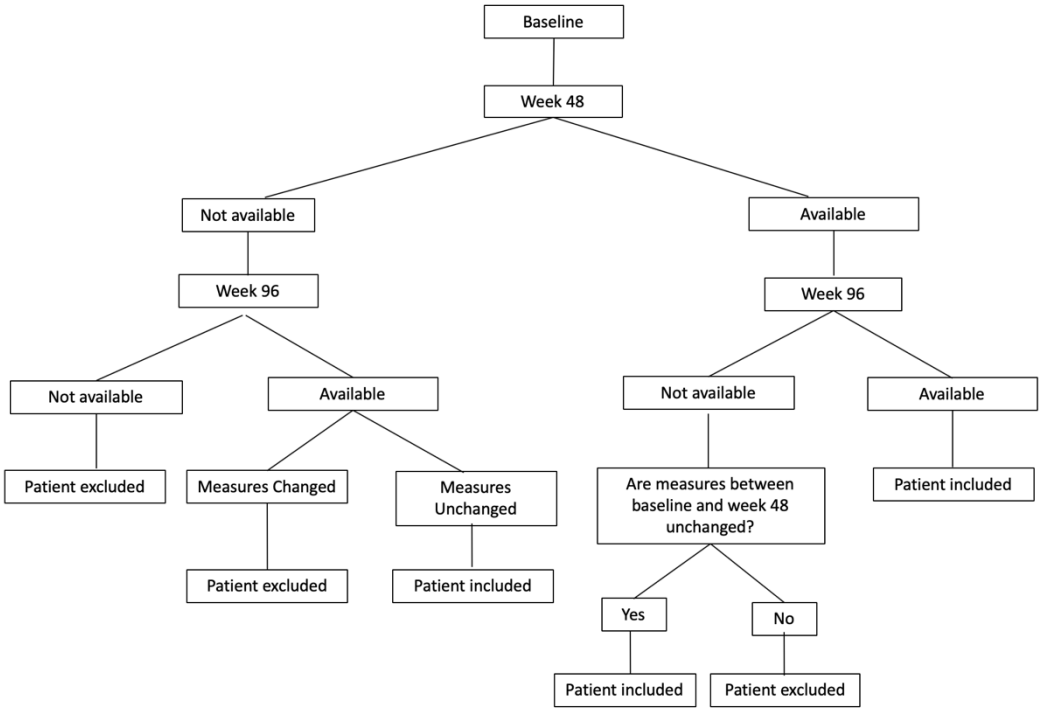

To calculate percentage worsening change, I used the following formula between baseline and week 48 data and between baseline and week 96 data:

$$\frac{|Xbl - Xfu|}{\left[\frac{Xbl + Xfu}{2}\right]} * 100 = Percentage\ change$$

For this logistic regression analysis, I used the two eye averaged OCT measures for patients without a history of optic neuritis; for patients with a history of unilateral optic neuritis, I used only the values for the eyes without optic neuritis. I excluded patients with history of bilateral optic neuritis.

Under the assumption of missing-at-random (MAR), missing data were handled by mathematical algorithms in the mixed effects model, which works by applying listwise deletions (i.e. an entire record is excluded from analysis if any single value

is missing) and maximum likelihood analysis to fit a suitable statistical model to all the observed data.

7.3.5.2. Trial analysis

Left and right eye OCT measures were analysed separately for the gRNFL (primary analysis) and the GCIPL (secondary analysis) measures.

The primary analysis was based on the global gRNFL thickness average excluding eyes with optic neuritis. The analysis used a multiple linear regression method adjusting for baseline and minimisation variables to calculate adjusted mean differences and 95% confidence intervals for the individual pairwise comparisons between each active treatment and placebo. Additionally, the temporal RNFL sector was also analysed using the same approach described above.

Secondary analysis repeated the primary analysis but including all eyes regardless of optic neuritis status, adjusting for the presence of optic neuritis.

The same analyses as above were performed for the GCIPL thickness average.

Where there were missing data for an outcome variable, those records were removed from any formal statistical analysis using a complete cases approach.

7.4. Results

7.4.1. PhD analysis

7.4.1.1. Baseline characteristics

Two-hundred-sixty-one patients enrolled in the MS-SMART trial (UCL n=172 and Edinburgh n=89) opted to take part in the optional OCT sub-study. Of these, one patient voluntarily withdrew from the sub-study before performing the scan; one patient was withdrawn by investigators due to poor collaboration during scan acquisition; for one patient, we were unable to perform OCT scans at baseline due to machine malfunctioning. Forty-four patients (17%) were excluded due to other eye pathology (including diabetic maculopathy and severe refractive errors) or severe nystagmus as reported in Figure 7.12.

.

Figure 7.12 Patient disposition OCT sub-study (London and Edinburgh pooled cohorts)

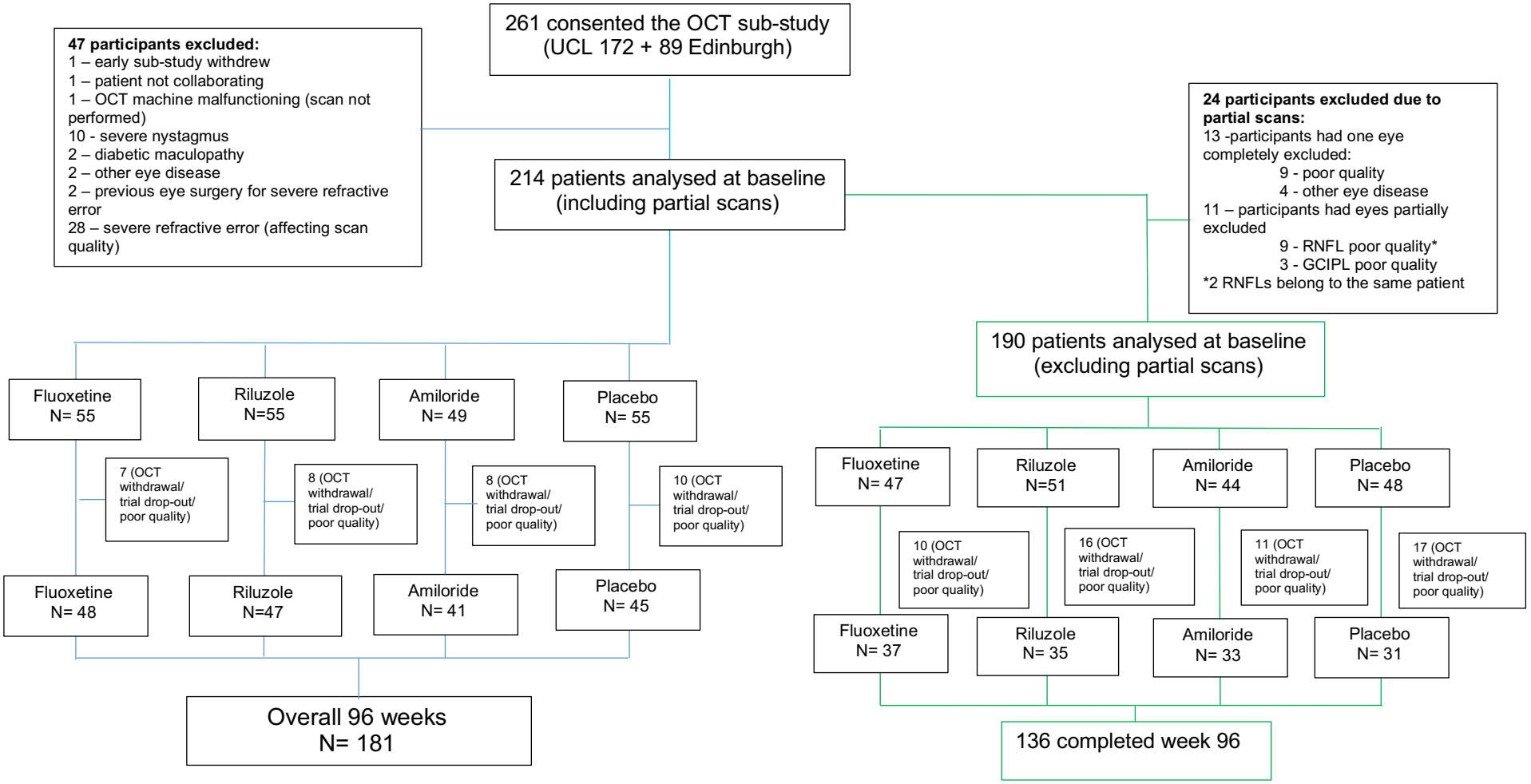

Of the remaining 214 patients scanned, 13 eyes (3%) were excluded (i.e. complete exclusion) due to poor quality scans. Additionally, 3 peripapillary RNFL (0.7%) scans and 7 GCIPL (1.7%) scans - and not the entire eyes – were excluded (i.e. partial exclusion) due to poor quality. Complete exclusion implies that both peripapillary RNFL and GCIPL scans from the same eye were rejected. Partial exclusion implies that only one of the two measures, RNFL or GCIPL, from the same eye were rejected. In regard to the optic neuritis (ON) history (Table 7.2), 113 patients (52.8%) reported no previous history of ON; 11 (5.1%) had history of bilateral ON; 66 (30.8%) had previous ON in one eye only, 5 (2.3%) patients had sub-clinical ON; 15 patients (7%) had previous history of ON but the involved eye was unknown; for 4 patients (1.8%) the ON status was indefinable

Table 7.2 Optic neuritis history

ON history	Patients (N)	Left eye (N)		Right eye (N)	
		gRNFL	GCIPL	gRNFL	GCIPL
No ON	113	109	111	110	111
ON in one eye*	71	66 (30 LEON)	66 (30 LEON)	68 (36 REON)	68 (36 REON)
Bilateral ON	11	9	10	10	10
Known for past ON but involved eye unknown	15	12	13	14	15
ON history undefinable	4	4	4	4	4
Total	**214**	**200**	**204**	**206**	**208**

* Including 5 eyes from 5 patients with sub-clinical optic neuritis in one eye based on gRNFL inter-eye difference >20% (the eye with lower gRNFL thickness was included in the group with history of ON in one eye).
ON: optic neuritis. RNFL: retinal nerve fibre layer; GCIPL: ganglion cell layer + inner plexiform layer. LEON: left eye optic neuritis. REON: right eye optic neuritis.

The baseline characteristics of the individual and pooled UCL and Edinburgh cohorts are shown in Table 7.3. Additionally, I created a table comparing characteristics of patients with no history of ON with the ones with history of ON (Table 7.4).

The baseline characteristics of the UCL and Edinburgh cohorts were very similar in terms of age, disease duration, disability levels and brain volume measures (Table 7.3). The T2 lesion volume appeared to be slightly higher for the Edinburgh group compared to the UCL group (i.e. 13.9 ml vs 11.0 ml); however, t-test analysis revealed no statically significant differences (p= 0.134) of this variable between the two groups.

When I compared patients with previous history of optic neuritis with patients without previous history of optic neuritis, I could not find any significant difference in terms of demographic and MRI measures. EDSS, PASAT, SDMT, MSFC were also non-statistically different between the two groups. However, as expected, there was statistically significant difference with respect of visual acuity and OCT measures, with the optic neuritis groups showing significantly lower values of SLCVA 2.5%, gRNFL, tRNFL, and GCIPL (Table 7.4).

Table 7.3 Baseline characteristics of the individual and pooled UCL and Edinburgh cohorts

	Pooled (*n* = 214)	**UCL (N=138)**	**Edinburgh (N=76)**
Age, years *[mean (sd)]*	54.4 (7.0)	54.2 (6.9)	54.9 (7.1)
Female Sex, % *(N)*	70% (151)	69% (96)	72% (55)
Disease duration, years *[mean (sd)]*	22.3 (9.9)	22.0 (9.4)	22.7 (10.5)
Progression duration, years *[mean (sd)]*	8.2 (5.8)	8.2 (5.6)	8.1 (6.2)
EDSS, score *[median (IQR)]*	6 (5.625–6.5)	6 (5.5–6.5)	6 (6.0–6.5)
MSFC, z-score *[mean (sd)]***	0.05 (0.76)	0.08 (0.83)	-0.02 (0.59)
SDMT, no. of correct answers *[median (IQR)]*	48 (38.75-53)	49.5 (42-54)	43 (35-51.75)
PASAT, no. of correct answers *[median (IQR)]*	43 (34-52)	44 (35-53)	41 (30-50.25)
SLCVA 2.5%, no. of correct answers *[left eye median (IQR)]**	18 (9-26)	18.5 (8.25-27)	18 (9-25)
SLCVA 2.5%, no. of correct answers *[right eye median (IQR)]**	19 (9-29)	19 (9-29.75)	18 (8-29)
gRNFL thickness, µm *[left eye mean (sd)]*	82.9 (13.7)	83.8 (13.7)	81.2 (13.6)
gRNFL thickness, µm *[right eye mean (sd)]*	82.1 (14.2)	82.1 (13.9)	82.1 (15)
gRNFL thickness, µm *[eye average mean (sd)]*	83.3 (13.5)	84.4 (13.2)	81.2 (13.7)

tRNFL thickness, µm *[left eye mean (sd)]*	50.0 (13.7)	49.9 (14.5)	50.2 (12.3)
tRNFL thickness, µm *[right eye mean (sd)]*	57.6 (18.1)	59.7 (18.8)	53.3 (16)
tRNFL thickness, µm *[eye average mean (sd)]*	54.6 (15.1)	56.1 (15.5)	51.9 (13.8)
GCIPL thickness, µm *[left eye mean (sd)]*	74.3 (14.7)	75.1 (14.9)	72.8 (14.2)
GCIPL thickness, µm *[right eye mean (sd)]*	73.5 (15.3)	74.4 (14.9)	71.9 (16.0)
GCIPL thickness, µm *[eye average mean (sd)]*	75.1 (13.9)	76.5 (13.6)	72.4 (14.2)
NBV, ml *[mean (sd)]*	1426.1 (75.3)	1421.3 (79.0)	1434.7 (67.7)
NDGMV, ml *[mean (sd)]*	45.2 (3.8)	45.7 (3.9)	44.3 (3.4)
NCGMV, ml *[mean (sd)]*	796.9 (39.5)	795.5 (41.9)	799.4 (35.0)
NWMV, ml *[mean (sd)]*	584.0 (40.1)	580.2 (41.0)	590.9 (37.5)
T2LV, ml *[mean (sd)]*	12.1 (11.6)	11.0 (9.1)	13.9 (15.0)

* I provided SLCVA for individual eyes; at the UCL site, but not at the Edinburgh site, also binocular visual acuity was measured.
**Reference population: whole MS-SMART cohort.

Abbreviations: EDSS=expanded disability status scale; GCIPL= ganglion cell layer + inner plexiform layer. IQR= inner quartile range. MSFC=multiple sclerosis functional composite; NBV=normalised (whole) brain volume. NCGMV= normalised cortical grey matter volume. NDGMV= normalised deep grey matter volume. NWMV= normalised white matter volume. PASAT= paced auditory serial addition test. SD= standard deviation. SDMT=symbol digit modalities test; SLCVA= Sloan low contrast visual acuity. g/tRNFL= peripapillary/temporal retinal nerve fibre layer. T2LV= T2 lesion volume.

Table 7.4 Baseline characteristics of subjects with and without previous history of optic neuritis (UCL and Edinburgh pooled cohort)

	NON (*n* = 113)	**ON (N=101)**	**NON vs ON, p value**
Age, years *[mean (sd)]*	54.8 (6.4)	54.0 (7.6)	*0.365*
Female Sex, % *(N)*	72% (82)	68% (69)	-
Disease duration, years *[mean (sd)]*	21.9 (10.0)	22.7 (9.6)	*0.551*
Progression duration, years *[mean (sd)]*	7.6 (5.2)	8.8 (6.4)	*0.135*
EDSS, score *[median (IQR)]*	6 (6.0–6.5)	6 (5.5–6.5)	*0.768*
MSFC, z-score *[mean (sd)]*	0.09 (0.70)	-0.005 (0.82)	*0.356*
SDMT, no. of correct answers *[median (IQR)]*	49.5 (41-53.25)	47.5 (36-53)	*0.238*
PASAT, no. of correct answers *[median (IQR)]*	42 (34-53)	43 (33-52)	*0.659*
SLCVA 2.5%, no. of correct answers *[left eye median (IQR)]*	22 (12-30)	14.5 (0-23)	***<0.001***
SLCVA 2.5%, no. of correct answers *[right eye median (IQR)]*	22 (14-32)	15 (4-25.25)	***<0.001***
gRNFL thickness, µm *[left eye mean (sd)]*	88.1 (11.2)	76.7 (13.9)	***<0.001***
gRNFL thickness, µm *[right eye mean (sd)]*	87.2 (11.8)	76.3 (14.5)	***<0.001***

tRNFL thickness, µm *[left eye mean (sd)]*	54.8 (12.1)	44.2 (13.4)	***<0.001***
tRNFL thickness, µm *[right eye mean (sd)]*	62.7 (15.4)	51.7 (19.3)	***<0.001***
GCIPL thickness, µm *[left eye mean (sd)]*	79.9 (11.1)	67.6 (15.7)	***<0.001***
GCIPL thickness, µm *[right eye mean (sd)]*	79.2 (12.6)	67.1 (15.7)	***<0.001***
NBV, ml *[mean (sd)]*	1427.2 (71.1)	1424.8 (80.1)	*0.815*
NDGMV ml *[mean (sd)]*	45.6 (3.5)	44.7 (4.1)	*0.067*
NCGMV ml *[mean (sd)]*	796.6 (39.1)	797.2 (40.2)	*0.922*
NWMV, ml *[mean (sd)]*	585.0 (36.7)	583.0 (43.7)	*0.718*
T2LV, ml *[mean (sd)]*	12.0 (13.3)	12.2 (9.4)	*0.907*

Abbreviations: EDSS=expanded disability status scale; GCIPL= ganglion cell layer + inner plexiform layer. IQR= inner quartile range. MSFC=multiple sclerosis functional composite; NBV=normalised (whole) brain volume. NCGMV= normalised cortical grey matter volume. NDGMV= normalised deep grey matter volume. NON= no history of optic neuritis. NWMV= normalised white matter volume. ON= history of optic neuritis in at least on eye. PASAT= paced auditory serial addition test. SD= standard deviation. SDMT=symbol digit modalities test; SLCVA= Sloan low contrast visual acuity. g/tRNFL= peripapillary/temporal retinal nerve fibre layer. T2LV= T2 lesion volume.

7.4.1.2. Cross-sectional analyses

There was no significant correlation between any of the OCT measures and EDSS or MSFC (Table 7.5). Very weak associations were found between gRNFL, GCIPL and PASAT. There were significant correlations between the three OCT measures, SDMT and SLCVA 2.5% (Table 7.5).

Table 7.5 Correlations between OCT measures clinical and MRI variables at baseline

		EDSS	MSFC	PASAT	SDMT	SLCVA 2.5%*	NBV	T2LV
gRNFL*	Correlation Coefficient	-0.08	0.11	0.17	0.35	0.43	0.18	- 0.17
	P-value	0.28	0.14	**0.018**	**<0.001**	**<0.001**	**0.017**	**0.02**
	Sample size N	181	181	181	181	181	181	181
tRNFL*	Correlation Coefficient	-0.08	0.17	0.13	0.38	0.41	0.17	- 0.24
	P-value	0.29	0.02	0.07	**<0.001**	**<0.001**	**0.02**	**0.001**
	Sample size N	181	181	181	181	181	181	181
GCIPL*	Correlation Coefficient	-0.12	0.17	0.19	0.40	0.48	0.16	- 0.25
	P-value	0.11	0.02	**0.009**	**<0.001**	**<0.001**	**0.04**	**<0.001**
	Sample size N	181	181	181	181	181	181	181

*For this analysis, I excluded patients with unknown optic neuritis history or bilateral optic neuritis. I averaged the values between left and right eye for patients without history of optic neuritis. I included only the values of the fellow eyes, in patients with history of optic neuritis in one eye only.

7.4.1.3. Longitudinal analysis

The annualised atrophy rates for mean gRNFL, tRNFL and mean GCIPL were different from zero over the course of the 96-week study. Estimated annualised rates of atrophy from the mixed-effects models (Figure 7.13) were as follows:

- gRNFL annualised mean atrophy rate was -0.47 (standard error [SE] 0.08) µm/year (p<0.001);
- tRNFL annualised mean atrophy rate was -0.28 (SE 0.09) µm/year (p=0.002);
- GCIPL annualised mean atrophy rate was -0.43 (SE 0.07) µm/year (p<0.001).

Figure 7.13 Annualised rate of change for GCIPL, gRNFL and tRNFL

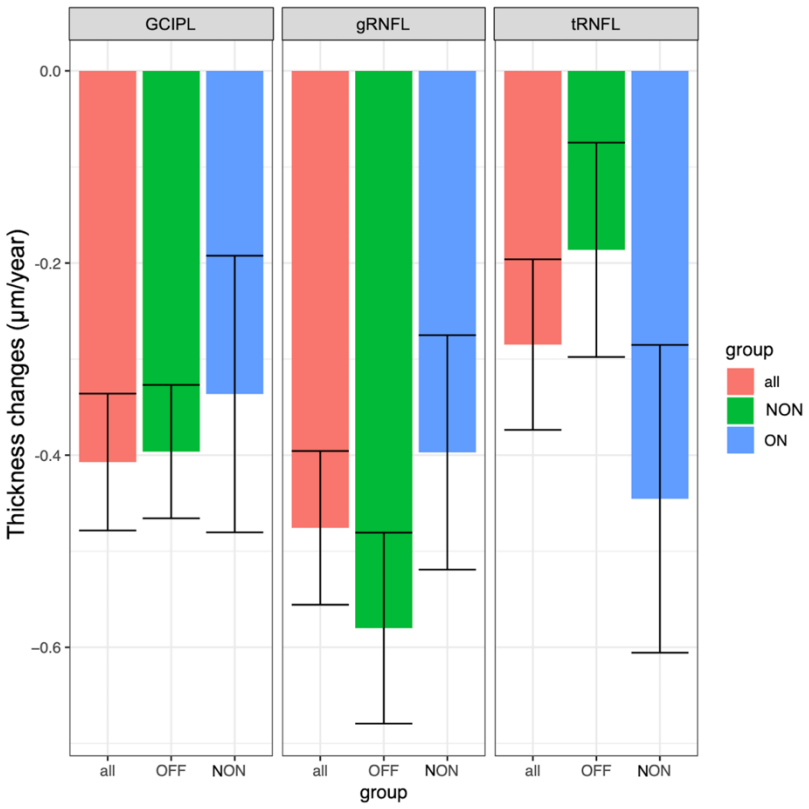

Bar graphs showing annualised mean change in GCIPL, gRNFL and tRNFL thickness for all patients and for subgroup of patients with or without history of previous ON. The bars represent annual mean changes in the three OCT measure thickness, and the vertical lines are 95% confidence intervals. Reductions in annual average thinning for GCIPL and gRNFL was greater for patient with no history of previous ON; tRNFL thinning was slightly higher in the group with previous ON. Abbreviations: GCIPL= ganglion cell + inner plexiform layer; gRNFL= global retinal nerve fibre layer; tRNFL= temporal retinal nerve fibre layer; NON= non-optic neuritis (group); ON= optic neuritis (group).

According to the same statistical model, the changes in EDSS, SDMT, MSFC (including the sub-scores T25FW and 9HPT), and MRI brain volume variables over the 96 weeks were also different from 0 (Table 7.6).

Table 7.6 Clinical and MRI variable change over 96 weeks

	Interval from baseline Value	**Standard Error**	**P value**
EDSS, score	0.29	0.06	**<0.001**
SDMT, no. of correct answers	0.84	0.26	**0.001**
MSFC, z-score	-0.18	0.05	**<0.001**
T25FW, sec (attempt average)	10.63	1.68	**<0.001**
9HPT, sec (hand average)	14.67	3.98	**<0.001**
SLCVA 2.5% no. of correct answers (eye average)	0.75	0.56	0.184
Brain volume, ml	-6.69	643.35	**<0.001**
Deep grey matter volume, ml	-0.16	27.21	**<0.001**
Cortical grey matter volume, ml	-5.20	423.83	**<0.001**

Abbreviations: 9HPT= 9-hole peg test. EDSS=expanded disability status scale; MSFC=multiple sclerosis functional composite; SDMT=symbol digit modalities test; SLCVA= Sloan low contrast visual acuity. T25FW= timed 25-foot walk.

There was no significant change of the SLCVA 2.5%, therefore, I did not include this variable in the mixed effects model analyses.

I also looked at the single rate of changes in the four treatment arms (Table 7.7 and Figure 7.14 below).

Table 7.7 Rate of changes in the four treatment arms

Variable	Treatment	Average change	Standard error	P value
gRNFL, µm/year	Placebo	-0.45	0.15	**0.004**
	Amiloride	-0.83	0.16	**<0.001**
	Fluoxetine	0.17	0.16	0.296
	Riluzole	-0.97	0.14	**<0.001**
tRNFL, µm/year	Placebo	-0.16	0.13	0.237
	Amiloride	-0.73	0.21	**0.001**
	Fluoxetine	0.10	0.18	0.569
	Riluzole	-0.50	0.16	**0.004**
GCIPL, µm/year	Placebo	-0.70	0.20	**0.001**
	Amiloride	-0.38	0.13	**0.004**
	Fluoxetine	-0.24	0.11	**0.030**
	Riluzole	-0.40	0.12	**0.001**

GCIPL= ganglion cell + inner plexiform layer; gRNFL= global retinal nerve fibre layer; tRNFL= temporal retinal nerve fibre layer.

Figure 7.14 rate of changes in the four treatment arms

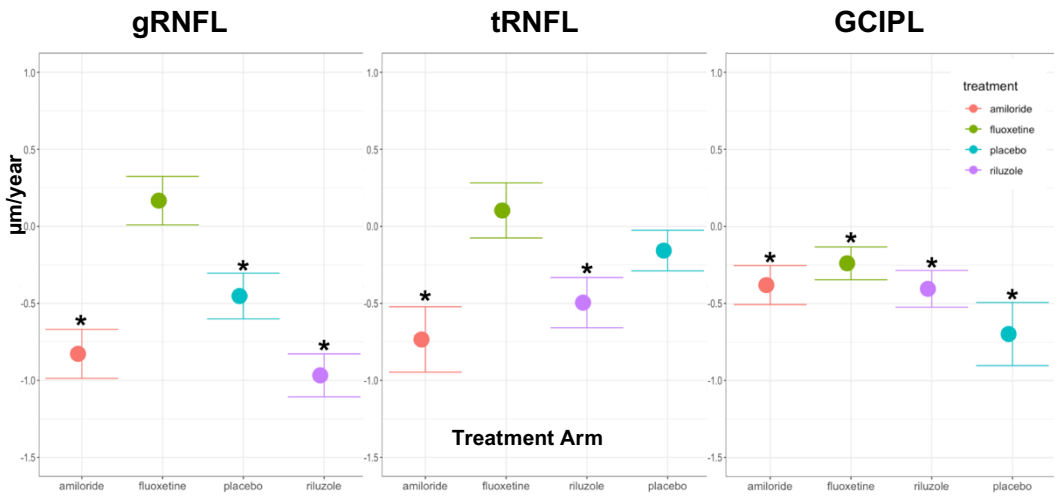

*Statistically significant. GCIPL= ganglion cell + inner plexiform layer; gRNFL= global retinal nerve fibre layer; tRNFL= temporal retinal nerve fibre layer.

Compared to placebo, the annualised rates of change split by treatment arm are shown in Table 7.8.

Table 7.8 annualised rates of change split by treatment arm

Variable	Treatment	Average change	Standard error	P value
gRNFL, µm/year	Placebo			
	Amiloride	-0.46	0.15	0.268
	Fluoxetine	0.45	0.21	**0.033**
	Riluzole	-0.37	0.21	0.087
tRNFL, µm/year	Placebo			
	Amiloride	-0.42	0.25	0.097
	Fluoxetine	0.34	0.24	0.152
	Riluzole	-0.25	0.24	0.301
GCIPL, µm/year	Placebo			
	Amiloride	0.30	0.20	0.150
	Fluoxetine	0.40	0.20	**0.045**
	Riluzole	0.35	0.20	0.082

GCIPL= ganglion cell + inner plexiform layer; gRNFL= global retinal nerve fibre layer; tRNFL= temporal retinal nerve fibre layer.

Patients in the fluoxetine arm had a significant lower rate of gRNFL and GCIPL thicknesses compared to placebo.

These relationships were mostly maintained when I added eyes with history of optic neuritis as a covariate in the mixed effects models (Table 7.9 below).

Table 7.9 annualised rates of change split by treatment arm adjusted for history of optic neuritis

Variable	Treatment	Average change	Standard error	P value
gRNFL, µm/year	*Placebo*			
	Amiloride	-0.25	0.22	0.267
	Fluoxetine	0.45	0.21	**0.035**
	Riluzole	-0.37	0.21	0.088
tRNFL, µm/year	*Placebo*			
	Amiloride	-0.42	0.25	0.098
	Fluoxetine	0.34	0.24	0.158
	Riluzole	-0.25	0.24	0.305
GCIPL, µm/year	*Placebo*			
	Amiloride	0.29	0.21	0.166
	Fluoxetine	0.39	0.20	**0.059**
	Riluzole	0.26	0.21	0.211

GCIPL= ganglion cell + inner plexiform layer; gRNFL= global retinal nerve fibre layer; tRNFL= temporal retinal nerve fibre layer.

Baseline OCT measures and their relationships with OCT measures atrophy rates are shown in table 7.10.

Table 7.10 Baseline OCT measures associated with changes of clinical variables over 96 weeks

	Beta	SE	*P* value
EDSS 96wk change, score			
gRNFL thickness, µm	-0.01	0.00	**0.003**
tRNFL thickness, µm	-0.01	0.00	**<0.001**
GCIPL, µm	-0.01	0.00	**0.003**
SDMT 96wk change, no correct letters			
gRNFL thickness, µm	0.03	0.03	0.289
tRNFL thickness, µm	0.02	0.02	0.568
GCIPL, µm	0.06	0.02	**0.017**
T25FW 96wk change, seconds			
gRNFL thickness, µm	-0.31	0.16	**0.048**
tRNFL thickness, µm	-0.31	0.12	**0.012**
GCIPL, µm	-0.48	0.14	**<0.001**
9HPT 96wk change (hand average) seconds			
gRNFL thickness, µm	0.54	0.29	0.062
tRNFL thickness, µm	0.22	0.23	0.330
GCIPL	0.47	0.27	0.083
MSFC 96wk change, z-score			
gRNFL thickness, µm	0.01	0.00	**0.029**
tRNFL thickness, µm	0.01	0.00	**0.008**
GCIPL, µm	0.01	0.00	**<0.001**

Beta= regression coefficient from the mixed effects model. Parameters are not standardised. GCIPL= ganglion cell + inner plexiform layer; EDSS: expanded disability status scale. gRNFL= global retinal nerve fibre layer; tRNFL= temporal retinal nerve fibre layer. SDMT: symbol digit modalities test. T25FW: times 25-foor walk. 9HPT: 9-hole peg test.

Table 7.11 shows baseline OCT measures that were associated with changes of MRI variables over 96 weeks.

Table 7.11 Baseline OCT measures associated with changes of MRI variables over 96 weeks

	Beta	SE	*P* value
PBVC at 96 weeks			
gRNFL thickness, µm	0.02	0.01	**0.005**
tRNFL thickness, µm	0.01	0.00	**0.012**
GCIPL, µm	0.02	0.00	**<0.001**

GCIPL= ganglion cell + inner plexiform layer; gRNFL= global retinal nerve fibre layer; tRNFL= temporal retinal nerve fibre layer.

Only GCIPL percentage change, and not gRNFL or tRNFL percentage changes, showed significant association with PBVC between baseline and week 96 (Table 7.12).

Table 7.12 Percentage OCT measure changes and PBVC between baseline and 96 weeks

	Beta	**SE**	***P* value**
PBVC at 96 weeks			
gRNFL percentage change	0.09	0.15	0.529
tRNFL percentage change	-0.36	0.25	0.151
GCIPL percentage change	0.25	0.12	**0.032**

GCIPL= ganglion cell + inner plexiform layer; gRNFL= global retinal nerve fibre layer; tRNFL= temporal retinal nerve fibre layer.

7.4.1.4. Logistic regression analysis

30 patients were excluded due to bilateral or undefinable history of optic neuritis. Four patients were also excluded due to eye or peripapillary RNFL rejected scans. Of the remaining patients, 33 were excluded due to missing data (EDSS, 9HPT, T25FW) to measure disease progression. Three patients were automatically excluded from the statistical model due to missing disease-duration. Of the remaining 145 patients, 52 had confirmed disability progression and 93 did not progress.

There was no significant association between gRNFL and GCIPL measures and occurrence of confirmed disability progression. tRNFL thickness could significantly predict confirmed disability progression after adjusting for age, gender, disease-duration, baseline EDSS score and trial site. The association between tRNFL and confirmed disability progression was negative: the higher the tRNFL, the lower the probability to have confirmed disability progression (OR: 0.97; 95% CI: 0.95 to 0.99; p=0.023). This means that, for every 1 standard deviation decrease in tRNFL, the chance of presenting with confirmed disability progression is increased by 3%.

7.4.2. Trial analysis

Summary statistics for the OCT measures for left eyes and right eyes at baseline and week 96 are reported in Table 7.13 and 7.14 for all patients' eyes, and in Table 7.15 and 7.16 for patients' eyes without previous history of optic neuritis.

For gRNFL and tRNFL, left eye measures were obtained from 159 participants (n=119 had not suffered from previous optic neuritis); and right eye measures from 163 participants (n=113 had not suffered from previous optic neuritis).

For GCIPL, left eye measures were obtained from 161 participants (n=121 had not suffered from previous optic neuritis); and right eye measures from 165 participants (n=117 had not suffered from previous optic neuritis).

The adjusted mean differences between active drug and placebo for gRNFL thickness and complex GCIPL thickness are shown in Table 7.17. There was no statistically significant difference between the any of the trial active arms and the placebo arm for all the OCT measures analysed.

Table 7.13 Peripapillary RNFL outcomes summary statistics for all patients at baseline and 96 weeks

		Fluoxetine	Riluzole	Amiloride	Placebo	Overall
Left Eye						
gRNFL baseline (µm)	N	43	39	36	41	159
	Mean	81.3	83.7	84.5	83.6	83.2
	SD	11.3	13.9	16.4	13.0	13.6
gRNFL 96 wks (µm)	N	43	39	36	41	159
	Mean	79.5	80.1	81.1	81.7	80.6
	SD	10.8	13.7	16.2	12.3	13.
tRNFL baseline (µm)	N	43	39	36	41	159
	Mean	48.4	50.0	51.4	52.3	50.5
	SD	14.0	13.7	16.3	12.4	14.1

		Fluoxetine	Riluzole	Amiloride	Placebo	Overall
Left Eye						
tRNFL 96 wks (µm)	N	43	39	36	41	159
	Mean	49.8	50.4	51.7	52.6	51.1
	SD	14.4	14.4	17.5	12.6	14.6
Right Eye						
gRNFL baseline (µm)	N	45	42	36	40	163
	Mean	80.2	81.1	86.5	81.2	82.1
	SD	12.2	16.4	15.5	14.1	14.6
gRNFL 96 wks(µm)	N	45	42	36	40	163
	Mean	80.6	79.9	85.5	80.6	81.5
	SD	12.5	16.4	15.3	14.2	14.6
tRNFL baseline (µm)	N	45	42	36	40	163
	Mean	55.3	57.0	64.0	57.9	58.3
	SD	16.3	19.4	20.0	19.0	18.8
tRNFL 96 wks (µm)	N	45	42	36	40	163
	Mean	53.1	53.8	59.6	55.7	55.4
	SD	15.1	17.5	17.7	17.7	17.0

gRNFL: global (peripapillary) retinal nerve fibre layer (global average). tRNFL: temporal (sector) retinal nerve fibre layer. nRNFL: nasal (sector) retinal nerve fibre layer. LE: left eye. RE: right eye. SD: standard deviation.

Table 7.14 GCIPL outcomes summary statistics for all patients at baseline and 96 weeks

		Fluoxetine	Riluzole	Amiloride	Placebo	Overall
Left eye						
GCIPL baseline (µm)	N	43	40	37	41	161
	Mean	74.9	75.0	75.3	77.4	75.6
	SD	13.4	14.7	16.9	13.1	14.4
GCIPL 96 wks (µm)	N	43	40	37	41	161
	Mean	74.1	74.2	74.6	76.3	74.8
	SD	13.5	14.8	16.6	13.1	14.4
Right Eye						
GCIPL baseline (µm)	N	43	43	41	38	165
	Mean	73.8	69.1	76.4	76.7	73.9
	SD	14.7	18.2	14.2	14.4	15.7
GCIPL 96 wks (µm)	N	43	43	41	38	165
	Mean	73.5	68.8	75.7	75.5	73.3
	SD	14.9	18.2	14.2	14.5	15.7

ETDRS: early treatment diabetic retinopathy study. SD: standard deviation. GCIPL: ganglion cell layer and inner plexiform layer. Only inner ETDRS sectors were included.

Table 7.15 Peripapillary RNFL outcomes summary statistics for patients with no history of optic neuritis at baseline and 96 weeks

		Fluoxetine	Riluzole	Amiloride	Placebo	Overall
Left Eye						
gRNFL baseline (µm)	N	35	27	26	31	119
	Mean	83.7	86.6	91.2	86.4	86.7
	SD	10.2	12.8	13.0	11.0	11.8
tRNFL baseline (µm)	N	35	27	26	31	119

		Fluoxetine	Riluzole	Amiloride	Placebo	Overall
Left Eye						
	Mean	51.6	52.4	57.5	54.4	53.8
	SD	13.3	11.3	14.0	10.3	12.4
gRNFL 96 wks(µm)	N	35	27	26	31	119
	Mean	81.6	83.0	87.8	84.3	84.0
	SD	9.7	12.4	12.9	10.1	11.3
tRNFL 96 wks (µm)	N	35	27	26	31	119
	Mean	53.1	52.7	58.3	54.8	54.6
	SD	13.7	12.1	15.0	10.5	12.9
Right Eye						
gRNFL baseline (µm)	N	33	29	27	24	113
	Mean	81.0	84.2	91.0	85.6	85.2
	SD	12.4	15.8	14.1	13.6	14.3
tRNFL baseline (µm)	N	33	29	27	24	113
	Mean	56.7	59.3	68.0	63.2	61.5
	SD	17.1	18.6	18.5	16.7	18.0
gRNFL 96 wks(µm)	N	33	29	27	24	113
	Mean	81.4	82.8	90.1	85.0	84.6
	SD	12.7	15.9	13.8	13.7	14.3
tRNFL 96 wks (µm)	N	33	29	27	24	113
	Mean	54.0	56.3	63.2	61.2	58.4
	SD	15.7	17.6	16.2	15.3	16.5

gRNFL: global (peripapillary) retinal nerve fibre layer. SD: standard deviation.

Table 7.16 GCIPL outcomes summary statistics for patients with no history of optic neuritis at baseline and 96 weeks

		Allocated Treatment				
		Fluoxetine	Riluzole	Amiloride	Placebo	Overall
Left eye						
GCIPL thickness at baseline (µm)	N	35	29	27	30	121
	Mean	78.9	77.6	82.4	79.6	79.6
	SD	10.7	12.0	12.3	11.2	11.5
GCIPL thickness at 96 weeks (µm)	N	35	29	27	30	121
	Mean	78.2	76.7	81.5	78.6	78.7
	SD	10.7	12.6	12.4	11.0	11.6
Right eye						
GCIPL thickness at baseline (µm)	N	33	29	31	24	117
	Mean	75.4	71.7	80.3	81.9	77.1
	SD	14.8	18.6	12.4	11.4	15.0
GCIPL thickness at 96 weeks (µm)	N	33	29	31	24	117
	Mean	75.1	71.1	79.5	81.2	76.5
	SD	14.9	18.7	12.6	11.2	15.0

ETDRS: early treatment diabetic retinopathy study. SD: standard deviation. GCIPL: ganglion cell layer and inner plexiform layer. MV: macular volume.

Table 7.17 Multiple regression analyses for the OCT outcomes at 96 weeks

Outcome variable	N	AMD (Amiloride – Placebo)	95% Confidence Limits for AMD		P-value	AMD (Fluoxetine – Placebo)	95% Confidence Limits for AMD		P-value	AMD (Riluzole – Placebo)	95% Confidence Limits for AMD		P-value
Left eye													
gRNFL thickness (µm), eyes with no ON only:	119	-0.819	-2.245	0.607	0.258	0.210	-1.126	1.547	0.756	-0.982	-2.387	0.422	0.169
gRNFL thickness (µm), all patients, adjusted for ON	159	-0.870	-2.080	0.339	0.157	0.429	-0.731	1.589	0.466	-1.053	-2.240	0.133	0.082
GCIPL overall thickness (µm), eyes with no ON only	121	0.157	-0.525	0.839	0.649	0.223	-0.424	0.869	0.497	-0.102	-0.776	0.572	0.765
GCIPL overall thickness (µm), all patients, adjusted for ON	161	0.196	-0.403	0.796	0.518	0.237	-0.343	0.817	0.420	0.058	-0.528	0.643	0.846
tRNFL thickness (µm), eyes with no optic neuritis only:	119	0.290	-1.015	1.595	0.661	0.746	-0.484	1.976	0.232	-0.338	-1.635	0.959	0.607
tRNFL thickness (µm), all patients, adjusted for ON	159	-0.213	-1.339	0.914	0.710	0.928	-0.157	2.012	0.093	-0.047	-1.152	1.059	0.934
Right eye													
gRNFL thickness (µm), eyes with no ON only:	113	-0.260	-1.334	0.814	0.632	0.961	-0.072	1.993	0.068	-0.868	-1.922	0.187	0.106
gRNFL thickness (µm), all patients, adjusted for ON	163	-0.037	-0.901	0.827	0.933	1.033	0.236	1.829	0.011	-0.408	-1.221	0.404	0.323
GCIPL overall thickness (µm), eyes with no ON only	117	-0.062	-0.628	0.503	0.828	0.452	-0.119	1.023	0.120	0.200	-0.397	0.796	0.508
GCIPL overall thickness (µm), all patients, adjusted for ON	165	0.331	-0.242	0.903	0.256	0.813	0.246	1.380	0.005	0.573	0.003	1.144	0.049
tRNFL thickness (µm), eyes with no ON only	113	-1.983	-3.848	-0.118	0.037	-1.012	-2.823	0.798	0.270	-1.326	-3.173	0.520	0.157
tRNFL thickness (µm), all patients, adjusted for ON	163	-0.978	-2.508	0.553	0.209	-0.181	-1.600	1.239	0.802	-0.845	-2.291	0.602	0.250

ETDRS: early treatment diabetic retinopathy study. GCIPL: ganglion cell layer and inner plexiform layer. MV: macular volume. gRNFL: global (peripapillary) retinal nerve fibre layer. gRNFL thickness of eyes with no optic neuritis was the primary OCT analysis. ON: optic neuritis.

7.5 Discussion

MRI techniques have been regarded as the most reliable and sensitive surrogate biomarkers for assessing inflammatory and axonal pathology in patients with MS. Brain atrophy measures are commonly used as primary outcomes of phase 2 trials for putative neuroprotective therapies in progressive MS. However, MRI is expensive, time consuming and not easily accessible. Thinning of the RNFL in patients with MS is believed to reflect axonal loss. This is supported by the anatomical notion that there is no myelin in the retina and, consequently, RNFL thickness principally reflects axonal density. OCT is capable of quantifying RNFL thinning, suggesting the possibility that this imaging technique could potentially substitute or complement MRI for monitoring disease progression in clinical trials (Gordon-Lipkin *et al.*, 2007; Frohman *et al.*, 2009; Martinez-Lapiscina *et al.*, 2016).

I have reported the largest prospective OCT study carried out so far in patients with SPMS. The results of this longitudinal study demonstrate that baseline measures of gRNFL, tRNFL and GCIPL are associated with clinical disability and brain atrophy after 96 weeks in SPMS. I have also found that CGIPL thinning occurs in SPMS after 96 weeks and is significantly associated with PBVC. These findings suggest that, together with brain axonal loss, there is also axonal loss in the anterior visual pathway in SPMS, and support OCT measures as candidate outcome measures for clinical trials looking at neuroprotection, as suggested by other previous studies (Garcia-Martin *et al.*, 2014; Martinez-Lapiscina *et al.*, 2016; Birkeldh *et al.*, 2019). However, a few considerations should be made.

MS-SMART participants had a mean gRNFL thickness of 81-82 µm and GCIPL thickness of 72-73 µm. I found a significant mean annual thinning of gRNFL and

GCIPL of -0.47 μm and -0.43 μm respectively, accounting for eyes with previous optic neuritis (measured with Heidelberg Spectralis OCT machine). These findings are in contrast with the ones recently reported by Winges et al., who carried a post hoc OCT analysis of the phase 2 randomised-controlled neuroprotective trial testing Lipoic acid versus placebo in SPMS (Spain *et al.*, 2017; Winges *et al.*, 2019). In this study, researchers analysed 47 subjects and used a Cirrus OCT machine (Carl Zeiss Meditec, Inc., Dublin, CA, USA) to acquire scans at baseline, year 1, and year 2. They found a non-statistically significant annualised mean gRNFL atrophy rate of −0.31 μm/year, and a mean GCIPL atrophy rate of −0.29 μm/year. Additionally, they did not find any correlation between OCT changes and MRI measured of whole-brain or grey matter atrophy. In this study from Winges et al, the baseline values of gRNFL and GCPL thickness were 77.3 μm and 67.4 μm respectively. Baseline gRNFL measure correlated with gRNFL atrophy rate over 2 years. They grouped all the trial participants under the assumption that the secondary OCT outcomes were negative. However, because the trial showed that Lipoic Acid was significantly associated with reduced brain atrophy loss, a neuroprotective effect of Lipoid Acid on the retina cannot be excluded, even though this did not reach statistical significance. Moreover, 45% of the subjects enrolled in the Lipoic Acid trial were on Interferon beta and glatiramer acetate, whereas the MS-SMART patients were not on any disease-modifying therapy. This fact could account for the discrepancy between the MS-SMART and Lipoc Acid trial results. Additionally, MS-SMART used a very strict inclusion criterion, that is, eligible patients had to have on-going and steadily progressive disability in the two years before the study. This information is not clearly stated as an inclusion criterion for the lipoic acid trial and it might be possible that SPMS stable participants had affected the rate of OCT measure atrophy. Finally, the number of patients that completed the OCT sub-study in MS-SMART was almost three-fold larger than the

one from the Lipoic Acid trial (n=136 vs n=47 respectively), which would result in a higher statistical power in favour of MS-SMART.

However, MS-SMART was certainly in agreement with other reported studies. For instance, in a longitudinal observational study including 20 patients with SPMS and 3 with PPMS, Pisa et al observed that people with progressive MS had a significant retinal thinning over time (measured with a Heidelberg Spectralis OCT machine) even when no disease activity was observed at routine clinical or brain MRI assessment (Pisa *et al.*, 2019).

In the SPRINT-MS study, a randomised controlled trial in a mixed cohort of patients with progressive MS that found a significant positive effect of ibudilast vs placebo on rates of brain atrophy (Fox *et al.*, 2018), investigators reported no differences on gRNFL measures between the two treatment arms after two years. In the placebo group of this trial, the annual rate of gRNFL atrophy was −0.26 μm/year. Both Heidelberg Spectralis or Zeiss Cirrus OCT machines were used in this trial. A full report of the OCT analysis is still pending and I cannot comment more about this study. However, it is worth noticing that OCT image acquired using different device models and vendors are not directly comparable in terms of results. Therefore, I can hypothesise that the annualised gRNFL atrophy rate in SPRINT-MS might have been lower than the one in MS-SMART due to use of different OCT machine models and make.

Another important question is whether rates of OCT measure changes were affected by ageing. However, normative OCT data for healthy ageing population are not easily accessible as there are a very few longitudinal studies. Most of the reference values used are inferred from cross-sectional studies. For instance, in a study reported by Mwanza et al. including healthy subjects between 18 and 84

years of age, the annualised rate of GCIPL thickness loss -0.43 μm/year (Mwanza *et al.*, 2011). In a longitudinal analysis carried out in 35 healthy Hong Kong Chinese subjects (mean age 56.43±6.69) using a Cirrus OCT machine, Leung et al. found a mean rate RNFL thicknesses change of −0.52 μm/year (95% CI: −0.86 to −0.17), with no detectable RNFL reduction in the nasal and temporal quadrants. A greater baseline gRNFL thickness was associated with a faster rate of change. They also found an age-related decline of the RNFL (Leung *et al.*, 2012). Ratchford et al. investigated longitudinally a mix cohort of 164 MS patients (including 24 SPMS) and 59 healthy controls. The overall rate of change in the MS cohort was −0.21 μm/year for RNFL thickness and −0.37 μm/year for GCIPL thickness. In healthy controls, the rate of change was −0.25 μm/year for RNFL thickness and −0.20 μm/year ($p < 0.001$) for GCIPL thickness. The rate of GCIPL thinning was 46% faster in patients with MS than healthy controls, whereas there was no significant difference in the rate of RNFL thinning between patients with MS and HCs. There were no healthy controls in the MS-SMART trials and I am unable to investigate whether the rate of OCT measures loss was mainly age related. Nevertheless, I adjusted all the statistical analyses for participants' age.

The primary intervention analysis from the MS-SMART trial observed no effect of amiloride, fluoxetine or riluzole on the rate of percentage brain volume change. In keeping with these findings, the OCT sub-study results did not show any difference between active and placebo arms in any of the OCT outcomes analysed in the pre-planned trial analysis. Nevertheless, the fluoxetine arm showed pseudoatrophy at 24 week and reduced number of new/enlarged T2 lesions, suggesting a possible immunomodulatory effect of fluoxetine. Using a different statistical approach in my PhD analysis, I found that the patients in fluoxetine arm had a significant lower annualised rate of RNFL and GCIPL thinning as compared with placebo. The longitudinal trial and PhD analyses are substantially different so it is not surprising

that they led to different results. In fact, the trial analysis was carried out using linear regression models, which could not account for within patient inter-eye correlations. Using mixed effects models in my PhD study, instead, I could account for this interpatient inter-eye correlations (i.e. two eyes that belongs to the same subject and two measures over time that belong to the same subject).

Although no significant association was found at baseline between OCT measures and EDSS or MSFC using unadjusted correlation analyses, when I looked at the longitudinal data using mixed effects models, the baseline OCT measures could significantly predict EDSS and MSFC changes. The cross-sectional analysis also showed that there were significant correlations between the three OCT measures, SDMT and SLCVA 2.5%. However, when I looked at the follow-up data, I found that there was no significant change in the SLCVA 2.5% ($p=0.184$). There is increasing interest in outcome measures of visual function and there have been several reports showing that low contrast charts are associated with disease severity in RRMS (Balcer *et al.*, 2007, 2017; Talman *et al.*, 2010). My findings of no significant change in the SLCVA 2.5% might be due to four possible reasons: 1) the RNFL loss detected by OCT was not severe enough to affect visual function or that compensatory mechanisms could attenuate the effects of the anterior visual pathway neurodegeneration; 2) the timeframe of 96 week is too short to detect significant visual acuity changes; 3) the baseline visual acuity has already reached a ceiling effect and, despite increasing RNFL thinning, the overall visual acuity remains unchanged; 4) although less likely, there might be a learning effect on SLCVA 2.5%..

The logistic regression study showed that tRNFL was the only OCT measure that could discriminate between patients with and without confirmed disability

progression. These findings should be validated in a study using more frequent outcomes as I measured confirmed disability progression at 12 months.

One of the limitations of my study, as mentioned above, is the lack of healthy controls to account for RNFL thinning due to ageing. Older age was associated strongly with thinner inner retinal thickness in previous studies (Mwanza *et al.*, 2011). However, in all my statistical models, I adjusted for both age and disease duration which should be able to compensate an ageing effect.

Another limitation of this study is that I did not look at other OCT-derived retinal layers, including inner nuclear layer (INL) and outer plexiform layer (OPL). Several studies have shown that INL, in combination with OPL, are associated with disease activity and can predict response to disease-modifying treatment (Saidha *et al.*, 2012; Knier *et al.*, 2016), suggesting that INL could serve as a biomarker to monitor central nervous system inflammation.

In conclusion, I showed that baseline OCT measures can predict clinical and MRI changes. OCT is sensitive enough to detect axonal loss in both RNFL and GCIPL in a population of SPMS with evidence of disease progression, not on disease-modifying therapy. As I showed, progressive loss of RNFL and GCIPL occurred in this study cohort, supporting the need for neuroprotection. Low contrast charts do not seem to be useful in a population like the one in MS-SMART possibly because the mean visual acuity is already low.

Chapter 8. **Conclusions and future directions**

The MS-SMART trial was ground-breaking in its design and approach to an intractable neuro-degenerative disease. It demonstrated that this type of highly efficient trial can be performed in SPMS, and supports application in further trials in progressive MS and potentially other neurodegenerative environments. Using such a trial design will enable the research community to accelerate the testing of drugs in these very demanding situations which have large healthcare costs and burdens associated with them.

The trial was well powered, blinding was robust, adherence was high, and retention was high. Additionally, the primary outcome progressed as expected in the placebo arm, similarly to what observed in other recent trials in SPMS (Chataway *et al.*, 2014; Spain *et al.*, 2017; Kappos *et al.*, 2018). Valuable information was obtained across the board for all secondary and exploratory measures and my PhD mostly focussed on analysing these.

Carrying out my PhD project analysis data from a multicentre double-blind trial has provided me with an in-depth knowledge of intrinsic problems linked to clinical research in SPMS. I had the possibility to see many patients and analyse considerable data.

I will summarise below some of the learning points from my PhD research:

1) A multi-arm trials in SMPS in feasible in the UK and offers several advantages.
2) Fluoxetine, riluzole and amiloride did not have neuroprotective effect as measured by brain MRI atrophy.
3) MRI atrophy measures are reliable in terms of reproducibility and can be used in phase 2 trial in SPMS.

4) Baseline cross-sectional analyses highlighted the importance of SDMT as a measure of overall disability and brain volume loss and that comorbidity (BMI and hypertension) should be considered when investigating patients with SPMS.
5) Cervical cord analysis findings showed that the percentage change of cord atrophy is less than what reported in previous studies and, with the current MRI analyses techniques, do not seem to offer a benefit over brain atrophy measures.
6) OCT-derived retinal layer measures suggested progressive axonal loss in the visual pathways of people with SPMS despite occurrence of acute optic neuritis.

Future directions will aim at:

- Analysing the value of SDMT and comorbidity in the longitudinal analyses;
- Improving the MRI analysis pipeline for the cervical cord scans by mean of registration-based techniques;
- Analysing the OCT data to calculate sample size for an ideal clinical trial using RNFL or GCIPL as primary outcomes;
- Extending the OCT analysis to other retinal layers (INL and ONL).

References

Active Biotech » Press Releases. Active Biotech announce results in ARPEGGIO Phase II trial with laquinimod in Primary Progressive MS [Internet]. [cited 2018 Apr 2] Available from: http://www.activebiotech.com/en/media/pressreleases/?id=2153402&date=1512129600

Agosta F, Absinta M, Sormani MP, Ghezzi A, Bertolotto A, Montanari E, et al. In vivo assessment of cervical cord damage in MS patients: a longitudinal diffusion tensor MRI study. Brain 2007; 130: 2211–2219.

Allaman I, Fiumelli H, Magistretti PJ, Martin J-L. Fluoxetine regulates the expression of neurotrophic/growth factors and glucose metabolism in astrocytes. Psychopharmacology (Berl). 2011; 216: 75–84.

Altmann DR, Jasperse B, Barkhof F, Beckmann K, Filippi M, Kappos LD, et al. Sample sizes for brain atrophy outcomes in trials for secondary progressive multiple sclerosis. Neurology 2009; 72: 595–601.

Amann M, Pezold S, Naegelin Y, Fundana K, Andělová M, Weier K, et al. Reliable volumetry of the cervical spinal cord in MS patient follow-up data with cord image analyzer (Cordial). J. Neurol. 2016; 263: 1364–1374.

Amato MP, Ponziani G. Quantification of impairment in MS : discussion of the scales in use. Mult. Scler. 1999; 5: 216–219.

Andersen O, Elovaara I, Färkkilä M, Hansen HJ, Mellgren SI, Myhr K-M, et al. Multicentre, randomised, double blind, placebo controlled, phase III study of weekly, low dose, subcutaneous interferon beta-1a in secondary progressive multiple sclerosis. J. Neurol. Neurosurg. Psychiatry 2004; 75: 706–10.

De Angelis F, John NA, Brownlee WJ. Disease-modifying therapies for multiple sclerosis. BMJ 2018a; 363: k4674.

De Angelis F, Plantone D, Chataway J. Pharmacotherapy in Secondary Progressive Multiple Sclerosis: An Overview. CNS Drugs 2018b; 32: 499–526.

Arrambide G, Rovira A, Sastre-Garriga J, Tur C, Castilló J, Río J, et al. Spinal cord lesions: A modest contributor to diagnosis in clinically isolated syndromes but a relevant prognostic factor. Mult. Scler. J. 2018; 24: 301–312.

Arun T, Tomassini V, Sbardella E, de Ruiter MB, Matthews L, Leite MI, et al. Targeting ASIC1 in primary progressive multiple sclerosis: evidence of neuroprotection with amiloride. Brain 2013; 136: 106–15.

Ascherio A, Munger KL. Environmental risk factors for multiple sclerosis. Part I: The role of infection. Ann. Neurol. 2007; 61: 288–299.

Ascherio A, Munger KL, Lünemann JD. The initiation and prevention of multiple sclerosis. Nat. Rev. Neurol. 2012; 8: 602–12.

Ashburn TT, Thor KB. Drug repositioning: identifying and developing new uses for existing drugs. Nat. Rev. Drug Discov. 2004; 3: 673–683.

Azevedo CJ, Cen SY, Khadka S, Liu S, Kornak J, Shi Y, et al. Thalamic atrophy in multiple sclerosis: A magnetic resonance imaging marker of neurodegeneration throughout disease. Ann. Neurol. 2018; 83: 223–234.

Bajorath J. Computational analysis of ligand relationships within target families. Curr. Opin. Chem. Biol. 2008; 12: 352–8.

Balcer LJ, Baier ML, Cohen JA, Kooijmans MF, Sandrock AW, Nano-Schiavi ML, et al. Contrast letter acuity as a visual component for the Multiple Sclerosis Functional Composite. Neurology 2003; 61: 1367–73.

Balcer LJ, Galetta SL, Calabresi PA, Confavreux C, Giovannoni G, Havrdova E, et al. Natalizumab reduces visual loss in patients with relapsing multiple sclerosis. Neurology 2007; 68: 1299–304.

Balcer LJ, Miller DH, Reingold SC, Cohen JA. Vision and vision-related outcome measures in multiple sclerosis. Brain 2015; 138: 11–27.

Balcer LJ, Raynowska J, Nolan R, Galetta SL, Kapoor R, Benedict R, et al. Validity of low-contrast letter acuity as a visual performance outcome measure for multiple sclerosis. Mult. Scler. 2017; 23: 734–747.

Balk LJ, Twisk JWR, Steenwijk MD, Daams M, Tewarie P, Killestein J, et al. A dam for retrograde axonal degeneration in multiple sclerosis? J. Neurol. Neurosurg. Psychiatry 2014; 85: 782–9.

Bano D, Ankarcrona M. Beyond the critical point: An overview of excitotoxicity, calcium overload and the downstream consequences. Neurosci. Lett. 2018; 663: 79–85.

Barkhof F. MRI in multiple sclerosis: correlation with expanded disability status scale (EDSS). Mult. Scler. J. 1999; 5: 283–286.

Barkhof F. Brain atrophy measurements should be used to guide therapy monitoring in MS – NO. Mult. Scler. J. 2016; 22: 1524–1526.

Barkhof F, Calabresi PA, Miller DH, Reingold SC. Imaging outcomes for neuroprotection and repair in multiple sclerosis trials. Nat. Rev. Neurol. 2009; 5: 256–66.

Barkhof F, Filippi M, Miller DH, Tofts P, Kappos L, Thompson AJ. Strategies for optimizing MRI techniques aimed at monitoring disease activity in multiple sclerosis treatment trials. J. Neurol. 1997; 244: 76–84.

Barnett MH, Prineas JW. Relapsing and remitting multiple sclerosis: pathology of the newly forming lesion. Ann. Neurol. 2004; 55: 458–68.

Batoulis H, Recks MS, Holland FO, Thomalla F, Williams RO, Kuerten S. Blockade of tumour necrosis factor-α in experimental autoimmune encephalomyelitis reveals differential effects on the antigen-specific immune response and central nervous

system histopathology. Clin. Exp. Immunol. 2014; 175: 41–8.

Bauer P, Kieser M. Combining different phases in the development of medical treatments within a single trial. Stat. Med. 1999; 18: 1833–48.

Beck RW, Gal RL, Bhatti MT, Brodsky MC, Buckley EG, Chrousos GA, et al. Visual function more than 10 years after optic neuritis: experience of the optic neuritis treatment trial. Am. J. Ophthalmol. 2004; 137: 77–83.

Bedard K, Krause K-H. The NOX Family of ROS-Generating NADPH Oxidases: Physiology and Pathophysiology. Physiol. Rev. 2007; 87: 245–313.

Belbasis L, Bellou V, Evangelou E, Ioannidis JPA, Tzoulaki I. Environmental risk factors and multiple sclerosis: an umbrella review of systematic reviews and meta-analyses. Lancet Neurol. 2015; 14: 263–273.

Benedict RH, DeLuca J, Phillips G, LaRocca N, Hudson LD, Rudick R, et al. Validity of the Symbol Digit Modalities Test as a cognition performance outcome measure for multiple sclerosis. Mult. Scler. J. 2017; 23: 721–733.

Benoit E, Escande D. Riluzole specifically blocks inactivated Na channels in myelinated nerve fibre. Pflugers Arch. 1991; 419: 603–9.

Bergers E, Bot JCJ, De Groot CJA, Polman CH, Lycklama à Nijeholt GJ, Castelijns JA, et al. Axonal damage in the spinal cord of MS patients occurs largely independent of T2 MRI lesions. Neurology 2002; 59: 1766–71.

Bermel RA, Bakshi R. The measurement and clinical relevance of brain atrophy in multiple sclerosis. Lancet. Neurol. 2006; 5: 158–170.

Bhat R, Mahapatra S, Axtell RC, Steinman L. Amelioration of ongoing experimental autoimmune encephalomyelitis with fluoxetine. J. Neuroimmunol. 2017; 313: 77–81.

Birkeldh U, Manouchehrinia A, Hietala MA, Hillert J, Olsson T, Piehl F, et al. Retinal nerve fiber layer thickness associates with cognitive impairment and physical disability in multiple sclerosis. Mult. Scler. Relat. Disord. 2019; 36: 101414.

Bjartmar C, Kinkel RP, Kidd G, Rudick RA, Trapp BD. Axonal loss in normal-appearing white matter in a patient with acute MS. Neurology 2001; 57: 1248–52.

Bjelobaba I, Begovic-Kupresanin V, Pekovic S, Lavrnja I. Animal models of multiple sclerosis: Focus on experimental autoimmune encephalomyelitis. J. Neurosci. Res. 2018; 96: 1021–1042.

Bogdan C. Nitric oxide and the immune response. Nat. Immunol. 2001; 2: 907–916.

Bot JCJ, Barkhof F, Polman CH, Lycklama à Nijeholt GJ, de Groot V, Bergers E, et al. Spinal cord abnormalities in recently diagnosed MS patients: added value of spinal MRI examination. Neurology 2004; 62: 226–33.

Bove R, Musallam A, Xia Z, Baruch N, Messina S, Healy BC, et al. Longitudinal

BMI trajectories in multiple sclerosis: Sex differences in association with disease severity. Mult. Scler. Relat. Disord. 2016; 8: 136–40.

Brochet B, Deloire MSA, Bonnet M, Salort-Campana E, Ouallet JC, Petry KG, et al. Should SDMT substitute for PASAT in MSFC? A 5-year longitudinal study. Mult. Scler. 2008; 14: 1242–9.

Brochet B, Deloire MSA, Perez P, Loock T, Baschet L, Debouverie M, et al. Double-Blind Controlled Randomized Trial of Cyclophosphamide versus Methylprednisolone in Secondary Progressive Multiple Sclerosis. PLoS One 2017; 12: e0168834.

Brown JWL, Coles AJ. Alemtuzumab: evidence for its potential in relapsing-remitting multiple sclerosis. Drug Des. Devel. Ther. 2013; 7: 131–8.

Browne P, Chandraratna D, Angood C, Tremlett H, Baker C, Taylor B V., et al. Atlas of Multiple Sclerosis 2013: A growing global problem with widespread inequity. Neurology 2014; 83: 1022–1024.

Brownlee W, Altmann D, Alves Da Mota P, Swanton J, Miszkiel K, Wheeler-Kingshott CG, et al. Association of asymptomatic spinal cord lesions and atrophy with disability 5 years after a clinically isolated syndrome. Mult. Scler. J. 2017; 23: 665–674.

Cambron M, Mostert J, D'Hooghe M, Nagels G, Willekens B, Debruyne J, et al. Fluoxetine in progressive multiple sclerosis: The FLUOX-PMS trial. Mult. Scler. J. 2019: 135245851984305.

Cambron M, Mostert J, Haentjens P, D'Hooghe M, Nagels G, Willekens B, et al. Fluoxetine in progressive multiple sclerosis (FLUOX-PMS): study protocol for a randomized controlled trial. Trials 2014; 15: 37.

Campillos M, Kuhn M, Gavin A-C, Jensen LJ, Bork P. Drug target identification using side-effect similarity. Science 2008; 321: 263–6.

Cardoso MJ, Modat M, Wolz R, Melbourne A, Cash D, Rueckert D, et al. Geodesic Information Flows: Spatially-Variant Graphs and Their Application to Segmentation and Fusion. IEEE Trans. Med. Imaging 2015; 34: 1976–1988.

Casserly C, Seyman EE, Alcaide-Leon P, Guenette M, Lyons C, Sankar S, et al. Spinal Cord Atrophy in Multiple Sclerosis: A Systematic Review and Meta-Analysis. J. Neuroimaging 2018; 28: 556–586.

Chataway J, Nicholas R, Todd S, Miller DH, Parsons N, Valdés-Márquez E, et al. A novel adaptive design strategy increases the efficiency of clinical trials in secondary progressive multiple sclerosis. Mult. Scler. 2011; 17: 81–8.

Chataway J, Schuerer N, Alsanousi A, Chan D, MacManus D, Hunter K, et al. Effect of high-dose simvastatin on brain atrophy and disability in secondary progressive multiple sclerosis (MS-STAT): a randomised, placebo-controlled, phase 2 trial. Lancet 2014; 383: 2213–21.

Choi JJ, Wang S, Tung Y-S, Morrison B, Konofagou EE. Molecules of Various

Pharmacologically-Relevant Sizes Can Cross the Ultrasound-Induced Blood-Brain Barrier Opening in vivo. Ultrasound Med. Biol. 2010; 36: 58–67.

Ciccarelli O, Barkhof F, Bodini B, De Stefano N, Golay X, Nicolay K, et al. Pathogenesis of multiple sclerosis: insights from molecular and metabolic imaging. Lancet. Neurol. 2014; 13: 807–22.

Ciccarelli O, Cohen JA, Reingold SC, Weinshenker BG, Amato MP, Banwell B, et al. Spinal cord involvement in multiple sclerosis and neuromyelitis optica spectrum disorders. Lancet Neurol. 2019; 18: 185–197.

Cocco E, Marrosu MG. The current role of mitoxantrone in the treatment of multiple sclerosis. Expert Rev. Neurother. 2014; 14: 607–616.

Cohen JA, Barkhof F, Comi G, Hartung H-P, Khatri BO, Montalban X, et al. Oral fingolimod or intramuscular interferon for relapsing multiple sclerosis. N. Engl. J. Med. 2010; 362: 402–15.

Cohen JA, Coles AJ, Arnold DL, Confavreux C, Fox EJ, Hartung H-P, et al. Alemtuzumab versus interferon beta 1a as first-line treatment for patients with relapsing-remitting multiple sclerosis: a randomised controlled phase 3 trial. Lancet (London, England) 2012a; 380: 1819–28.

Cohen JA, Cutter GR, Fischer JS, Goodman AD, Heidenreich FR, Kooijmans MF, et al. Benefit of interferon beta-1a on MSFC progression in secondary progressive MS. Neurology 2002; 59: 679–87.

Cohen JA, Imrey PB, Calabresi PA, Edwards KR, Eickenhorst T, Felton WL, et al. Results of the Avonex Combination Trial (ACT) in relapsing-remitting MS. Neurology 2009; 72: 535–41.

Cohen JA, Reingold SC, Polman CH, Wolinsky JS. Disability outcome measures in multiple sclerosis clinical trials: current status and future prospects. Lancet Neurol. 2012b; 11: 467–476.

Coles AJ, Cox A, Le Page E, Jones J, Trip SA, Deans J, et al. The window of therapeutic opportunity in multiple sclerosis: evidence from monoclonal antibody therapy. J. Neurol. 2006; 253: 98–108.

Coles AJ, Twyman CL, Arnold DL, Cohen JA, Confavreux C, Fox EJ, et al. Alemtuzumab for patients with relapsing multiple sclerosis after disease-modifying therapy: a randomised controlled phase 3 trial. Lancet (London, England) 2012; 380: 1829–39.

Compston A, Coles A. Multiple sclerosis. Lancet 2008; 372: 1502–17.

Compston A, Coles A, Compston D, Brophy P, Carswell R, Barbellion W, et al. Multiple sclerosis. Lancet 2008; 372: 1502–1517.

Confavreux C, Compston DA, Hommes OR, McDonald WI, Thompson AJ. EDMUS, a European database for multiple sclerosis. J. Neurol. Neurosurg. Psychiatry 1992; 55: 671–6.

Connick P, De Angelis F, Parker RA, Plantone D, Doshi A, John N, et al. Multiple Sclerosis-Secondary Progressive Multi-Arm Randomisation Trial (MS-SMART): a multiarm phase IIb randomised, double-blind, placebo-controlled clinical trial comparing the efficacy of three neuroprotective drugs in secondary progressive multiple sclerosis. BMJ Open 2018; 8: e021944.

Conway D, Cohen JA. Combination therapy in multiple sclerosis. Lancet Neurol. 2010; 9: 299–308.

Conway DS, Thompson NR, Cohen JA. Influence of hypertension, diabetes, hyperlipidemia, and obstructive lung disease on multiple sclerosis disease course. Mult. Scler. J. 2017; 23: 277–285.

Costello F. Vision Disturbances in Multiple Sclerosis. Semin. Neurol. 2016; 36: 185–195.

Cotton F, Weiner HL, Jolesz FA, Guttmann CRG. MRI contrast uptake in new lesions in relapsing-remitting MS followed at weekly intervals. Neurology 2003; 60: 640–6.

Craner MJ, Damarjian TG, Liu S, Hains BC, Lo AC, Black JA, et al. Sodium channels contribute to microglia/macrophage activation and function in EAE and MS. Glia 2005; 49: 220–229.

Cruz-Herranz A, Balk LJ, Oberwahrenbrock T, Saidha S, Martinez-Lapiscina EH, Lagreze WA, et al. The APOSTEL recommendations for reporting quantitative optical coherence tomography studies. Neurology 2016; 86: 2303–2309.

Cuatrecasas P. Drug discovery in jeopardy. J. Clin. Invest. 2006; 116: 2837–2842.

Cutter GR, Baier ML, Rudick RA, Cookfair DL, Fischer JS, Petkau J, et al. Development of a multiple sclerosis functional composite as a clinical trial outcome measure. Brain 1999; 122: 871–882.

Dean G. Annual incidence, prevalence, and mortality of multiple sclerosis in white South-African-born and in white immigrants to South Africa. Br. Med. J. 1967; 2: 724–30.

Dekker I, Sombekke MH, Balk LJ, Moraal B, Geurts JJ, Barkhof F, et al. Infratentorial and spinal cord lesions: Cumulative predictors of long-term disability? Mult. Scler. J. 2019: 135245851986493.

Deloire M, Ruet A, Hamel D, Bonnet M, Brochet B. Early cognitive impairment in multiple sclerosis predicts disability outcome several years later. Mult. Scler. J. 2010; 16: 581–587.

DeLuca GC, Williams K, Evangelou N, Ebers GC, Esiri MM. The contribution of demyelination to axonal loss in multiple sclerosis. Brain 2006; 129: 1507–1516.

Denic A, Johnson AJ, Bieber AJ, Warrington AE, Rodriguez M, Pirko I. The relevance of animal models in multiple sclerosis research. Pathophysiology 2011; 18: 21–9.

Diamond M, Kelly JP, Connor TJ. Antidepressants suppress production of the Th1 cytokine interferon-γ, independent of monoamine transporter blockade. Eur. Neuropsychopharmacol. 2006; 16: 481–490.

Dutta R, McDonough J, Yin X, Peterson J, Chang A, Torres T, et al. Mitochondrial dysfunction as a cause of axonal degeneration in multiple sclerosis patients. Ann. Neurol. 2006; 59: 478–489.

Edan G, Comi G, Le Page E, Leray E, Rocca MA, Filippi M, et al. Mitoxantrone prior to interferon beta-1b in aggressive relapsing multiple sclerosis: a 3-year randomised trial. J. Neurol. Neurosurg. Psychiatry 2011; 82: 1344–50.

Edan G, Le Page E. Induction Therapy for Patients with Multiple Sclerosis: Why? When? How? CNS Drugs 2013; 27: 403–409.

Elliott C, Belachew S, Wolinsky JS, Hauser SL, Kappos L, Barkhof F, et al. Chronic white matter lesion activity predicts clinical progression in primary progressive multiple sclerosis. Brain 2019; 142: 2787–2799.

Enzinger C, Fazekas F, Matthews PM, Ropele S, Schmidt H, Smith S, et al. Risk factors for progression of brain atrophy in aging: six-year follow-up of normal subjects. Neurology 2005; 64: 1704–11.

Eshaghi A, Kievit RA, Prados F, Sudre CH, Nicholas J, Cardoso MJ, et al. Applying causal models to explore the mechanism of action of simvastatin in progressive multiple sclerosis. Proc. Natl. Acad. Sci. U. S. A. 2019; 116: 11020–11027.

Eshaghi A, Marinescu R V, Young AL, Firth NC, Prados F, Jorge Cardoso M, et al. Progression of regional grey matter atrophy in multiple sclerosis. Brain 2018a; 141: 1665–1677.

Eshaghi A, Prados F, Brownlee WJ, Altmann DR, Tur C, Cardoso MJ, et al. Deep gray matter volume loss drives disability worsening in multiple sclerosis. Ann. Neurol. 2018b; 83: 210–222.

Estevez AG, Stutzmann JM, Barbeito L. Protective effect of riluzole on excitatory amino acid-mediated neurotoxicity in motoneuron-enriched cultures. Eur. J. Pharmacol. 1995; 280: 47–53.

European Study Group on interferon beta-1b in secondary progressive MS. Placebo-controlled multicentre randomised trial of interferon beta-1b in treatment of secondary progressive multiple sclerosis. Lancet (London, England) 1998; 352: 1491–7.

Evangelou N, DeLuca GC, Owens T, Esiri MM. Pathological study of spinal cord atrophy in multiple sclerosis suggests limited role of local lesions. Brain 2005; 128: 29–34.

Evangelou N, Konz D, Esiri MM, Smith S, Palace J, Matthews PM. Regional axonal loss in the corpus callosum correlates with cerebral white matter lesion volume and distribution in multiple sclerosis. Brain 2000; 123 (Pt 9): 1845–9.

Faissner S, Mishra M, Kaushik DK, Wang J, Fan Y, Silva C, et al. Systematic

screening of generic drugs for progressive multiple sclerosis identifies clomipramine as a promising therapeutic. Nat. Commun. 2017; 8: 1990.

Fambiatos A, Jokubaitis V, Horakova D, Kubala Havrdova E, Trojano M, Prat A, et al. Risk of secondary progressive multiple sclerosis: A longitudinal study. Mult. Scler. J. 2019: 135245851986899.

Fan Q, Teo Y-Y, Saw S-M. Application of Advanced Statistics in Ophthalmology. Investig. Opthalmology Vis. Sci. 2011; 52: 6059.

Feys P, Lamers I, Francis G, Benedict R, Phillips G, LaRocca N, et al. The Nine-Hole Peg Test as a manual dexterity performance measure for multiple sclerosis. Mult. Scler. J. 2017; 23: 711–720.

Filippi M, Preziosa P, Rocca MA. Magnetic resonance outcome measures in multiple sclerosis trials: time to rethink? Curr. Opin. Neurol. 2014; 27: 290–9.

Filippi M, Rovaris M, Iannucci G, Mennea S, Sormani MP, Comi G. Whole brain volume changes in patients with progressive MS treated with cladribine. Neurology 2000; 55: 1714–8.

Filippini G. Ocrelizumab appears to reduce relapse and disability in multiple sclerosis but quality of evidence is moderate. Evid. Based Med. 2017; 22: 215–216.

Fischer JS, Rudick RA, Cutter GR, Reingold SC. The Multiple Sclerosis Functional Composite Measure (MSFC): an integrated approach to MS clinical outcome assessment. National MS Society Clinical Outcomes Assessment Task Force. Mult. Scler. 1999; 5: 244–50.

Fisher E, Chang A, Fox RJ, Tkach JA, Svarovsky T, Nakamura K, et al. Imaging correlates of axonal swelling in chronic multiple sclerosis brains. Ann. Neurol. 2007; 62: 219–228.

Fisher E, Lee J-C, Nakamura K, Rudick RA. Gray matter atrophy in multiple sclerosis: a longitudinal study. Ann. Neurol. 2008; 64: 255–65.

Fisniku LK, Chard DT, Jackson JS, Anderson VM, Altmann DR, Miszkiel KA, et al. Gray matter atrophy is related to long-term disability in multiple sclerosis. Ann. Neurol. 2008; 64: 247–54.

Fitzgibbon T, Taylor SF. Retinotopy of the human retinal nerve fibre layer and optic nerve head. J. Comp. Neurol. 1996; 375: 238–251.

Fliri AF, Loging WT, Thadeio PF, Volkmann RA. Biological spectra analysis: Linking biological activity profiles to molecular structure. Proc. Natl. Acad. Sci. U. S. A. 2005; 102: 261–6.

Foltynie T. Glycolysis as a therapeutic target for Parkinson's disease. Lancet. Neurol. 2019; 18: 1072–1074.

Fox RJ, Beall E, Bhattacharyya P, Chen JT, Sakaie K. Advanced MRI in multiple sclerosis: current status and future challenges. Neurol. Clin. 2011; 29: 357–80.

Fox RJ, Coffey CS, Conwit R, Cudkowicz ME, Gleason T, Goodman A, et al. Phase 2 Trial of Ibudilast in Progressive Multiple Sclerosis. N. Engl. J. Med. 2018; 379: 846–855.

Fox RJ, Coffey CS, Cudkowicz ME, Gleason T, Goodman A, Klawiter EC, et al. Design, rationale, and baseline characteristics of the randomized double-blind phase II clinical trial of ibudilast in progressive multiple sclerosis. Contemp. Clin. Trials 2016; 50: 166–177.

Fox RJ, Thompson A, Baker D, Baneke P, Brown D, Browne P, et al. Setting a research agenda for progressive multiple sclerosis: the International Collaborative on Progressive MS. Mult. Scler. 2012; 18: 1534–40.

Frank JA, Richert N, Bash C, Stone L, Calabresi PA, Lewis B, et al. Interferon-beta-1b slows progression of atrophy in RRMS: Three-year follow-up in NAb- and NAb+ patients. Neurology 2004; 62: 719–25.

Franke K, Hagemann G, Schleussner E, Gaser C. Changes of individual BrainAGE during the course of the menstrual cycle. Neuroimage 2015; 115: 1–6.

Freedman MS, Bar-Or A, Oger J, Traboulsee A, Patry D, Young C, et al. A phase III study evaluating the efficacy and safety of MBP8298 in secondary progressive MS. Neurology 2011; 77: 1551–1560.

Friese MA, Craner MJ, Etzensperger R, Vergo S, Wemmie JA, Welsh MJ, et al. Acid-sensing ion channel-1 contributes to axonal degeneration in autoimmune inflammation of the central nervous system. Nat. Med. 2007; 13: 1483–1489.

Frischer JM, Weigand SD, Guo Y, Kale N, Parisi JE, Pirko I, et al. Clinical and pathological insights into the dynamic nature of the white matter multiple sclerosis plaque. Ann. Neurol. 2015; 78: 710–21.

Frohman E, Costello F, Zivadinov R, Stuve O, Conger A, Winslow H, et al. Optical coherence tomography in multiple sclerosis. Lancet. Neurol. 2006; 5: 853–63.

Frohman EM, Dwyer MG, Frohman T, Cox JL, Salter A, Greenberg BM, et al. Relationship of optic nerve and brain conventional and non-conventional MRI measures and retinal nerve fiber layer thickness, as assessed by OCT and GDx: A pilot study. J. Neurol. Sci. 2009; 282: 96–105.

Frohman EM, Fujimoto JG, Frohman TC, Calabresi PA, Cutter G, Balcer LJ. Optical coherence tomography: a window into the mechanisms of multiple sclerosis. Nat. Clin. Pract. Neurol. 2008; 4: 664–675.

Furby J, Hayton T, Altmann D, Brenner R, Chataway J, Smith KJ, et al. A longitudinal study of MRI-detected atrophy in secondary progressive multiple sclerosis. J. Neurol. 2010; 257: 1508–16.

Furby J, Hayton T, Anderson V, Altmann D, Brenner R, Chataway J, et al. Magnetic resonance imaging measures of brain and spinal cord atrophy correlate with clinical impairment in secondary progressive multiple sclerosis. Mult. Scler. 2008; 14: 1068–75.

Galea I, Ward-Abel N, Heesen C. Relapse in multiple sclerosis. BMJ 2015; 350: h1765.

Garcia-Martin E, Polo V, Larrosa JM, Marques ML, Herrero R, Martin J, et al. Retinal layer segmentation in patients with multiple sclerosis using spectral domain optical coherence tomography. Ophthalmology 2014; 121: 573–9.

Gass A, Rocca MA, Agosta F, Ciccarelli O, Chard D, Valsasina P, et al. MRI monitoring of pathological changes in the spinal cord in patients with multiple sclerosis. Lancet. Neurol. 2015; 14: 443–54.

Gilgun-Sherki Y, Panet H, Melamed E, Offen D. Riluzole suppresses experimental autoimmune encephalomyelitis: implications for the treatment of multiple sclerosis. Brain Res. 2003; 989: 196–204.

Giovannoni G, Comi G, Cook S, Rammohan K, Rieckmann P, Sørensen PS, et al. A Placebo-Controlled Trial of Oral Cladribine for Relapsing Multiple Sclerosis. N. Engl. J. Med. 2010; 362: 416–426.

Goodman AD, Rossman H, Bar-Or A, Miller A, Miller DH, Schmierer K, et al. GLANCE Results of a phase 2, randomized, double-blind, placebo-controlled study. Neurology 2009; 72: 806–812.

Gordon-Lipkin E, Chodkowski B, Reich DS, Smith SA, Pulicken M, Balcer LJ, et al. Retinal nerve fiber layer is associated with brain atrophy in multiple sclerosis. Neurology 2007; 69: 1603–1609.

De Groot CJ, Bergers E, Kamphorst W, Ravid R, Polman CH, Barkhof F, et al. Post-mortem MRI-guided sampling of multiple sclerosis brain lesions: increased yield of active demyelinating and (p)reactive lesions. Brain 2001; 124: 1635–45.

Group british and duch mutiple sclerosis azathiprine trial. Double-masked trial of azathioprine in multiple sclerosis. British and Dutch Multiple Sclerosis Azathioprine Trial Group. Lancet (London, England) 1988; 2: 179–83.

Hamdan R, Gonzalez RG, Ghostine S, Caussin C. Optical coherence tomography: From physical principles to clinical applications. Arch. Cardiovasc. Dis. 2012; 105: 529–534.

Hampton DW, Anderson J, Pryce G, Irvine K-A, Giovannoni G, Fawcett JW, et al. An experimental model of secondary progressive multiple sclerosis that shows regional variation in gliosis, remyelination, axonal and neuronal loss. J. Neuroimmunol. 2008; 201–202: 200–11.

Hardingham GE, Bading H. Synaptic versus extrasynaptic NMDA receptor signalling: implications for neurodegenerative disorders. Nat. Rev. Neurosci. 2010; 11: 682–96.

Hardmeier M, Wagenpfeil S, Freitag P, Fisher E, Rudick RA, Kooijmans M, et al. Rate of brain atrophy in relapsing MS decreases during treatment with IFN -1a. Neurology 2005; 64: 236–240.

Hartung H-P, Gonsette R, Konig N, Kwiecinski H, Guseo A, Morrissey SP, et al.

Mitoxantrone in progressive multiple sclerosis: a placebo-controlled, double-blind, randomised, multicentre trial. Lancet 2002; 360: 2018–2025.

Hauser S, Waubant E, Arnold DL, Vollmer T, Antel J, Fox RJ, et al. B-Cell Depletion with Rituximab in Relapsing–Remitting Multiple Sclerosis. N. Engl. J. Med. 2008; 358: 676–88.

Hauser SL, Chan JR, Oksenberg JR. Multiple sclerosis: Prospects and promise. Ann. Neurol. 2013; 74: 317–27.

Hawker K, O'Connor P, Freedman MS, Calabresi PA, Antel J, Simon J, et al. Rituximab in patients with primary progressive multiple sclerosis: results of a randomized double-blind placebo-controlled multicenter trial. Ann. Neurol. 2009; 66: 460–71.

Healy BC, Arora A, Hayden DL, Ceccarelli A, Tauhid SS, Neema M, et al. Approaches to normalization of spinal cord volume: application to multiple sclerosis. J. Neuroimaging 2012; 22: e12-9.

Hemmer B, Kerschensteiner M, Korn T. Role of the innate and adaptive immune responses in the course of multiple sclerosis. Lancet Neurol. 2015; 14: 406–419.

Henderson APD, Altmann DR, Trip AS, Kallis C, Jones SJ, Schlottmann PG, et al. A serial study of retinal changes following optic neuritis with sample size estimates for acute neuroprotection trials. Brain 2010a; 133: 2592–602.

Henderson APD, Trip SA, Schlottmann PG, Altmann DR, Garway-Heath DF, Plant GT, et al. A preliminary longitudinal study of the retinal nerve fiber layer in progressive multiple sclerosis. J. Neurol. 2010b; 257: 1083–1091.

Henry ME, Schmidt ME, Hennen J, Villafuerte RA, Butman ML, Tran P, et al. A comparison of brain and serum pharmacokinetics of R-fluoxetine and racemic fluoxetine: A 19-F MRS study. Neuropsychopharmacology 2005; 30: 1576–83.

Hickman SJ, Brex PA, Brierley CM, Silver NC, Barker GJ, Scolding NJ, et al. Detection of optic nerve atrophy following a single episode of unilateral optic neuritis by MRI using a fat-saturated short-echo fast FLAIR sequence. Neuroradiology 2001; 43: 123–8.

Hobart J, Cano S. Improving the evaluation of therapeutic interventions in multiple sclerosis: the role of new psychometric methods. Health Technol. Assess. (Rockv). 2009; 13: iii, ix–x, 1–177.

Hobart J, Lamping D, Fitzpatrick R, Riazi A, Thompson A. The Multiple Sclerosis Impact Scale (MSIS-29): a new patient-based outcome measure. Brain 2001; 124: 962–73.

Hopkins AL, Groom CR. The druggable genome. Nat. Rev. Drug Discov. 2002; 1: 727–30.

Horsfield MA, Sala S, Neema M, Absinta M, Bakshi A, Sormani MP, et al. Rapid semi-automatic segmentation of the spinal cord from magnetic resonance images: Application in multiple sclerosis. Neuroimage 2010; 50: 446–455.

Howell OW, Reeves CA, Nicholas R, Carassiti D, Radotra B, Gentleman SM, et al. Meningeal inflammation is widespread and linked to cortical pathology in multiple sclerosis. Brain 2011; 134: 2755–2771.

Hulst HE, Thompson AJ, Geurts JJ. The measure tells the tale: Clinical outcome measures in multiple sclerosis. Mult. Scler. 2017; 23: 626–627.

Ikuta F, Zimmerman HM. Distribution of plaques in seventy autopsy cases of multiple sclerosis in the United States. Neurology 1976; 26: 26–8.

Inglese M, Madelin G, Oesingmann N, Babb JS, Wu W, Stoeckel B, et al. Brain tissue sodium concentration in multiple sclerosis: a sodium imaging study at 3 tesla. Brain 2010; 133: 847–57.

International Multiple Sclerosis Genetics Consortium (IMSGC), Beecham AH, Patsopoulos NA, Xifara DK, Davis MF, Kemppinen A, Cotsapas C, Shah TS, Spencer C, Booth D, Goris A, Oturai A, Saarela J, Fontaine B, Hemmer B, Martin C, Zipp F, D'Alfonso S, Martine MJ. Analysis of immune-related loci identifies 48 new susceptibility variants for multiple sclerosis. Nat Genet 2013; 45: 1353–1360.

James ND, Sydes MR, Mason MD, Clarke NW, Anderson J, Dearnaley DP, et al. Celecoxib plus hormone therapy versus hormone therapy alone for hormone-sensitive prostate cancer: first results from the STAMPEDE multiarm, multistage, randomised controlled trial. Lancet Oncol. 2012; 13: 549–558.

Jehle T, Bauer J, Blauth E, Hummel A, Darstein M, Freiman TM, et al. Effects of riluzole on electrically evoked neurotransmitter release. Br. J. Pharmacol. 2000; 130: 1227–34.

Jolliffe IT. Principal Component Analysis [Internet]. Second Edition. New York: Springer; 2002. Available from: http://cda.psych.uiuc.edu/statistical_learning_course/Jolliffe I. Principal Component Analysis (2ed., Springer, 2002)(518s)_MVsa_.pdf

Kalincik T, Cutter G, Spelman T, Jokubaitis V, Havrdova E, Horakova D, et al. Defining reliable disability outcomes in multiple sclerosis. Brain 2015; 138: 3287–3298.

Kalkers NF, Barkhof F, Bergers E, van Schijndel R, Polman CH. The effect of the neuroprotective agent riluzole on MRI parameters in primary progressive multiple sclerosis: a pilot study. Mult. Scler. J. 2002; 8: 532–533.

Kalkers NF, Bergers E, Castelijns JA, van Walderveen MA, Bot JC, Adèr HJ, et al. Optimizing the association between disability and biological markers in MS. Neurology 2001; 57: 1253–8.

Kandel ER. JHSTMJ. Principles of Neural Science. 2000.

Kapoor R. Neuroprotection in multiple sclerosis: therapeutic strategies and clinical trial design. Curr. Opin. Neurol. 2006; 19: 255–9.

Kapoor R, Furby J, Hayton T, Smith KJ, Altmann DR, Brenner R, et al. Lamotrigine for neuroprotection in secondary progressive multiple sclerosis: a randomised,

double-blind, placebo-controlled, parallel-group trial. Lancet. Neurol. 2010; 9: 681–8.

Kapoor R, Ho P-R, Campbell N, Chang I, Deykin A, Forrestal F, et al. Effect of natalizumab on disease progression in secondary progressive multiple sclerosis (ASCEND): a phase 3, randomised, double-blind, placebo-controlled trial with an open-label extension [Internet]. Lancet Neurol. 2018[cited 2018 Mar 29] Available from: https://www.sciencedirect.com/science/article/pii/S1474442218300693?_rdoc=1&_fmt=high&_origin=gateway&_docanchor=&md5=b8429449ccfc9c30159a5f9aeaa92ffb

Kappos L, Antel J, Comi G, Montalban X, O'Connor P, Polman CH, et al. Oral fingolimod (FTY720) for relapsing multiple sclerosis. N. Engl. J. Med. 2006; 355: 1124–40.

Kappos L, Bar-Or A, Cree BAC, Fox RJ, Giovannoni G, Gold R, et al. Siponimod versus placebo in secondary progressive multiple sclerosis (EXPAND): a double-blind, randomised, phase 3 study [Internet]. Lancet 2018[cited 2018 Mar 29] Available from: http://linkinghub.elsevier.com/retrieve/pii/S0140673618304756

Kawachi I, Lassmann H. Neurodegeneration in multiple sclerosis and neuromyelitis optica. J. Neurol. Neurosurg. Psychiatry 2016: jnnp-2016-313300.

Kearney H, Altmann DR, Samson RS, Yiannakas MC, Wheeler-Kingshott CAM, Ciccarelli O, et al. Cervical cord lesion load is associated with disability independently from atrophy in MS. Neurology 2015a; 84: 367–373.

Kearney H, Miller DH, Ciccarelli O. Spinal cord MRI in multiple sclerosis--diagnostic, prognostic and clinical value. Nat. Rev. Neurol. 2015b; 11: 327–38.

Kearney H, Yiannakas MC, Abdel-Aziz K, Wheeler-Kingshott CAM, Altmann DR, Ciccarelli O, et al. Improved MRI quantification of spinal cord atrophy in multiple sclerosis. J. Magn. Reson. Imaging 2014; 39: 617–23.

Keiser MJ, Setola V, Irwin JJ, Laggner C, Abbas AI, Hufeisen SJ, et al. Predicting new molecular targets for known drugs. Nature 2009; 462: 175–81.

Kemanetzoglou E, Andreadou E. CNS Demyelination with TNF-α Blockers. Curr. Neurol. Neurosci. Rep. 2017; 17: 36.

Keshavan A, Paul F, Beyer MK, Zhu AH, Papinutto N, Shinohara RT, et al. Power estimation for non-standardized multisite studies. Neuroimage 2016; 134: 281–294.

De Keyser J, Wilczak N, Leta R, Streetland C. Astrocytes in multiple sclerosis lack beta-2 adrenergic receptors. Neurology 1999; 53: 1628–33.

Khan O. Can clinical outcomes be used to detect neuroprotection in multiple sclerosis? Neurology 2007; 68: S64-71; discussion S91-6.

Killestein J, Kalkers NF, Polman CH. Glutamate inhibition in MS: the neuroprotective properties of riluzole. J. Neurol. Sci. 2005; 233: 113–5.

Kipp M, Nyamoya S, Hochstrasser T, Amor S. Multiple sclerosis animal models: a clinical and histopathological perspective. Brain Pathol. 2017; 27: 123–137.

Klein JP, Arora A, Neema M, Healy BC, Tauhid S, Goldberg-Zimring D, et al. A 3T MR imaging investigation of the topography of whole spinal cord atrophy in multiple sclerosis. AJNR. Am. J. Neuroradiol. 2011; 32: 1138–42.

Knier B, Schmidt P, Aly L, Buck D, Berthele A, Mühlau M, et al. Retinal inner nuclear layer volume reflects response to immunotherapy in multiple sclerosis. Brain 2016; 139: 2855–2863.

Koch M, Kingwell E, Rieckmann P, Tremlett H, UBC MS Clinic Neurologists. The natural history of secondary progressive multiple sclerosis. J. Neurol. Neurosurg. Psychiatry 2010; 81: 1039–43.

Komori M, Lin YC, Cortese I, Blake A, Ohayon J, Cherup J, et al. Insufficient disease inhibition by intrathecal rituximab in progressive multiple sclerosis. Ann. Clin. Transl. Neurol. 2016; 3: 166–79.

Kong EKC, Peng L, Chen Y, Yu ACH, Hertz L. Up-regulation of 5-HT2B receptor density and receptor-mediated glycogenolysis in mouse astrocytes by long-term fluoxetine administration. Neurochem. Res. 2002; 27: 113–20.

Kornek B, Lassmann H. Axonal pathology in multiple sclerosis. A historical note. Brain Pathol. 1999; 9: 651–6.

Korteweg T, Rovaris M, Neacsu V, Filippi M, Comi G, Uitdehaag B, et al. Can rate of brain atrophy in multiple sclerosis be explained by clinical and MRI characteristics? Mult. Scler. J. 2009; 15: 465–471.

Kosa P, Ghazali D, Tanigawa M, Barbour C, Cortese I, Kelley W, et al. Development of a Sensitive Outcome for Economical Drug Screening for Progressive Multiple Sclerosis Treatment. Front. Neurol. 2016; 7: 131.

Kragt JJ, van der Linden FAH, Nielsen JM, Uitdehaag BMJ, Polman CH. Clinical impact of 20% worsening on Timed 25-foot Walk and 9-hole Peg Test in multiple sclerosis. Mult. Scler. 2006; 12: 594–8.

Kurtzke JF. Rating neurologic impairment in multiple sclerosis: an expanded disability status scale (EDSS). Neurology 1983; 33: 1444–52.

Kurtzke JF. Epidemiology in multiple sclerosis: a pilgrim's progress. Brain 2013; 136: 2904–2917.

Kutzelnigg A, Lucchinetti CF, Stadelmann C, Brück W, Rauschka H, Bergmann M, et al. Cortical demyelination and diffuse white matter injury in multiple sclerosis. Brain 2005; 128: 2705–12.

Lamanauskas N, Nistri A. Riluzole blocks persistent Na^{+} and Ca^{2+} currents and modulates release of glutamate via presynaptic NMDA receptors on neonatal rat hypoglossal motoneurons *in vitro*. Eur. J. Neurosci. 2008; 27: 2501–2514.

Langdon DW, Amato MP, Boringa J, Brochet B, Foley F, Fredrikson S, et al.

Recommendations for a Brief International Cognitive Assessment for Multiple Sclerosis (BICAMS). Mult. Scler. 2012; 18: 891–8.

Langer-Gould A, Brara SM, Beaber BE, Koebnick C. Childhood obesity and risk of pediatric multiple sclerosis and clinically isolated syndrome. Neurology 2013; 80: 548–52.

Lassmann H. Hypoxia-like tissue injury as a component of multiple sclerosis lesions. J. Neurol. Sci. 2003; 206: 187–191.

Lassmann H. Targets of therapy in progressive MS. Mult. Scler. J. 2017; 23: 1593–1599.

Lassmann H. Multiple Sclerosis Pathology. Cold Spring Harb. Perspect. Med. 2018; 8: a028936.

Leary SM, Miller DH, Stevenson VL, Brex PA, Chard DT, Thompson AJ. Interferon beta-1a in primary progressive MS: an exploratory, randomized, controlled trial. Neurology 2003; 60: 44–51.

De Leener B, Cohen-Adad J, Kadoury S. Automatic Segmentation of the Spinal Cord and Spinal Canal Coupled With Vertebral Labeling. IEEE Trans. Med. Imaging 2015; 34: 1705–1718.

De Leener B, Kadoury S, Cohen-Adad J. Robust, accurate and fast automatic segmentation of the spinal cord. Neuroimage 2014; 98: 528–536.

Leist TP, Comi G, Cree BAC, Coyle PK, Freedman MS, Hartung H-P, et al. Effect of oral cladribine on time to conversion to clinically definite multiple sclerosis in patients with a first demyelinating event (ORACLE MS): a phase 3 randomised trial. Lancet Neurol. 2014; 13: 257–267.

Leung CKS, Yu M, Weinreb RN, Ye C, Liu S, Lai G, et al. Retinal Nerve Fiber Layer Imaging with Spectral-Domain Optical Coherence Tomography: A Prospective Analysis of Age-Related Loss. Ophthalmology 2012; 119: 731–737.

Likosky WH, Fireman B, Elmore R, Eno G, Gale K, Goode GB, et al. Intense immunosuppression in chronic progressive multiple sclerosis: the Kaiser study. J. Neurol. Neurosurg. Psychiatry 1991; 54: 1055–60.

Lin X, Tench CR, Turner B, Blumhardt LD, Constantinescu CS. Spinal cord atrophy and disability in multiple sclerosis over four years: application of a reproducible automated technique in monitoring disease progression in a cohort of the interferon beta-1a (Rebif) treatment trial. J. Neurol. Neurosurg. Psychiatry 2003; 74: 1090–4.

Lisak RP, Benjamins JA, Nedelkoska L, Barger JL, Ragheb S, Fan B, et al. Secretory products of multiple sclerosis B cells are cytotoxic to oligodendroglia in vitro. J. Neuroimmunol. 2012; 246: 85–95.

Lisak RP, Nedelkoska L, Benjamins JA, Schalk D, Bealmear B, Touil H, et al. B cells from patients with multiple sclerosis induce cell death via apoptosis in neurons in vitro. J. Neuroimmunol. 2017; 309: 88–99.

Lo AC, Saab CY, Black JA, Waxman SG. Phenytoin Protects Spinal Cord Axons and Preserves Axonal Conduction and Neurological Function in a Model of Neuroinflammation In Vivo. J. Neurophysiol. 2003; 90: 3566–3571.

Lorscheider J, Buzzard K, Jokubaitis V, Spelman T, Havrdova E, Horakova D, et al. Defining secondary progressive multiple sclerosis. Brain 2016; 139: 2395–405.

Losseff NA, Wang L, Lai HM, Yoo DS, Gawne-Cain ML, McDonald WI, et al. Progressive cerebral atrophy in multiple sclerosis. A serial MRI study. Brain 1996a: 2009–19.

Losseff NA, Webb SL, O 'riordan JI, Page R, Wang L, Barker GJ, et al. Spinal cord atrophy and disability in multiple sclerosis A new reproducible and sensitive MRI method with potential to monitor disease progression. Brain 1996b; 119: 701–708.

Lovera J, Ramos A, Devier D, Garrison V, Kovner B, Reza T, et al. Polyphenon E, non-futile at neuroprotection in multiple sclerosis but unpredictably hepatotoxic: Phase I single group and phase II randomized placebo-controlled studies. J. Neurol. Sci. 2015; 358: 46–52.

Lublin F, Miller DH, Freedman MS, Cree BAC, Wolinsky JS, Weiner H, et al. Oral fingolimod in primary progressive multiple sclerosis (INFORMS): a phase 3, randomised, double-blind, placebo-controlled trial. Lancet 2016; 387: 1075–1084.

Lublin FD, Baier M, Cutter G. Effect of relapses on development of residual deficit in multiple sclerosis. Neurology 2003; 61: 1528–32.

Lublin FD, Cofield SS, Cutter GR, Conwit R, Narayana PA, Nelson F, et al. Randomized study combining interferon and glatiramer acetate in multiple sclerosis. Ann. Neurol. 2013; 73: 327–340.

Lublin FD, Reingold SC. Defining the clinical course of multiple sclerosis: results of an international survey. National Multiple Sclerosis Society (USA) Advisory Committee on Clinical Trials of New Agents in Multiple Sclerosis. Neurology 1996; 46: 907–11.

Lublin FD, Reingold SC, Cohen JA, Cutter GR, Sørensen PS, Thompson AJ, et al. Defining the clinical course of multiple sclerosis: the 2013 revisions. Neurology 2014; 83: 278–86.

Lucchinetti CF, Popescu BFG, Bunyan RF, Moll NM, Roemer SF, Lassmann H, et al. Inflammatory cortical demyelination in early multiple sclerosis. N. Engl. J. Med. 2011; 365: 2188–97.

Luchetti S, Fransen NL, van Eden CG, Ramaglia V, Mason M, Huitinga I. Progressive multiple sclerosis patients show substantial lesion activity that correlates with clinical disease severity and sex: a retrospective autopsy cohort analysis. Acta Neuropathol. 2018; 135: 511–528.

Lukas C, Knol DL, Sombekke MH, Bellenberg B, Hahn HK, Popescu V, et al. Cervical spinal cord volume loss is related to clinical disability progression in multiple sclerosis. J. Neurol. Neurosurg. Psychiatry 2015; 86: 410–8.

Lukas C, Sombekke MH, Bellenberg B, Hahn HK, Popescu V, Bendfeldt K, et al. Relevance of spinal cord abnormalities to clinical disability in multiple sclerosis: MR imaging findings in a large cohort of patients. Radiology 2013; 269: 542–52.

Lundmark J, Reis M, Bengtsson F. Serum concentrations of fluoxetine in the clinical treatment setting. Ther. Drug Monit. 2001; 23: 139–47.

Mackenzie IS, Morant S V., Bloomfield GA, MacDonald TM, O'Riordan J. Incidence and prevalence of multiple sclerosis in the UK 1990-2010: a descriptive study in the General Practice Research Database. J. Neurol. Neurosurg. Psychiatry 2014; 85: 76–84.

Maes M, Kenis G, Kubera M, De Baets M, Steinbusch H, Bosmans E. The negative immunoregulatory effects of fluoxetine in relation to the cAMP-dependent PKA pathway. Int. Immunopharmacol. 2005; 5: 609–618.

Magliozzi R, Howell O, Vora A, Serafini B, Nicholas R, Puopolo M, et al. Meningeal B-cell follicles in secondary progressive multiple sclerosis associate with early onset of disease and severe cortical pathology. Brain 2006; 130: 1089–1104.

Mahad DH, Trapp BD, Lassmann H. Pathological mechanisms in progressive multiple sclerosis. Lancet Neurol. 2015; 14: 183–193.

Mandolesi G, Gentile A, Musella A, Fresegna D, De Vito F, Bullitta S, et al. Synaptopathy connects inflammation and neurodegeneration in multiple sclerosis. [Internet]. Nat. Rev. Neurol. 2015[cited 2015 Nov 22] Available from: http://www.ncbi.nlm.nih.gov/pubmed/26585978

Mann RS, Constantinescu CS, Tench CR. Upper cervical spinal cord cross-sectional area in relapsing remitting multiple sclerosis: Application of a new technique for measuring cross-sectional area on magnetic resonance images. J. Magn. Reson. Imaging 2007; 26: 61–65.

Marracci GH, Jones RE, McKeon GP, Bourdette DN. Alpha lipoic acid inhibits T cell migration into the spinal cord and suppresses and treats experimental autoimmune encephalomyelitis. J. Neuroimmunol. 2002; 131: 104–14.

Marrie RA, Elliott L, Marriott J, Cossoy M, Blanchard J, Leung S, et al. Effect of comorbidity on mortality in multiple sclerosis. Neurology 2015; 85: 240–7.

Marrie RA, Horwitz R, Cutter G, Tyry T. Cumulative impact of comorbidity on quality of life in MS. Acta Neurol. Scand. 2012; 125: 180–186.

Marrie RA, Horwitz RI, Cutter G, Tyry T, Vollmer T. Association between comorbidity and clinical characteristics of MS. Acta Neurol. Scand. 2011; 124: 135–141.

Marrie RA, Rudick R, Horwitz R, Cutter G, Tyry T, Campagnolo D, et al. Vascular comorbidity is associated with more rapid disability progression in multiple sclerosis. Neurology 2010; 74: 1041–7.

Martin D, Thompson MA, Nadler J V. The neuroprotective agent riluzole inhibits release of glutamate and aspartate from slices of hippocampal area CA1. Eur. J.

Pharmacol. 1993; 250: 473–6.

Martinez-Lapiscina EH, Arnow S, Wilson JA, Saidha S, Preiningerova JL, Oberwahrenbrock T, et al. Retinal thickness measured with optical coherence tomography and risk of disability worsening in multiple sclerosis: A cohort study. Lancet Neurol. 2016; 15: 574–584.

McGuigan C, Hutchinson M. The multiple sclerosis impact scale (MSIS-29) is a reliable and sensitive measure. J. Neurol. Neurosurg. Psychiatry 2004; 75: 266–9.

McKee JB, Cottriall CL, Elston J, Epps S, Evangelou N, Gerry S, et al. Amiloride does not protect retinal nerve fibre layer thickness in optic neuritis in a phase 2 randomised controlled trial. Mult. Scler. J. 2017: 135245851774297.

Metz L, Li D, Traboulsee A, Myles M, Duquette P, Godin J, et al. Glatiramer acetate in combination with minocycline in patients with relapsing—remitting multiple sclerosis: results of a Canadian, multicenter, double-blind, placebo-controlled trial. Mult. Scler. J. 2009; 15: 1183–1194.

Metz LM, Liu W-Q. Effective treatment of progressive MS remains elusive. Lancet (London, England) 2018; 391: 1239–1240.

Miller DH, Barkhof F, Frank JA, Parker GJM, Thompson AJ. Measurement of atrophy in multiple sclerosis: pathological basis, methodological aspects and clinical relevance. Brain 2002a; 125: 1676–95.

Miller DH, Barkhof F, Frank JA, Parker GJM, Thompson AJ. Measurement of atrophy in multiple sclerosis: pathological basis, methodological aspects and clinical relevance. Brain 2002b; 125: 1676–95.

Miller DH, Khan OA, Sheremata WA, Blumhardt LD, Rice GPA, Libonati MA, et al. A controlled trial of natalizumab for relapsing multiple sclerosis. N. Engl. J. Med. 2003; 348: 15–23.

Miller DH, Soon D, Fernando KT, MacManus DG, Barker GJ, Yousry TA, et al. MRI outcomes in a placebo-controlled trial of natalizumab in relapsing MS. Neurology 2007; 68: 1390–401.

Milo R, Panitch H. Combination therapy in multiple sclerosis. J. Neuroimmunol. 2011; 231: 23–31.

Minagar A, Barnett MH, Benedict RHB, Pelletier D, Pirko I, Sahraian MA, et al. The thalamus and multiple sclerosis: modern views on pathologic, imaging, and clinical aspects. Neurology 2013; 80: 210–9.

Mizoule J, Meldrum B, Mazadier M, Croucher M, Ollat C, Uzan A, et al. 2-Amino-6-trifluoromethoxy benzothiazole, a possible antagonist of excitatory amino acid neurotransmission--I. Anticonvulsant properties. Neuropharmacology 1985; 24: 767–73.

Mizuno T, Kurotani T, Komatsu Y, Kawanokuchi J, Kato H, Mitsuma N, et al. Neuroprotective role of phosphodiesterase inhibitor ibudilast on neuronal cell death induced by activated microglia. Neuropharmacology 2004; 46: 404–411.

Moccia M, Lanzillo R, Palladino R, Chang KC-M, Costabile T, Russo C, et al. Cognitive impairment at diagnosis predicts 10-year multiple sclerosis progression. Mult. Scler. J. 2016; 22: 659–667.

Moccia M, Prados F, Filippi M, Rocca MA, Valsasina P, Brownlee WJ, et al. Longitudinal spinal cord atrophy in multiple sclerosis using the generalized boundary shift integral. Ann. Neurol. 2019: ana.25571.

Montalban X, Hauser SL, Kappos L, Arnold DL, Bar-Or A, Comi G, et al. Ocrelizumab versus Placebo in Primary Progressive Multiple Sclerosis. N. Engl. J. Med. 2017; 376: 209–220.

Montalban X, Sastre-Garriga J, Tintoré M, Brieva L, Aymerich F, Río J, et al. A single-center, randomized, double-blind, placebo-controlled study of interferon beta-1b on primary progressive and transitional multiple sclerosis. Mult. Scler. J. 2009; 15: 1195–1205.

Morini M, Roccatagliata L, Dell'Eva R, Pedemonte E, Furlan R, Minghelli S, et al. α-Lipoic acid is effective in prevention and treatment of experimental autoimmune encephalomyelitis. J. Neuroimmunol. 2004; 148: 146–153.

Mostert J, Heersema T, Mahajan M, Van Der Grond J, Van Buchem MA, De Keyser J. The effect of fluoxetine on progression in progressive multiple sclerosis: a double-blind, randomized, placebo-controlled trial. ISRN Neurol. 2013; 2013: 370943.

Mostert JP, Admiraal-Behloul F, Hoogduin JM, Luyendijk J, Heersema DJ, van Buchem MA, et al. Effects of fluoxetine on disease activity in relapsing multiple sclerosis: a double-blind, placebo-controlled, exploratory study. J. Neurol. Neurosurg. Psychiatry 2008; 79: 1027–31.

Mowry EM, Azevedo CJ, McCulloch CE, Okuda DT, Lincoln RR, Waubant E, et al. Body mass index, but not vitamin D status, is associated with brain volume change in MS. Neurology 2018; 91: e2256–e2264.

Mullard A. Drug repurposing programmes get lift off. Nat. Rev. Drug Discov. 2012; 11: 505–506.

Munger KL, Bentzen J, Laursen B, Stenager E, Koch-Henriksen N, Sørensen TIA, et al. Childhood body mass index and multiple sclerosis risk: a long-term cohort study. Mult. Scler. 2013; 19: 1323–9.

Mwanza J-C, Durbin MK, Budenz DL, Girkin CA, Leung CK, Liebmann JM, et al. Profile and Predictors of Normal Ganglion Cell–Inner Plexiform Layer Thickness Measured with Frequency-Domain Optical Coherence Tomography. Investig. Opthalmology Vis. Sci. 2011; 52: 7872.

Nakamura K, Brown RA, Narayanan S, Collins DL, Arnold DL, Alzheimer's Disease Neuroimaging Initiative. Diurnal fluctuations in brain volume: Statistical analyses of MRI from large populations. Neuroimage 2015; 118: 126–132.

Nandoskar A, Raffel J, Scalfari AS, Friede T, Nicholas RS. Pharmacological Approaches to the Management of Secondary Progressive Multiple Sclerosis. Drugs 2017; 77: 885–910.

Noseworthy JH, O'Brien P, Erickson BJ, Lee D, Sneve D, Ebers GC, et al. The Mayo Clinic-Canadian Cooperative trial of sulfasalazine in active multiple sclerosis. Neurology 1998; 51: 1342–52.

Noseworthy JH, Wolinsky JS, Lublin FD, Whitaker JN, Linde A, Gjorstrup P, et al. Linomide in relapsing and secondary progressive MS: part I: trial design and clinical results. North American Linomide Investigators. Neurology 2000; 54: 1726–33.

Nourbakhsh B, Azevedo C, Maghzi A-H, Spain R, Pelletier D, Waubant E. Subcortical grey matter volumes predict subsequent walking function in early multiple sclerosis. J. Neurol. Sci. 2016; 366: 229–233.

O'Gorman C, Bukhari W, Todd A, Freeman S, Broadley SA. Smoking increases the risk of multiple sclerosis in Queensland, Australia. J. Clin. Neurosci. 2014; 21: 1730–3.

O Y. Brain and cervical spinal cord atrophy in primary progressive multiple sclerosis: results from a placebo-controlled phase III trial (INFORMS). In: ECTRIMS Online Library.

Oh J, Seigo M, Saidha S, Sotirchos E, Zackowski K, Chen M, et al. Spinal cord normalization in multiple sclerosis. J. Neuroimaging 2014; 24: 577–84.

Ontaneda D, Fox RJ, Chataway J. Clinical trials in progressive multiple sclerosis: lessons learned and future perspectives. Lancet Neurol. 2015; 14: 208–223.

Opexa Therapeutics. Phase 2b Abili-T Trial of Tcelna® (imilecleucel-T) in Secondary Progressive Multiple Sclerosis Did Not Meet Primary Endpoint [Internet]. [cited 2017 May 1] Available from: http://www.opexatherapeutics.com/investors-relations/press-releases/press-release-details/2016/Opexa-Therapeutics-Announces-Phase-2b-Abili-T-Trial-of-Tcelna-imilecleucel-T-in-Secondary-Progressive-Multiple-Sclerosis-Did-Not-Meet-Primary-Endpoint/default.a

Oprea TI, Mestres J. Drug repurposing: far beyond new targets for old drugs. AAPS J. 2012; 14: 759–63.

Orton S-M, Herrera BM, Yee IM, Valdar W, Ramagopalan S V, Sadovnick AD, et al. Sex ratio of multiple sclerosis in Canada: a longitudinal study. Lancet. Neurol. 2006; 5: 932–6.

Le Page E, Leray E, Edan G, French Mitoxantrone Safety Group. Long-term safety profile of mitoxantrone in a French cohort of 802 multiple sclerosis patients: a 5-year prospective study. Mult. Scler. 2011; 17: 867–75.

Pakpoor J, Disanto G, Gerber JE, Dobson R, Meier UC, Giovannoni G, et al. The risk of developing multiple sclerosis in individuals seronegative for Epstein-Barr virus: a meta-analysis. Mult. Scler. J. 2013; 19: 162–166.

Paling D, Solanky BS, Riemer F, Tozer DJ, Wheeler-Kingshott CAM, Kapoor R, et al. Sodium accumulation is associated with disability and a progressive course in multiple sclerosis. Brain 2013; 136: 2305–17.

Panitch H, Miller A, Paty D, Weinshenker B. Interferon beta-1b in secondary progressive MS: results from a 3-year controlled study. Neurology 2004; 63: 1788–95.

Parikh RH, Patel RJ. Nanoemulsions for Intranasal Delivery of Riluzole to Improve Brain Bioavailability: Formulation Development and Pharmacokinetic Studies. Curr. Drug Deliv. 2016; 13: 1130–1143.

Parmenter BA, Weinstock-Guttman B, Garg N, Munschauer F, Benedict RHB. Screening for cognitive impairment in multiple sclerosis using the Symbol digit Modalities Test. Mult. Scler. 2007; 13: 52–7.

Peterson JW, Bö L, Mörk S, Chang A, Trapp BD. Transected neurites, apoptotic neurons, and reduced inflammation in cortical multiple sclerosis lesions. Ann. Neurol. 2001; 50: 389–400.

Petrova N, Carassiti D, Altmann DR, Baker D, Schmierer K. Axonal loss in the multiple sclerosis spinal cord revisited. Brain Pathol. 2018; 28: 334–348.

Petzold A, de Boer JF, Schippling S, Vermersch P, Kardon R, Green A, et al. Optical coherence tomography in multiple sclerosis: a systematic review and meta-analysis. Lancet Neurol. 2010; 9: 921–932.

Peyro Saint Paul L, Debruyne D, Bernard D, Mock DM, Defer GL. Pharmacokinetics and pharmacodynamics of MD1003 (high-dose biotin) in the treatment of progressive multiple sclerosis. Expert Opin. Drug Metab. Toxicol. 2016: 1–18.

Pisa M, Ratti F, Vabanesi M, Radaelli M, Guerrieri S, Moiola L, et al. Subclinical neurodegeneration in multiple sclerosis and neuromyelitis optica spectrum disorder revealed by optical coherence tomography. Mult. Scler. J. 2019: 135245851986160.

Pitt D, Werner P, Raine CS. Glutamate excitotoxicity in a model of multiple sclerosis. Nat. Med. 2000; 6: 67–70.

Pitteri M, Romualdi C, Magliozzi R, Monaco S, Calabrese M. Cognitive impairment predicts disability progression and cortical thinning in MS: An 8-year study. Mult. Scler. J. 2017; 23: 848–854.

Plantone D, De Angelis F, Doshi A, Chataway J. Secondary Progressive Multiple Sclerosis: Definition and Measurement. CNS Drugs 2016; 30: 517–526.

Pöhlau D, Przuntek H, Sailer M, Bethke F, Koehler J, König N, et al. Intravenous immunoglobulin in primary and secondary chronic progressive multiple sclerosis: a randomized placebo controlled multicentre study. Mult. Scler. J. 2007; 13: 1107–1117.

Polman CH, O'Connor PW, Havrdova E, Hutchinson M, Kappos L, Miller DH, et al. A randomized, placebo-controlled trial of natalizumab for relapsing multiple sclerosis. N. Engl. J. Med. 2006; 354: 899–910.

Polman CH, Reingold SC, Banwell B, Clanet M, Cohen JA, Filippi M, et al.

Diagnostic criteria for multiple sclerosis: 2010 Revisions to the McDonald criteria. Ann. Neurol. 2011; 69: 292–302.

Polman CH, Rudick RA. The multiple sclerosis functional composite a clinically meaningful measure of disability. Neurology 2010; 74

Poorolajal J, Bahrami M, Karami M, Hooshmand E. Effect of smoking on multiple sclerosis: a meta-analysis. J. Public Health (Oxf). 2016: fdw030.

Popescu BFG, Lucchinetti CF. Pathology of Demyelinating Diseases. Annu. Rev. Pathol. Mech. Dis. 2012; 7: 185–217.

Popescu BFG, Pirko I, Lucchinetti CF. Pathology of multiple sclerosis: where do we stand? Continuum (Minneap. Minn). 2013; 19: 901–21.

Prados F, Barkhof F. Spinal cord atrophy rates. Neurology 2018; 91: 157–158.

Prados F, Cardoso MJ, MacManus D, Wheeler-Kingshott CAM, Ourselin S. A modality-agnostic patch-based technique for lesion filling in multiple sclerosis. Med. Image Comput. Comput. Assist. Interv. 2014; 17: 781–8.

Press Release Innate Immunotherapeutics. Top-line results for trial of MIS416 in patients with secondary progressive multiple sclerosis [Internet]. 2017[cited 2018 Apr 2] Available from: http://www.innateimmuno.com/irm/PDF/1424_0/TopLineResultsforTrialofMIS416

Prineas JW, Kwon EE, Cho ES, Sharer LR, Barnett MH, Oleszak EL, et al. Immunopathology of secondary-progressive multiple sclerosis. Ann. Neurol. 2001; 50: 646–57.

Prineas JW, Lee S. Multiple Sclerosis: Destruction and Regeneration of Astrocytes in Acute Lesions. J. Neuropathol. Exp. Neurol. 2019; 78: 140–156.

Raftopoulos R, Hickman SJ, Toosy A, Sharrack B, Mallik S, Paling D, et al. Phenytoin for neuroprotection in patients with acute optic neuritis: a randomised, placebo-controlled, phase 2 trial. Lancet Neurol. 2016; 15: 259–269.

Rammohan KW. MULTIPLE SCLEROSIS AS A NEURONAL DISEASE. Neurology 2007; 68: 2161–2161.

Rashid W, Davies GR, Chard DT, Griffin CM, Altmann DR, Gordon R, et al. Upper cervical cord area in early relapsing-remitting multiple sclerosis: Cross-sectional study of factors influencing cord size. J. Magn. Reson. Imaging 2006; 23: 473–476.

Ratchford JN, Saidha S, Sotirchos ES, Oh JA, Seigo MA, Eckstein C, et al. Active MS is associated with accelerated retinal ganglion cell/inner plexiform layer thinning. Neurology 2013; 80: 47–54.

Ratzer R, Iversen P, Börnsen L, Dyrby TB, Romme Christensen J, Ammitzbøll C, et al. Monthly oral methylprednisolone pulse treatment in progressive multiple sclerosis. Mult. Scler. J. 2016; 22: 926–934.

Reuter M, Tisdall MD, Qureshi A, Buckner RL, van der Kouwe AJW, Fischl B. Head

motion during MRI acquisition reduces gray matter volume and thickness estimates. Neuroimage 2015; 107: 107–115.

Riazi A, Hobart JC, Lamping DL, Fitzpatrick R, Thompson AJ. Multiple Sclerosis Impact Scale (MSIS-29): reliability and validity in hospital based samples. J. Neurol. Neurosurg. Psychiatry 2002; 73: 701–4.

Rice GP, Filippi M, Comi G. Cladribine and progressive MS: clinical and MRI outcomes of a multicenter controlled trial. Cladribine MRI Study Group. Neurology 2000; 54: 1145–1155.

Rinker JR et al. Results of a pilot trial of lithium in progressive multiple sclerosis. ECTRIMS Online Library. Rinker II J. Sep 16 2016; 145965 [Internet]. ECTRIMS Online Libr. Rinker II J. Sep 16 2016; 145965[cited 2017 Apr 19] Available from: http://onlinelibrary.ectrims-congress.eu/ectrims/2016/32nd/145965/john.rinker.ii.results.of.a.pilot.trial.of.lithium.in.progressive.multiple.html?f=m2

Rocca MA, Horsfield MA, Sala S, Copetti M, Valsasina P, Mesaros S, et al. A multicenter assessment of cervical cord atrophy among MS clinical phenotypes. Neurology 2011; 76: 2096–102.

Rocca MA, Iannucci G, Rovaris M, Comi G, Filippi M. Occult tissue damage in patients with primary progressive multiple sclerosis is independent of T2-visible lesions--a diffusion tensor MR study. J. Neurol. 2003; 250: 456–60.

Rocca MA, Sormani MP, Rovaris M, Caputo D, Ghezzi A, Montanari E, et al. Long-term disability progression in primary progressive multiple sclerosis: a 15-year study. Brain 2017; 140: 2814–2819.

Rolan P, Hutchinson M, Johnson K. Ibudilast: a review of its pharmacology, efficacy and safety in respiratory and neurological disease. Expert Opin. Pharmacother. 2009; 10: 2897–2904.

Romme Christensen J, Ratzer R, Börnsen L, Lyksborg M, Garde E, Dyrby TB, et al. Natalizumab in progressive MS: results of an open-label, phase 2A, proof-of-concept trial. Neurology 2014; 82: 1499–1507.

Rudick R, Antel J, Confavreux C, Cutter G, Ellison G, Fischer J, et al. Recommendations from the National Multiple Sclerosis Society Clinical Outcomes Assessment Task Force. Ann. Neurol. 1997; 42: 379–82.

Rudick RA, Kappos L. Measuring disability in relapsing-remitting MS. Neurology 2010; 75: 296–7.

Rudick RA, Stuart WH, Calabresi PA, Confavreux C, Galetta SL, Radue E-W, et al. Natalizumab plus Interferon Beta-1a for Relapsing Multiple Sclerosis. N. Engl. J. Med. 2006; 354: 911–923.

Saidha S, Al-Louzi O, Ratchford JN, Bhargava P, Oh J, Newsome SD, et al. Optical coherence tomography reflects brain atrophy in multiple sclerosis: A four-year study. Ann. Neurol. 2015; 78: 801–13.

Saidha S, Sotirchos ES, Ibrahim MA, Crainiceanu CM, Gelfand JM, Sepah YJ, et al. Microcystic macular oedema, thickness of the inner nuclear layer of the retina, and disease characteristics in multiple sclerosis: a retrospective study. Lancet Neurol. 2012; 11: 963–972.

Saidha S, Syc SB, Durbin MK, Eckstein C, Oakley JD, Meyer SA, et al. Visual dysfunction in multiple sclerosis correlates better with optical coherence tomography derived estimates of macular ganglion cell layer thickness than peripapillary retinal nerve fiber layer thickness. Mult. Scler. 2011a; 17: 1449–63.

Saidha S, Syc SB, Ibrahim MA, Eckstein C, Warner C V., Farrell SK, et al. Primary retinal pathology in multiple sclerosis as detected by optical coherence tomography. Brain 2011b; 134

Sastre-Garriga J, Ingle GT, Chard DT, Cercignani M, Ramió-Torrentà L, Miller DH, et al. Grey and white matter volume changes in early primary progressive multiple sclerosis: a longitudinal study. Brain 2005; 128: 1454–1460.

Sawcer S, Franklin RJM, Ban M. Multiple sclerosis genetics. Lancet. Neurol. 2014; 13: 700–9.

Sawcer S, Hellenthal G, Pirinen M, Spencer CC, Patsopoulos NA, Moutsianas L, et al. Genetic risk and a primary role for cell-mediated immune mechanisms in multiple sclerosis. Nature 2011; 476: 214–219.

Sbardella E, Tona F, Petsas N, Pantano P, Sbardella E, Tona F, et al. DTI Measurements in Multiple Sclerosis: Evaluation of Brain Damage and Clinical Implications. Mult. Scler. Int. 2013; 2013: 671730.

Scalfari A, Neuhaus A, Degenhardt A, Rice GP, Muraro PA, Daumer M, et al. The natural history of multiple sclerosis: a geographically based study 10: relapses and long-term disability. Brain 2010; 133: 1914–29.

Van Schependom J, D'hooghe MB, Cleynhens K, D'hooge M, Haelewyck MC, De Keyser J, et al. The Symbol Digit Modalities Test as sentinel test for cognitive impairment in multiple sclerosis. Eur. J. Neurol. 2014; 21

Schippling S, Balk L, Costello F, Albrecht P, Balcer L, Calabresi P, et al. Quality control for retinal OCT in multiple sclerosis: validation of the OSCAR-IB criteria. [Internet]. Mult. Scler. 2014[cited 2014 Nov 13] Available from: http://www.ncbi.nlm.nih.gov/pubmed/24948688

Schlaeger R, Papinutto N, Zhu AH, Lobach I V, Bevan CJ, Bucci M, et al. Association Between Thoracic Spinal Cord Gray Matter Atrophy and Disability in Multiple Sclerosis. JAMA Neurol. 2015; 72: 897–904.

Schreiber K, Magyari M, Sellebjerg F, Iversen P, Garde E, Madsen CG, et al. High-dose erythropoietin in patients with progressive multiple sclerosis: A randomized, placebo-controlled, phase 2 trial. Mult. Scler. J. 2017; 23: 675–685.

Schuffenhauer A, Floersheim P, Acklin P, Jacoby E. Similarity metrics for ligands reflecting the similarity of the target proteins. J. Chem. Inf. Comput. Sci.; 43: 391–405.

Scolding N, Barnes D, Cader S, Chataway J, Chaudhuri A, Coles A, et al. Association of British Neurologists: revised (2015) guidelines for prescribing disease-modifying treatments in multiple sclerosis. Pract. Neurol. 2015; 15: 273–279.

Secondary Progressive Efficacy Clinical Trial of Recombinant Interferon-beta-1a in MS (SPECTRIMS) Study Group. Randomized controlled trial of interferon- beta-1a in secondary progressive MS: Clinical results. Neurology 2001; 56: 1496–504.

Sedel F, Papeix C, Bellanger A, Touitou V, Lebrun-Frenay C, Galanaud D, et al. High doses of biotin in chronic progressive multiple sclerosis: a pilot study. Mult. Scler. Relat. Disord. 2015; 4: 159–69.

Simpson S, Blizzard L, Otahal P, Van der Mei I, Taylor B. Latitude is significantly associated with the prevalence of multiple sclerosis: a meta-analysis. J. Neurol. Neurosurg. Psychiatry 2011; 82: 1132–1141.

Sipe JC, Romine JS, Koziol JA, McMillan R, Zyroff J, Beutler E. Cladribine in treatment of chronic progressive multiple sclerosis. Lancet (London, England) 1994; 344: 9–13.

Smith A. Symbol Digit Modalities Test (SDMT) Manual (revised) [Internet]. Los Angeles West. Psychol. Serv. 1982Available from: http://www.ncbi.nlm.nih.gov/pubmed/22190573

Smith KJ, Kapoor R, Hall SM, Davies M. Electrically active axons degenerate when exposed to nitric oxide. Ann. Neurol. 2001; 49: 470–6.

Smith S., Zhang Y, Jenkinson M, Chen J, Matthews PM, Federico A, et al. Accurate, robust and automated longitudinal and cross-sectional brain change analysis. Neuroimage 2002; 17: 479–489.

Smith SM, Jenkinson M, Woolrich MW, Beckmann CF, Behrens TEJ, Johansen-Berg H, et al. Advances in functional and structural MR image analysis and implementation as FSL. Neuroimage 2004; 23 Suppl 1: S208-19.

Sombekke MH, Wattjes MP, Balk LJ, Nielsen JM, Vrenken H, Uitdehaag BMJ, et al. Spinal cord lesions in patients with clinically isolated syndrome: A powerful tool in diagnosis and prognosis. Neurology 2013; 80: 69–75.

Spain R, Powers K, Murchison C, Heriza E, Winges K, Yadav V, et al. Lipoic acid in secondary progressive MS: A randomized controlled pilot trial. Neurol. Neuroimmunol. neuroinflammation 2017; 4: e374.

Stankiewicz JM, Neema M, Alsop DC, Healy BC, Arora A, Buckle GJ, et al. Spinal cord lesions and clinical status in multiple sclerosis: A 1.5 T and 3 T MRI study. J. Neurol. Sci. 2009; 279: 99–105.

De Stefano N, Airas L, Grigoriadis N, Mattle HP, O'Riordan J, Oreja-Guevara C, et al. Clinical Relevance of Brain Volume Measures in Multiple Sclerosis. CNS Drugs 2014; 28: 147–156.

De Stefano N, Giorgio A, Battaglini M, Rovaris M, Sormani MP, Barkhof F, et al.

Assessing brain atrophy rates in a large population of untreated multiple sclerosis subtypes. Neurology 2010; 74: 1868–1876.

Steinman L. Multiple sclerosis: a two-stage disease. Nat. Immunol. 2001; 2: 762–764.

Stevenson VL, Leary SM, Losseff NA, Parker GJ, Barker GJ, Husmani Y, et al. Spinal cord atrophy and disability in MS: a longitudinal study. Neurology 1998; 51: 234–8.

Stys PK. Axonal degeneration in multiple sclerosis: is it time for neuroprotective strategies? Ann. Neurol. 2004; 55: 601–3.

Stys PK, Waxman SG, Ransom BR. Ionic mechanisms of anoxic injury in mammalian CNS white matter: role of Na+ channels and Na(+)-Ca2+ exchanger. J. Neurosci. 1992; 12: 430–9.

Su KG, Banker G, Bourdette D, Forte M. Axonal degeneration in multiple sclerosis: the mitochondrial hypothesis. Curr. Neurol. Neurosci. Rep. 2009; 9: 411–7.

Takao H, Hayashi N, Ohtomo K. Effect of scanner in longitudinal studies of brain volume changes. J. Magn. Reson. Imaging 2011; 34: 438–444.

Talman LS, Bisker ER, Sackel DJ, Long DA, Galetta KM, Ratchford JN, et al. Longitudinal study of vision and retinal nerve fiber layer thickness in multiple sclerosis. Ann. Neurol. 2010; 67: 749–60.

Thompson AJ, Banwell BL, Barkhof F, Carroll WM, Coetzee T, Comi G, et al. Diagnosis of multiple sclerosis: 2017 revisions of the McDonald criteria [Internet]. Lancet Neurol. 2017[cited 2018 Jan 1] Available from: http://www.ncbi.nlm.nih.gov/pubmed/29275977

Toosy AT, Mason DF, Miller DH. Optic neuritis. Lancet Neurol. 2014; 13: 83–99.

Tourbah A, Lebrun-Frenay C, Edan G, Clanet M, Papeix C, Vukusic S, et al. MD1003 (high-dose biotin) for the treatment of progressive multiple sclerosis: A randomised, double-blind, placebo-controlled study. [Internet]. Mult. Scler. 2016[cited 2016 Sep 19] Available from: http://www.ncbi.nlm.nih.gov/pubmed/27589059

Toussaint D, Périer O, Verstappen A, Bervoets S. Clinicopathological study of the visual pathways, eyes, and cerebral hemispheres in 32 cases of disseminated sclerosis. J. Clin. Neuroophthalmol. 1983; 3: 211–20.

Trapp BD, Nave K-A. Multiple sclerosis: an immune or neurodegenerative disorder? Annu. Rev. Neurosci. 2008; 31: 247–69.

Trapp BD, Peterson J, Ransohoff RM, Rudick R, Mörk S, Bö L. Axonal transection in the lesions of multiple sclerosis. N. Engl. J. Med. 1998; 338: 278–85.

Trapp BD, Stys PK. Virtual hypoxia and chronic necrosis of demyelinated axons in multiple sclerosis. Lancet. Neurol. 2009; 8: 280–91.

Trapp BD, Vignos M, Dudman J, Chang A, Fisher E, Staugaitis SM, et al. Cortical neuronal densities and cerebral white matter demyelination in multiple sclerosis: a retrospective study. Lancet. Neurol. 2018; 17: 870–884.

Tremlett H, Yinshan Zhao Y, Devonshire V. Natural history of secondary-progressive multiple sclerosis. Mult. Scler. J. 2008; 14: 314–324.

Tsagkas C, Magon S, Gaetano L, Pezold S, Naegelin Y, Amann M, et al. Spinal cord volume loss. Neurology 2018; 91: e349–e358.

Tur C, Moccia M, Barkhof F, Chataway J, Sastre-Garriga J, Thompson AJ, et al. Assessing treatment outcomes in multiple sclerosis trials and in the clinical setting. Nat. Rev. Neurol. 2018; 14: 75–93.

Vandemeulebroecke M, Coffey CS, Thomann MA, Muller KE, Barsdorf A, Arbing R, et al. Group Sequential and Adaptive Designs - A Review of Basic Concepts and Points of Discussion. Biometrical J. 2008; 50: 541–557.

Vercellino M, Plano F, Votta B, Mutani R, Giordana MT, Cavalla P. Grey matter pathology in multiple sclerosis. J. Neuropathol. Exp. Neurol. 2005; 64: 1101–7.

Vergo S, Craner MJ, Etzensperger R, Attfield K, Friese MA, Newcombe J, et al. Acid-sensing ion channel 1 is involved in both axonal injury and demyelination in multiple sclerosis and its animal model. Brain A J. Neurol. 2011; 134: 571–584.

Vesterinen HM, Peter C, Irvine CMJ, Sena ES, Egan KJ, Carmichael GG, et al. PLOS ONE: Drug Repurposing: A Systematic Approach to Evaluate Candidate Oral Neuroprotective Interventions for Secondary Progressive Multiple Sclerosis. PLoS One 2015: 10(4): 1-18.

van Waesberghe JH, Kamphorst W, De Groot CJ, van Walderveen MA, Castelijns JA, Ravid R, et al. Axonal loss in multiple sclerosis lesions: magnetic resonance imaging insights into substrates of disability. Ann. Neurol. 1999; 46: 747–54.

Wang Y-Y, Nacher JC, Zhao X-M. Predicting drug targets based on protein domains. Mol. Biosyst. 2012; 8: 1528–34.

Waubant E, Maghzi A-H, Revirajan N, Spain R, Julian L, Mowry EM, et al. A randomized controlled phase II trial of riluzole in early multiple sclerosis. Ann. Clin. Transl. Neurol. 2014; 1: 340–7.

Waxman SG. Axonal conduction and injury in multiple sclerosis: the role of sodium channels. Nat. Rev. Neurosci. 2006; 7: 932–941.

Wheeler-Kingshott CA, Stroman PW, Schwab JM, Bacon M, Bosma R, Brooks J, et al. The current state-of-the-art of spinal cord imaging: applications. Neuroimage 2014; 84: 1082–93.

Whitaker JN, McFarland HF, Rudge P, Reingold SC. Outcomes assessment in multiple sclerosis clinical trials: a critical analysis. Mult. Scler. 1995; 1: 37–47.

Wingerchuk DM, Weinshenker BG. Disease modifying therapies for relapsing multiple sclerosis. BMJ 2016; 354: i3518.

Winges KM, Murchison CF, Bourdette DN, Spain RI. Longitudinal optical coherence tomography study of optic atrophy in secondary progressive multiple sclerosis: Results from a clinical trial cohort. Mult. Scler. J. 2019; 25: 55–62.

Witte ME, Schumacher A-M, Mahler CF, Naumann R, Misgeld T, Correspondence MK, et al. Calcium Influx through Plasma-Membrane Nanoruptures Drives Axon Degeneration in a Model of Multiple Sclerosis. Neuron 2019; 101: 615-624.e5.

Wolinsky JS, Narayana PA, O'Connor P, Coyle PK, Ford C, Johnson K, et al. Glatiramer acetate in primary progressive multiple sclerosis: results of a multinational, multicenter, double-blind, placebo-controlled trial. Ann. Neurol. 2007; 61: 14–24.

World Health Organization. Atlas multiple sclerosis resources in the world 2008. ANNE X E S 2 WHO Libr. Cat. Data 2008

Xiong Z-G, Zhu X-M, Chu X-P, Minami M, Hey J, Wei W-L, et al. Neuroprotection in Ischemia. Cell 2004; 118: 687–698.

Yang H-T, Ju J-H, Wong Y-T, Shmulevich I, Chiang J-H. Literature-based discovery of new candidates for drug repurposing. [Internet]. Brief. Bioinform. 2016[cited 2016 Oct 3] Available from: http://www.ncbi.nlm.nih.gov/pubmed/27113728

Yates RL, Esiri MM, Palace J, Jacobs B, Perera R, DeLuca GC. Fibrin(ogen) and neurodegeneration in the progressive multiple sclerosis cortex. Ann. Neurol. 2017; 82: 259–270.

Zajicek J, Ball S, Wright D, Vickery J, Nunn A, Miller D, et al. Effect of dronabinol on progression in progressive multiple sclerosis (CUPID): a randomised, placebo-controlled trial. Lancet Neurol. 2013; 12: 857–865.

Zivadinov R, Reder AT, Filippi M, Minagar A, Stüve O, Lassmann H, et al. Mechanisms of action of disease-modifying agents and brain volume changes in multiple sclerosis. Neurology 2008; 71: 136–44.

Neurostatus.net [Internet]. Available from: https://www.neurostatus.net/index.php?file=about

Managing multiple sclerosis - NICE Pathways [Internet]. Available from: http://pathways.nice.org.uk/pathways/multiple-sclerosis#path=view%3A/pathways/multiple-sclerosis/managing-multiple-sclerosis.xml&content=view-node%3Anodes-disease-modifying-therapies

A timeline of the research process | Multiple Sclerosis Society UK [Internet]. Available from: https://www.mssociety.org.uk/ms-research/how-we-decide-what-we-fund/research-process-timeline

Santhera Reports Outcome of Exploratory Trial with Idebenone in PPMS Conducted at the NIH [Internet]. [cited 2018 Mar 7] Available from: http://www.santhera.com/assets/files/press-releases/2018-03-05_PR_PPMS_e_final.pdf

Photocoagulation for diabetic macular edema. Early Treatment Diabetic Retinopathy Study report number 1. Early Treatment Diabetic Retinopathy Study research group. Arch. Ophthalmol. (Chicago, Ill. 1960) 1985; 103: 1796–806.

Efficacy and toxicity of cyclosporine in chronic progressive multiple sclerosis: a randomized, double-blinded, placebo-controlled clinical trial. The Multiple Sclerosis Study Group. Ann. Neurol. 1990; 27: 591–605.

The Canadian cooperative trial of cyclophosphamide and plasma exchange in progressive multiple sclerosis. The Canadian Cooperative Multiple Sclerosis Study Group. Lancet (London, England) 1991; 337: 441–6.

Optical Coherence Tomography [Internet]. Cham: Springer International Publishing; 2015. [cited 2019 Dec 20] Available from: http://link.springer.com/10.1007/978-3-319-06419-2